UNIVERSITÀ DEGLI STUDI DI SALERNO



DIPARTIMENTO DI INGEGNERIA INDUSTRIALE

Corso di Dottorato in Ingegneria industriale Curriculum in Ingegneria chimica - XXXV Ciclo

Tesi di dottorato in
"FUNCTIONALIZATION OF PASTA
THROUGH THE INCORPORATION OF
ACTIVE INGREDIENTS OF NATURAL
ORIGINS"

Tutor

Prof. Ing. Giovanna Ferrari

Serena Carpentieri

Dottoranda

- (

Dr. Sergio De Gennaro

Coordinator del Corso di dottorato

Prof. Francesco Donsì

nno accademico: 2021/2022

UNIVERSITÀ DEGLI STUDI DI SALERNO



DIPARTIMENTO DI INGEGNERIA INDUSTRIALE

Corso di Dottorato in Ingegneria industriale Curriculum in Ingegneria chimica - XXXV Ciclo

Tesi di dottorato in
"FUNCTIONALIZATION OF PASTA
THROUGH THE INCORPORATION OF
ACTIVE INGREDIENTS OF NATURAL
ORIGINS"

Tutor

Dottoranda

Serena Carpentieri

r. Sergio De Gennaro

Prof. Ing. Giovanna Ferrari

Coordinatore del Corso di dottorato

Prof. Francesco Donsì

Anno accademico: 2021/202

Aknowledgements

I would thank Prof. Giovanna Ferrari, who has supported me in these years of PhD and since my Bachelor Degree. I owe her the ability to develop a critical and problem-solving approach that has taught me to go in deep and face-up the arising challenges.

I would like to gratefully thank Prof. Donsì and Prof. Pataro, Dr. Roberta Ferrari, all the colleagues and the people I met and with whom I have collaborated these three years in ProdAl S.c.a.r.l.

I also thank Pastificio Lucio Garofalo S.p.a. and Dr. Sergio De Gennaro for their collaboration within the Pasta for fun project which my PhD is part.

I thank Prof. Bonofiglio and Giusy from the Department of Pharmacy and Health and Nutrition Sciences of the University of Calabria for their invaluable kindness and support to my research activities.

I also thank Prof. Joanna Harasym and Agnieszka Orkusz, who welcomed me to their university in Wroclaw for a short but intense period, for the hospitality, gratitude and appreciation shown to me.

Many thanks to my whole family, representing for me a precious and constant source of inspiration and support, and huge thanks to Davide, my wingman, my safe harbour. I thank him for his constant presence, support and understanding during this challenging path.

Thanks also to those who are no longer here, leaving an unbridgeable void, thank you for being constantly present despite your absence.

List of contributions

Publications on international peer reviewed journals

- Nutrizio, M., Pataro, G., Carullo, D., Carpentieri, S., Mazza, L., Ferrari, G., Chemat, F., Banović, M., Režek Jambrak, A. (2020). High Voltage Electrical Discharges as an Alternative Extraction Process of Phenolic and Volatile Compounds from Wild Thyme (Thymus serpyllum L.): In Silico and Experimental Approaches for Solubility Assessment. Molecules, 25, 4131. https://doi.org/10.3390/molecules25184131
- Carpentieri, S., Pataro, G., Mazza, L., Nutrizio, M., Režek Jambrak A., Ferrari, G. (2021). Pulsed Electric Fields- and Ultrasound-assisted green Extraction of valuable compounds from Origanum vulgare L. and Thymus serpyllum L. Food Research International, 56, 4834–4842. https://doi.org/10.1111/ijfs.15159
- Carpentieri, S., Soltanipour, F., Ferrari, G., Pataro, G., Donsì, F. (2021). Emerging Green Techniques for the Extraction of Antioxidants from Agri-Food By-Products as Promising Ingredients for the Food Industry. Antioxidants, 10, 1417. https://doi.org/10.3390/antiox10091417
- Carpentieri, S., Režek Jambrak, A., Ferrari, G., Pataro, G. (2022).
 Pulsed electric field-assisted extraction of aroma and bioactive compounds from aromatic plants and food by-products. Frontiers in Nutrition Food Chemistry, 8, 792203.
 https://doi.org/10.3389/fnut.2021.792203
- Carpentieri, S., Larrea-Wachtendorff, D., Donsì, F., Ferrari, G. (2022). Functionalization of pasta through the incorporation of bioactive compounds from agri-food by-products: fundamentals, opportunities, and drawbacks. Trends in Food Science and Technology, 122, 49-65. https://doi.org/10.1016/j.tifs.2022.02.011
- Carpentieri, S., Ferrari, G., Pataro, G. (2022). Optimization of Pulsed Electric Fields-Assisted Extraction of Phenolic Compounds From White Grape Pomace Using Response Surface Methodology.

- Frontiers in Sustainable Food Systems, 6, 854968. DOI: 10.3389/fsufs.2022.854968
- Carpentieri, S., Augimeri, G., Ceramella, J., Vivacqua, A., Sinicropi, M. S., Pataro, G., Bonofiglio, D., Ferrari, G. (2022). Antioxidant and Anti-Inflammatory Effects of Extracts from Pulsed Electric Field-Treated Artichoke By-Products in Lipopolysaccharide-Stimulated Human THP-1 Macrophages. Foods, 11, 2250. https://doi.org/10.3390/foods11152250
- Eslami, E., **Carpentieri, S.**, Pataro, G., Ferrari, G. (2023). A comprehensive overview of tomato by-products valorization by conventional methods versus emerging technologies. Foods, 12, 166. https://doi.org/10.3390/foods12010166
- Carpentieri, S., Ferrari, G., Pataro, G. (2023). Pulsed electric fields-assisted extraction of valuable compounds from red grape pomace: process optimization using response surface methodology. Frontiers in Nutrition, 10, 1-20. https://doi.org/10.3389/fnut.2023.1158019
- Carpentieri, S., Ferrari, G., Donsì, F. (2022). All-natural wheat gliadin-gum arabic nanocarriers for encapsulation and delivery of grape by-products phenolics obtained through different extraction procedures. Food Chemistry. *Submitted*, Manuscript ID: FOODCHEM-D-22-10789

Publications on proceedings of international conferences

- Carpentieri, S., Ferrari, G., Pataro, G. (2022). Optimization of Pulsed Electric Fields-Assisted Extraction of phenolic compounds from white and red grape pomace using Response Surface Methodology. Proceedings of the 9th International Conference on sustainable solid waste management, June 15 - 18, 2022, Corfu, Greece.
- Carpentieri, S., Augimeri, G., Ceramella, J., Vivacqua, A., Sinicropi, M. S., Pataro, G., Bonofiglio, D., Ferrari, G. (2022). Antioxidant and

Anti-Inflammatory Effects of Extracts from Pulsed Electric Field-Treated Artichoke By-Products in Lipopolysaccharide-Stimulated Human THP-1 Macrophages. Proceedings of the 4th World Congress on Electroporation & Pulsed Electric Fields in Biology, Medicine, Food and Environmental Technologies, October 9-13, 2022, Copenhagen, Denmark.

Carpentieri, S., Ferrari, G., Pataro, G. (2022). Optimization through Response Surface Methodology of Pulsed Electric Fields-Assisted Extraction of Bioactive Compounds From Red Grape Pomace. Proceedings of 9th International Conference on sustainable solid waste management, October 9-13, 2022, Copenhagen, Denmark

Summary

Aknowledgements	5
List of Figures	VIII
List of Tables	XV
Abstract	XIX
Nomenclature	.XXII
Chapter I	1
Introduction	1
Chapter II	5
State of the art	5
PART A – Functionalization of pasta	5
II.1 Pasta production process	5
II.1.1 Raw materials	7
II.1.2 Mixing	9
II.1.3 Extrusion.	10
II.1.4 Drying	10
II.2 Functional pasta	11
II.2.1 Agri-food by-products: a cheap source of functional compound	ls 11
II.2.1.1 Fruit and vegetables	22
II.2.1.2 Oil crops	22
II.2.1.3 Cereals	23
II.2.1.4 Other by-products	24
II.3 Functional pasta production: benefits and drawbacks	24
II.3.1 Health-beneficial pasta with high-quality attributes	26
II.3.2 Strategies to mitigate the negative impact of by-products' addit on the sensory features of pasta	
II.4 Factors affecting the functional attributes of pasta	

PART B – Functional ingredients: waste valorisation	34
II.5 Opportunities	34
II.6 Emerging green techniques for the extraction of bioactives from agrifood by-products as promising ingredients for the food industry	35
II.6.1 Emerging green technologies and involved mechanisms of cell disintegration.	35
Pure Extracts	37
II.6.1.1 Pulsed Electric Fields (PEF)	37
Total recovery of the biomass	39
II.6.1.2 High-Pressure Homogenization (HPH)	39
II.6.2 Green Extraction Process: Synergism between Solvents and Technology	41
II.6.2.1 Bio-Based Solvents	45
II.6.2.1.1 Ethanol	46
II.6.2.1.2 Water	47
Chapter III	49
Objectives of the work	49
Chapter IV	55
Materials & Methods	55
PART A - Functional ingredients	55
IV.1 Raw materials	55
IV.1.1 Characterisation of the raw materials in terms of phenolic profile	57
IV.2 Solvents and chemicals	59
IV.3 Pulsed Electric Fields (PEF)-assisted extraction	60
IV.3.1 Experimental apparatus	60
IV.3.1.1 Lab-scale PEF system	60
IV.3.1.2 Pilot scale PEF system	61
IV.3.1.3 Continuous PEF system	62
IV.3.2 Experimental procedure	63
IV.3.2.1 Sample processing (G300G)	63
IV.3.2.1.1 Cell membrane electroporation induced by PEF	63

IV.3.2.1.2 PEF-assisted extraction	64
IV.3.2.1.3 Experimental Design	65
IV.3.2.2 Sample processing (A113H)	66
IV.3.2.3 Sample processing (N433W)	67
IV.4 High-pressure homogenization-assisted extraction	68
IV.4.1 Experimental apparatus	68
IV.4.2 Experimental procedure	69
IV.4.2.1 Sample processing (E706IT)	69
IV.4.2.2 Sample processing (A781M, and B651S)	70
IV.4.2.3 Downstream processes	71
IV.5 Analytical determinations	71
IV.5.1 Total Phenolic Content (TPC)	71
IV.5.2 Flavonoid content (FC)	71
IV.5.3 Ferric Reducing Antioxidant Power (FRAP)	72
IV.5.4 Free-radical-scavenging capacity (DPPH)	72
IV.5.5 Evaluation of total anthocyanin content (TAC)	72
IV.5.6 Evaluation of tannin content (TC)	73
IV.5.7 Determination of lycopene content	73
IV.5.8 Particle size distribution (PSD) analysis	74
IV.5.9 Optical microscopy analysis	74
IV.5.10 Colour measurements	74
IV.5.11 HPLC-PDA analyses of the extracts	75
IV.5.12 Thermal stability kinetics	76
IV.5.13 Water absorption capacity and solubility index	76
IV.6 Statistical analysis	76
Materials & Methods	77
PART B - Functional pasta	77
IV.7 Raw materials	77
IV.8 Solvents and chemicals	78
IV.9 Pasta Production – Sample processing	79

IV.10 Analytical determinations	84
IV.10.1 Colourimetric analysis	84
IV.10.2 Sensory analysis	85
IV.10.3 Texture profile analysis	85
IV.10.4 Cooking quality	85
IV.10.5 Thermal properties	86
IV.10.6 Pasting analysis	86
IV.10.7 Microstructure	86
IV.10.8 Chemical profile	87
IV.11 Simulated gastrointestinal digestion	87
IV.11.1 Oral phase	87
IV.11.2 Gastric phase	88
IV.11.3 Intestinal phase	88
IV.11.4 Total phenolic content (TPC) release	88
IV.11.5 Starch digestibility	88
IV.11.5.1 Starch nutritional fractions	88
IV.11.5.2 Total starch content	89
IV.11.5.3 Hydrolysed starch	90
IV.12 Biological activity	90
IV.12.1 Sample preparation	90
IV.12.2 Cell Viability Assay	91
IV.12.3 Real-Time RT-PCR Assays	91
IV.12.4 Enzyme-Linked Immunosorbent Assay (ELISA)	91
IV.12.5 Glucose uptake	91
IV.13 Statistical analysis	92
Section I	95
Natural-based ingredients from agri-food by-products and herbs: product	tion
and characterisation	95
Chantar V	05

extraction of intracellular compounds from selected agri-food and herbs	• 1
V.1 Introduction	96
V.2 Materials and Methods	97
V.2.1 Raw materials and samples preparation	97
V.2.2 Samples processing	97
V.2.3 Analytical determinations	98
V.3 Results and discussion	98
V.3.1 Pulsed electric field-assisted extraction (G300G)	98
V.3.1.1 Optimization of PEF processing conditions	98
V.3.1.2 Effect of PEF-assisted extraction on the recover compounds from G300G	•
V.3.1.2.1 Model fitting	101
V.3.1.2.2 Optimization of the extraction processing c	onditions 105
V.3.1.3 Quantification of the main phenolic compounds PDA analysis	
V.3.2 Pulsed electric field-assisted extraction (A113H)	115
V.3.2.1 Total phenolic content, antioxidant activity and HI analysis of A113H extracts	
V.3.3 Pulsed electric field-assisted extraction (N433W)	117
V.3.4 High-Pressure Homogenization-assisted extraction ((E706IT) 119
V.3.4.1 Effect of HPH-treatment on the recovery of bioacompounds from E706IT	
V.3.4.2 Effect of HPH-treatment on the colourimetric processions	
V.3.4.3 Effect of HPH-treatment on the particle size of suspensions	
V.3.5 High-Pressure Homogenization-assisted extraction ((A781M) 128
V.3.5.1 Effect of HPH-treatment on the recovery of bioacompounds and particle size of A781M suspensions	
V.3.6 High-Pressure Homogenization-assisted extraction (

1
4
7
7
8
9
9
9
9
9
8
0
9
9
3
3
4
5
5
5
5
5
5
8
2
3
5

VII.3.1.6 Pasting analysis	166
VII.3.1.7 Microstructural analysis	168
VII.3.1.8 Chemical profile	171
VII.4 Conclusions	174
Chapter VIII	175
Health validation of the new functional pasta: in vitro digestibility and biological activity	175
VIII.1 Introduction	176
VIII.2 Materials and Methods	177
VIII.2.1 Raw materials and samples preparation	177
VIII.2.2 Analytical determinations	177
VIII.3 Results and discussion	177
VIII.3.1 In vitro digestion studies	177
VIII.3.2 Biological activity of the pasta samples	181
VIII.3.2.1 Cytotoxicity	181
VIII.3.2.2 Anti-inflammatory effects in LPS stimulated human macrophages	182
VIII.3.2.3 Glucose uptake	185
VIII.4 Conclusions	187
Chapter IX	189
General conclusion and future	189
perspectives	189
P afarances	103

List of Figures

Figure I.1 Scientific publications on functional pasta in the last years (Science Direct database, September 2022, search string: "functional	2
AND pasta").	2
Figure II.1 Traditional flowsheet of the fresh and dry pasta manufacturing process with the indication, in yellow, of the eventual	
modifications and integrations needed to produce functional pasta. UHT, HT, and LT: Ultra High Temperature, High Temperature, and Low	-
Temperature, respectively.	6
Figure II.2 Main classification of agri-food by-products incorporated into pasta, their main bioactive compounds, and expected main beneficial properties (based on the content of Table I.2). LDL: Low-Density	
Lipoprotein.	21
Figure II.3 Main critical factors affecting the overall quality	21
characteristics of the final pasta functionalized with the addition of	
valuable compounds.	25
Figure II.4 Main critical aspects associated with the pasta	
functionalization and potential solutions.	29
Figure II.5 Schematics of a typical continuous flow PEF system, and	
cross-sectional views of different treatment chamber configurations; (a)	
parallel plate, (b) co-axial, (c) co-linear, (the grey arrows are	
representative of the product flow).	38
Figure II.6 Mechanism of cell disintegration induced by PEF:	
electroporation phenomenon.	38
Figure II.7 Schematics of the operating principle of a typical HPH	
system and focus on the homogenization valve.	40
Figure II.8 Mechanism of cell disintegration induced by HPH.	41
Figure II.9 Classification of the green extraction technologies as a	
function of the solvent used and the food residues source.	45
Figure III.1 Schematization of the main objective of this Ph.D. thesis	
investigation.	51
Figure III.2 Schematic work plan of this Ph.D. thesis investigation.	52
Figure IV.1 Effect of the type of solvent and its concentration on the	
extraction yield of TPC from E706IT. The added blue dot in each graph	
refers to pure water added as a comparative model.	58
Figure IV.2 Extraction kinetics of TPC (mgGAE/gDW) from E706IT,	.
by using 80% acetone-water (v/v).	59
Figure IV.3 Schematization of the batch PEF system used in this Ph.D.	<i>(</i> 1
investigation. VIII	61
VIII	

Figure IV.4 Schematic overview of the continuous flow PEF system	
used in this Ph.D. investigation.	63
Figure IV.5 Working principle of High Shear Homogenizer.	68
Figure IV.6 Schematization of the HPH plant used in this Ph.D.	
investigation.	69
Figure IV.7 Bronze die used in this Ph.D. investigation. Internal top view	
(a), external top view (b).	79
Figure IV.8 3D representation of the forced air convection chamber designed in ProdAl Scarl.	80
Figure IV.9 Schematization of the pasta production process implemented at lab-scale and related investigated parameters.	81
Figure IV.10 Temperature profile of the dough, pasta and extruder after 15 min of mixing.	82
Figure IV.11 Acceptability by panelists in terms of colour of the E700I and R430E pasta samples.	83
Figure IV.12 Schematization of the main pasta production processing	
phases conducted at FAVA S.p.a.	84
Figure V.1 Response surface for the permeabilization index (Zp) of PEF	
treated G300G tissues as a function of electric field strength (kV/cm) and	
the energy input (kJ/kg).	101
Figure V.2 Response surfaces for Total Phenolic Content (TPC) of	
extracts obtained from untreated (Control) (A,C,E) and PEF-treated (E =	
4.6 kV/cm; WT = 20 kJ/kg) (B,D,F) G300G as a function of extraction	
time and ethanol concentration, with the extraction temperature set at	
20°C (A,B), 35°C (C,D), 50°C (E,F).	108
Figure V.3 Response surfaces for Flavonoid Content (FC) of extracts obtained from untreated (Control) (A,C,E) and PEF-treated (E = 4.6 kV/cm; WT = 20 kJ/kg) (B,D,F) G300G as a function of extraction time and ethanol concentration, with the extraction temperature set at 20° C (A,B), 35° C (C,D), 50° C (E,F).	100
	109
Figure V.4 Response surfaces for antioxidant activity (FRAP) of extracts obtained from untreated (Control) (A,C,E) and PEF-treated (E = 4.6 kV/cm; WT = 20 kJ/kg) (B,D,F) G300G as a function of extraction time and ethanol concentration, with the extraction temperature set at 20° C (A,B), 35° C (C,D), 50° C (E,F).	110
Figure V.5 Response surfaces for Total Anthocyanin Content (TAC) of extracts obtained from untreated (Control) (A,C,E) and PEF-treated (E = 4.6 kV/cm; WT = 20 kJ/kg) (B,D,F) G300G as a function of extraction time and ethanol concentration, with the extraction temperature set at	
20°C (A,B), 35°C (C,D), 50°C (E,F).	111
Figure V.6 Response surfaces for Tannin Content (TC) of extracts obtained from untreated (Control) (A,C,E) and PEF-treated (E = 4.6 kV/cm; WT = 20 kJ/kg) (B,D,F) G300G as a function of extraction time	
	IX

and ethanol concentration, with the extraction temperature set at 20°C (A,B), 35°C (C,D), 50°C (E,F).	112
Figure V.7 HPLC-PDA chromatograms of 50% (v/v) ethanol-water	
extracts obtained after 300 min of extraction at 50 °C from untreated	
G300G (red line) and PEF-treated G300G (black line) (Eopt =4.6 kV/cm;	
WT,opt = 20 kJ/kg). Peak identification: gallic acid (1); chlorogenic acid	
(2); caffeic acid (3); epicatechin (4), p-coumaric acid (5); naringin (6);	
rutin (7); phlorizin (8).	114
Figure V.8 HPLC-PDA chromatograms of 50% (v/v) ethanol-water	
extracts obtained after 300 min of extraction at 50 °C from untreated	
G300G (red line) and PEF-treated G300G (black line) (Eopt = 4.6 kV/cm;	
WT,opt = 20 kJ/kg) G300G. Peak identification: (1) peonidin 3-O-	115
glucoside. Figure V.9 HPLC-PDA chromatograms of the extract from untreated	113
A113H (black line), and the extract from PEF-treated A113H (red line).	
Peak identification: gallic acid (1), catechin (2), chlorogenic acid (3),	
epicatechin (4), cynarine (5), sinapic acid (6), naringin (7), rutin (8),	
phlorizin (9).	116
Figure V.10 HPLC-PDA chromatograms of the extract from untreated	
N433W (black line), and the extract from PEF-treated N433W (red line).	
Peak identification: gallic acid (1), catechin (2), chlorogenic acid (3),	
epicatechin (4), cynarine (5), sinapic acid (6), naringin (7), rutin (8),	
phlorizin (9).	118
Figure V.11 Response surfaces for TPC, antioxidant activity and	
lycopene content in the untreated and HPH-treated suspensions at 80	
MPa (A,C,E) and 100 MPa (B,D,F) as function of the process	100
temperature and the number of passes through the homogenization valve.	122
Figure V.12 Mean particle size of untreated (np = 0), and HPH-treated	
(P = 80 MPa, T = 5 °C – 50 °C, np = $2 - 15$) E706IT suspensions.	
	127
Figure V.13 Particle size distribution (PDI) of untreated (np = 0), and	,
HPH-treated (P = 80 MPa, T = 25 °C, np = $2-15$) E706IT suspensions.	127
Figure V.14 Micrographs at 10x of untreated (np = 0, control) and HPH-	
treated (P = 80 MPa, T = 5 °C -50 °C, np = $2-15$) E706IT suspensions.	128
Figure V.15 HPLC-PDA chromatograms of the untreated A781M	
suspension (red line), and HPH-treated A781M suspension (black line).	129
E. MACM. C. 1. C. 1. 1. O. 1. IDM 1	
Figure V.16 Mean particle size of untreated (np = 0), and HPH-treated	
(P = 80 MPa, T = 5 °C - 50 °C, np = 2 - 15) A781M suspensions.	121
Figure V.17 HPLC-PDA chromatograms of the untreated B651S	131
suspension (red line), and HPH-treated B651S suspension (black line).	
Peak identification: gallic acid (1), catechin (2), chlorogenic acid (3),	
X	

phlorizin (9).	133
Figure V.18 Mean particle size of untreated (np = 0), and HPH-treated (P = 80 MPa , T = $5 ^{\circ}\text{C} - 50 ^{\circ}\text{C}$, np = $2 - 15$) B651S suspensions.	134
Figure VI.1 Isothermal degradation of lycopene in E706IT suspension, obtained upon HPH treatment, exposed at different temperatures (25, 40, 70, 100 °C). The lines represent model fits to the experimental data. The bars represent the mean ± standard deviation. Figure VI.2 Isothermal degradation of antioxidant activity in E706IT suspension, obtained upon HPH treatment, exposed at different temperatures (25, 40, 70, 100 °C). The lines represent model fits to the experimental data. The bars represent the mean ± standard deviation. Figure VI.3 Isothermal degradation of TPC in A781M suspension, obtained upon HPH treatment, exposed at different temperatures (25, 40, 70, 100 °C). The lines represent model fits to the experimental data. The	140 140
bars represent the mean \pm standard deviation.	142
Figure VI.4 Isothermal degradation of antioxidant activity in A781M suspension, obtained upon HPH treatment, exposed at different temperatures (25, 40, 70, 100 °C). The lines represent model fits to the experimental data. The bars represent the mean \pm standard deviation.	142
Figure VI.5 Picture of A781M suspensions, obtained upon HPH treatment, exposed at different temperatures (25, 40, 70, 100 °C) after 8 hours of exposure.	143
Figure VI.6 Isothermal degradation of TPC in B651S suspension, obtained upon HPH treatment, exposed at different temperatures (25, 40, 70, 100 °C). The lines represent model fits to the experimental data. The bars represent the mean ± standard deviation. Figure VI.7 Isothermal degradation of antioxidant activity in B651S suspension, obtained upon HPH treatment, exposed at different	144
temperatures (25, 40, 70, 100 °C). The lines represent model fits to the experimental data. The bars represent the mean \pm standard deviation. Figure VI.8 Isothermal degradation of TPC in G300G extract, obtained upon PEF-assisted extraction, exposed at different temperatures (25, 40,	145
70, 100 °C). The lines represent model fits to the experimental data. The bars represent the mean \pm standard deviation. Figure VI.9 Isothermal degradation of antioxidant activity in G300G	146
extract, obtained upon PEF-assisted extraction, exposed at different temperatures (25, 40, 70, 100 °C). The lines represent model fits to the experimental data. The bars represent the mean \pm standard deviation. Figure VI.10 Isothermal degradation of TPC in A113H extract, obtained upon PEF-assisted extraction, exposed at different temperatures (25, 40,	147
- · · · · ·	XI

epicatechin (4), p-coumaric acid (5), naringin (6), rutin (7), quercetin (8),

70, 100 °C). The lines represent model fits to the experimental data. The	
bars represent the mean \pm standard deviation.	146
Figure VI.11 Isothermal degradation of antioxidant activity in A113H	
extract, obtained upon PEF-assisted extraction, exposed at different	
temperatures (25, 40, 70, 100 °C). The lines represent model fits to the	
experimental data. The bars represent the mean \pm standard deviation.	147
Figure VI.12 Isothermal degradation of TPC in N433W extract, obtained	
upon PEF-assisted extraction, exposed at different temperatures (25, 40,	
70, 100 °C). The lines represent model fits to the experimental data. The	
bars represent the mean \pm standard deviation.	147
Figure VI.13 Isothermal degradation of antioxidant activity in N433W	
extract, obtained upon PEF-assisted extraction, exposed at different	
temperatures (25, 40, 70, 100 °C). The lines represent model fits to the	
1	148
Figure VII.1 Pictures of the traditional pasta (control) and the pasta	150
functionalized with the obtained natural extracts.	156
Figure VII.2 Colourimetric profile of the different types of functional	
and traditional pasta (control).	
Different letters above the bars indicate significant differences (p≤0.05)	
among the mean values of each colourimetric parameter of the	150
investigated samples.	156
Figure VII.3 Overall difference (ΔE^*) between the main colourimetric	
parameters of functional pasta samples and those of traditional pasta (control). Different letters above the bars indicate significant differences	
(control). Different fetters above the bars indicate significant differences $(p \le 0.05)$ among the mean values of the samples.	158
Figure VII.4 Descriptive analysis of the main investigated attributes for	150
functional pasta samples.	159
Figure VII.5 Acceptability by panelists in terms of colour (a) and odour	10)
(b) of the functional pasta samples.	161
Figure VII.6 Texture profile of functional and traditional pasta samples	
(control). Different letters above the bars indicate significant differences	
$(p \le 0.05)$ among the mean values of the samples.	162
Figure VII.7 Water absorption index (WAI) of functional and traditional	
pasta samples (control), at cooling time of 0 min and 10 min after	
cooking. Different lowercase letters above the bars indicate significant	
differences (p \leq 0.05) among the mean values of the same samples at	
different cooling times (0 min, 10 min). Different uppercase letters above	
the bars indicate significant differences (p≤0.05) among the mean values	
of the different samples at the same cooling time.	163
Figure VII.8 Scanning electron micrographs of raw pasta surface.	169
Figure VII.9 Scanning electron micrographs of raw pasta section.	170
Figure VII.10 Chemical profile in terms of total polyphenols (a) and	
antioxidant activity (b) of functional and traditional pasta samples	
(control), downstream of the main phases of dry pasta production and	
XII	

$(p \le 0.05)$ among the mean values of the same samples at different	172
processing phases.	
Figure VII.11 Chromatogram (HPLC) of extracts from B520GP dry	
pasta (blue curve) and cooked pasta (black curve) samples and change in	
the concentration of the identified phenolic compounds between B520GP	
pasta before and after cooking. *Peak 2: unidentified compound at 11.30	
min, that could correspond to hydroxybenzoic acid, being one of the most	
abundant free phenolic acids in durum wheat semolina (Bueno-Herrera	
and Pérez-Magariño, 2020).	173
Figure VIII.1 Release of total phenolic compounds (TPC) during the	
digestive phases of functional and traditional pasta (control) samples.	
Different letters above the bars indicate significant differences (p≤0.05)	
among the mean values of the different samples at the same digestive	
phase.	178
Figure VIII.2 Digestibility of starch in functional and traditional pasta	
(control) samples during each digestive phase.	
Different letters above the bars indicate significant differences (p≤0.05)	
among the mean values of the different samples at the same digestive	
phase.	179
Figure VIII.3 Nutritional fractions of starch in functional and traditional	
pasta (control) samples. RDS: rapid digestible starch, SDS: slowly	
digestible starch, RS: resistant starch.	
Different letters above the bars indicate significant differences (p≤0.05)	
among the mean values of the different samples at the same digestive	
rate.	180
Figure VIII.4 MTT (3-(4,5-Dimethylthiazol-2-yl)-2,5-	
Dinhanyltetrazolium Bromide) growth in Caco 2 (a) and HanG2 (b)	

cooking. Different letters above the bars indicate significant differences

Figure VIII.4 MTT (3-(4,5-Dimethylthiazol-2-yl)-2,5-Diphenyltetrazolium Bromide) growth in Caco-2 (a), and HepG2 (b) cells untreated (CTRL) or treated for 12 - 24 h with R430E pasta digestate (C₁<C₂<C₃<C₄). Cell viability is expressed as % of control (CTRL). The value represents the means \pm SEMs of three different experiments, each performed with triplicate samples. * p < 0.05, *** p < 0.005, *** p < 0.001, **** p < 0.0001.

Figure VIII.5 MTT (3-(4,5-Dimethylthiazol-2-yl)-2,5-Diphenyltetrazolium Bromide) growth in Caco-2 (a), and HepG2 (b) cells untreated (CTRL) or treated for 12 - 24 h with B520GP pasta digestate (C₁<C₂<C₃<C₄). Cell viability is expressed as % of control (CTRL). The value represents the means \pm SEMs of three different experiments, each performed with triplicate samples. * p < 0.05, *** p < 0.005, *** p < 0.001, **** p < 0.0001.

Figure VIII.6 Anti-inflammatory effects of R430E digestate in M1 macrophages. Real Time RT-PCR assay for (a) Monocyte Chemoattractant Protein (MCP)-1/C-C motif chemokine ligand 2 (CCL-

182

181

2) and (b) interleukin-6 (IL-6), mRNA expression in human THP-1 derived macrophages untreated (-) or treated for 1 h with digestate $(C_1 < C_2 < C_3 < C_4)$ and then stimulated with 10 ng/mL of lipopolysaccharides (LPS) for 24 h.

Enzyme-linked immunosorbent assay (ELISA) for (c) CCL-2 and (d) IL-6 and in human THP-1 derived macrophages. The values represent the means \pm SEMs of three different experiments, performed in duplicate. * p < 0.05, ** p < 0.005, *** p < 0.001, **** p < 0.0001.

183

184

185

Figure VIII.7 Anti-inflammatory effects of B520GP digestate in M1 macrophages. Real Time RT-PCR assay for (a) Monocyte Chemoattractant Protein (MCP)-1/C-C motif chemokine ligand 2 (CCL-2) and (b) interleukin-6 (IL-6), mRNA expression in human THP-1 derived macrophages untreated (-) or treated for 1 h with digestate $(C_1 < C_2 < C_3 < C_4)$ and then stimulated with 10 ng/mL of lipopolysaccharides (LPS) for 24 h.

Enzyme-linked immunosorbent assay (ELISA) for (c) CCL-2 and (d) IL-6 and in human THP-1 derived macrophages. The values represent the means \pm SEMs of three different experiments, performed in duplicate. * p < 0.05, ** p < 0.005, *** p < 0.001, **** p < 0.0001.

Figure VIII.8 Effect of the exposure of SW872 cells for 24 h at R430E digestate ($C_2 < C_3$) on glucose uptake (MFI).

The values represent the means \pm SEMs of three different experiments, performed in triplicate. * p < 0.05, *** p < 0.005, *** p < 0.001, **** p < 0.0001.

Figure VIII.9 Effect of the exposure of SW872 cells for 24 h at B520GP digestate ($C_2 < C_3 < C_4$) on glucose uptake (MFI).

The values represent the means \pm SEMs of three different experiments, performed in triplicate. * p < 0.05, ** p < 0.005, *** p < 0.001, **** p < 0.0001.

List of Tables

Table II.1 Main steps of the pasta manufacturing process, their conditions traditionally used, and the main critical variables to monitor and/or modify in the case of functional pasta production Table II.2 Main agri-food by-product sources of bioactive compounds used for pasta functionalization, with the indication of their main functional components, their concentration added to pasta, expected	8
beneficial effects, and techno-functional properties of the final pasta product.	12
Table II.3 Physicochemical stability of the bioactive compounds added to pasta during the transformation process and the cooking phases. Table II.4 Advantages and disadvantages of green extraction technologies.	32
	36
Table II.5 Extraction of bioactive compounds from agri-food by-products using green solvents and/or assisted by non-conventional technologies.	42
Table IV.1 Physicochemical characterisation of the investigated matrices.	56
Table IV.2 Experimental design obtained by RSM with the combinations of the independent variables investigated (type of solvent, solvent	
concentration).	58
Table IV.3 Experimental design obtained by RSM with the combinations of the independent variables investigated (E, WT).	65
Table IV.4 Experimental design obtained by RSM with the combinations of the independent variables investigated (E-W, ethanol percentage in	
ethanol-water mixture (%, v/v); t, diffusion time (min) T, extraction	66
temperature (°C)). Table IV.5 Experimental design obtained by RSM with the combinations	00
of the independent variables investigated (P, pressure (MPa); np, number of passes through the micrometric valve, T, extraction temperature (°C)). Table IV.6 Chemical and colour parameters of the durum wheat semolina.	70
	78
Table IV.7 Chemical and physical characteristics of tap water used in this Ph.D. investigation.	78
Table V.1 Actual values of the two independent variables investigated and response of the dependent variable (Zp) of the PEF-treated G300G tissues.	98
Table V.2 Analysis of variance (ANOVA) of the second polynomial model for the cell disintegration index (Zp) of PEF treated G300G tissues.	100

Table V.3 Actual values of the three independent variables investigated
and responses of the dependent variable (TPC, FC, and FRAP) in G300G
extracts from either conventional SLE or PEF (4.6 kV/cm, 20 kJ/kg)-
assisted extraction process. 103
Table V.4 Actual values of the three independent variables investigated
and responses of the dependent variable (TAC, TC) in G300G extracts
from either conventional SLE or PEF (4.6 kV/cm, 20 kJ/kg)-assisted
extraction process.
Table V.5 Analysis of variance (ANOVA) of the two-factor interaction
(2FI) models for the TPC, FC, and antioxidant activity (FRAP) in G300G
extracts from either conventional SLE or PEF (4.6 kV/cm, 20 kJ/kg)-
assisted extraction process. 104
Table V.6 Analysis of variance (ANOVA) of the two-factor interaction
(2FI) models for the TAC, TC in G300G extracts from either conventional
SLE or PEF (4.6 kV/cm, 20 kJ/kg)-assisted extraction process. 105
Table V.7 Concentrations (mg/gDW) of gallic acid, chlorogenic acid,
caffeic acid, epicatechin, p-coumaric acid, naringin, rutin and phlorizin
(HPLC/PDA analysis) in the extracts from untreated and PEF-treated
G300G. 114
Table V.8 Concentrations (in mg/gDW) of gallic acid, catechin,
chlorogenic acid, epicatechin, cynarine, sinapic acid, naringin, rutin, and
phlorizin (HPLC/PDA analysis) in the extracts from the untreated and
PEF-treated A113H. Values with different lowercase letter within the
same row are significantly different ($p \le 0.05$).
Table V.9 Concentrations (in mg/gDW) of gallic acid, catechin,
chlorogenic acid, epicatechin, cynarine, sinapic acid, naringin, rutin, and
phlorizin (HPLC/PDA analysis) in the extracts from the untreated and
PEF-treated N433W. Values with different lowercase letter within the
same row are significantly different ($p \le 0.05$).
Table V.10 Actual values of the three independent variables investigated
and responses of the dependent variables (TPC, FRAP, and lycopene) in
untreated and HPH-treated E706IT suspensions. 119
Table V.11 Optimal extraction conditions for each response variable
analysed, for untreated and HPH-treated E706IT suspensions. 123
Table V.12 Colour parameters, colour differences (ΔE^*) among untreated
and HPH-treated E706IT suspensions, hue angle, and chroma (C*) of
E706IT suspensions as a function of HPH processing conditions ($P = 80$
MPa, $T = 5$ °C -50 °C, $np = 0 - 15$).
Table V.13 Optimal extraction conditions for each response variable
analysed, for untreated and HPH-treated A781M suspensions. 128
Table V.14 Concentrations (in mg/gDW) of catechin, epicatechin,
chlorogenic acid, rutin, and phlorizin (HPLC/PDA analysis) in the
untreated and HPH-treated A781M suspensions.
and carea and in it deduced 11/01101 suspensions.

Table V.15 Optimal extraction conditions for each response variable analysed, for untreated and HPH-treated B651S suspensions.	32
Table V.16 Concentrations (in mg/gDW) of catechin, chlorogenic acid,	
epicatechin, p-coumaric acid, naringin, rutin, quercetin, and phlorizin	
(HPLC/PDA analysis) in the untreated and HPH-treated B651S	
suspensions. 13	33
Table V.17 Optimal HPH processing conditions for E706IT, A781M, and	
B651S samples.	36
Table V.18 Optimal PEF-assisted extraction processing conditions for	
G300G, A113H, and N433W samples.	36
Table V.19 Water solubility index (WSI) and water absorption index	
(WAI) of E706IT, A781M, B651S HPH-treated suspensions, and G300G,	
A113H, N433W extracts from PEF-treated samples.	48
Table VI.1 Optimal cooking time (OCT), and cooking losses (CL) of	
functional and traditional pasta samples (control).	64
Table VII.2 Thermal properties of the analysed samples: ΔH , transition	
enthalpy, Ton, onset temperature; Tpeak, peak temperature; Tend, end	
1	65
Table VII.3 Pasting properties of the analysed samples.	67

Abstract

The food industry is undergoing a constant evolution process to meet the dynamic requirements of a growing population, increasingly concerned about diet-related diseases.

However, global strategies promoting healthy diets have rarely succeeded because of the resistance posed to the modification of consumers' preferences. In this scenario, the addition of bioactive compounds to highly consumed foods, such as pasta, represents an opportunity to promote healthier lifestyles through the consumption of functional products, without drastically changing consumer habits. Pasta, one of the most consumed products worldwide, can be re-designed as a carrier for bioactive compounds, which are not consumed in sufficient amounts in the daily diet.

The emerging concept of exploiting natural and cheap sources, such as agrifood residues, for developing high added-value and innovative food products, containing health-promoting ingredients, could contribute to satisfying the increasing consumers' demand for greener products and cleaner labels.

However, the techno-functional properties and beneficial effects of bioactive compounds are the most critical factors to be controlled during pasta production and preparation, due to intensive processing conditions, for preserving the quality attributes of the final pasta. Likewise, the incorporation of non-conventional ingredients without affecting the sensory aspects of pasta, is a rather challenging task, which requires a fundamental understanding of the effects of the different functional ingredients added into the pasta on the structural, nutritional, and sensorial properties of the novel product.

To preserve the traditional pasta-like sensory profile and to improve its health-promoting effect, the introduction of innovative technologies on the recovery and extraction of natural bioactive compounds could be an opportunity and a strength in the development of functional pasta.

In the frame of the "zero waste economy", the exploitation of nonthermal technologies to fully unlock bioactive components from agri-food by-products represents an opportunity for the pasta industry to satisfy the increasing consumers' demand for sustainable processes.

Therefore, the main aim of this Ph.D. thesis was to develop a new functional pasta with health-beneficial properties related to the prevention of metabolic syndrome, through the incorporation of active principles recovered from agrifood by-products by using Pulsed electric fields (PEF) and High-Pressure Homogenization (HPH) technologies. These novel cell disruption technologies could represent suitable and effective operational strategies to tackle the main processing challenges associated with pasta functionalization, able to enhance the extraction yields of target bioactive compounds, to mitigate the impact of the addition of novel ingredients on the pasta quality, as well as to improve its health-beneficial properties.

A comprehensive understanding of the most critical factors involved in the pasta functionalization process, the preservation of the quality attributes, as well as the potential beneficial effects of the functional pasta on human cell lines, have also been investigated to fill the knowledge gap in the current research on the demonstration of the actual beneficial effects arising from the consumption of the newly formulated pasta, and to further support its eventual industrial transferability.

To this purpose, six different raw materials, including agri-food by-products and herbaceous matrices, have been selected based on commercial considerations, scientific impact, and a comprehensive physicochemical, toxicological, and biological characterisation. These raw materials have been subjected to PEF-assisted extraction and HPH treatment at optimized processing conditions and according to their proximate composition and physical appearance.

Subsequently, the standardisation and optimization of the product formulation and pasta production process were carried out and the obtained pasta was comprehensively characterised in terms of microstructure, sensory, cooking, pasting, and thermal properties, bioactivity through the production process and cooking phase, *in vitro* digestibility, and biological activity on human cell lines.

Several analytical methods have been used to investigate the properties of the pasta samples, namely proximate analysis (AOAC guidelines), differential scanning calorimetry (DSC), rheometer, texturometer, colourimeter, scanning electron microscopy (SEM), among others.

The results obtained highlighted the potential use of the investigated matrices as potential sources of bioactive compounds and strengthened the potentiality of PEF and HPH technologies to unlock intracellular target compounds, enhancing their extraction efficiency. The efficacy of HPH to disrupt the plant cells was confirmed also by particle size analysis and microscopy, allowing to formulate hypothesis for the implementation of such innovative treatment in a real plant for total extracts production.

The obtained extracts showed a good stability when subjected to processing conditions similar to those utilized for pasta preparation and production. This behaviour was detected especially for HPH-treated suspensions that could

have induced changes in the microstructure of macromolecules (e.g., fibres, proteins) naturally present in total extracts tending to form complex bioactive molecules with enhanced stability.

The extracts incorporated in the pasta matrix demonstrated to positively contribute to its bioactivity, which remained constant even after the pilot scale production process and cooking phase. Interestingly, the different types of functional pasta produced (R430E, E700I, O112H, N309BN, D701GN, B520GP) showed texture, residual moisture properties, water absorption capacity, cooking losses, and microstructure comparable to those of traditional pasta.

Overall, all the samples exhibited a similar *in vitro* digestion profile. It is interesting, however, to highlight that the total extracts used to functionalize E700I, R430E, and D701GN pasta samples, induced a significant increase in resistant starch fraction (less easily digestible) during the intestinal phase, and a corresponding reduction in rapidly digestible starch fraction compared to the control pasta. This behaviour could be attributed to the protective effect induced by the macromolecules, naturally present in the total HPH-treated suspensions, on the starch granules, making them less accessible to amylolytic enzymes. The slowed starch digestibility and controlled release of glucose through digestion, being one of the main factors responsible for the metabolic syndrome, support the conclusion that functional pasta could potentially prevent the occurrence of glycaemic peaks.

Consistently with the findings of starch digestibility, R430E sample was found to be particularly promising in terms of glucose uptake when evaluating the biological effects of its digestate on liposarcoma cell lines (SW872 cells). Likewise, B520GP sample showed powerful anti-inflammatory properties in LPS-stimulated human macrophages when compared to the traditional pasta. The results obtained so far allow to highlight that the addition of natural extracts in pasta formulation did not affect the processability of the dough and affected only slightly the sensorial characteristics of the final product. Moreover, the different phases of the pasta production process do not affect the bioavailability of the bioactive compounds that are able to resist the gastrointestinal tract and can be delivered in the target organs.

Nevertheless, *in vivo* studies on the biological activity of the novel functional pasta and a study of the techno-economic feasibility of the product innovation are fundamental to support the possible upscaling to an industrial level.

Nomenclature

Acronyms and abbreviations

PEF Pulsed Electric Fields

HPH High Pressure Homogenization

US Ultrasounds

UAE
 WItrasound-Assisted-Extraction
 Microwave-Assisted-Extraction
 HVED
 High Voltage Electrical Discharges

HSH High Shear Homogenizer

FDA Food and Drug Administration

NCDs Non Communicable Deseases

VHT Very-High Temperature
UHT Ultra-High Temperature

HT High TemperatureLT Low TemperatureOMWW Olive mill wastewater

OP Oil pomace

EWPEgg White PowderEVFEverVita FibraEVPEverVita Pro

LDL Low-Density Lipoprotein

EFSA European Food Safety Authority

PUFA Polyunsaturated fatty acid

PGH Pistachio green hull

PEM Protein-energy malnutrition

XXII

CMC Carboxymethylcellulose

RH Relative humidity TG Transglutaminase ILs Ionic Liquids

DESDeep Eutectic SolventsSCFsSupercritical FluidsSUPRASSupramolecular SolventsPPOPolyphenol oxidase

AOAC Association of Official Agricultural

Chemists

AACC American Association of Cereal Chemists

MRL Maximum Residue Levels
TPC Total Phenolic Content

RSM Response Surface Methodology

FC-CCD Face-centred central composite design

2FI Two-factor interaction

FRAP Ferric Reducing Antioxidant Power

DPPH 2,2-diphenyl-1-picrilidrazil
HPLC-PDA High Performance Liquid

Chromatography-Photodiode array

detector

GAE

Gallic acid equivalent

QE

Quercetin equivalent

AAE

Ascorbic acid equivalent

SLE

Solid-liquid extraction

FC

Flavonoid content

TAC Total anthocyanin content

TC Tannin content

NF Nanofiltration

C3G Cyanidin-3-glucoside

WAC Water absorption capacity

WSI Water solubility index

OCT Optimal cooking time

XXIII

CL Cooking loss

ANOVA Analysis of variance

DLS Dynamic light scattering

CFU Colony forming unit

DSC Differential Scanning Calorimetry

SSF Simulated salivary fluid
SGF Simulated gastric fluid
SIF Simulated intestinal fluid

Gastrointestinal

RDS Rapidly digestible starch
SDS Slowly digestible starch

RS Resistant starch

GOPOD Glucose oxidase/ peroxidase

Hep-G2 Hepatocarcinoma cells

CACO-2 Colorectal adenocarcinoma cells

SW-872 Liposarcoma cells

THP-1 Circulating monocytes of leukemia MTT 3-(4,5-dimethylthiazol- 2-yl)-2,5-

diphenyltetrazolium

MCP-1 Monocyte Chemoattractant Protein
ELISA Enzyme-Linked Immunosorbent Assay
2-NBDG (2-(N-(7-Nitrobenz-2-oxa-1,3-diazol-4-

yl)Amino)-2-Deoxyglucose)

MFIMean Fluorescent IntensityPSDParticle size distributionRMSERoot Mean Square Error

Eq. Equation

SEM Scanning electron microscopy

LPS Lipopolysaccharide

CTRL Control

HCl Hydrochloric acid CO_2 Carbon dioxide

XXIV

Symbols

 T_S

*g*_{DW} Grams (dry weight)

 $Z_{untr(0,1 kHz)}$ Absolute value of the complex impedance

of untreated tissue

 $Z_{tr(0,1 kHz)}$ Absolute value of the complex impedance

of PEF treated tissue in the low (0.1 kHz)

frequency range

 $Z_{tr\,(1\,MHz)}$ Absolute value of the complex impedance

of PEF treated tissue in the high (1 MHz)

frequency range

 Y_k Response variable Xi, Xj independent variables

 β_0 , α_0 Intercept

 β_i , α_i Regression coefficients of the linear terms β_{ii} Regression coefficients of the quadratic

terms

 β_{ij} , α_{ij} Regression coefficients of the interaction

terms

 ABS_s Absorbance of the sample ABS_B Absorbance of the blank

DF Dilution factor

 ε Molar extinction coefficient (L/mol/cm) H_{20} Amount of starch hydrolysed within 20 min of the intestinal digestion (mg)

inition the intestinal digestion (ing)

 H_{120} Amount of starch hydrolysed within 120 min of the intestinal digestion (mg)

Initial weight of starch in the sample (mg)

 ΔA Absorbance of sample solution EV Sample extraction volume (mL)

W Sample weight (mg)

t time (min)

T Temperature (°C)

L* Lightness

a* Red/green coordinate

 b^* Yellow/blue coordinate v/w Volume/weight (mL/g) w/w Weight/weight (g/g)

v/vVolume/volume (mL/mL)L/SLiquid to Solid ratio (mL/g)EElectric field strength (kV/cm) W_T Specific energy input (kJ/kg) Z_p Cell disintegration index

 E_{opt} Optimal Electric field strength (kV/cm) $W_{T,opt}$ Optimal specific energy input (kJ/kg) n_P Number of passes through the valve

 P_{MAX} Maximum pressure (bar) ΔE^* Overall difference in colour

 C^*_{ab} Chroma

 h^*_{ab} Hue angle (°)

 C_1 , C_2 , C_3 , C_4 Concentration (1-4) (mg/mL) ΔH Transition enthalpy (J/g)

 T_{on} Transition onset temperature (°C) T_{peak} Transition peak temperature (°C) T_{end} Transition end temperature (°C) R^2 Coefficient of determination

Chapter I Introduction

Nowadays, food consumption is intended to be focused not only on satisfying the primal urge of hunger but also on promoting consumers' health (Dias et al., 2015). Food industries are currently striving to reduce artificial food additives and develop novel food products containing health-beneficial ingredients, overcoming the existing limitations of conventional food processing (Faustino et al., 2019). This occurs also as a response to the consumers' awareness of the correlation between a healthy lifestyle and dietary habits with the reduced incidence of chronic diseases, such as neurodegenerative diseases, diabetes, and cancer, of an increasingly aging population (European Commission, 2013). Therefore, in the last decades, pharmaceutical and food industries have started to research and develop functional foods as attractive economic commodities (Dias et al., 2015). Nowadays, European consumers defined their consuming preferences based on the novelty and nutritional profile of food products. For instance, a study conducted by Nielsen in 2018 stated that as many as 45 Italians out of 100 declare to look for new foods when they go food shopping (Osservatorio Immagino, 2020).

"Functional foods" are defined as foods, which, through the incorporation of bioactive compounds, can be demonstrated to exert health benefits beyond the intrinsic nutritive effect (Romero et al., 2019). However, the approach for promoting healthy diets through the consumption of functional foods, characterised by formulations far from those the consumers are used to, has, to date, barely succeeded, because consumers' preferences are difficult to modify. In contrast, the addition of bioactive compounds to staple foods, such as pasta, represents an opportunity to promote a healthier diet, without requiring the consumers to change their eating habits.

The concept of functional food first appeared 40 years ago, with a growing interest in this type of product, both from industry and academia, observed already from the second half of the 1990s.

U.S. Food and Drug Administration (FDA) identified pasta as an excellent vehicle for functional compounds with demonstrated biological activity, such

Chapter I

as antioxidants and dietary fibres, because its wide global consumption is likely to contribute to incrementing the intake of healthy elements (Nilusha et al., 2019). Moreover, the worldwide pasta consumption grows annually due to its excellent nutritional properties, ease, and versatility of preparation, as well as cheapness. Since 1949, the FDA approved pasta enrichment with vitamins and iron, as well as the inclusion of health-beneficial ingredients that can contribute to reducing the risk of noncommunicable diseases (NCDs), such as cardiovascular and respiratory diseases, cancers, and diabetes (Wahanik et al., 2018). Based on these premises, the interest in functional pasta has exponentially increased, as shown in Figure I.1, which reports the number of publications per year related to "functional pasta" in the last years.

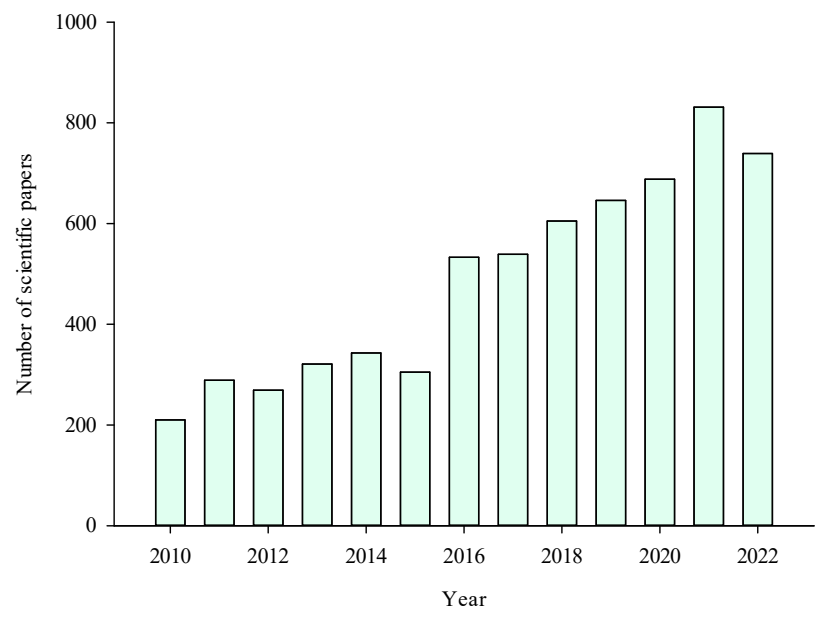


Figure I.1 Scientific publications on functional pasta in the last years (Science Direct database, September 2022, search string: "functional AND pasta").

Different bioactive ingredients have been investigated for pasta functionalization. For example, dietary fibres have attracted noteworthy attention because of their wide availability, e.g., they can be recovered from different agri-food residues and wastes, as well as their role in the prevention and cure of a diverse range of diseases (constipation, gastrointestinal problems) (Wahanik et al., 2018). Antioxidant compounds and proteins have also been considered as health-promoting ingredients of interest for pasta functionalization (Sharma et al., 2016; Wahanik et al., 2018).

Globally, the demand for natural bioactive compounds and the exploration of functional ingredients have continuously increased in parallel with the consumers' preference for functional foods (Boggia et al., 2020). Agri-food

by-products are still rich in natural valuable intracellular compounds that, when effectively recovered, can be exploited as functional ingredients by the food, pharmaceutical, and cosmetic industries, contributing to creating new market opportunities (Ben-Othman et al., 2020). Seeds, pods, peels, pomace, hulls, husks, stems, rinds, and kernels from fruits and vegetable processing have also been widely demonstrated to be sustainable sources of bioactive compounds (Sharma et al., 2016).

The modern food industry and agri-food research have identified as a priority the reduction of industrial wastes in fruits and vegetable production either by valorizing the agri-food by-products or improving food production methods, in line with the 17 sustainable development goals adopted by all United Nations Member States (UN, 2021). The valorisation of agri-food by-products and residues, through proper extraction and stabilization methods, represents an invaluable opportunity for contributing to the sustainable development of the sector, bringing also economic and social benefits to the population. However, processing conditions, product design, and formulation represent critical aspects to be carefully considered, because their lack of optimization could hinder the successful development of novel products, such as functional pasta. The incorporation of non-conventional ingredients represents one of the main drawbacks of pasta functionalization, for the effect on product quality attributes, as recently reviewed (Dey et al., 2021; Nilusha et al., 2019). However, several strategies, based on the careful selection of the characteristics of the raw materials and optimization of the manufacturing processes, can be applied to improve the overall quality of the final pasta product.

Dey et al. (2021) provided an overview of the impact of the extrusion process on the quality of extruded products, functionalized through the incorporation of food processing by-products. However, to date, there is a lack of a comprehensive study addressing all the relevant, interlinked technological challenges involved in processing high-quality functional pasta, considering, at the same time, the opportunities, and strategies to mitigate the negative impact of the incorporation of agri-food by-products.

Moreover, although several studies dealing with the valorisation of agri-food by-products exist, they are mainly focused on the optimization of the extraction conditions, while studies involving the final applications of the obtained extracts into real food matrices are much scarcer. Additionally, there is a strong need to deeply investigate the beneficial effects of the functionalized food product on human health through *in vitro* and then *in vivo* studies to further support the development and validation of the new formulated food product.

Therefore, the following chapter of this work addressed the recent advancements in the production of pasta functionalized with agri-food by-products, focusing on how the addition of bioactive compounds to pasta affects not only the pasta-making process, but also the technological,

Chapter I

structural, sensorial, and nutritional properties of pasta. It also critically analysed the main technological strategies, including the application of green emerging technologies, and the opportunities to mitigate the impact of the addition of unconventional ingredients on the quality of pasta, as well as to improve its health-beneficial properties.

Chapter II State of the art PART A – Functionalization of pasta

II.1 Pasta production process

Pasta is a worldwide-known food product, obtained through durum wheat semolina and water processing, according to its ancient traditionality. Starch (74 – 76% dry basis) and proteins (12 – 15% dry basis) are the major components of durum wheat semolina (Garcia-Valle et al., 2021). These components undergo sequential structural changes during the pasta-making process, which involves three fundamental steps: mixing/kneading, extrusion, and drying (Marti et al., 2016), as shown in Figure II.1, and whose operating conditions are described in Table II.1. The main insights on how the manufacturing process and its crucial operational parameters influence the structural and sensorial properties of pasta are briefly described in this section, as a basis for understanding the impact the incorporation of functional ingredients might have.

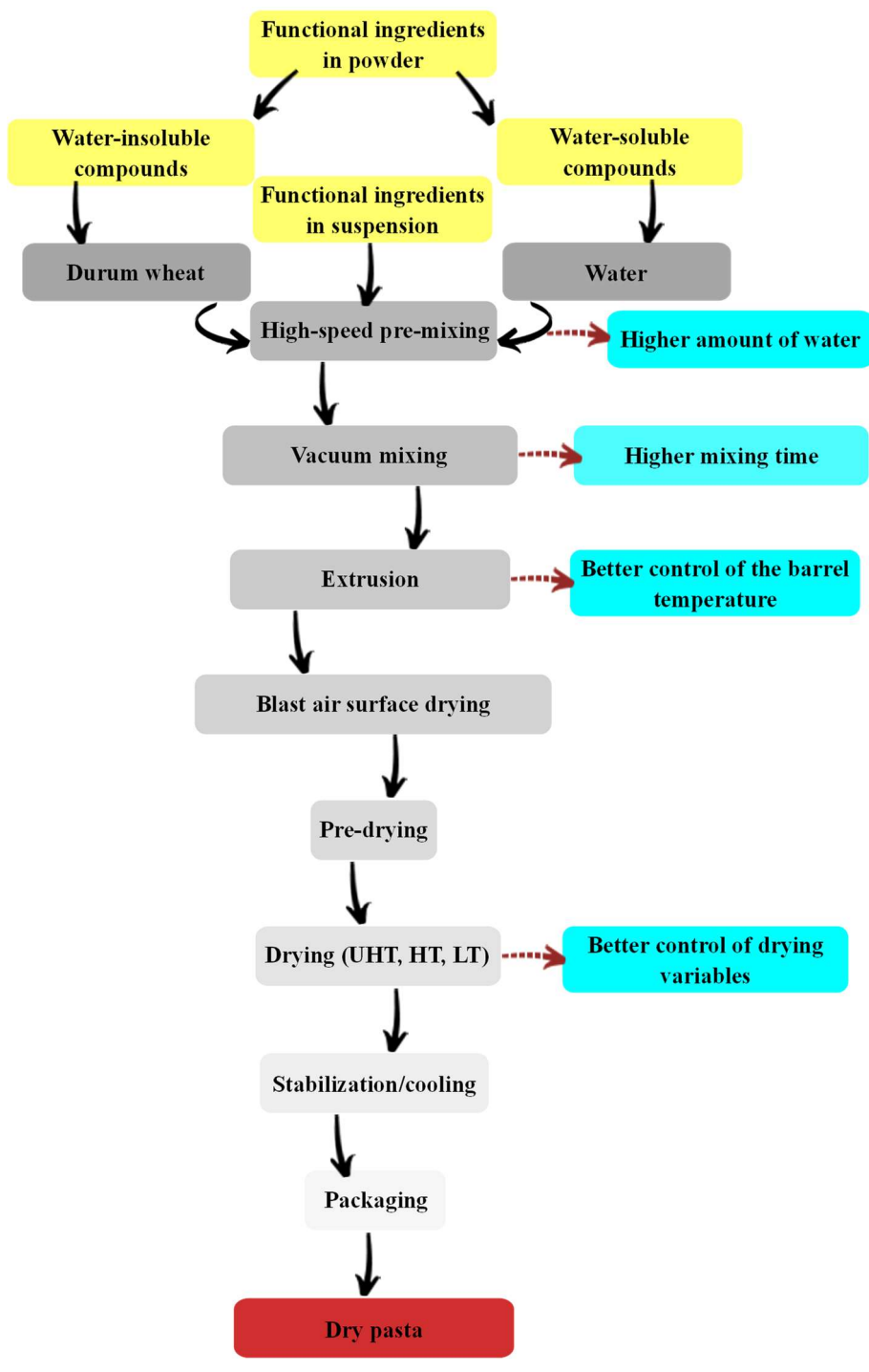


Figure II.1 Traditional flowsheet of the fresh and dry pasta manufacturing process with the indication, in yellow, of the eventual modifications and 6

integrations needed to produce functional pasta. UHT, HT, and LT: Ultra High Temperature, High Temperature, and Low Temperature, respectively.

II.1.1 Raw materials

Durum wheat semolina is the preferred raw material for high-quality pasta production, because of the unpaired role of its chemical and physical characteristics playing on pasta processing (Garcia-Valle et al., 2021). A highquality pasta should have a moisture content within an optimum range from 10 to 16% for dry pasta and around 24% for fresh pasta, both values depending on the food entities regulation, and a relatively high protein content (13.5 -14.5%), with the right balance between glutenins and gliadins to give the desired elasticity and extensibility to the dough (Grassi et al., 2021). A low amount of gluten proteins results in a pasta product with low mechanical strength, whereas a high amount promotes uniform hydration of the semolina during mixing and the "overstretch" of the pasta during extrusion (Grassi et al., 2021). Factors related to semolina characteristics, such as yellow colour and particle size distribution, have shown an important influence on the overall quality of the pasta products (Hare, 2017; Nilusha et al., 2019). Traditionally, semolina with a b* value higher than 30 units, in CIELab colourimetric coordinates, corresponds to a level of yellowness characteristic of high-quality pasta (Hare, 2017). However, mixing, and kneading increase oxygen availability through the water incorporation and the mechanical action, promoting pigments oxidation. Thus, at an industrial scale, mixing generally takes place under vacuum (Hare, 2017).

Another critical requirement to consider for high-quality pasta production is semolina particle size since it affects its water absorption capacity (Banach et al., 2021). The particle size distribution in semolina preferentially ranges from 250 to 350 µm for commercial application (Jalgaonkar and Jha, 2016). This size is preferred to reduce the mixing time and improve the homogeneity of the dough (Banach et al., 2021). Indeed, uniform granulation is important for proper hydration. Small particles tend to over-hydrate, resulting in a soft, sticky dough that requires more energy to dry, whereas large particles tend to under-hydrate, resulting in a stiff dough, which requires more energy for extrusion, resulting in "white specks" in the product (Sicignano, 2015).

Along with the traditional utilization of durum wheat semolina for pasta production, new sources have been introduced to replace semolina in the production of gluten-free products (Nilusha et al., 2019; Romano et al., 2021). Despite the paramount role of gluten proteins in high-quality dough formation is widely known, the need for a safe alternative for people suffering from the celiac disease has forced pasta manufacturers to find adequate solutions for the production of high-quality gluten-free pasta (Nilusha et al., 2019). Composite flours, obtained by mixing gluten-free cereals and different protein sources, such as rice, corn, buckwheat (de Arcangelis et al., 2020), quinoa

(Ramos-Diaz et al., 2020), dairy (Manoj Kumar et al., 2019), egg (Torres et al., 2021) and vegetable proteins (Bolarinwa and Oyesiji, 2021; Bouasla et al., 2017), are commonly utilized to produce gluten-free pasta products. Hydrocolloids from chia (*Salvia hispanica*) have attracted significant attention due to their capability to emulate the role of the gluten network in gluten-free pasta production (Chiang et al., 2021). The newer ingredients and their quality attributes as well as processing conditions for nonconventional "gluten-free" pasta production have been thoroughly reviewed by (Nilusha et al., 2019) and discussed by (de Arcangelis et al., 2020).

In addition, for optimal pasta quality, the water used in the pasta production is required to have specific physical and chemical characteristics, such as the absence of chemicals, iron salts, bacterial contamination and off-flavors, and pH, mineral content, and temperature in a well-defined range (Manthey and Twombly, 2005), as summarized in Table II.1.

Table II.1 Main steps of the pasta manufacturing process, their conditions traditionally used, and the main critical variables to monitor and/or modify in the case of functional pasta production.

Processing step		Traditional processing conditions	Functional pasta processing conditions	References
Raw materials formulation	Durum wheat semolina	Protein content: 13.5 and 14.5% Moisture: 10- 16% Colour: b* = 25 Particle size: 250-350 µm	Optimization of particle size of the functional ingredients	(Alzuwaid et al., 2020; Ciccoritti et al., 2019)
	Water	pH: 6.6-6.9 Mineral content ≤ 400-500 mg/L Calcium and magnesium carbonates ≤ 180- 200 mg/L Temperature: 40- 50 °C Amount: 28-33% of semolina	Optimization of amount and temperature of water and hydration method, depending on the concentration and the physical characteristics of the functional ingredients, to avoid under-hydration, and "white specks" in the final pasta	(la Gatta et al., 2017)
Vacuum mixing		Pressure: 63-80 kPa time: 10-15 min	Optimization of the mixing conditions to improve the distribution of the functional ingredients through the dough and to avoid the loss	(Merendino et al., 2014; Pasqualone et al., 2016)

		of their biological activity	
Extrusion	Pressure: 100 ± 20 bars Barrel temperature: 45-50 °C	Control of the barrel temperature and pressure to grant the preservation of the thermolabile compounds and the integrity of the pasta network.	(de Paula et al., 2017)
Blast air surface drying	Air temperature: 40 Time: 1-2 min	0-50 °C	
Pre-drying	Moisture of the pasta entering the stage: $29 \pm 2\%$ Reduction of the total water ($\sim 10\%$)	Optimization of	(Giannetti et al., 2021a)
Drying	Low Temperature: 40- 60 °C High Temperature: 60< T<80 °C Very High Temperature: T ≥90 °C	drying cycles according to the chemical stability of the functional compounds	
Cooling and stabilization	Ambient condition ~50%, to minimize cracking.	s, relative humidity the possibility of	

II.1.2 Mixing

The mixing process strongly influences dough development and the technological transformations required for pasta production. Pasta quality factors, such as gluten network formation, starch encapsulation, and water distribution, are determined by processing parameters, namely mixing time, temperature, and speed rate. Mixing times ranging from 10 to 15 min have been reported as optimal conditions for doughs formed with semolina at standardised chemical and physical properties (as previously discussed) (de Cindio and Baldino, 2015). At overmixing conditions, the crosslinks among proteins of the gluten network begin to break, and the dough becomes sticky (Meerts et al., 2017).

Dough rheological properties are also correlated with the amount of added water, whose correct dosage is required to develop a cohesive and viscoelastic dough with optimum gluten strength. A freshly formed dough should contain between 28-32% moisture, depending on semolina properties and pasta shape (Czaja et al., 2018; Dey et al., 2021). Proper dough development requires that semolina particles are completely hydrated: incomplete hydration typically

results in pasta with a higher tendency to crack, whereas excess hydration may result in sticky pasta with low mechanical strength, poor colour, and low cooking quality (de la Peña and Manthey, 2017).

II.1.3 Extrusion

At the extrusion stage, polymerization, which is the central phenomenon, is modulated by the synergistic effect of pressure, temperature, and water content. Generally, pressures around 100 ± 20 bars and barrel temperatures between 45 and 50 °C have been reported as proper conditions for pasta shaping with the lowest cooking losses and highest firmness (Czaja et al., 2018; Dey et al., 2021). Process temperatures above 55 °C impact negatively the gluten network structure by triggering the formation of covalent links, resulting in a soft, sticky product when cooked (Martin et al., 2019).

Moreover, dye material plays an essential role in extruded pasta surface properties (Boukid, 2021). Teflon dies, which have a low coefficient of friction, thus reducing the pressure needed for extrusion and increasing the rate of extruded pasta, result in smooth pasta with a bright-yellow appearance. On the contrary, a rough, uneven, and porous pasta is produced utilizing bronze dies (Boukid, 2021). Interestingly, higher effective moisture diffusivity coefficients were measured for pasta extruded with a bronze die than with a Teflon die, suggesting that the use of bronze dies could reduce the drying time (Ogawa and Adachi, 2017).

II.1.4 Drying

The pasta drying process can be classified into three main phases: pre-drying, final drying, and cooling/stabilization. The objective of the pre-drying phase is to maintain the desired pasta shape during the process, preventing pieces from sticking together. The moisture content of the product when entering the final drying stage is ~ 18 - 21%. The rate of moisture removal in this phase is critical because of the product's elastic state. If drying is too fast, the superficial tensions exceed the strength of the pasta and checking occurs. Finally, the product is equilibrated with the ambient conditions to minimize the possibility of cracking. Sometimes, it is necessary to perform humidification in the drier through steam injection to eliminate residual superficial tensions and enhance product stabilization (Baiano et al., 2019). Three drying modalities can be defined as a function of processing temperatures and relative humidity ranges: conventional or low temperature (LT, T < 60 °C), high temperature (HT, 70 < T < 80 °C), and very high-temperature drying (VHT, T \geq 90 °C) (Giannetti et al., 2021b).

The different drying cycles were reported to influence the sensory and cooking quality of pasta (Giannetti et al., 2021a; Masato et al., 2021). In general, HT drying improved cooking properties and organoleptic characteristics, as 10

shown by lower cooking losses, higher firmness, hardness, cohesiveness, springiness, breaking energy, and lower surface stickiness and bulkiness, attributed to a higher proportion of amylose in the starch, than pasta processed by LT drying cycles. However, HT and VHT drying might promote the formation of strong protein networks, making the protein fraction less sensitive to changes during cooking and starch less available to imbibition (Masato et al., 2021). During HT drying, the protein fraction might undergo also structural and compositional changes, which might impair the product's nutritional properties. Severe thermal treatments decreased the in vitro digestibility of starch and wheat proteins, due to the formation of large protein aggregates (Sissons et al., 2021). Therefore, despite high-temperature drying being economically advantageous, it requires accurate control to obtain a high-quality product. Some undesired effects, including non-enzymatic browning and thermo-mechanical stresses, may be induced by high heating and drying rates (Gasparre et al., 2019). Pasta cracking can be reduced by increasing the relative humidity in the chamber, hence slowing down the drying process (Baiano et al., 2019). However, if drying is too slow, pasta might spoil or become moldy (Jalgaonkar et al., 2018a).

II.2 Functional pasta

Pasta generally contains a high amount of starch but a low concentration of health-promoting elements such as dietary fibre, minerals, vitamins, and phenolic compounds (Nilusha et al., 2019). To enhance the health-beneficial value of pasta, several studies have focused on adding functional ingredients recovered from agri-food by-products which contributed to enhancing specific physiological responses and reducing the risk of diseases (Melini et al., 2020). Different dietary fibre, proteins, antioxidants, and omega-3 fatty acids have been added to pasta as functional ingredients (Oliviero and Fogliano, 2016). The benefit of consumption of functional pasta includes antidiabetic (Attanzio et al., 2019; Conte A et al., 2015; Lalegani et al., 2018; Marinelli et al., 2015), antioxidant (Espinosa-Solis et al., 2019), anti-inflammatory (Parizad et al., 2020), and antibiotic effects (Espinosa-Solis et al., 2019; Spinelli et al., 2019). In addition, several bioactive compounds, such as dietary fibres, phenolic compounds, minerals, and vitamins among others, have been reported to contribute to reducing the glycaemic index and combating cardiovascular disorders and many other health diseases (Gull et al., 2018).

II.2.1 Agri-food by-products: a cheap source of functional compounds

Table II.2 summarizes the main bioactive compounds from agri-food byproducts such as fruit, vegetables, oil crops, and cereals by-products used for pasta functionalization, their source, the incorporated amount, the expected

beneficial effects, and techno-functional properties of the obtained functional pasta. Figure II.2 serves as a help to the reader to navigate through Table II.2, by providing a classification of the main agri-food by-products as sources of bioactive compounds as functional ingredients in pasta, and the associated beneficial effects.

Table II.2 Main agri-food by-product sources of bioactive compounds used for pasta functionalization, with the indication of their main functional components, their concentration added to pasta, expected beneficial effects, and techno-functional properties of the final pasta product.

Sources	Functional ingredients	Added or substituted amount	Expected beneficial effects	Effects on techno- functional properties*	References
Fruit Prickly pear cladodes' extract	Soluble dietary fibres: arabinose, galactose, rhamnose, xylose, and galacturonic acid	Replacing 33.3, 66.7, 100% of water, corresponding to 10, 20, 30% (v/w) of dough	Blood cholesterol- and glucose- lowering capabilities	+ Acceptable quality and sensory parameters up to 20% (v/w) of dough replacing	(Attanzio et al., 2019)
Unripe apple flour	Antioxidants: flavonoids and anthocyanins	Replacing 50% of semolina	Antioxidant, antimicrobia l, antifungal, and anticarcinog enic properties	+ Increase in antioxidant activity by 97%	(Espinosa- Solis et al., 2019)
Grape marc	Dietary fibres and antioxidants	Addition of 15% of semolina (three formulation s: 500 µm, 125 µm, and 125 µm with 0.6% (w/w) of transglutami nase (TG))	Anti-cancer, protection against oxidative stress, cardiovascul ar diseases, and diabetes	+ Sensory acceptable quality, higher content of phenolic compounds, and antioxidant activity than control spaghetti	(Marinelli et al., 2015)

State of the art

			tate of the art
	Addition of 2.5, 5, and 7.5% of the dough	+ Increase in total phenolics, condensed tannins, monomeric anthocyanins, and antioxidant capacity - Reduced acceptance of aroma, aftertaste, flavor, and appearance	(Sant'Anna et al., 2014)
	Addition of 7% of the dough	+ Increase in fibre content (3%), the phenols retained after cooking were 6.21 mg/100 g of pasta + Good cooking properties	(Balli et al., 2021)
Grape peels	Replacing 0-5% of the dough	- Substitution ≥3% led to high cooking losses, firmer pasta, heterogenic surface, and undesired sensory characteristics	(Ungureanu -Iuga et al., 2020)

		Addition of 4.94% of the dough		+ Increase in polyphenols, dietary, fibre, and resistant starch - Reduction in chewiness, higher dough complex modulus and pasta brittleness	(Iuga and Mironeasa, 2021)
Banana peels	Antioxidants and polyphenols	Replacing 5% of corn flour	Antifungal, antibiotic properties	+ Not significantly affected colour and texture profile of pasta	(Puraikalan, 2018)
Orange by- product	Dietary fibres, phenolics, and carotenoids	Addition of 2.5, 5, 7.5% of the dough	Antioxidant properties and reduced hyperglyce mia	+ Pasta with 2.5% of orange by- products can be considered a "source fibre" product - Significant increase in solid loss with incorporation ≥5%	(Crizel et al., 2015)
Tomato peel flour	Minerals, vitamins C and E, β- carotene, lycopene, flavonoids,	Replacing 15% of whole meal flour; 2% hydrocolloi ds (agar, carboxymet hylcellulose, guar seed flour, and xanthan gum)	Antioxidant and antimutagen ic activities	+ Increase in carotenoids and dietary fibres - Lower sensory scores for elasticity, odour, and firmness than the control	(Padalino et al., 2017)
	organic acids, phenolics, and chlorophyll	Addition of 10%, 15%, 20% and 25% of whole-meal flour Subsequent experimenta 1 phase:		+ Pasta with the fine particles showed the greatest sensory score + Prolonged glucose release for the	(Conte A et al., 2015)

		addition at different particle size (63, 125, and 250 µm)		pasta enriched with coarse particles	
Vegetables Carrot pomace	Dietary fibres, antioxidants: α-carotene and β- carotene, and ascorbic acid	Replacing 2, 4, 6, 8, 10% of semolina	Antioxidant properties	+ Increase in phenolic content and antioxidant activity than the control - Substitution ≥4% might lead to low cooking qualities	(Gull et al., 2015)
Artichoke canning by-products' extracts	Phenolic compounds, hydroxycinna mates, and flavonoids	Replacing 100% of water, corresponding to 35.5% (v/w) of the dough Ultrasounds -assisted extraction: L/S = 3 ethanol: water (30:70, v/v) then centrifuged and concentrate d at up to 40% of the initial volume	Inhibition of LDL oxidation, hepatoprote ctive, hypocholest erolemia, and antioxidant properties	+ Higher phenolic compounds and antioxidant activity than control pasta + Textural and cooking properties similar to control pasta - Increase in pasta brownness and decrease in yellowness	(Pasqualone et al., 2017)
Potato peel autohydro lysis extract	Fibres, minerals, and antioxidants	Addition of 4% w/w of psyllium husk, dry basis Subcritical water extraction: ground peel/water, L/S = 15:1 (w/w)	Prevention of oxidative damage, microbial infections, hypercholes terolemia, and diabetes	+ Suitable technological properties, attractive colour, and increased total phenolic content and antioxidant activity	(Fradinho et al., 2020)

Oil Crops

		OMWW		+ OP	(Cedola et
Olive oil by- products (pomace (OP), mill wastewate r (OMWW))	Phenolic compounds, fatty acids such as oleic, palmitic, and linoleic acids	OMWW replacing 100% of water, corresponding to 30% of the dough. OP replacing 10% of semolina with 0.6% transglutaminase	Anti-cancer, anti-aging properties, protection against oxidative stress	+ OP improved both total polyphenols and antioxidant activity ± OMWW slightly improved the chemical quality without compromising the sensory properties - Reduced sensory acceptability due to the bitter and spicy taste of OP + 63g of pasta would be sufficient to	(Cecchi et al., 2019)
(OMWW))		Replacing 5- 10% (OP) of durum wheat semolina		meet the EFSA health claim for olive oil phenols - Appearance of pasta strongly affected - Reduced cooking loss properties, higher Increased swelling index and, water absorption, and cooking loss	(Simonato e al., 2019)

		Addition of 10-15% (OP) and 0.6% of the dough transglutami nase		+ Good sensory acceptability of pasta with 10% OP and 0.6% transglutamin ase + Increase in flavonoids and total polyphenols	(Padalino et al., 2018)
		Addition of 7% (OP) of the dough	-	+ Increase in fibre content (3%), the phenols retained after cooking were 9 mg/100 g of pasta + Good cooking properties	(Balli et al., 2021)
Pistachio green hulls (PGH) extract	Polyphenols such as gallic, 4-hydroxybenzo ic, protocatechuic acids, quercetin-3-O-rutinoside, and catechin	Replacing 0.5, 1, and 1.5% of durum wheat semolina Aqueous extraction: 10 g of powdered PGH, (L/S=15:1) concentrate d and freeze-dried	Antioxidant and antimicrobia l properties, reduction of the risk of type 2 diabetes mellitus	+ Significant reduction <i>in vitro</i> starch digestibility and glycaemic index of pasta (1.5%) than the control	(Lalegani et al., 2018)
De-oiled chia flour	Poly- unsaturated fatty acids, essential amino acids, dietary fibres, antioxidants	Replacing 2.5, 5, 10% of wheat flour	Protection against oxidative damage of cells and tissues, prevention of cancer, diabetes, and cardiovascul ar problems	+ Increase in total dietary fibres and omega-3 content. The ratio of ω-3/ω-6 fatty acids also increased significantly from 0 to 2.14	(Aranibar et al., 2018)

Defatted soy flour	All essential amino acids except methionine, iso-flavones, genistein, and daidzein	Replacing 5, 15, and 25% of 50:50 pearl millet flour: semolina blend	Multifunctio nal antioxidant activities	+ Acceptable quality parameters of pasta with 15% of soy flour Lower cooking and sensory qualities at higher levels of substitution	(Jalgaonkar et al., 2018b)
Defatted peanut flout	Dietary fibres, including cellulose, hemicellulose, pectin, mucilage, and gums, proteins	Replacing of 8.3% of semolina	Solving the existing problem of protein-calorie malnutrition	+ This pasta will solve the problem of protein- calorie malnutrition	(Badwaik et al., 2014)
Cereals					
Oat bran	Dietary fibres and antioxidants such as tocopherols and tocotrienols, sterols, and vanillic acid	Replacing 50% of semolina	Control blood glucose level, lowering of serum cholesterol and obesity	+ Increase in total dietary fibres content (16.43% w/w) with a decrease in the digestibility of starch components - Increase in cooking loss and water absorption index	(Espinosa- Solis et al., 2019)
Cereal brans (Wheat, Rice, Rye, and Oat)	Dietary fibres (cellulose and hemicellulose) , proteins, vitamins, and minerals	Replacing 20% of semolina	Antilipemic, antiatheroge nic, antihyperten sive, hypoglycae mic properties	+ Increase in total dietary fibre content by 1.7–2.9 times. + Increase in total phenolic content and antioxidant activity compared to control pasta	(Levent et al., 2020)
Wheat bran, germ, and debrannin g fractions	Dietary fibres (cellulose, pentosans, and	Replacing 20, 25% of semolina	Hypercholes terolemia effect, effects on fecal	+ Significant improvement in sensory attributes and cooking	(la Gatta et al., 2017)

	lignin), proteins, antioxidants	Addition of 10, 20, 25, 30% of the dough	bulking and laxation, reduction of glycaemic and insulinemic responses	quality parameters with separated hydration method + Increase in proteins, fibres, and reduction in available carbohydrates - Higher cooking loss due to starch granules swelling and rupture	(Laureati et al., 2016)
Maize bran and brewer's spent grain	Dietary fibres, essential amino acids, lipids, minerals, antioxidants, and vitamins	2.5, 5, 7.5, 10, 12.5, and 15%, for maize bran; 17.5 and 20% for brewer's spent grain Replacing 3-25% of the dough, and Egg White Powder (EWP) 0- 12% of the dough	- Lowering glycaemic index, and risk of cancer, cardiovascul ar diseases, and obesity	- Reduction in the sensory quality of all types of pasta by 14% than the control - Significant reduction of the average break strain of pasta + The addition of EWP improved the mechanical properties of cooked pasta due to the	(Spinelli et al., 2019) (Cappa and Alamprese, 2017)
Brewer's spent grainderived ingredient s (high in fibre, and high in protein) Other by-pr	Dietary fibres, proteins, vitamins, minerals, antioxidants, and essential fatty acids	Replacing 0.8-9.5% of semolina with EVF, 1-12.5% of semolina with EVP	Enhanced glycaemic control, cholesterol- lowering capacity, prebiotics effect	tight protein network + Increase in pasta firmness and tensile strength and a decrease in the predicted glycaemic index compared to the control	(Sahin et al., 2021)

Pangas processin g waste	Proteins, essential amino acids	Addition of 0, 2.5, 5.0, 7.5, 10% of semolina	Protein fortification of low- protein foods	+ Significant increase in the protein content, and water absorption capacity Good colour and functionality up to 5% of pangas waste	(Reddy Surasani et al., 2019)
Whey powder	Proteins	Replacing 0-15% of the starch- corn flour mix	Antihyperte nsive effects, sense of satiety	+ Reduction in cooking loss, dough and pasta firmness, smooth pasta surface, and acceptable sensory quality	(Ungureanu -Iuga et al., 2020)

^{* +, -, ±} denotes positive, negative, or neutral effects, respectively, on techno-functional properties

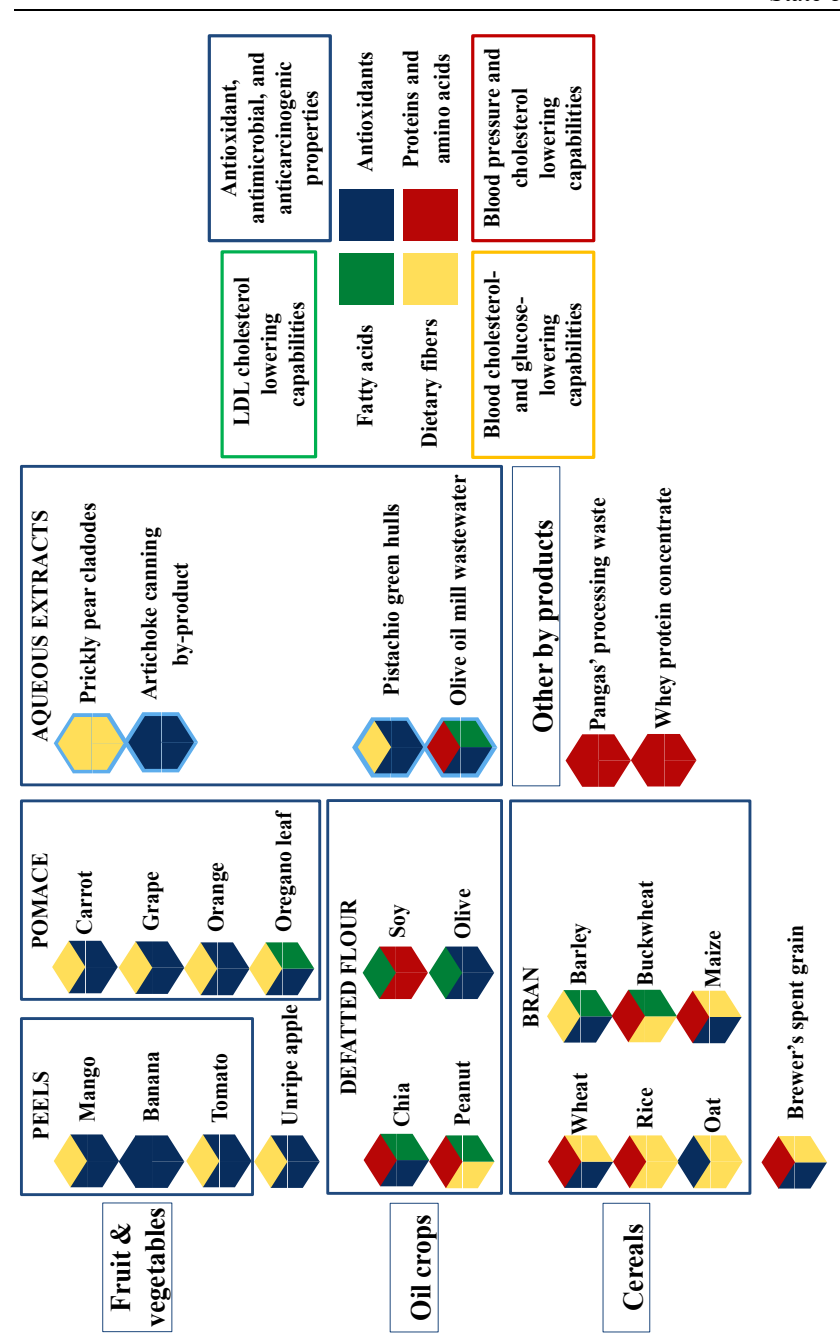


Figure II.2 *Main classification of agri-food by-products incorporated into pasta, their main bioactive compounds, and expected main beneficial*

properties (based on the content of Table II.2). LDL: Low-Density Lipoprotein.

II.2.1.1 Fruit and vegetables

Bioactive compounds of natural origin have attracted increasing interest as food additives because of their potential health-beneficial properties, due to their content in minerals, vitamins, fibres, and phytochemicals, such as polyphenols. For instance, the by-products of winemaking, especially red grape marc, including seeds, are considered as an economical and widely available source of valuable compounds being antioxidants, polyphenols, such as phenolic acids and anthocyanins, and fibres (Marinelli et al., 2015; Özcan et al., 2017; Sant'Anna et al., 2014; Spinelli et al., 2019). However, although these residues are valuable source of bioactive compounds, their composition and physicochemical properties largely vary depending on the grape variety, geographical and environmental factors, as well as on the winemaking process, including the harvesting step (Özcan et al., 2017). Their direct incorporation into spaghetti was reported to increase the bioaccessibility of antioxidant compounds, improving the health-beneficial properties, through the reduction of the glycaemic index, of the consumed product (Marinelli et al., 2018). Carrot pomace is also a good source of dietary fibres, as well as antioxidants, such as α- and β-carotene, and ascorbic acid (Badwaik et al., 2014). Its incorporation into pasta products led to a significant increase in the content of phenolic compounds and the resulting antioxidant activity (Gull et al., 2018).

Peels are the main by-products of fruit and vegetable processing. Jurić et al. (2019a); Padalino et al. (2017); Pataro et al. (2020a) reported that tomato peels were rich in health-beneficial compounds, such as minerals, vitamins C and E, β -carotene, lycopene, flavonoids, organic acids, phenolics, chlorophyll, and dietary fibres, and therefore could be suitable for pasta functionalization. Mango and banana peels, when added to pasta, showed antifungal, antibiotic, antioxidant properties, and contributed to reducing carbohydrate digestibility (Jalgaonkar et al., 2018b; Puraikalan, 2018).

Generally, the incorporation of plant bioactive compounds in pasta worsened the overall quality, causing high cooking loss, rigidity, and low sensory acceptance. Therefore, to date, the main technological challenges associated with the addition of these types of by-products to pasta concern the amelioration of sensory characteristics for aroma, aftertaste, flavor, and appearance of functionalized pasta (Padalino et al., 2017; Ungureanu-Iuga et al., 2020) as well as its cooking qualities (Crizel et al., 2015; Gull et al., 2015).

II.2.1.2 Oil crops

Oilcake, the major by-product of the oil extraction industry, is rich in total dietary fibre, phenolic compounds, and fatty acids. Olive, chia, soy, and 22

peanuts are the most remarkable industrial sources for oilcake. After the oil is extracted, a by-product rich in fibres, proteins, and polyphenols remains as a waste fraction. Olive oil by-products are well-known for their anti-cancer, anti-aging properties, and protection against oxidative stress (Cecchi et al., 2019; Cedola et al., 2020). Chia seeds represent one of the richest sources of polyunsaturated fatty acid (PUFA) (Aranibar et al., 2018). Soybean byproducts contain essential amino acids and high concentrations of isoflavones (Singh et al., 2017). These by-products could be successfully used as natural additives to ameliorate the nutritional properties and the antioxidant activity of pasta and other cereal-based products (Aranibar et al., 2018; Jalgaonkar et al., 2018b). Another oil crop popular in southern Italy is pistachio, whose industrial processing leaves a green hull as one of the main by-products. Pistachio green hull (PGH) contains different polyphenols, such as gallic, 4hydroxybenzoic, protocatechuic acids, naringin, quercetin-3-O-rutinoside, and catechin, as reported by (Lalegani et al., 2018). PGH incorporated into pasta formulation showed high antioxidant activity, good ability to inhibit αamylase and α -glucosidase activity in vitro, and a significant reduction in the in vitro starch digestibility and glycaemic index (Lalegani et al., 2018). Despite the beneficial effects observed in the pasta functionalized with oilbased by-products, the undesirable sensory characteristics due to bitter taste, dark colour (Cecchi et al., 2019; Cedola et al., 2020), and the poor cooking qualities (Simonato et al., 2019) represent severe limitations that should be overcome to promote their further exploitation.

II.2.1.3 Cereals

Cereal bran, especially from wheat, barley, corn, and oat, represents the major processing by-product of the food grain industry and an important source of dietary fibre, which has a fundamental role in the human diet (Wahanik et al., 2018). Dietary fibre from cereal bran includes polysaccharides. oligosaccharides, lignin, and associated substances, which exhibit several health-beneficial physiological effects, such as laxation, blood-glucose concentration, and cholesterol reduction (Rezende et al., 2021). However, the poor techno-functional properties of bran, combined with the potentially negative effect on pasta properties due to its interactions with other food components, represent significant drawbacks when formulating high fibre products. Cereal brans from wheat, buckwheat, oat, corn, barley, and rice, have been added to pasta as functional ingredients to make it a prophylactic/therapeutic food, able to contribute to preventing several diseases (Levent et al., 2020). However, some studies have reported the antinutritional effects of cereal brans, due to the presence of phytic acid, capable of binding minerals, proteins, and starch, resulting in the alteration of their functionality and availability (Levent et al., 2020).

The main drawbacks deriving from the incorporation of fibre-rich by-products into pasta are related to the decrease in the technological quality of the product: different authors reported higher cooking losses and water absorption due to starch granules swelling and rupture (Espinosa-Solis et al., 2019; Laureati et al., 2016). A significant reduction of the average break strain of pasta enriched with fibres was also observed due to the disruption of the protein matrix by the cereal bran particles (Cappa and Alamprese, 2017; Laureati et al., 2016)

Broken rice kernels represent potentially valuable by-products, because of their rich nutritional profile (Amagliani et al., 2017). Broken rice is an inexpensive material compared to head rice, traditionally generated in the industrial milling process with volumes of around 10% to 15% of the starting cereal (Bodie et al., 2019). Broken rice kernels are typically processed into flour (Amagliani et al., 2017), and utilized as a major ingredient for glutenfree pasta production (Bouasla et al., 2017). Even though rice dough showed lower mechanical properties than wheat semolina pasta, the tailored dosage of the main ingredients and the use of different enhancers enabled to obtain a good-quality gluten-free pasta enriched with this cheap cereal by-product with superior nutritional profiles (Bolarinwa and Oyesiji, 2021).

II.2.1.4 Other by-products

Protein fortification of low-protein foods is an alternative way to overcome the protein-energy malnutrition (PEM) issue. The use of high-protein flours (soybean, pea, lupine, bean, chickpea) in pasta resulted in the nutritional improvement of the product, contributing also to achieving satisfactory sensory and functional properties, due to the reinforcement of the protein network (Messia et al., 2021). Interestingly, the addition of lupine flour significantly decreased the glycaemic index of the chips samples (Çoban et al., 2021). Remarkably, fish proteins can also serve as an excellent source of proteins, especially to supplement pasta, as they contain all the essential amino acids and are characterised by excellent digestibility (Reddy Surasani et al., 2019). Another by-product rich in high-quality proteins is whey, a major by-product of dairy industries, which was demonstrated to have antihypertensive effects when added to pasta (Ungureanu-Iuga et al., 2020).

II.3 Functional pasta production: benefits and drawbacks

In recent years, new formulations for functional pasta have been developed, in addition to providing nutrients and energy, also to beneficially modulating one or more target functions in the body while avoiding alterations of the technological and qualitative characteristics of the final pasta product (Melini et al., 2020). As discussed in § II.1, the overall quality characteristics of pasta are affected by several factors related to raw materials quality, formulation,

and pasta production process, including cooking and sensory response. Moreover, as reported in § II.2.1, the incorporation of functional ingredients from agri-food by-products may cause several undesired technological quality characteristics in pasta, depending on ingredients' physicochemical properties and their formulation. Thus, the incorporation of non-conventional ingredients requires balancing the formulations and using appropriate processing conditions in the main critical steps (as highlighted in Figure II.1 and Table II.1, § II.1), to minimize the deterioration of the technological and functional properties of pasta, as conferred by the addition of these ingredients (Gull et al., 2018). Figure II.3 summarizes these main critical factors associated with the functionalization of pasta, all contributing to the final technological characteristics and health-beneficial effects of the obtained product.

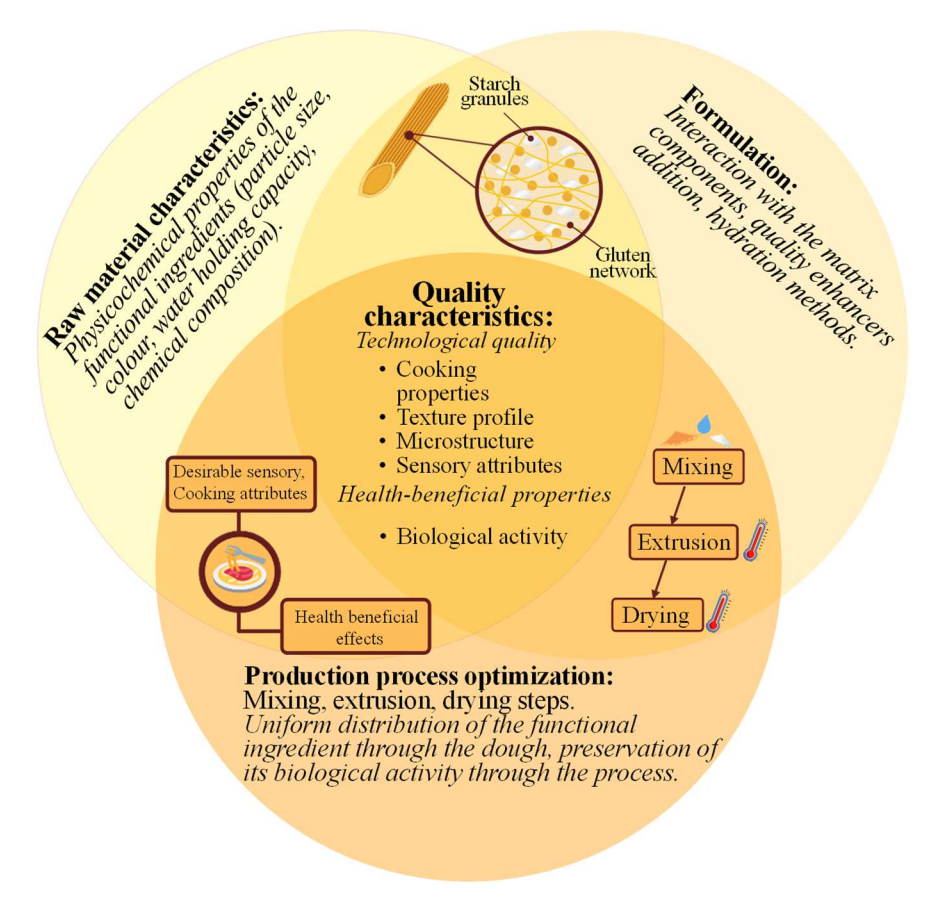


Figure II.3 *Main critical factors affecting the overall quality characteristics of the final pasta functionalized with the addition of valuable compounds.*

II.3.1 Health-beneficial pasta with high-quality attributes

The incorporation of functional ingredients in staple foods without changing their overall quality and sensory characteristics, while maintaining the biological functionality of the added bioactive compounds, represents an arduous technological challenge for researchers and food manufacturers (Laureati et al., 2016). Many authors have tested consumers' acceptance of fortified pasta by exploring their opinions about the use of agri-food byproducts as functional ingredients for pasta products and evaluating their purchase intentions. According to Cecchi et al. (2019), consumers responded positively to the idea of recovering food wastes for supplementing the nutritional content of foods. Indeed, several participants associated the darkened colour of fortified products with the appearance of "healthy" highfibre foods. Previous studies have indicated that the consumers, mainly females and the elderly, were interested in enriched food products of improved nutritional values and can accept lower sensorial properties of functional foods to receive health benefits. The belief that functional foods deliver health benefits emerged as the strongest positive reason for the willingness to compromise on taste (Jaworska et al., 2020). Moreover, the study conducted by Altamore et al. (2017) confirmed that consumers' choices in pasta purchasing are mainly driven by concerns about health benefits, the origin of raw materials, and the environment (Altamore et al., 2017). Identifying consumer segments with common characteristics is, therefore, crucial for the food industry to position new products on the market, and develop effective strategies to break down barriers to acceptance (Perito et al., 2019).

Remarkably, the mechanisms of interaction of plant residues, incorporated in the formulation, with the complex pasta matrix remain largely unexplored, especially for what concerns the synergistic or antagonistic action of antioxidants, fibre, polysaccharides, proteins against gluten formation and starch gelatinization. As reported in Table II.2, the incorporation of these ingredients led to crucial changes in the technological characteristics of pasta, such as increased cooking loss (Alzuwaid et al., 2020; Jalgaonkar et al., 2018b; Simonato et al., 2019), and water uptake (Gull et al., 2018) and reduced pasta firmness, due to their interference with the proper formation of the gluten network (Laureati et al., 2016; Sant'Anna et al., 2014). For instance, the addition of grape powder to pasta increased its hardness due to the interactions established between water and the hydroxyl groups of polysaccharides through hydrogen bonding, hence decreasing the sensory acceptance (Sant'Anna et al., 2014). In contrast, Pasqualone et al. (2017) and Puraikalan (2018) observed that the addition of artichokes and banana byproducts, respectively, did not affect the proper formation of the gluten network, and, thus, did not alter the texture and cooking parameters of pasta. Similarly, Foschia et al. (2015) reported an improvement in cooking

characteristics when oat bran flour was added to pasta in combination with other dietary fibres.

As functional pasta production through the incorporation of natural bioactive compounds generally worsens the product quality, depending on the byproduct used and the processing conditions, adequate strategies must be adopted to reduce the likelihood that consumers reject these novel products (see § II.3.2). The main factors influencing the quality of functional pasta are, instead, discussed in detail in § II.4.

II.3.2 Strategies to mitigate the negative impact of by-products' addition on the sensory features of pasta

Pasta manufacturers have adopted different strategies in the development of functional pasta products to minimize the deterioration of the sensory and functional attributes of the final product, and, hence, making it suitable to be introduced in the market, matching consumers' expectations. Figure II.4 schematically summarizes in a flowchart how such strategies are generally articulated, focusing on the main critical aspects and the possible solutions. The hydration method and particle size distribution of the ingredients are reported as the most important parameters to overcome the negative impact

reported as the most important parameters to overcome the negative impact on sensory properties of pasta functionalization.

The pasta obtained through the separated hydration of wheat and bran powder

The pasta obtained through the separated hydration of wheat and bran powder showed a significant improvement of the organoleptic properties and cooking quality, in comparison with the pasta obtained through traditional hydration (la Gatta et al., 2017). The hydration method markedly affects the formation of disulfide bonds. More specifically, separate hydration was suggested to increase the number of disulfide bonds and improve the gluten network's strength.

Recently, micronisation, as a size reduction method applied to the semolina and functional additives, was reported to greatly contribute to producing functional pasta with enhanced health benefits, while ensuring that the technological and sensory properties of the pasta are not negatively affected (Ciccoritti et al., 2019). Conte et al. (2015) investigated the influence of particle size of tomato peels' powder on the sensory quality of pasta. Their results indicated that the spaghetti produced with fine particles (mean size of 63 µm) showed a significant increase in starch digestibility and higher consumer acceptability, due to the lower fibrous content, good adhesiveness, low bulkiness, improved water absorption, and soft mouthfeel. The particle size of wheat bran resulted to have a significant effect on the technological and functional properties of durum wheat pasta. A finer wheat bran particle size minimized the impact on dough properties, resulting in pasta with good sensory acceptability and enhanced phytochemical profile (Alzuwaid et al., 2020; Steglich et al., 2015).

One of the most commonly used solutions to minimize the antagonistic effects of functional additives on pasta is the incorporation of quality-enhancers, which contribute to improving shelf-stability, cooking quality, texture, and appearance (Padalino et al., 2017). For example, the addition of carboxymethylcellulose (CMC) (la Gatta et al., 2017; Yadav et al., 2014), guar gum (Padalino et al., 2017), egg white powder (Cappa and Alamprese, 2017), and transglutaminase (Cedola et al., 2020; Marinelli et al., 2018) to pasta functionalized with different powdery agri-food by-products contributed to a measurable improvement in cooking and sensorial qualities.

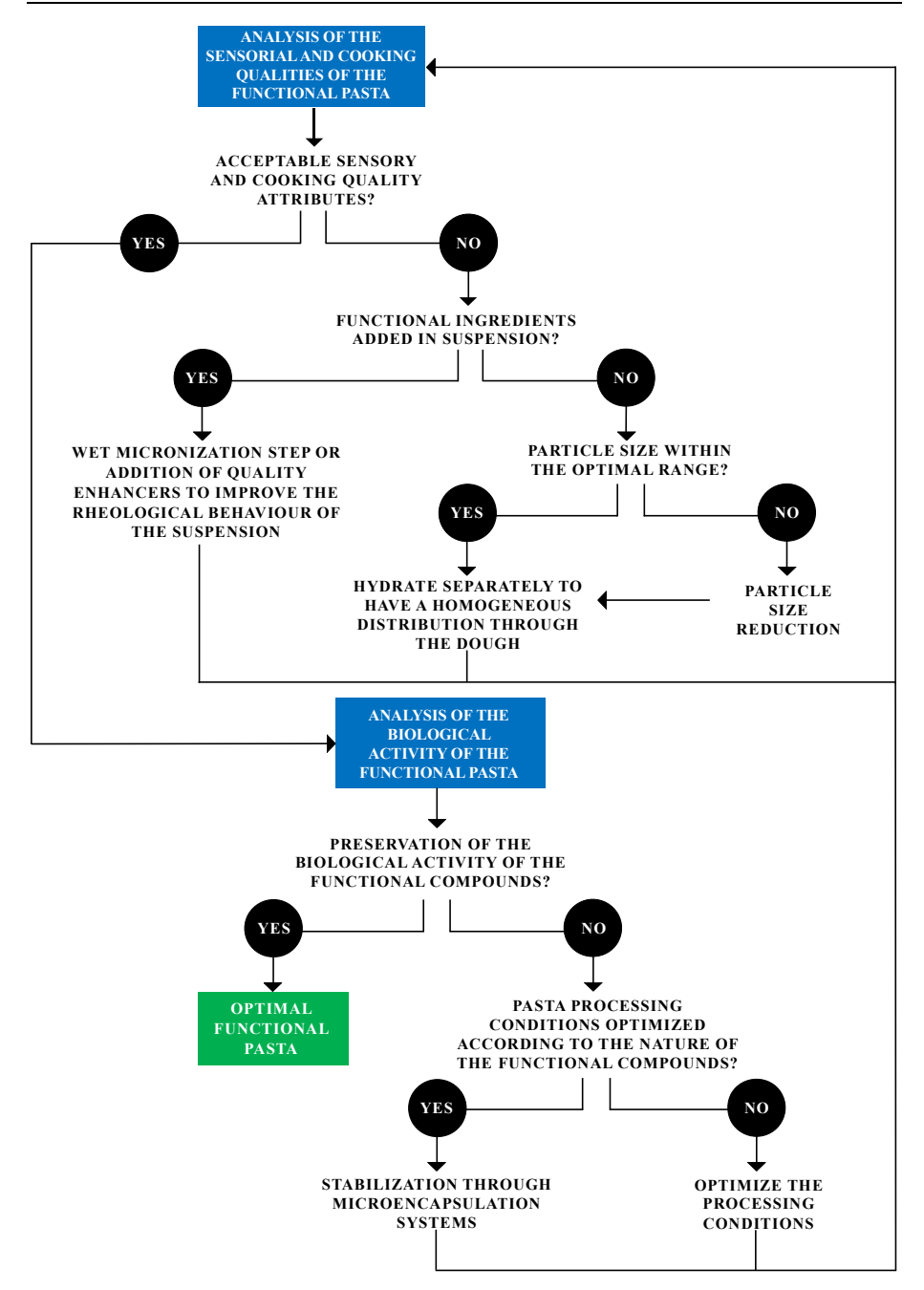


Figure II.4 *Main critical aspects associated with the pasta functionalization and potential solutions.*

II.4 Factors affecting the functional attributes of pasta

Demonstration of efficient incorporation of the bioactives into food products, ensuring that their functionality is preserved, is essential for commercializing new functional foods (Maskey et al., 2020). Although the product's quality is important, it is even more critical to ensure that, after product processing, storage, and cooking, the active ingredients exhibit high bioavailability, and therefore are capable of entering circulation after consumption to exert an active effect (Preedy, 2014). A prerequisite for the bioavailability of any compound is its bioaccessibility, defined as the amount that can be potentially absorbed from the lumen because is released from the food matrix during digestion (Dima et al., 2020). The bioaccessibility of active compounds is strictly correlated to the effect of the food manufacturing process, as well as to eventual interactions with the food matrix components. For instance, dietary fibres can interfere with polyphenols bioavailability during mastication and/or digestion processes. For example, pectin was shown to strongly decrease the bioavailability of β-carotene during human consumption. Polyphenols bound to dietary fibres need to be hydrolyzed in the intestine's upper area, to improve their absorption in the human intestine (Padayachee et al., 2017). Therefore, a complex food structure, intensive food processing, or preparation conditions, might endanger the bioaccessibility of bioactive compounds and, thus, their bioavailability. For these reasons, numerous applications have been reported in the field of liquid food functionalization, whereas a more limited number of studies focused on the functionalization of solid foods, such as meat or pasta (Day et al., 2009).

Previous studies on the physicochemical stability of bioactive compounds added to pasta, through the pasta-making process (mixing, extrusion, drying) and cooking steps, are reported in Table II.3.

As shown in Table II.3, kneading and extrusion phases may cause significant reductions in the content of bioactive compounds. Phenolic compounds during extrusion may undergo decarboxylation due to high barrel temperature, while high moisture content may promote polymerization, and, hence, reduce extractability and antioxidant activity (Obiang-Obounou and Ryu, 2013). The significant reduction in the content of total phenolic acids after extrusion might be due to oxidizing reactions triggered by water, oxygen, and heat (De Paula et al., 2017a). However, the level of bioactive compounds was reported to increase in some extruded products. For example, in berry-enriched pasta, and chia flour-enriched pasta an increase in bioactive compounds was observed after kneading and sheeting steps (Bustos et al., 2020) and along the manufacturing process (Aranibar et al., 2018), likely because unlocked and released from the cell wall matrix by the mechanical treatments.

Moreover, further losses in phenolics may occur during pasta drying. The degradation of antioxidant components could be the outcome of the high-temperature drying process, which is often essential for achieving high-quality

pasta (Balli et al., 2021). However, the loss of bioactive compounds might also be associated with their interaction with other components of the pasta matrix (gluten, starch), altering their solubility and availability (Balli et al., 2021). It must be remarked that, often, the observed decrease in bioactive compounds might be an artifact, due to the difficulties in recovering them from the highly structured protein matrix developed during kneading and drying (Parizad et al., 2020).

Significant losses of bioactive compounds might occur also during pasta cooking. It was reported that cooking significantly reduced total phenolic compounds, isoprenoids, and carotenoids due to their release in the cooking water or their degradation at high temperatures (Biernacka et al., 2021; Parizad et al., 2020; Pasqualone et al., 2016). However, in other cases, it was observed that the cooking process increased the content of bound phenolic acids and total phenolic compounds, which are released from cell walls during cooking (Ciccoritti et al., 2017; Podio et al., 2019). These results are consistent with those previously obtained by Merendino and coworkers, who explained the increase in the antioxidant capacity either with the release or exposition of some bioactive compounds during the cooking process, as well as with the formation of some Maillard reaction products that contributed to the overall antioxidant activity. The same authors observed that, during cooking, rutin was transformed into quercetin, characterised by a higher antioxidant activity (Merendino et al., 2014).

Microencapsulation might represent an effective strategy to maintain or even increase the antioxidant activity, stability, and bioavailability of bioactive compounds during food processing and cooking (Vieira et al., 2020). For example, polysaccharides- and whey protein-based delivery systems were tested to encapsulate ω -3 fatty acids and *Garcinia cowa* fruit extract, before incorporation in pasta (Iafelice et al., 2008; Pillai et al., 2012). Remarkably, the drying process did not affect the stability of encapsulated bioactive compounds, providing effective protection against their deterioration and improving the nutritional value, cooking characteristics, and sensory acceptability of the final pasta (Iafelice et al., 2008; Pillai et al., 2012).

However, only scarce data are available for the validation of microencapsulation of bioactives for pasta additives, especially for what concerns their behavior in the product and after consumption (Dias et al., 2015).

Table II.3 Physicochemical stability of the bioactive compounds added to pasta during the transformation process and the cooking phases.

·	v i	0.1	
Pasta product formulation	Process conditions	Effect on bioactive compounds	Reference
Grape pomace (tagliatelle)	Drying: 40 °C, 20 h Cooking: 8 min, 6 L of salted (≈ 40 g of sodium chloride) water	Drying: loss of phenols, phenols from pasta = 47% of the initial amount in the added pomace Cooking: loss of phenols, phenols from cooked pasta = 32% of the initial amount in the added pomace	(Balli et al., 2021)
Red grape marc flour (spaghetti)	Mixing: 25 °C, 20 min Drying: 1 st step, 20 min at 55 °C; 2 nd step, 580 min at 75 °C; 3 rd step, 40 min at 60 °C; 4 th step, 20 min at 45 °C; 5 th step, 840 min at 40 °C	Cooking: -7% total phenolic compounds, +3% total antioxidant capacity	(Marinelli et al., 2018)
Berry fruits pasta	Drying: 30 °C, 30 min and at 45 °C, 75%, 17.5 h Cooking: 14 min	Cooking: reduction of antioxidant activity	(Bustos et al., 2020)
Lyophilized tomato and durum wheat bran extracts (spaghetti)	Kneading: 15 min, 1 bar vacuum Extrusion: 40 °C, 25 rpm Drying: linear decrease in RH from 95% to 40%, 8 h, and 50 min, T max 78 °C	Cooking: -15–20% isoprenoids, -23–27% lycopene	(Pasqualone et al., 2016)
Chia flour pasta	Pre-drying: 30 °C, 30 min Drying: 24 h at 30 °C in a closed chamber	Drying: increase of individual polyphenols of 3 times the theoretical value expected Cooking: not significant differences in polyphenols	(Pigni et al., 2020)
Cereal coffee (fettuccine)	Drying: 25 °C, 24 h, 30% relative humidity Cooking: 50 g of pasta, 500 mL of water	Cooking: decrease in the amount of total phenolic compounds from 12 to 15%	(Biernacka et al., 2021)
Debranning fractions of purple wheat (macaroni)	Mixing and extrusion: 20 min Drying: 60 °C for 12 h Cooking: 1 L water, 100 g pasta	Processing: reduction in total antioxidant capacity (TAC) and total phenolic compounds (TPC) because of the drying steps Cooking: -65,2% TAC; -51,1% TPC	(Parizad et al., 2020)
Micronised debranning fractions of durum wheat (spaghetti)	Drying: 50 °C for 20 h Cooking: 1 L of water, 100 g of pasta, 13 min	Cooking: +73% total phenolic acids; +90% total phenolic compounds; -free phenolic compounds	(Ciccoritti et al., 2017)

Tartary buckwheat sprouts	Pre-mixing: 15 min at room temperature Kneading: 10 min in vacuum at 40 °C Extrusion: 9.1–12.1 MPa and vacuum of 70 mmHg Drying: 30 °C for predrying, 4 h at 50–58 °C for drying	Processing: increase in the antioxidant capacity Cooking: -40% total phenolic compounds	(Merendino et al., 2014)
Barley pasta	Mixing: 6 min Drying: 80 °C for 4 h	Extrusion: significant reduction in total phenolic acids	(de Paula et al., 2017)
Whole wheat pasta	Drying: 50 °C Cooking: 1 L of water, 100 g of pasta, 13 min	Processing: -40% and - 89% total antioxidant capacity (TAC) and phenolic acids (PA) mainly during the milling process (-25% and -84% decrease of TAC and PA, respectively)	(Martini et al., 2018)
	Drying: 30 °C, 30 min, then 45 °C in a humidity-controlled (75%), 17.5 h Cooking: 400 mL of water, 8 g of pasta, 8 min	Cooking: increase in the release of bound polyphenols, and antioxidant activity	(Podio et al., 2019)
Gluten-free pre-cooked buckwheat pasta	Extrusion: extruder screw (60, 80, 100 and 120 rpm), raw material moisture (30, 32 and 34%) Drying: < 40 °C in an air oven overnight	Extrusion: increase in free phenolic acids in pasta produced at 30% and 34% of moisture content, at the screw speed of 60 rpm, while at 32%, at the screw speed of 100 rpm	(Oniszczuk et al., 2019)
Gluten-free pasta (pasta enriched with black rice, chickpea, red lentil, sorghum, amaranth, and quinoa)	Cooking: 1 g of pasta, 30 mL of water, 7-8 min	Cooking: decrease in the bound-to-free ratio of phenolic compounds, by a factor ranging from 14-folds for flavonoids to 5-folds for other phenolics	(Rocchetti et al., 2017)

PART B – Functional ingredients: waste valorisation

II.5 Opportunities

The use of pre-processing steps on raw materials (such as extraction or micronization) represents a valuable approach to increase the content of bioactive components in pasta while reducing the impact on the final pasta sensorial properties. Emerging green technologies could be exploited to obtain high purity extracts suitable to be added to pasta, or to unlock valuable compounds. Ultrasound- (Lin et al., 2018), microwave- (Chuyen et al., 2018), supercritical fluid- (Gallego et al., 2019), pulsed electric fields- (Pataro et al., 2020) high-pressure homogenization- (Donsì and Velikov, 2020) assisted extractions are green technologies frequently used in the recovery of valuable compounds from agri-food by-products, which are generally selected according to the nature of the target compounds and the characteristics of the food matrix (Melini et al., 2020). These technologies have recently been proposed as an alternative to conventional plant cell permeabilization operations to shorten the processing time, increase recovery yield of target intracellular bioactive compounds, improve the quality and the functionality of the extracts (Galanakis, 2021; Comunian et al., 2021; Jurić et al., 2019; Pataro et al., 2020). In general, the application of emerging technologies in extraction processes represents a sustainable technology platform for the valorisation of agri-food industrial residues, which also contributes to decreasing the environmental impact. However, only a few studies have investigated these technologies to extract bioactives from agri-food byproducts for their addition to pasta. For example, the addition to pasta of different extracts obtained through emerging technologies, such as bran oleoresin recovered through supercritical carbon dioxide extraction (Pasqualone et al., 2016) or antioxidants recovered through US-assisted extraction from artichoke canning by-products (Pasqualone et al., 2017), did not alter the textural and cooking parameters of the product and represented an excellent vehicle to increase the antioxidant dietary intake. These results contributed to demonstrating that emerging technologies may represent effective and non-toxic treatments for extracting bioactive compounds. As purely mechanical pre-processing steps, further efforts should be addressed to elucidate the potential contribution of novel micronisation technologies, such as high-pressure homogenization (HPH) as a wet milling technique (Gali et al., 2022), to control the particle size distribution of the residues (Dons) and Velikov, 2020) and improve the rheological behavior of the suspensions

(Mustafa et al., 2018). The HPH-treated aqueous suspensions, where the intracellular compounds are fully unlocked, can potentially be used as a texture or rheology modifier, emulsifier, or stabilizer agent, as well as a health-beneficial food ingredient. The HPH process can be designed to micronise the plant residue suspended in the aqueous phase in a finely milled sub-cellular particle suspension, contributing to its homogeneous and smooth appearance, and favoring the exploitation of the total by-product aiming at "zero waste economy" (Donsì and Velikov, 2020; Jurić et al., 2019; Mustafa et al., 2018).

II.6 Emerging green techniques for the extraction of bioactives from agri-food by-products as promising ingredients for the food industry

The integration into a biorefinery of green solvents (water or naturally derived solvents) coupled with the use of innovative technologies can be expected to holistically support the development of "sustainable" extraction processes (Clarke et al., 2018; John Camm, 2012).

More specifically, the improvement of process efficiency requires both to maintain a sustained driving force for the extraction process, for example by acting on the affinity and solubilization of the target solutes in the selected solvent, and to reduce the mass transfer resistances, for example through the permeabilization or destruction of the plant cell envelope, which represents the main physical barrier for the diffusion of target compounds.

II.6.1 Emerging green technologies and involved mechanisms of cell disintegration

Mass transfer enhancement represents the challenge for the efficient extraction of valuable bioactive compounds from biomass. The main mass transfer resistances lay in the membranes that separate the intracellular compounds, such as polyphenols located in vacuoles and chloroplasts of plant cells, from the outside environment, hindering their diffusion (Tzima et al., 2021). The permeabilization or physical rupture of cell membranes can, therefore, facilitate the diffusion of the target molecules, and thus reduce extraction time and increase process efficiency (Siemer et al., 2012). Different techniques based on mechanical, chemical, thermal, or electrical methods can be used to affect the cell membrane.

Conventional extraction processes heavily rely on the use of organic solvents, long processing times, high temperatures, and large expenditure of energy that might negatively impact both human health and the environment. To overcome these limitations, innovative processes have been proposed and widely investigated (Dobrinčić et al., 2020).

The most promising innovative extraction techniques include Pulsed Electric Fields (PEF), Ultrasound-Assisted Extraction (UAE), Microwave-Assisted Extraction (MAE), High Voltage Electrical Discharges (HVED), for the production of pure functional extracts obtained after the removal of the exhausted matrix, and High-Pressure Homogenization (HPH) aimed to fully recover the target biomass. The main advantages and drawbacks associated with these technologies, according to the different cell rupture mechanisms induced by each technique are summarized in Table II.4.

Table II.4 Advantages and disadvantages of green extraction technologies.

Extraction Method	Advantages	Disadvantages
PEF	Non-destructive, high selectivity, no thermal effect, no need for energy-intensive drying pretreatment, energetically efficient, continuous operability, easy to scale up	Dependence on medium composition (conductivity), high cost of the equipment (Niu et al., 2020)
UAE	Significant savings in maintenance, low equipment cost, low operating temperature, efficient extraction of thermolabile compounds	Separation and purification steps required, lack of uniformity in the distribution of ultrasound energy, potential change in the constitutive molecules, large amount of solvent, difficulty in scaling (Roselló-Soto et al., 2015)
MAE	High extraction yields, small equipment size, easy industrial escalation, low solvent consumption, possibility to develop a solvent-free process, low power consumption, good reproducibility	High equipment cost, non- selective extraction separation, and purification steps required, very poor efficiency for volatile compounds, lack of studies on modeling of the heating process to improve its uniformity (Coelho et al., 2020; Vinatoru et al., 2017)
HVED	High extraction yields, efficient extraction of thermolabile compounds, low solvent consumption, low energy consumption, possibility to extract thermolabile compounds	Batch mode operation, hard to be scaled-up, free radicals would be produced leading to oxidative cell damage, but may also oxidize the target compounds, requires precise control of input energy, less selective than PEF (Barba et al., 2015; Dalvi-Isfahan et al., 2016)

HPH	High extraction yields, high scalability, ability to overcome high cell wall rigidity, effective in	Non-selective extraction, cell debris can bring downstream complications and costs,
	aqueous environments (eliminating the need for energy-	temperature increase undesirable for heat-sensitive
	intensive drying), one of the most used mechanical methods for large-scale cell disruption	extracts, cooling needed, high energy consumption (Barba et al., 2014)

The following sections focus on the application of PEF technology to achieve a high-purity extract, and on the use of HPH treatment to fulfil the total recovery of the target by-product and the subsequent "zero waste" concept. Nevertheless, insights regarding the other abovementioned cell disruption technologies have been reported and described elsewhere by Carpentieri et al. (2021b).

Pure Extracts

II.6.1.1 Pulsed Electric Fields (PEF)

Extraction aided by PEF is an innovative process for the recovery of bioactive compounds from the residues of the agri-food chain (Barba et al., 2016). The effectiveness of PEF treatment depends on several parameters, including electric field strength, total specific energy input, and treatment temperature (Zhang et al., 2018). A typical PEF system comprises a high-voltage pulse generator, a treatment chamber (parallel plate, co-axial, collinear configurations), a pump (for continuous mode operation), a temperature control system, as well as devices like oscilloscope, voltage, and current probes for process monitoring and data acquisition (Figure II.5). In PEF processing, a plant matrix in wet form is physically and electrically contacted with the metal electrodes of a treatment chamber, operated either batch-wise or in continuous, and exposed to repetitive (Hz-kHz) very short (µs-ms) electric field pulses of moderate intensity (E = 1-10 kV/cm) and relatively low energy input ($W_T = 1-20 \text{ kJ/kg}$) supplied by the pulse generator. The pulse shapes commonly used in PEF treatments are either exponential or squarewave pulses, monopolar or bipolar (Raso et al., 2016). Depending on the treatment intensity, size, and morphological characteristics of biological cells, the application of electric pulses may cause reversible or irreversible pore formation on the cell membranes, referred to as electroporation or electropermeabilization, as schematized in Figure II.6, (Raso et al., 2016). This has been proved to improve the efficiency of the conventional extraction processes of valuable compounds from several plant tissues of fruit and vegetable origin, by facilitating the penetration of the solvent into the cells and the selective release of valuable compounds towards the extracting medium (Puértolas and Barba, 2016).

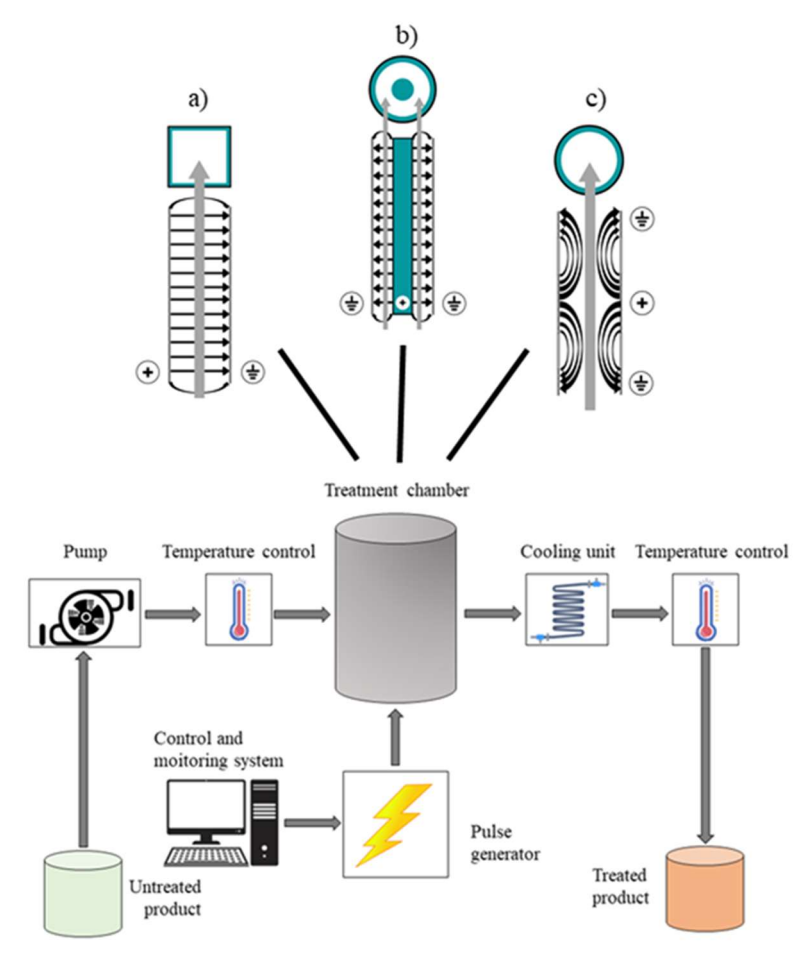


Figure II.5 Schematics of a typical continuous flow PEF system, and cross-sectional views of different treatment chamber configurations; (a) parallel plate, (b) co-axial, (c) co-linear, (the grey arrows are representative of the product flow).

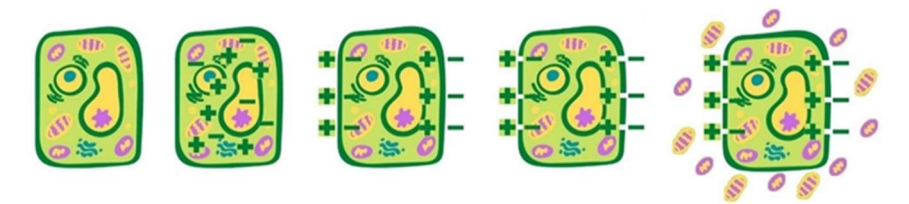


Figure II.6 *Mechanism of cell disintegration induced by PEF: electroporation phenomenon.*

Although the technology is heading for wider industrial application, several limitations still hinder the commercialization of PEF technology. One of the challenges is the development of more reliable and affordable pulse generation 38

systems with sufficient electrical field strength, power, and repetition rate, as well as the optimization of the overall PEF system design, to fulfill current industrial requirements in terms of throughput and treatment uniformity. Moreover, several technological issues, economical pitfalls, consumer acceptance, and regulatory aspects, as well as toxicity risks remain and have to be addressed prior to the full exploitation of PEF technology in different sectors of the food industry (Niu et al., 2020).

Total recovery of the biomass

II.6.1.2 High-Pressure Homogenization (HPH)

The growing interest in environmental protection and food sustainability has attracted greater attention to alternative technologies such as high-pressure homogenization (HPH). It is a green technology with low energy consumption that does not generate high CO₂ emissions or polluting effluents. In the homogenization process, the process fluid flows through the homogenization valve, where intense fluid mechanical forces are generated, which cause the particles suspended in the fluid to disintegrate (Figure II.7). In the case of biomass, the particle disintegration corresponds to full cell disruption, with the associated release of intracellular material (Donsì and Velikov, 2020; Jurić et al., 2019). Moreover, also the total surface area of the newly formed particles increases, resulting in a significant improvement in the physical stability of the product. The fluid undergoes mechanical stress (shear, hydrodynamic, and cavitation effects) and a temperature increase (thermal effect) of about 2-3 °C for every 10 MPa of homogenization pressure (Mesa et al., 2020). The particle size decreases, and a more homogeneous distribution is obtained, facilitating operations such as mixing and emulsifying.

The existence of valves of different geometries has given rise to the design of equipment capable of working at pressures higher than 400 MPa. Therefore, three types of homogenizations are distinguished, according to the valve geometry:

- Standard homogenization for pressures between 0 and 50 MPa;
- High-pressure homogenization (HPH) for pressures between 50 and 300 MPa;
- Homogenization at very high pressure (UHPH) for pressures equal to or greater than 400 MPa.

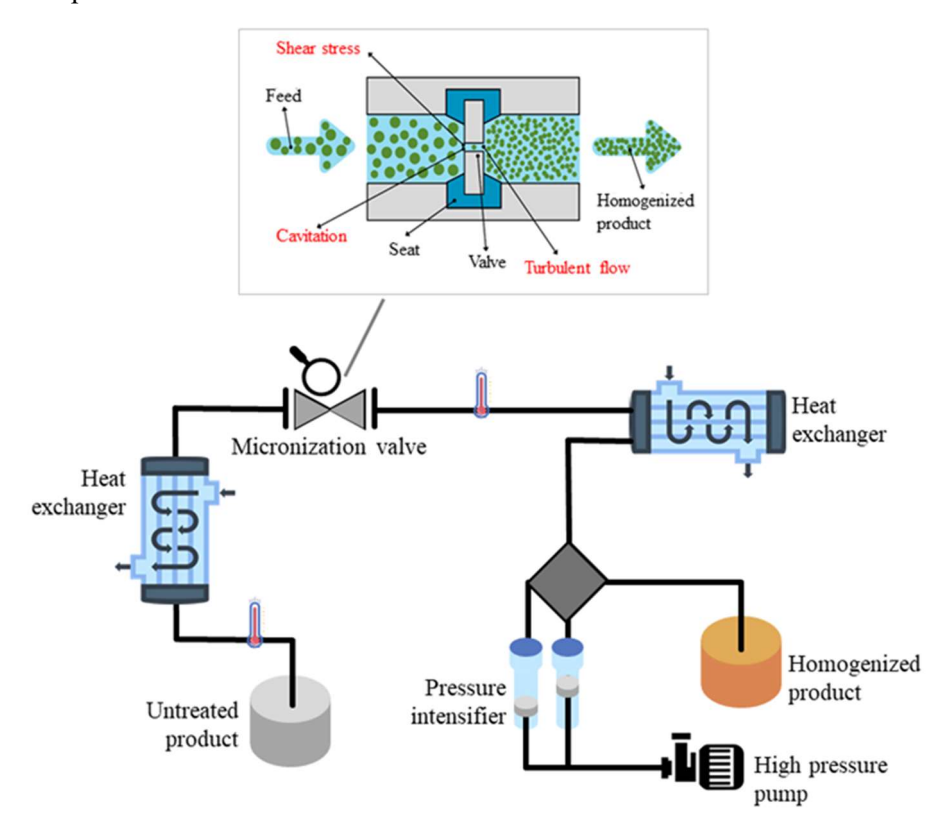


Figure II.7 *Schematics of the operating principle of a typical HPH system and focus on the homogenization valve.*

The possibility of operating continuously for a great diversity of pumpable fluids has made it possible to extend the applications to the activation or inactivation of enzymes, reduction of the microbial load, processes of mixing, dispersion, emulsion, or encapsulation, processes of cell disruption, and protein modification. The use of HPH to valorise food residues has two objectives:

- improving the extraction capacity of intracellular structural components;
- improving the technological functionality of bioactive compounds.

The application of HPH treatment leads to the destruction of plant tissues, cell walls, membranes, and organelles (Figure II.8), improving the mass transfer of solvents into materials and recovering high-added value compounds (Plazzotta and Manzocco, 2018).

The degree of cell destruction appears to be strongly dependent on the characteristics of the matrix and the intensity of the HPH in terms of working pressure and the number of passages through the homogenization valve (Comuzzo and Calligaris, 2019).

The theory of homogenization is based on the flow-induced deformation of macromolecules.

During the passage through the valve, suspended particles undergo fluid dynamic stresses, leading to their rupture above a certain pressure. The sudden pressure drops at the valve exit induce sample acceleration and cavitation, leading to high kinetic energy, responsible for intensive collisions among particles and between particles and instrument walls (Plazzotta and Manzocco, 2018).



Figure II.8 Mechanism of cell disintegration induced by HPH.

II.6.2 Green Extraction Process: Synergism between Solvents and Technology

The added value associated with the extraction of bioactive compounds from agri-food by-products is a crucial step for their minimization and environment-friendly valorisation. In this context, approaching greener extraction alternatives using the above-mentioned emerging technologies and solvents with tunable properties, could be the desirable direction (Saini and Panesar, 2020). In the following section, a comprehensive and up-to-date analysis of the combined application of green solvents and emerging technologies in the extraction of bioactive compounds from agri-food byproducts is reported. Moreover, a classification of the used solvents and applied technologies, highlighting its affinity with the type of solvent, matrix, and target bioactive compounds is presented in Table II.5. Figure II.9 is intended to give a qualitative and immediate idea of Table II.5, guiding the reader throughout it. This investigation mainly focused on the application of the most suitable, biocompatible solvents for foods, primarily ethanol and water, coupled with the emerging cell disruption technologies described so far. However the extended version of Table II.5 and Figure II.9, including a deep analysis that involved the study of other solvents, namely Ionic Liquids (ILs), Deep Eutectic Solvents (DES), Supercritical Fluids (SCFs), Supramolecular Solvents (SUPRAS), glycerol, and terpenes such as limonene, can be found in a recently published paper available in literature (Carpentieri et al., 2021b).

Chapter II

Table II.5 Extraction of bioactive compounds from agri-food by-products using green solvents and/or assisted by non-conventional technologies.

Raw Materials	Target Compounds	Technology	Extraction Approach	Main Findings	Reference
		Bio-ba	sed solvents		
Ethanol					
White grape pomace	Phenolic compounds	PEF	E = 3.8 kV/cm, W = 10 kJ/kg, ethanol = 50% v/v, T = 50 °C time = 190 min	Reduced solvent consumption (3–12%) and extraction time (23–103 min), increased TPC (8%), FC (31%), and FRAP (36%) values	Carpentier i et al. (2022)
Peach waste	Total phenolic content, total flavonoid, anthocyanins	PEF	$W = 0.0014$ kJ/kg, ethanol = 70% v/v , treatment time = 16 μ s	PEF led to a reduction of extraction times (16 µs), compared to thermal extraction (40 min), reaching the same yields	(Plazzotta et al., 2021)
Pomelo peels	Naringin	PEF	E = 4 kV/cm, pulses = 30, ethanol = 40% ν/ν , T = 40 °C, L/S = 90 mL/g	PEF improved the extraction yields of naringin by 20% compared with the untreated sample	(Niu et al., 2021)
Lettuce waste	Polyphenols	НРН, UAE	Ethanol = 50– 75% v/v, HPH: P = 50 MPa, US: P = 400 W, f = 24 kHz, time = 120 s, L/S = 50 mL/g	HPH led to a reduction in phenolic yields compared to UAE, possibly due to the 40% activation of polyphenol oxidase	(Plazzotta and Manzocco , 2018)
Potato peels	Phenolic acids	НРН	Ethanol and NaOH (0-0.4 mol/L), T = 40 °C, L/S = 25 mL/g, P = 158.58 MPa, n of passes = 2	The combination of NaOH and HPH improved the extraction yield of total phenolic acid. The highest contribution is	(Zhu et al., 2016)

				associated with HPH	
Fresh rosemary and thyme by- products	Phenolics	PEF pre- treatment, then, UAE	PEF: $n = 167$, pulse width = 30μ , 0.1% aqueous NaCl, L/S = 1.4 mL/g for rosemary, and 1.5 mL/g for thyme, E = $1.1 \pm 0.2 \text{ kV}$ cm -1 , W = $0.36 \text{ and } 0.46 \text{ kJ kg}{-1}$ for rosemary and thyme US: T = 40 °C , P = 200 W , ethanol = $55.19\% \text{ v/v}$, L/S = 20 mL/g , time = 12.48 min	PEF pretreatment enhanced (p < 0.05) the recovery of phenolics and antioxidant activity compared to US individually	(Tzima et al., 2021)
Water					
Artichoke stems	Polyphenols	PEF	E = 3 kV/cm, W = 5 kJ/kg, T = 20 °C, L/S = 10 mL/g, time = 120 min	Increment in the recovery of chlorogenic acid (+28% compared to the control)	Carpentier i et al. (2022)
Mango peels	Polyphenols, proteins, carbohydrates	PEF, HVED	E (PEF) = 13.3 kV/cm, (HVED) = 40 kV/cm, n = 2000, W = 1000 kJ/kg distance between pulses = 2 s, T = 20 °C, L/S = 10 mL/g	HVED is more effective than PEF, however, PEF is more selective	(Parniako v et al., 2016b)
Fermented grape pomace	Total phenolic compounds, anthocyanins	UAE, PEF, HVED	US: power = 400 W f = 24 kHz PEF: E = 13.3 kV/cm, W = 0-564 kJ/kg, HVED: W = 0-218 kJ/kg,	HVED led to the highest phenolic compound's recovery with lower energy requirement than PEF and US	(Barba et al., 2015)

Chapter II

			L/S = 10		
			mL/g		
Tomato peels	Polyphenols, proteins	НРН	P = 100 MPa, n = 10 passes, L/S = 10 mL/g	Increase in proteins (+70.5%), polyphenols (+32.2%), antioxidant activity (+23.3%)	(Jurić et al., 2019)
Potato peels	Phenolic compounds	PEF	Pre-treatment: E = 1 kV/cm, W = 5 kJ/kg, treatment time = 6 ms, L/S = 1 mL water/g S/L extraction: Ethanol = 52%, time = 230 min, T = 50 °C	PEF reduced time, temperature, and solvent, improved the extraction yield (10%) and antioxidant activity (9%) than the untreated sample	(Frontuto et al., 2019)
Custard apple leaves	Phenolic compounds	PEF	Pre-treatment: E = 2, 4 or 6 kV/cm, W = 45, 94 or 142 kJ/kg, treatment time = 2.5–5 min, L/S = 2,5 mL/g S/L extraction: Ethanol = 70, L/S = 15:1 (v/w)	PEF improved the extraction yields (+5.2%) and the antioxidant activity than the untreated sample	(Ahmad Shiekh et al., 2021)
Sesame cake	Polyphenols, proteins	PEF, HVED	Pre-treatment: E = 13.3 kV/cm, W = 83 kJ/kg, treatment time = 1-7 ms, holding time = 4-28 min, T = 20-60 °C, L/S = 10 mL/g S/L extraction: Ethanol = 10%, L/S = 20 mL/g, time = 1 h	PEF and HVED accelerated the diffusion kinetics, making the impact of temperature smaller	(Sarkis et al., 2015)

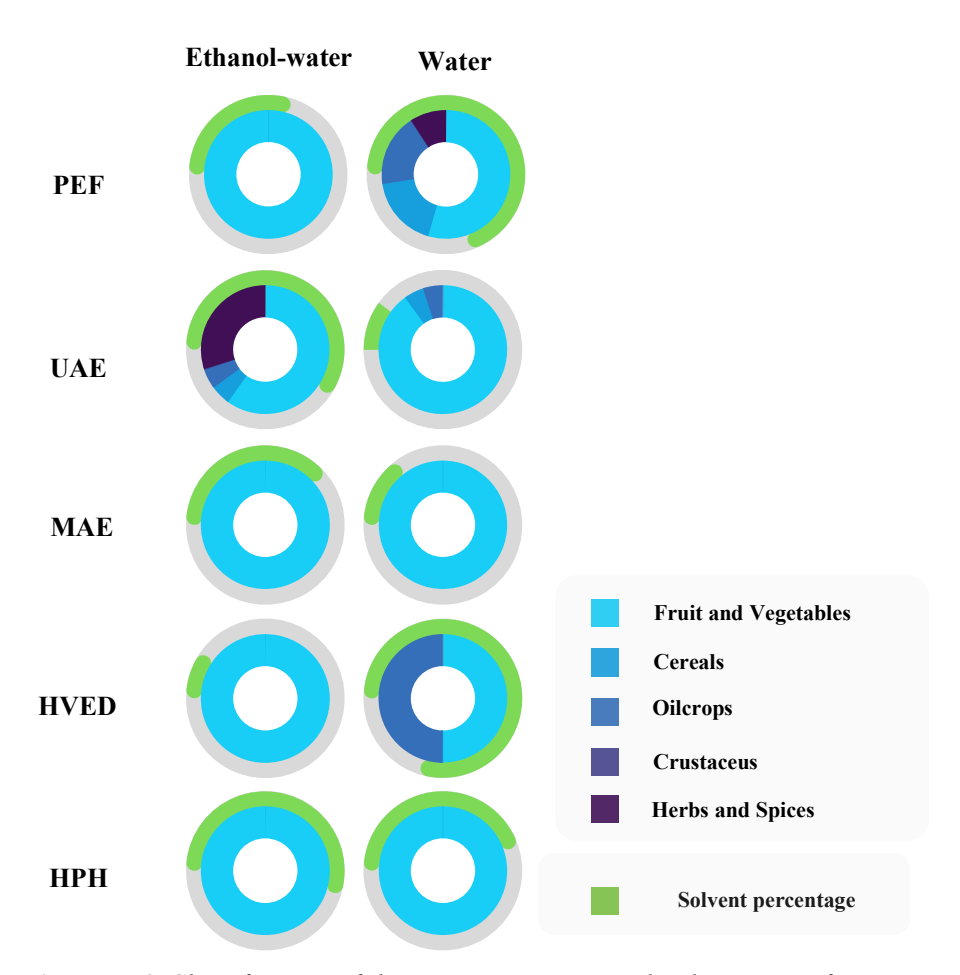


Figure II.9 Classification of the green extraction technologies as a function of the solvent used and the food residues source.

II.6.2.1 Bio-Based Solvents

Bio-based solvents are defined as solvents produced from renewable biomass sources such as wood, starch, vegetable oils, or fruits (Naidu et al., 2018). They are produced in a biorefinery that aims at maximum recovery and production of products with high-added value. Despite their great potential, the scale of biorefineries is still mainly limited to pilot or laboratory scale plants (Byun and Han, 2020), since the sustainability of biomass production highly depends on the implementation of land-management practices (Clarke et al., 2018).

Chapter II

These bio-solvents have a high solvent power, are non-toxic, non-flammable, and biodegradable. Their drawbacks are related to high viscosity and boiling point, high cost, and generation of off-flavors (Chemat et al., 2012). Ethanol is the most common bio-solvent, obtained from the fermentation of sugar-rich materials, such as sugar beet and cereals. Despite its flammability and potential explosivity, ethanol is used on a large scale thanks to its availability at high purity, cheapness, and biodegradability.

II.6.2.1.1 Ethanol

The most used green solvent for extraction processes is bioethanol, produced through the anaerobic fermentation of sugars (Sarris and Papanikolaou, 2016). To obtain a high percentage of polyphenol recovery, ethanol is always combined with an adequate amount of water. However, the final composition of the solvent is defined by the nature of the solute. For example, an aqueous solution of 80% (v/v) ethanol was found to be very effective for pomace of various red grape varieties, providing total polyphenol yields of 69.3–131.7 mg of gallic acid per g of dry weight (Tournour et al., 2015). For the extraction of polyphenols from seeds, 50% (v/v) of ethanol is much more effective than water and aqueous acetone (Duba et al., 2015). Ethanol-water solutions showed higher efficiency in extracting antioxidant compounds than a monocomponent solvent system (water, pure ethanol) because the mixture, inferring the change in the polarity of the compounds, reaches the polarity of diverse compounds (Gadioli Tarone et al., 2021; Setford et al., 2019). Many authors proved the strong influence of the interaction between emerging technologies and the hydroethanolic mixture composition on the extraction efficiency of bioactive compounds from agri-food by-products. The effect of the combination of PEF pre-treatment to achieve cell permeabilization and the subsequent UAE with 55% (v/v) ethanol on the extractability of bioactive compounds from fresh rosemary and thyme by-products demonstrated to be the most efficient solution that is attracting considerable interest (Tzima et al., 2021). PEF pre-treatment enhanced the antioxidant capacity of rosemary extracts resulting in a 1.3-fold increase, when compared to UAE individually applied (Tzima et al., 2021). Additionally, the effect of the cell tissue disruption of ultrasounds on lettuce waste hydro-alcoholic dispersions (50-75% (v/v) ethanol) was also compared to the one associated with the mechanisms involved in the HPH treatment (Plazzotta and Manzocco, 2018). Different from UAE, which induced progressive destruction of cellular structures (vacuoles), HPH-induced disruption was not gradual, so that lower energy was required to obtain higher tissue disruption. Although HPH promoted a much more intense cellular rupture, as a pre-treatment to UAE, it resulted in lower phenolic yields (25%) as compared to UAE. These results could be possibly be explained by the decompartmentalizing effect of HPH on

the oxidative enzymes entrapped in the plant matrix, while US did not cause changes in the polyphenol oxidase (PPO) conformation (Meullemiestre et al., 2016).

II.6.2.1.2 Water

Water can be considered as a potentially green solvent since it is non-toxic to health, it has a low environmental impact, it is low cost in terms of production, transportation, and disposal. In addition, the capability of this solvent to tune its properties by changing the conditions (e.g., temperature, pressure) has contributed to the increasing interest in using water as an extraction solvent (Clarke et al., 2018).

The use of water as a green extraction solvent has been widely combined with the application of emerging extraction technologies, to enhance the extractability of antioxidant intracellular compounds from agri-food byproducts. In particular, several authors have compared the effect of different technologies, namely PEF, HVED, and UAE, on the improvement of the extraction yields of bioactive compounds from agri-food peels and pomace (Barba et al., 2015; Parniakov et al., 2016; Sarkis et al., 2015), according to the cell rupture mechanisms related to each technology, to the plant matrix and tissue (stems, seeds, peels, pomace), to the physical and chemical properties of the target compounds (solubility, polarity).

HVED treatment resulted to be more efficient in terms of energy input than PEF to achieve a higher cell permeabilization degree and to improve phenolic compounds aqueous extraction from mango peels (Parniakov et al., 2016). These results could be related to the ability of HVED to induce fragmentation of the cell tissue due to the propagation of shock waves and the explosion of cavitation bubbles (Boussetta and Vorobiev, 2014). However, the extracts obtained by HVED were less clear and stable than the extracts obtained by PEF, which is characterised by a better selectivity related to the electroporation phenomenon, facilitating the subsequent separation and purification processes (Parniakov et al., 2016). These results were in accordance with the main findings of Barba et al. (2015), who proved that HVED was the best technology to achieve the highest phenolic compounds recovery from grape pomace with lower energy requirement than PEF and US. However, HVED was less selective than PEF and US regarding the anthocyanins recovered, because of the different mechanisms involved. HVED was able to induce the release of cell-wall-linked phenolic compounds and particularly proanthocyanidins, which may interact with polysaccharides. However, US and PEF were more efficient than HVED in promoting localized fractures in the inner layer of the epidermis, where vacuolar anthocyanins were located.

Chapter II

Given these considerations, the most promising application of HVED could be for enhancing the extraction of oil and phenolic compounds from seeds, with hard and lignocellulosic tissue, due to the cell disruptive mechanisms involved in the process (Sarkis et al., 2015).

Another technology, based on cell tissue disruptive mechanism and on the total recovery of the matrix, is high-pressure homogenization (HPH), used as a mechanical disruption method to recover valuable compounds from agrifood by-products, aiming at their total valorisation, using water as solvent (Gali et al., 2020). This technique is mainly applied as a wet milling technique, to improve the rheological behavior of the suspensions controlling the particle size distribution of the residues (Donsì and Velikov, 2020; Mustafa et al., 2018). HPH-induced micronisation of tomato peels suspensions promoted the complete disruption of the plant cells. HPH enabled the increased release of intracellular compounds (proteins 70.5%), polyphenols (32.2%)), and the recovery of up to 56.1% of the initial lycopene content (Jurić et al., 2019).

Chapter III Objectives of the work

Several challenges have been identified for functional pasta production, including the combination of intensive processing conditions with the stability of the added functional ingredients, their interaction with the complex structure of the pasta matrix, as well as the consumer's acceptance of these novel products. Hence, effective strategies to promote consumer preferences for functional pasta will be important to increase their purchase decision-making. The raw materials used for pasta formulation play a crucial role in the physical, nutritional, and textural properties of pasta.

Therefore, the incorporation of non-conventional ingredients without affecting the quality attributes of pasta is a rather challenging task, which requires a fundamental understanding of the effects of the different functional ingredients added into the pasta matrix on the structural, and nutritional properties of the functionalized pasta, as well as the standardisation of the processing and cooking conditions.

To preserve the traditional pasta-like sensory profile and to improve its healthpromoting effect, the introduction of innovative technologies on the recovery and extraction of natural bioactive compounds could be an opportunity and a strength in further exploiting functional pasta.

However, the extraction process constitutes a critical issue for the valorisation of agri-food by-products since it depends not only on the source composition and the tissue considered (peels, stems, seeds, shell) but also on the physical and chemical properties of the desired compounds.

The use of the most suitable, biocompatible solvents, primarily ethanol and water, coupled with environmentally friendly technologies, represents an integrated approach towards the development of "green" extraction processes. In spite of the fact that these cutting-edge extraction techniques can be very beneficial for food waste valorisation, they possess their own limitations which may pose significant barriers to their implementation and utilization. However, the introduction of these technologies into an integrated process might facilitate their industrial implementation by reusing a low-cost source for the development of valuable naturally-derived products.

Chapter III

Nevertheless, although great advances have been made in terms of extraction and formulation of functional ingredients from agri-food by-products, there is a lack in proof of concept for their final application in food products and still a knowledge gap in the current research on the demonstration of the actual beneficial effects arising from their consumption.

Therefore, the main objective of this Ph.D. thesis (depicted in Figure III.1), as part of the "Pasta for fun" project, funded by MISE (Ministry of economic development) and made in collaboration with the pasta producer Lucio Garofalo S.p.a., was to develop a standardised production process of functional pasta contributing to prevent the metabolic syndrome, investigating the use of PEF and HPH technologies to assist the extraction of functional ingredients from agri-food by-products in view of their future exploitation. These emerging cell disruption technologies could represent effective strategies to enhance the extraction yields of target bioactive compounds, to mitigate the impact of the addition of novel ingredients on the quality of pasta, as well as to improve its specific health-beneficial properties.

Moreover, PEF and HPH technologies, producing two different types of functional ingredients, supernatant and total suspension, respectively, allow to discriminate the aforementioned aspects according to the main physicochemical characteristics of the obtained functional components.

A comprehensive understanding of the factors involved in the pasta functionalization process, as well as the beneficial effects of the functional pasta on human cell lines, after undergoing an *in vitro* digestion process, have been also investigated to further support the eventual industrial transferability of the newly formulated pasta.

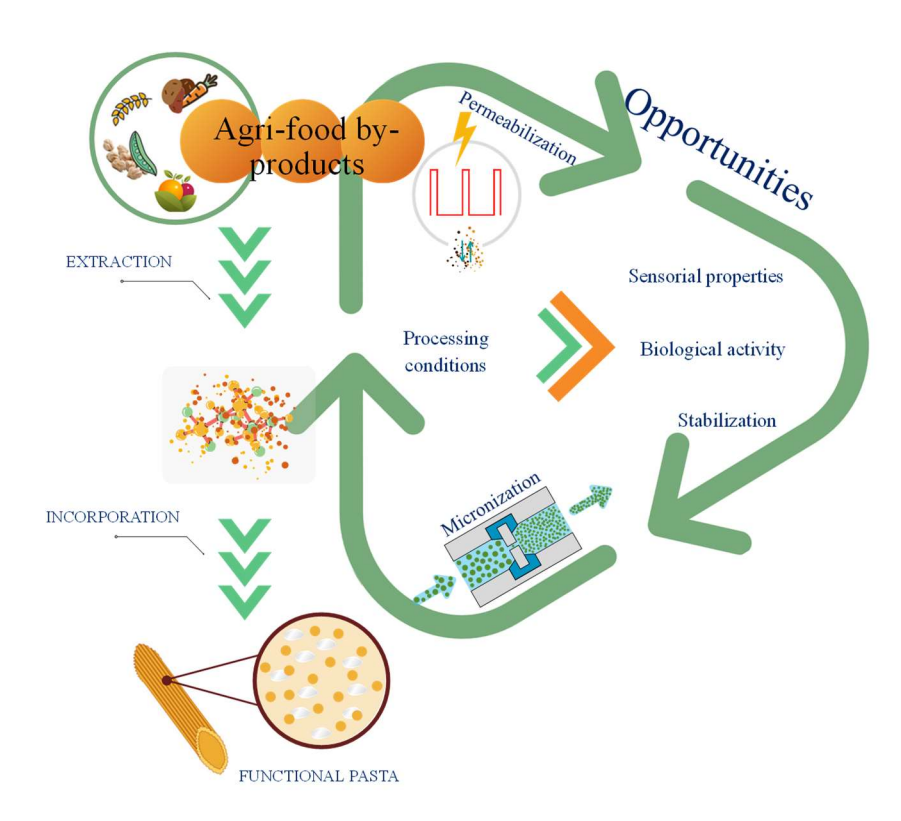


Figure III.1 Schematization of the main objective of this Ph.D. thesis investigation.

The sub-objectives considered to fulfill the proposed objective of this Ph.D. thesis are shown in the following scheme (Figure III.2).

Chapter III

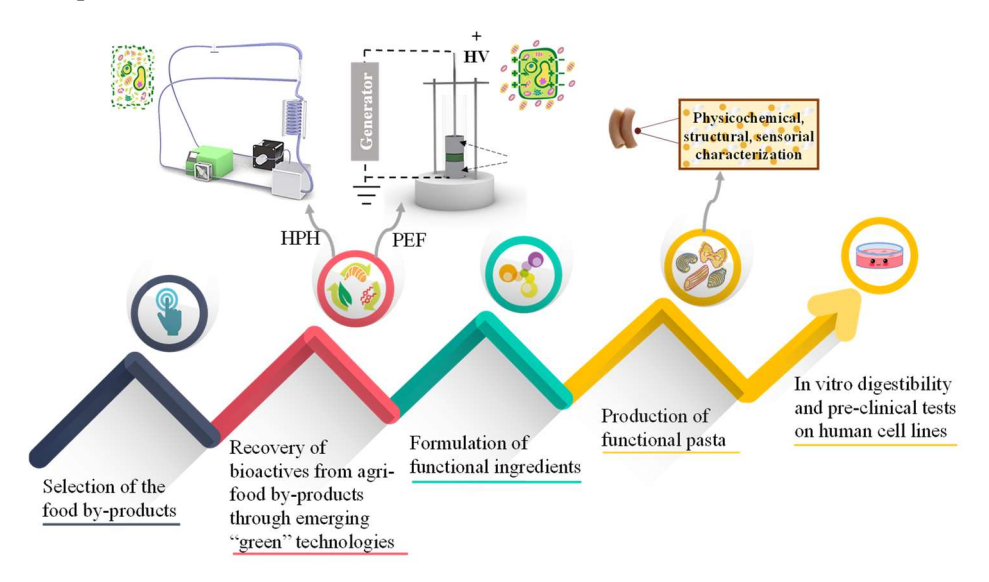


Figure III.2 *Schematic work plan of this Ph.D. thesis investigation.*

For the sake of achieving the attempted goals this thesis work has been structured in 2 different sections:

- Section I - "Natural-based ingredients from agri-food by-products: production and characterisation" (Chapter V - VI): in this section the possibility to utilize the more selective PEF technology and the more destructive HPH technology to produce pure extracts or total suspensions, respectively, identifying the optimal process parameters and the physicochemical properties of the obtained extracts to assess their potentiality to be used as functional ingredients was evaluated.

In **Chapter V**, the production of the different extracts by using PEF- and HPH-assisted extraction processes, evaluating the influence of processing conditions on extraction yields and physical characteristics of the obtained products was performed.

In **Chapter VI**, the formulation and realization of the functional ingredients were achieved, by stabilizing the previously obtained extracts and investigating their physicochemical stability under conditions simulating the transformation and preparation of the dry pasta.

Results of Chapters V-VI allowed to produce functional ingredients from agrifood by-products in standardised conditions and to discriminate them in function of their characteristics and phenolic profile, and according to the type of cell disintegration technology applied, in view of further utilization. In

particular, four different ingredients from agri-food by-products, and two of herbaceous origins have been identified.

- Section II - "Production of functional pasta on pilot scale and its comprehensive characterisation and techno-scientific validation" (Chapters VII-VIII): in this section, the production of the different types of functional pasta, as well as a complete physicochemical, sensorial, biological characterisation of the functionalized final products were attempted.

In Chapter VII, after the standardisation of the formulations and production process of functional pasta at lab-scale, the production of the functionalized pasta at pilot scale and its physicochemical, microstructural, and sensorial characterisation were carried out.

Chapter VIII was focused on health validation of the new functional pasta evaluating its biological activity as well as *in vitro* bioaccessibility of the added bioactive compounds and starch digestibility. In this Chapter a complete *in vitro* digestibility model mimicking the human digestive system was implemented and tailor-designed. The beneficial effects, including antioxidant, anti-inflammatory properties and glucose uptake of the digested functional pasta on selected human cell lines have been also investigated to support the possible upscaling to an industrial level.

- General conclusion and future perspectives (Chapter IX): the major outcomes, bottlenecks and remaining knowledge gaps regarding the pasta functionalization were summarized. Moreover, economic considerations related to the proposed extraction processes from the selected agri-food byproducts were reported in view of the potential integration of PEF and HPH technologies in the food industry. Finally, future perspectives in the frame of determining the technical and economic feasibility of the product innovation, as well as its health validation are presented.

Chapter IV Materials & Methods PART A - Functional ingredients

IV.1 Raw materials

In this thesis work, a screening of thirteen different raw materials, provided by local producers, as natural and low-cost sources of high-added value intracellular compounds has been conducted. The selection of industrial agrifood residues arises, firstly, from an in-depth analysis of the literature highlighting the scientific relevance of these matrices, due to their bioactivity and potential beneficial effects, secondly, from commercial considerations and availability throughout the year, finally, from a complete physicochemical characterisation of the investigated matrices.

The chemical composition of the raw materials was determined according to the standardised methods 923.03, 920.152, 922,06 ascribed by the AOAC (2005) official guidelines for the determination of ash, protein, and fat content, respectively. Moisture content was determined through the gravimetric method using an oven (Heraeus Group, Hanau, Germany) at 105 °C until a constant mass was reached (AOAC, 2003). Total dietary fibre was determined by a commercial kit (Megazyme K-TS, Wicklow, Irlanda) according to the method AOAC 991.43 (AOAC, 2005). Total carbohydrates were evaluated by subtracting the sum of the percentages of the other proximate components for 100 g of extract (Kostas et al., 2016). In addition, the pH and electrical conductivity have been determined according to the methods UNI EN 13037 (2012) and UNI EN 13038 (2002), respectively.

In the following table (Table IV.1) the moisture content ($g/100~g_{FW}$) and the proximate analysis on dry weight of the investigated raw materials ($g/100~g_{DW}$) are reported.

The raw materials, as well as the obtained extracts and the functional pasta samples reported throughout this Ph.D. thesis have been coded due to a non-

disclosure agreement signed with the company (Lucio Garofalo S.p.a.) within the 'Pasta for Fun' project of which this Ph.D. investigation is part.

 Table IV.1 Physicochemical characterisation of the investigated matrices.

A113H	88.1 ± 0.3	10.3 ± 0.3	16.1±0.6	15.2 ± 0.2	75.6±2.2	55.9±1.2	6.5±0.3
N433W	3.7±0.2	5.0 ± 0.1	17.4±0.5	2.0±0.2	9.8±3.1	65.8±0.6	7.5±0.2
B651S	6.3±0.3	3.2 ± 0.2	12.3±0.6	1.5±0.1	11.5±1.2	68.5±1.2	7.0±0.4
E706IT	80.7±0.8	4.9±0.3	14.7±0.2	1.3±0.1	5.8±0.5	73.3±0.9	4.6±0.1
F500A	80.4±0.1	10.5±3.1	9.3±1.3	1.55 ± 0.1	46.8±4.4	31.9±1.5	3.3±0.3
G300G	62.6±0.1	12.9±1.8	8.3±0.3	2.7±0.1	20.7±8.2	55.4±2.3	3.7±0.1
R840C	52.3±0.4	1.8±0.5	16.5±0.4	0.6±0.0	20.2±0.3	£0.9±0.7	3.6±0.1
Y210H	39.1±0.8	2.3 ± 0.1	13.3±1.3	0.6 ± 0.0	24.3±0.4	59.5±0.8	3.7±0.5
T760P	64.9±0.4	1.0±0.1	1.6±0.2	1.1±0.1	35.4 ± 0.3	60.9±1.1	3.9±0.3
A781M	67.9±0.1	2.0±0.1	9.0±0.1	0.9±0.1	13.5±0.5	74.6±0.9	3.9±0.1
R550R	6.7±0.1	15.3±0.2	2.2±0.4	0.5±0.1	0.1 ± 0.0	82.1±1.5	6.4 ± 0.3
S329G	10.8±0.3	5.9±0.1	24.3±1.3	2.3±0.1	12.6±1.4	54.9±0.9	5.9±0.1
X700H	8.0±0.1	6.4±0.1	24.8±0.5	5.3±0.1	24.3±0.5	39.2±0.5	6.1 ± 0.1
Agri-food by-products	Moisture (g/100 g)	Ash (g/100 g _{DW})	Protein (g/100 g _{DW})	Fat (g/100 gDw)	Carbohydrates (g/100 gpw)	Total fibre (g/100 gpw)	(-) Hd

EC (mS/cm)	2.1±0.1	3.3±0.1	0.6±0.1	1.1±0.1	1.0±0.1	1.6 ± 0.1	2.4±0.1	2.0±0.1	2.3±0.1	1.1 ± 0.1	0.7±0.1	0.6 ± 0.1	1.4±0.1
------------	---------	---------	---------	---------	---------	-------------	---------	---------	---------	-------------	---------	---------------	---------

From the data reported in Table IV.1, it was possible to identify four representative groups based on the protein content, very high (> 20%, Y700H, S329G), high (15% – 20%, R840C, E706IT), medium (8 - 14%, A781M, Y210H, F500A, G300G, B651S) and low protein content (<3%, R550R, T760P). Among the investigated raw materials R840C, Y210H, and R550R demonstrated to possess the lowest fat content.

However, an important obstacle to the development of the secondary market is related to the uncertainty of the quality of secondary raw materials and, in particular, to the presence of chemical substances dangerous to human health. Therefore, a preliminary analysis was conducted on the detection of the presence of pesticides using Agri-Screen Ticket Pesticide Detection Kit (Neogen corporation, Lesher place, Lansing, USA). This kit is used to detect all major organophosphates, thiophosphates and carbamates in air, water, soil, plant matrices, surfaces. This method, accurate and simple, has been approved by AOAC International, AOAC Research Institute, AFNOR Certified, IUPAC, USDA / GIPSA (FGIS) USDA / FSIS and is based on a simple biochemical principle. The analysed samples were free of pesticides or contained quantities below the maximum residue levels (MRL) for human consumption (Regulation (EC) No. 396/2005).

IV.1.1 Characterisation of the raw materials in terms of phenolic profile

To characterise the selected matrices also in terms of phenolic profile, and to define the optimal extraction conditions that maximize the extraction yield in terms of Total Phenolic Content (TPC), Response surface methodology (RSM) and a two-factor three-level face-centred central composite design (FC-CCD) were used to relate the response variable (TPC) to the selected process variables (type of solvent - ethanol, acetone, methanol, and water - and its concentration - 20% - 100% in water, v/v). The obtained experimental design is summarized in Table IV.2.

Table IV.2 Experimental design obtained by RSM with the combinations of the independent variables investigated (type of solvent, solvent concentration).

Run Number	Type of solvent	Solvent concentration (%, v/v)
1	Acetone	31
2	Acetone	100
3	Ethanol	20
4	Ethanol	64.8
5	Ethanol	58.8
6	Ethanol	100
7	Ethanol	20
8	Ethanol	65.6
9	Methanol	20
10	Methanol	100
11	Methanol	57.2

The raw materials were subjected to a solid-liquid extraction process with a fixed solid-to-liquid ratio of 1:10 (g/mL), for 24 h, at 25 °C under a gentle agitation (160 rpm, orbital incubator S150, PBI international, Milan, Italy). The obtained extracts were, then, centrifuged at 14,000 rpm for 10 min at 25 °C and the supernatant analysed in terms of TPC using the Folin Ciocalteu assay (§ IV.5.1), (data not shown). As an example, the curves obtained from the software, depicting the effect of the type of solvent, and solvent concentration on TPC level of E706IT extract, are reported in Figure IV.1.

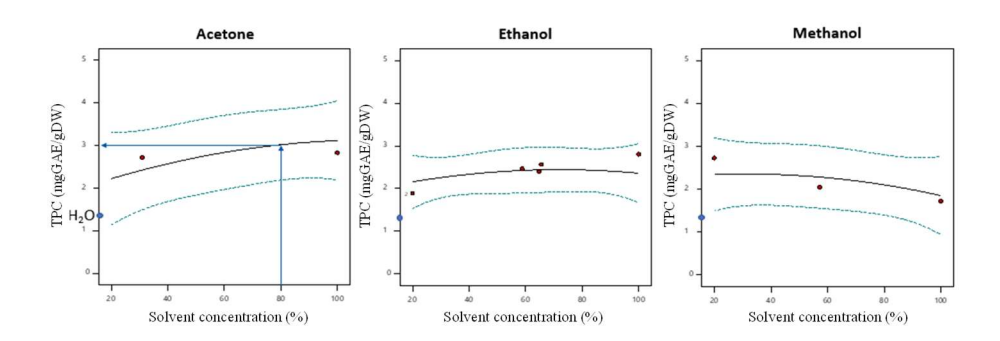


Figure IV.1 Effect of the type of solvent and its concentration on the extraction yield of TPC from E706IT. The added blue dot in each graph refers to pure water added as a comparative model.

To determine the optimal diffusion time, extraction kinetics in terms of TPC were conducted at the previously optimized extraction conditions. In particular, an aliquot of extract was taken at different times (5 min - 24 h) and furtherly analysed. Finally, the extracts obtained after 24 hours of extraction were characterised in terms of antioxidant activity by means of the spectrophotometric assays FRAP (Ferric Reducing Antioxidant Power) and DPPH (2,2-diphenyl-1-picrilidrazil), and subjected to HPLC analysis to identify their phenolic profile (§ IV.5.3, § IV.5.4, § IV.5.11, respectively), (data not shown). As an example the TPC extraction kinetics from E706IT, by using 80% acetone-water (v/v) as optimal extracting solvent (Figure IV.1), is reported in Figure IV.2.

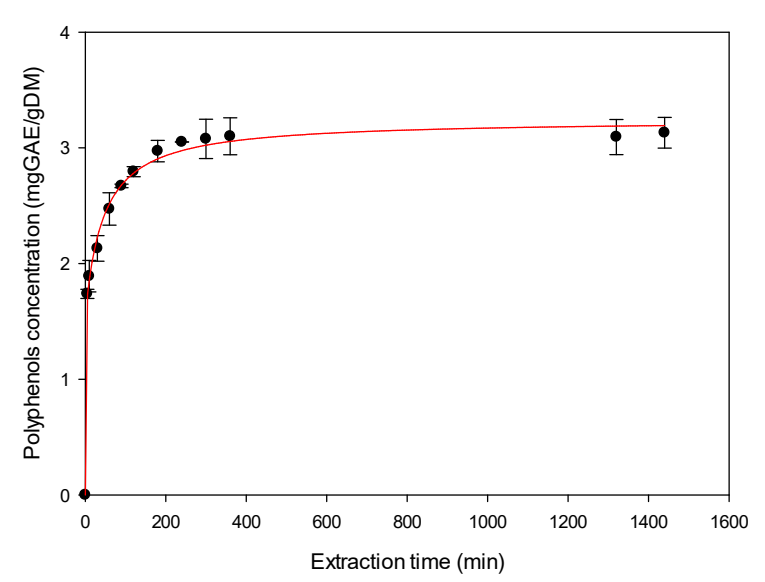


Figure IV.2 Extraction kinetics of TPC ($mgGAE/g_{DW}$) from E706IT, by using 80% acetone-water (v/v).

The results obtained from this conventional extraction process, using organic solvents and long diffusion times will be a benchmark for those obtained from PEF- or HPH-assisted extraction processes, using water, or a solution of water and ethanol, and for lower diffusion times.

IV.2 Solvents and chemicals

Ethanol, and all reagents and standards involved in the analyses were purchased from Sigma Aldrich (Steinheim, Germany).

IV.3 Pulsed Electric Fields (PEF)-assisted extraction

The extraction process constitutes a critical issue for the valorisation of agrifood by-products since it depends not only on the source composition and the tissue considered (peels, stems, seeds, shell) but also on the physical and chemical properties of the desired compounds. Therefore, the selection of the most appropriate extraction technique between PEF and HPH relied on the nature of the matrix, physical appearance, and the localization of the target compound inside the cell, which the different cell rupture mechanisms associated with each technique depend on.

The target matrices subjected to PEF treatment are S329G and F500A (data not shown), G300G, A113H, and N433W. However, only the results of the most promising raw materials have been reported and discussed in this Ph.D. thesis.

IV.3.1 Experimental apparatus

The experimental campaign of this Ph.D. investigation on PEF-assisted extraction was performed in two different treatment chambers and are specifically designed for lab-scale and pilot scale operations. Additionally, in the case of PEF treatment of N433W a bench-scale PEF continuous system was used. The main features and characteristics of the PEF equipment utilized are reported in detail in the following section.

IV.3.1.1 Lab-scale PEF system

PEF treatments of G300G, F500A, A113H, and N433W were performed using a laboratory scale batch system, previously described elsewhere (Donsì et al., 2010). Briefly the system consisted of a high voltage pulsed power (25 kV-500 A) generator (Modulator PG, ScandiNova, Uppsala, Sweden), able to generate monopolar square wave pulses with different pulse width (3-25 μ s) and frequency (1-450 Hz). A high voltage cable connected the pulse generator to a treatment chamber (Figure IV.3) made of two parallel plate cylindrical electrodes (3 cm in diameter) separated by a polycarbonate tube (electrode gap up to 5 cm). The actual voltage and current passing through the chamber were measured by a high voltage probe (Tektronix, P6015A, Wilsonville, OR, USA) and a Rogowsky coil (2-0.1, Stangenes, Inc., USA) connected to a 300 MHz oscilloscope (Tektronix, TDS 3034B, Wilsonville, OR, USA). The maximum electric field intensity (E, kV/cm) and the total specific energy input (W_T, kJ/kg) were calculated as reported by Carpentieri et al. (2022).

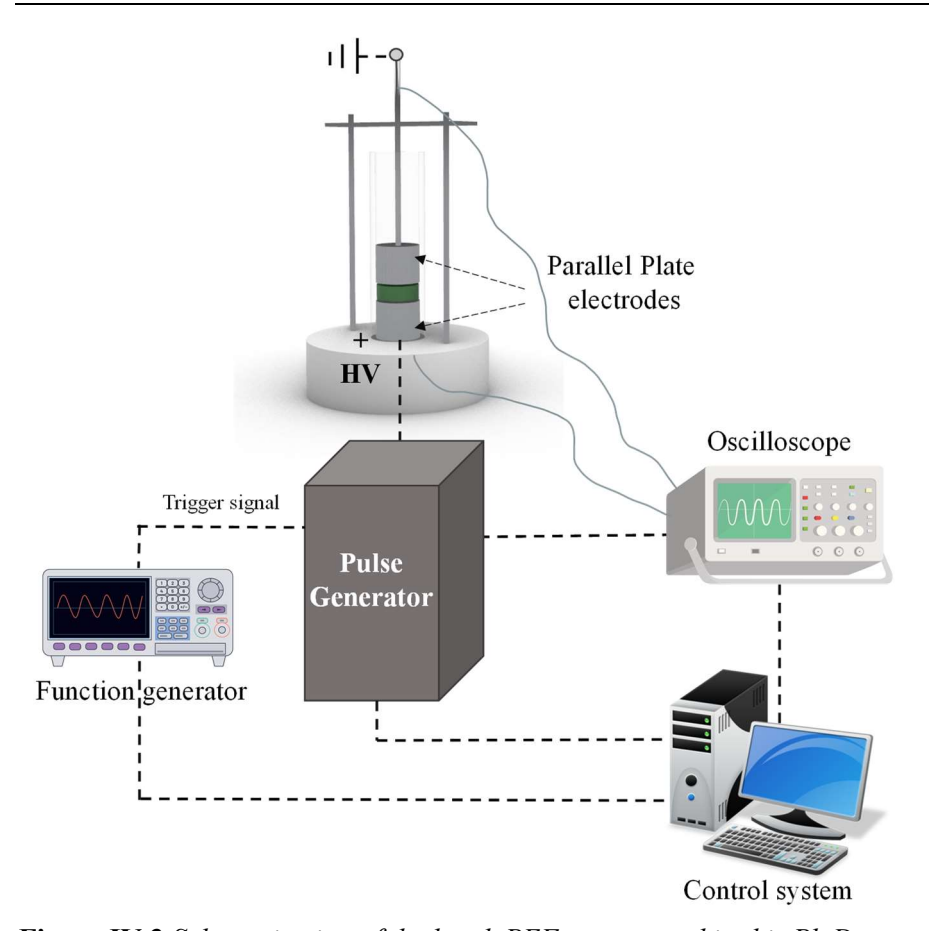


Figure IV.3 *Schematization of the batch PEF system used in this Ph.D. investigation.*

IV.3.1.2 Pilot scale PEF system

The PEF treatment of larger quantities of raw material was conducted on the A113H sample by using a pilot scale conveyor belt treatment chamber. The belt consisted of a series of perforated baskets with a feeding rate that can be varied between 0.21 and 2.78 cm/s. The PEF treatment zone, consisted of four consecutive couples of parallel plate electrodes ($A = 20 \text{ cm}^2$, Gap = 10 cm), which were alternatively disposed in vertical and horizontal way, to increase the efficiency and uniformity of the treatment. In addition, to ensure electrical continuity between each couple of electrodes, the whole PEF chamber was filled with tap water.

IV.3.1.3 Continuous PEF system

Briefly, the unit consisted of a peristaltic pump (EP MINI 20, Liverani, Ravenna, Italy) equipped with an inverter (Optidrive ODE-3-120070-1F12, Invertek Drives, Powys, UK) to set the flow rate of the suspension through the system. The PEF treatment zone consisted of co-linear cylindrical treatment chamber made of stainless steel electrodes separated by Plexiglas insulator. The inner diameter of the treatment zone was 2 cm and the electrode gap was 2 cm

The treatment chamber was connected to the output of a high voltage pulsed power (20 kV-100 A) generator (Diversified Technology Inc., Bedford, WA, USA) able to deliver both mono- and bipolar square wave pulses (1-10 μs, 1-1000 Hz), with a maximum average power of 25 kW. The peak electric field intensity (E, kV/cm) and total specific energy input (W_T, kJ/kg) were measured and calculated as reported in (Postma et al., 2016). Voltage and current signals at the treatment chambers were measured, respectively, by a high voltage probe (Tektronix, P6015A, Wilsonwille, OR, USA) and a rogowsky coil (2– 0.1 Stangenes, Inc., USA) and displayed on a 300 MHz digital oscilloscope (Tektronix, TDS 3034B, Wilsonwille, OR, USA). The PEF system used in this investigation is reported in Figure IV.4.

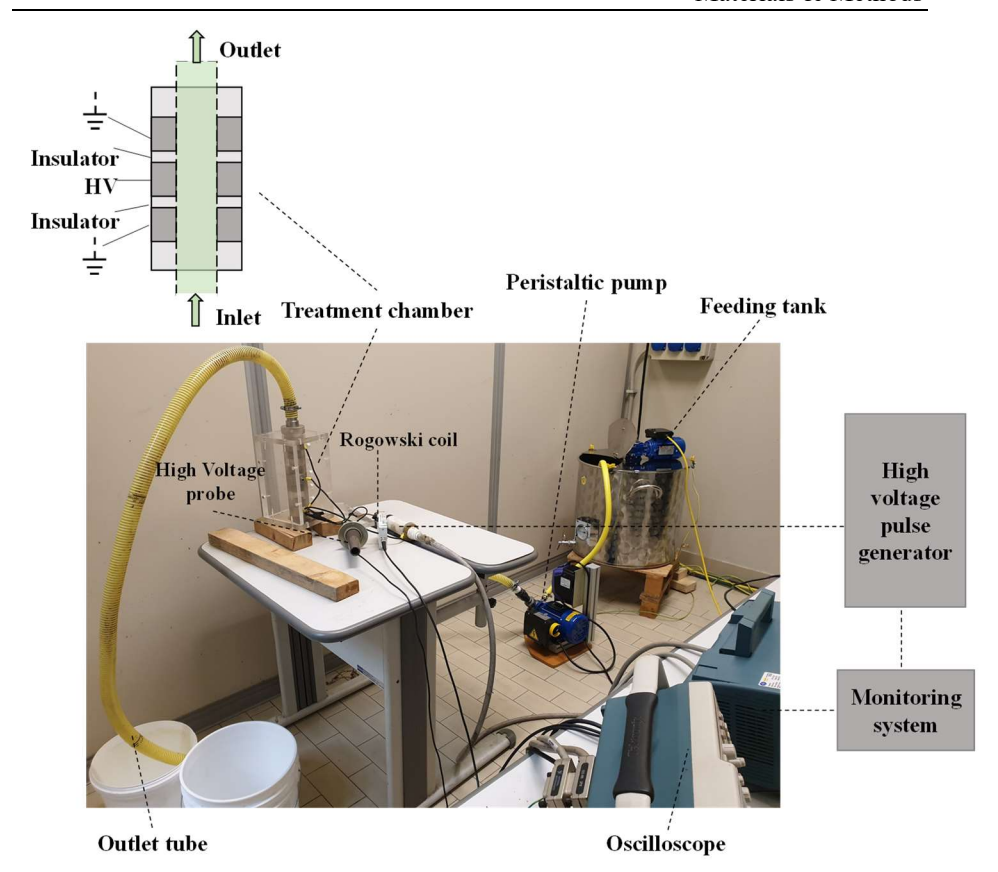


Figure IV.4 *Schematic overview of the continuous flow PEF system used in this Ph.D. investigation.*

IV.3.2 Experimental procedure

IV.3.2.1 Sample processing (G300G)

IV.3.2.1.1 Cell membrane electroporation induced by PEF

To evaluate the permeabilization degree of cell membrane of the investigated tissues upon PEF treatment, the cell disintegration index (Z_p) was determined via impedance analyses by measuring the electrical complex impedance of untreated and PEF-treated samples, according to the method described by Carpentieri et al. (2022).

The measuring cell was the same batch treatment chamber described in § IV.3.3.1. For the impedance measurements, approximately 5 g of each sample were loaded into the cell along with 1 mL of distilled water, necessary to ensure electrical continuity between the electrodes.

The electrodes were connected to an impedance analyser (Solartron 1260, UK), which provides a frequency response of the complex impedance of the

sample in the range of 10^2 – 10^6 Hz PEF treatments were carried out at different field strength (E = 0.5 - 5 kV/cm) and total specific energy input (W_T= 1 - 20 kJ/kg) at a constant pulse repetition frequency (5 Hz) and pulse width (20 μ s). The initial temperature of the samples was set at 20 ± 1 °C and no remarkable temperature increase was observed due to the relatively low energy input delivered during the treatment.

The Z_p value, which varies between 0 (for intact tissue) and 1 (for fully permeabilized tissue), was calculated on the basis of the measurement of the absolute value of the complex impedance of untreated ($|\mathbf{Z}_{untr}|$) and PEF treated tissue ($|\mathbf{Z}_{tr}|$) in the low (0.1 kHz) and high (1 MHz) frequency ranges, using the Eq. (1) (Frontuto et al., 2019):

$$Z_p = \frac{|Z_{untr(0,1 kHz)}| - |Z_{tr(0,1 kHz)}|}{|Z_{untr(0,1 kHz)}| - |Z_{tr(1 MHz)}|}$$
(1)

All the measurements were carried out in triplicate.

The obtained Z_p values were used to define the optimal treatment conditions in terms of electric field strength (E_{opt}) and total specific energy input ($W_{T,opt}$), that allowed to obtain the highest cell membrane permeabilization degree with the minimum treatment severity (Carpentieri et al., 2022a, 2021a; Frontuto et al., 2019).

IV.3.2.1.2 PEF-assisted extraction

For PEF-assisted extraction experiments, 5 g (on average) of the investigated matrix were loaded into the treatment chamber and treated under the previously determined optimal conditions (E_{opt} , $W_{T,opt}$). After the PEF treatment, the samples were immediately transferred into 100 mL Pyrex flasks where a water-ethanol mixture was added at a constant solid to liquid ratio (1:10 g/mL). The flasks were placed in an orbital incubator S150 (PBI international, Milan, Italy) and subjected to constant shaking at 160 rpm for different times (0–300 min), temperatures (20–50 °C), and ethanol concentration (0–50%, (v/v)). For the sake of comparison, the same experimental design and extraction protocol was used for untreated (control) samples subjected to conventional SLE without the application of PEF pretreatment.

After the extraction process, the extracts from untreated and PEF treated samples were centrifuged at 5289xg (PK130R model, ALC International, Cologno Monzese, IT) for 10 min at 4 °C to obtain the supernatants, which were then stored at 4 °C until further analysis.

IV.3.2.1.3 Experimental Design

Response surface methodology (RSM) was used to relate the response variables to the process variables, to define the optimal PEF processing conditions (E_{opt} in kV/cm, $W_{T,opt}$ in kJ/kg), which maximize the Z_p value, as well as the optimal conditions of the SLE process that maximize the extraction yields of TPC, flavonoid content (FC), total anthocyanin content (TAC), tannin content (TC), and antioxidant activity of extracts for untreated (control) and PEF-treated G300G samples.

A two-factor three-level face-centred central composite design (FC-CCD) was used to determine how the electric field strength (X_1 , 0.5-5 kV/cm) and total specific energy input (X_2 , 1-20 kJ/kg) affected the permeabilization degree of tissues upon PEF pre-treatment. The obtained experimental design consisted of 9 runs (Table IV.3), with the Z_p (Y_1) of PEF-treated samples considered as response variable. A second-order polynomial model reported in Eq. (2) was used to predict the response variable as a function of the investigated independent variables:

$$Y_k = \beta_0 + \sum_{i=1}^2 \beta_i X_i + \sum_{i=1}^2 \beta_{ii} X_i^2 + \sum_{i=1}^2 \sum_{j=i+1}^3 \beta_{ij} X_i X_j$$
(2) where Y_k is the response variable; X_i and X_j are the independent variables; β_0 ,

 β_{ij} , β_{ij} , and β_{ij} are the intercept, regression coefficients of the linear, quadratic, and interaction terms of the model, respectively.

Table IV.3 Experimental design obtained by RSM with the combinations of the independent variables investigated (E, W_T) .

Run	Variables		
	Е	W_T	
	(kV/cm)	(kJ/kg)	
1	0.5	1	
2	0.5	10.5	
3	0.5	20	
4	2.75	1	
5	2.75	10.5	
6	2.75	20	
7	5.0	1	
8	5.0	10.5	
9	5.0	20	

The same experimental design was used to analyse the effect of ethanol percentage $(X_3, 0-50\%, v/v)$ in a water-ethanol solvent mixture, extraction time $(X_4, 30-165 \text{ min})$, and extraction temperature $(X_5, 20-50 \text{ °C})$ on the response variables, namely total phenolic content (Y_2) , flavonoid content (Y_3) , antioxidant activity (Y_4) , anthocyanin content (Y_5) , tannin content (Y_6) , of untreated and PEF-treated samples. The experimental design consisted of 15

runs including five replicates of central points (Table IV.4). A two-factor interaction (2FI) model reported in Eq. (3) were applied to predict the response variables as function of the input variables for G300G:

$$Y_k = \alpha_0 + \sum_{i=1}^3 \alpha_i X_i + \sum_{i=1}^3 \sum_{j=i+1}^4 \alpha_{ij} X_i X_j + \sum_{i=1}^3 \sum_{j=i+2}^5 \alpha_{ij} X_i X_j$$
 (3)

where Y_k is the predicted response variables; X_i and X_j are the independent variables; α_0 , α_i , and α_{ij} are the intercept, regression coefficients of the linear, and interaction terms of the model, respectively.

Table IV.4 Experimental design obtained by RSM with the combinations of the independent variables investigated (E-W, ethanol percentage in ethanolwater mixture (%, v/v); t, diffusion time (min) T, extraction temperature (°C)).

Run	Variables				
•	E-W	t	T		
	(%, v/v)	(min)	(°C)		
1	0	30	20		
2	0	30	20		
3	25	300	20		
4	50	300	20		
5	50	165	20		
6	0	30	35		
7	25	165	35		
8	25	165	35		
9	25	165	35		
10	50	300	35		
11	0	30	50		
12	0	30	50		
13	25	300	50		
14	50	300	50		
15	50	165	50		

IV.3.2.2 Sample processing (A113H)

Prior to the PEF processing, A113H samples were cut into pieces of 10 cm length with a knife and then loaded into a pilot dicer machine (Giulio Raiola, Angri, Italy) to obtain 1 cm³ cubes. The cubes were immediately immersed in water with 1% (w/v) citric acid, prior to further experiments to avoid oxidation.

In this Ph.D. investigation, based on our experimental results (data not shown) an electric field strength (E) of 3 kV/cm and a specific energy input of 5 kJ/kg, defined upon the impedance measurements (data not shown) were utilized as optimal PEF treatment conditions for the permeabilization of A113H tissues. 66

Lab-scale PEF-assisted extraction experiments were performed by loading 5 g of food wastes into the lab-scale treatment cell, along with distilled water at constant S/L ratio of 1:1 and subsequently subjecting them to the optimal PEF treatments conditions, at a constant pulse repetition frequency (10 Hz) and pulse width (20 μ s).

After the electrical treatment, the biomass was put into 200 mL flasks together with distilled water and hydrochloric acid 0.01% (v/v) at the optimized solid-to-liquid ratio (1:5 g/mL) and allowed to stand in an incubator for 120 min, under a gentle agitation (160 rpm) at a diffusion temperature of 25 °C.

At the end of the extraction process, untreated and PEF treated biomasses were discarded and the extracts were centrifuged at 5700x g for 10 min (PK121R model, ALC International, Cologno Monzese, Milan, Italy) in order to obtain clear supernatants, which were stored at 4 °C for further quali-quantitative analyses.

Additionally pilot scale PEF-assisted extraction process was also carried out only on A113H samples. During PEF treatment, A113H were transported through the treatment zone at a flow rate of 150 kg/h and exposed to the same treatment intensity as for lab-scale tests. Approximately 500 g of stem cubes were loaded into each basket and a total amount of about 8 kg of raw material was processed. Afterwards, the untreated and treated A113H were subjected to the aqueous extraction step into a 100 L agitated tank at the same extraction conditions previously described.

IV.3.2.3 Sample processing (N433W)

Prior to the PEF processing, N433W tissues were subjected to a size reduction step by means of a mincer (Kenwood Corporation, Tokio, Japan) for 1 min, then, based on preliminary experimental results (data not shown) an electric field strength (E) of 3 kV/cm and a specific energy input (W_T) of 10 kJ/kg, were used for the permeabilization of N433W tissues. Lab-scale PEF-assisted extraction experiments were performed by loading 5 g of food wastes into the lab-scale treatment cell, along with distilled water at constant S/L ratio of 1:1 and subsequently subjecting them to the optimal PEF treatments conditions, at a constant pulse repetition frequency (5 Hz) and pulse width (20 μs).

The treated matrix was, then, subjected to a solid-liquid extraction step with distilled water at previously optimized extraction conditions (solid-to-liquid ratio of 1:50 g/mL, diffusion time of 3 h, agitation (160 rpm), diffusion temperature of 25 °C).

The PEF treatments were also conducted on N433W tissues by using the continuous PEF system, applying the same PEF processing conditions, at fixed suspension flow rate (250 L/h). The untreated and treated suspension were subjected to the aqueous extraction step into a 100 L agitated tank at the same extraction conditions previously described.

IV.4 High-pressure homogenization-assisted extraction

IV.4.1 Experimental apparatus

With the aim to completely recover the by-products and to induce total cell disruption, Y700H (data not shown), E706IT, A781M, and B651S were subjected to High Pressure Homogenization treatment (HPH).

Prior to perform complete cell disruption and to avoid clogging of the micrometric orifice of HPH plant, the samples were homogenized by using Ultra turrax system (T25 HSH, IKA Labortechnik, Germany), which allowed to finely disperse the solid component in the solvent. The HSH system consists of a rotor inserted in a fixed stator. The high rotational speed and the minimum distance between the rotor and stator produces strong cutting forces which result in better dispersion of the particles, as shown in Figure IV.5.

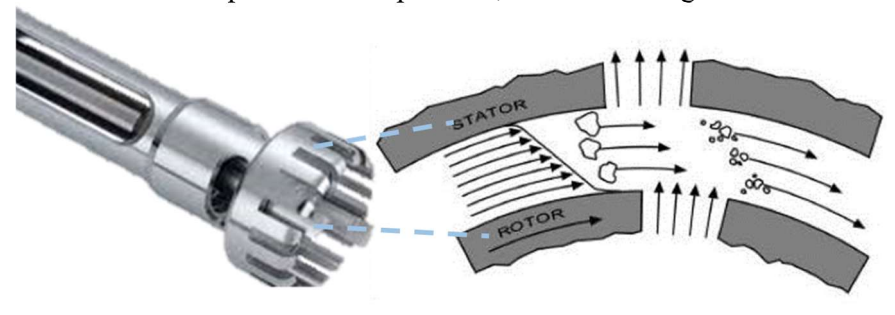


Figure IV.5 *Working principle of High Shear Homogenizer.*

The HPH technology, instead, is able to provoke the complete cell break down, causing a complete lysis of the cells and an instantaneous release of all the intracellular material towards the external environment (liquid phase). The full disintegration of the sample cells has been performed in an in-house developed lab-scale high-pressure homogenizer, schematized in Figure IV.6. The suspension was forced to pass through a micrometric orifice valve (model WS1973, Maximator JET GmbH, Schweinfurt, Germany) upon pressurization by means of an air driven Haskel pump (model DSHF 300, HPSC S.r.l., Varese, Italy).

The pressure drop across the orifice can range between 100 MPa and 200 MPa. The system is equipped with a tube-in-tube exchanger, located downstream of the orifice valve, to prevent excessive heating of the suspension.

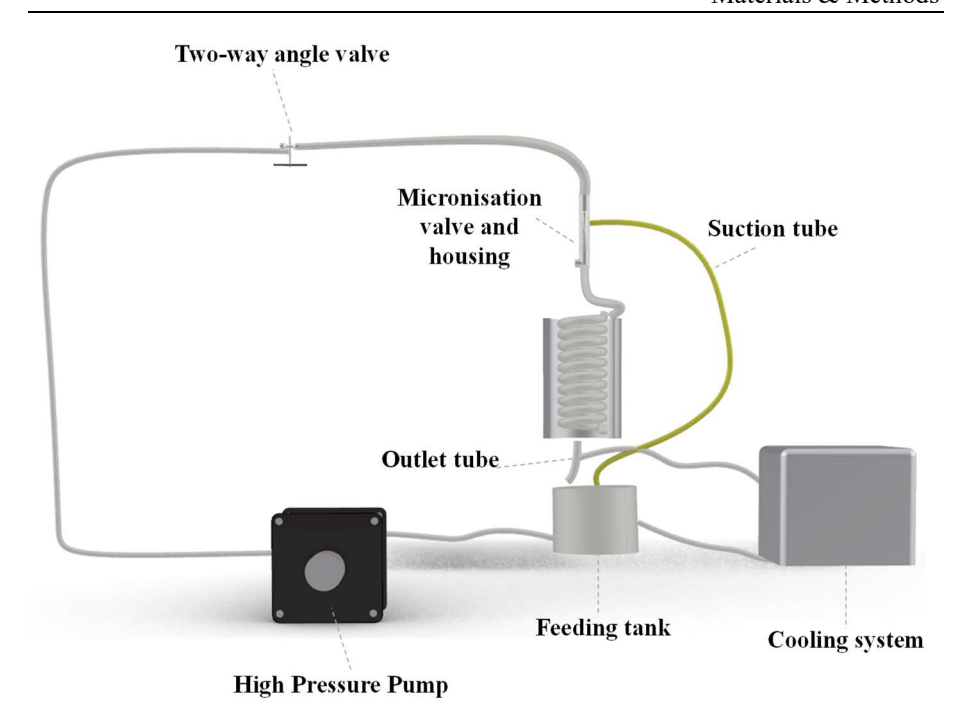


Figure IV.6 *Schematization of the HPH plant used in this Ph.D. investigation.*

IV.4.2 Experimental procedure

IV.4.2.1 Sample processing (E706IT)

In this thesis investigation, prior to perform complete cell disruption, the matrix was dissolved in distilled water with a previously optimized solid-to-liquid ratio of 1:10~g/mL and homogenized by using Ultraturrax at 20000 rpm for 10~minutes.

The obtained suspension was, then, subjected to HPH processing at variable pressure (P = 80 - 100 MPa), number of passes ($n_P = 1 - 15$ min), and treatment temperature (5 – 50 °C). Response surface methodology (RSM) was used to relate the response variables (TPC, antioxidant activity, lycopene content) to the investigated process variables, to define the optimal HPH processing conditions. The experimental design consisted of 24 runs reported in Table IV.5.

Table IV.5 Experimental design obtained by RSM with the combinations of the independent variables investigated (P, pressure (MPa); np, number of passes through the micrometric valve, T, extraction temperature (°C)).

Run	Variables		•
	P (MPa)	n_P	T (°C)
1	80	2	5
2	80	2	25
3	80	2	50
4	100	2	5
5	100	2	25
6	100	2	50
7	80	5	5
8	80	5	25
9	80	5	50
10	100	5	5
11	100	5	25
12	100	5	50
13	80	10	5
14	80	10	25
15	80	10	50
16	100	10	5
17	100	10	25
18	100	10	50
19	80	15	5
20	80	15	25
21	80	15	50
22	100	15	5
23	100	15	25
24	100	15	50

At the end of each treatment, samples were collected and stored at 4 °C until further analysis.

IV.4.2.2 Sample processing (A781M, and B651S)

In this investigation, based on our experimental results (data not shown) A781M, and B651S samples were dissolved in distilled water with a solid-to-liquid ratio of 1:15 g/mL, and 1:40 g/mL, respectively, and homogenized by using Ultraturrax at 20000 rpm for 10 minutes. The obtained suspensions were, then, subjected to HPH processing at a pressure of 80 MPa, for a number of passes of 15 (corresponding to about 15 min), at 25 °C.

IV.4.2.3 Downstream processes

The extracts from untreated and PEF treated samples with pilot scale batch and continuous systems were clarified by means of a stack of sieves of decreasing pore size $(500-25~\mu m)$ in order to remove any suspended solids, prior to be subjected to a nanofiltration (NF) process in a pilot scale plant (Sepra, Cesano Maderno, Italy).

Briefly, the system consisted of a loading tank of 100 L capacity, equipped with a cooling coil to control the processing temperature, a stainless steel housing for both a pre-filter cartridge (20 μ m of mean pore size) and a 18x1.2 in² spiral wound membrane module, a pre-feeding ($P_{MAX} = 10$ bar), a pressurization pump ($P_{MAX} = 45$ bar), and a pressure control valve.

The membrane used in this investigation is a NF polymeric membrane (GE Osmonics Desal DL 1812, Lenntech, Delfgauw, NE).

Nanofiltration tests were carried out by loading 80 L of water extracts from untreated and PEF treated samples and subjecting them to concentration at constant temperature and pressure (T = 25 °C; P = 20 bar), until reaching a volume reduction of 50-60%. The retentate stream was recovered and furtherly concentrated by using a R-200/205 Rotavapor (BÜCHI Labortechnik AG, Flawil, Switzerland) until achieving a volume reduction up to 90%, prior being subjected to a freeze drying process into a 25 L VirTis Genesis freeze-drier (SP Scientific, USA) at P = 50 mbar for 24 h, by setting the plate temperature at 25°C. Likewise the supernatants of the extracts from PEF-treated samples at lab-scale obtained after centrifugation, and the HPH-treated suspensions were concentrated by using a R-200/205 Rotavapor until achieving a volume reduction up to 90% and 80%, respectively, and subsequently subjected to freeze-drying. The dried extracts were then stored under refrigerated conditions to be furtherly characterised.

IV.5 Analytical determinations

IV.5.1 Total Phenolic Content (TPC)

The total phenolic content (TPC) of the obtained extracts was determined using the Folin-Ciocalteau method as reported by Carpentieri et al. (2022a). Gallic acid, dissolved in the different extracting solvents used to obtain each extract analysed, was used as a standard to create five-point calibration curves in a concentration range of 1-100 mg/L. Results were expressed as milligrams of gallic acid equivalents (GAE) per g of dry weight (g_{DM}) of the raw material.

IV.5.2 Flavonoid content (FC)

The flavonoid content (FC) of the obtained extracts was determine using the Aluminum-chloride colourimetric assay as previously described by

Carpentieri et al., (2022a). Quercetin, dissolved in the different extracting solvents used to obtain each extract analysed, was used as a standard to create five-point calibration curves in a concentration range of 20-100 mg/L. The absorbance of the samples and the standard solutions were measured at 510 nm. The obtained results were expressed as mg of quercetin equivalent (QE) per g_{DM} of the raw material.

IV.5.3 Ferric Reducing Antioxidant Power (FRAP)

FRAP assay of the extracts from both untreated and PEF- and HPH- treated samples was carried out according to the method described by Benzie and Strain (1996) with slight modifications. Ascorbic acid, dissolved in the different extracting solvents used to obtain each extract analysed, was used to generate five-point external standard calibration curves in a concentration range comprised between 0 and 2 mmol/L. The FRAP values were expressed as mg of ascorbic acid equivalents (mg AAE) per g_{DM} of the raw material.

IV.5.4 Free-radical-scavenging capacity (DPPH)

The antioxidant power of the extracts has been evaluated by DPPH spectrophotometric assay with the procedure reported by Rapisarda et al. (1999), with slight modifications. Briefly, 3.9 mL of a 25 ppm DPPH solution in methanol was mixed with 0.1 mL of extract and immediately incubated in the dark for 5 min. The absorbance of the reacting mixture was red at fixed wavelength (515 nm). Results were expressed as percentage decrease with respect to blank values, and the inactivation level evaluated as reported in the following equation (Eq. (4)):

$$\%I = 100 - \left(\frac{ABS_S}{ABS_B}\right) * 100 \tag{4}$$

where ABS_s is the absorbance of the sample and ABS_B is the absorbance of the blank.

IV.5.5 Evaluation of total anthocyanin content (TAC)

Total anthocyanin content (TAC) of the obtained extracts was determined using the pH differential method described by Lee et al. (2001) with slight modifications.

Briefly, two mixtures were prepared per each extract by diluting, with a dilution factor equal to 5, one sample with pH 1.0 buffer (0.19% (w/v)) of potassium chloride in water) and the other with pH 4.5 buffer (5.44% (w/v)) of sodium acetate in water). The absorbance of the diluted reacting solutions was

then measured at 520 and 700 nm using a V-650 spectrophotometer (Jasco Inc. Easton, MD, USA) within 30 min of their preparation.

Results are determined by means of the following formula (Eq. (5)) and expressed as mg of C3G (cyanidin-3-glucoside) per g_{DM} of the raw material:

$$C = \frac{A*MW*DF*10^3}{\varepsilon} * \frac{L}{S} * \frac{m_{TOT}}{m_{DW}}$$
 (5)

where:

 $A = (A520 nm - A700 nm)_{pH=1} - (A520 nm - A700 nm)_{pH=4.5}$

MW (molecular weights of cyanidin-3-glucoside) = $449.2 \ g/mol$;

DF= dilution factor;

 $\varepsilon = (\text{molar extinction coefficient}) = 26900 L/mol/cm;$

 10^3 = conversion factor from g to mg;

L/S = liquid-to-solid ratio;

 m_{TOT}/m_{DW} = ratio between the total mass of the raw material and the mass of the dry matrix.

IV.5.6 Evaluation of tannin content (TC)

The total tannin content was determined using the colourimetric method described by Tempel, (1982) with slight modifications. Briefly, to 4 ml of sample an amount of 2 mL of distilled water and 6 mL of concentrated HCl were added. One of the two vials was heated up to 100 °C for 30 min and then cooled down. After an amount equal to 1 mL of EtOH at 95% is added and the absorbance of the obtained sample is read at 550 nm. The concentration of tannins, expressed as mg of tannin content per g_{DM} of the raw material was calculated by using the following equation (Eq. (6)):

$$C = 19.33 * \Delta D * \frac{L}{S} * \frac{m_{TOT}}{m_{DW}} \tag{6}$$

where, $\Delta D = D2 - D1$;

D1 is the absorbance of the unheated vial, D2 is the absorbance of the heated vial;

L/S = liquid-to-solid ratio;

 m_{TOT}/m_{DW} = ratio between the total mass of the raw material and the mass of the dry matrix.

IV.5.7 Determination of lycopene content

The lycopene content of the samples was determined following the reduced volume lycopene assay reported by Fish et al. (2002), with slight modifications. Briefly, the mixture consisting of 0.05% (*w/v*) BHT in acetone, 95% ethanol, and hexane, in a 1:1:2 ratio, was added to the sample with a solid-to liquid ratio of 0.05 (g/mL). Vials were laid on their sides in a

container, covered with a second container that contained ice and placed in an orbital shaker at 180 rpm for 15 min. After 15 min of shaking, 3 mL of distilled water were added to each vial, and the samples shaken for another 5 min. Shaking was stopped, and vials were left at room temperature for 5 min to allow for phase separation. The absorbance of the hexane (upper) layer was measured at 503 nm, and the lycopene content evaluated as reported by Fish et al. (2002) and expressed as mg of lycopene per g_{DM} of the raw material.

IV.5.8 Particle size distribution (PSD) analysis

PSD of untreated and HPH-treated suspensions was analysed by laser diffraction, using a MasterSizer 2000 particle size analyser (Malvern, UK), with water at 25 °C as dispersant medium (refraction index = 1.33). The Fraunhofer approximation and equivalent sphere model was used to determine the size distribution of the suspension, from which the mean particle size expressed as volume moment mean diameter D [4,3] was evaluated for each investigated HPH processing condition.

IV.5.9 Optical microscopy analysis

The suspensions obtained after HPH treatment were analysed microscopically to investigate the effectiveness of HPH treatment in disrupting the vegetal cells. An optical inverted microscope Nikon Eclipse (TE 2000S, Nikon instruments Europe B.V., Amsterdam, Netherlands) equipped with a polarization filter, with a 10×, 20× and 40x objective, coupled to a DS Camera Control Unit (DS-5M-L1, Nikon Instruments Europe B.V, Amsterdam, The Netherlands) was used for image acquisition. Before the observation, few drops of sample were spread on a microscope slide and covered with a cover glass.

IV.5.10 Colour measurements

The effect of the HPH processing conditions on the colourimetric profile of the C suspensions, particularly reach in natural pigments, was evaluated through absolute measurements of colour parameters, namely lightness (L*), redness (a*) and yellowness (b*), of the suspensions, by the colourimeter CR-400 (Konica Minolta Inc., Tokyo, Japan). The colour difference (Δ E*) between the untreated and the HPH-treated suspensions at each investigated processing conditions was calculated according to Eq. (7), as reported by (Dattner and Bohn, 2015). The chroma (C*_{ab}), that indicates the colour purity, intensity or saturation, and the hue angle (h*_{ab}), that describes the relative amounts of redness (0°/360°) and yellowness (90°) of the sample, were evaluated according to the Eq. (8) and Eq. (9), respectively.

$$\Delta E^* = \sqrt{(\Delta L^*)^2 + (\Delta a^*)^2 + (\Delta b^*)^2}$$

$$C^*_{ab} = \sqrt{a^{*2} + b^{*2}}$$
(8)

$$C_{ab}^* = \sqrt{a^{*2} + b^{*2}} \tag{8}$$

$$h^*_{ab} = \arctan\left(\frac{b^*}{a^*}\right) \tag{9}$$

Ten measurements were conducted for each sample.

IV.5.11 HPLC-PDA analyses of the extracts

The identification of the most abundant bioactive compounds of the extracts was performed by High-Performance Liquid Chromatography - Photodiode Array Detection (HPLC-PDA) analyses, according to the method reported by Carpentieri et al. (2022a). A Waters 1525 Separation Module equipped with a photodiode array detector Water 2996 (Waters Corporation, USA) was used. Analytical separation of the analysed compounds was carried out in a Waters Spherisorb C18 reverse phase column (5 µm ODS2, 4,6 mm x 250 mm, Water Corporation, USA). Prior to HPLC analysis, the extracts were filtered with 0.20 µm filters and then diluted with the extracting solvent used to obtain each extract analysed. The mobile phase consisted of (A) phosphoric acid in water (0.1%, v/v), and (B) methanol. For compounds separation, the following gradient was used: 0-30 min from 5% B to 80% B, 30-33 min 80% B, 33-35 min from 80% B to 5% B. The injection volume and the flow rate of the mobile phase were 5 µL and 0.8 mL/min, respectively. The quantification of each compound was carried out at the wavelength of maximum absorbance λ = 271 nm for gallic acid, 320 nm for chlorogenic acid and cynarine, caffeic acid and p-coumaric acid, 280 nm for catechin, epicatechin and phlorizin, 283 nm for naringin, 260 nm for rutin, and 330 nm for sinapic acid. The commercial standards were dissolved into the extraction solvent to generate standard calibration curves ($R^2 = 0.980 - 0.998$). The results were expressed as mg of the target compound/g_{DM} of the raw material.

The same equipment was utilized for the identification of anthocyanins in the extracts by following the method described by Lee et al. (2008). The mobile phase consisted of (A) 100%, v/v acetonitrile, and (B) 10%, v/v acetic acid and 1%, v/v phosphoric acid in water. The injection volume and the flow rate of the mobile phase were 25 µL and 1.0 mL/min, respectively. A linear gradient consisting of 0-25 min from 2% A to 20% A, 25-30 min from 20% A to 40% A was used, with simultaneous detection at the wavelength of 280 and 520 nm. The commercial standard was dissolved into the extraction solvent to generate standard calibration curves ($R^2 = 0.988$). The results were expressed as mg of the target anthocyanin/g_{DM} of the raw material.

IV.5.12 Thermal stability kinetics

Although the quality of the product is important, it is even more important to ensure that, after the processing, storage, and preparation (cooking) of the product, the active ingredients possess a high bioavailability, and therefore are able to enter into circulation after consumption to exercise an active and beneficial effect (Preedy, 2014). To this purpose, the obtained dry extracts were then subjected to thermal stability analysis, in terms of total polyphenols (§ IV.5.1), antioxidant activity (§ IV.5.3), and lycopene content (§ IV.5.7). The extracts were solubilized in distilled water, and placed in ovens (Heraeus, Hanau, Germany) and subjected to four different temperatures simulating the pasta production process and cooking phases (25 °C, 40 °C, 70 °C, 100 °C). Aliquots of extracts were taken at different exposure times (60 min – 8 h) and furtherly analysed to obtain thermal stability kinetics. The obtained results were expressed as mg GAE, mg AAE, and mg lycopene per g_{DW} of the dry extract, for TPC, antioxidant activity, and lycopene content, respectively.

IV.5.13 Water absorption capacity and solubility index

The water absorption capacity and the solubility index of the dry extracts as the capacity of re-suspension after the stabilization process by freeze-drying were determined. Water absorption capacity was determined by the method of Gull et al. (2015). 2.5 g of sample were dispersed in 25 g of distilled water, and then stirred for 30 min. The dispersions were rinsed into centrifuge tubes, made up to 32.5 g and then centrifuged ($4000 \times g$, 15 min). The supernatant was decanted for determination of its solid content and sediment was weighed. WAC was calculated as grams of sediment (obtained after removal of the supernatant) per unit weight of original dry solid sample. As an index of water solubility, the amount of dried solids recovered by evaporating the supernatant was expressed as percentage of dry solids in the sample (Yousf et al., 2017).

IV.6 Statistical analysis

All the analyses were carried out in triplicate and the results were reported as means \pm standard deviations. Differences among mean values were analysed by one-way variance (ANOVA), by using SPSS 20 (SPSS IBM., Chicago, USA) statistical package. Tukey test was performed to determine statistically significant differences (p < 0.05).

The FC-CCD design and the analysis of the data were performed using the software package Design Expert Version 12 software (Minneapolis, MN). Five replicates of the optimal conditions were performed to validate the models.

Materials & Methods PART B - Functional pasta

IV.7 Raw materials

In this thesis work, durum wheat semolina was provided by a local pasta producer company (Lucio Garofalo S.p.a., Gragnano, Italy) and stored in sealed BOPP bags until use. The semolina was completely characterised and its chemical composition was determined according to the AOAC Official Methods 925.10, 920.152 (conversion factor 5.70), 923.03 and 922.06 for moisture, protein, ash and fat content, respectively. Total dietary fibre was determined as described in § IV.1. The extraction of gluten was carried out manually using a solution of monosodium phosphate and bisodic phosphate, in accordance with the method described by Tateo (1980). Total starch (TS) content was determined by a commercial kit (Amyloglucosidase/α-Amylase Method, Megazyme K-TS, Wicklow, Ireland) according to AOAC Method 996.11 and AACC Method 76-13.01. The amylose content was determined by a commercial kit (Megazyme K-TS, Wicklow, Ireland) according to the official assay procedure K-Amyl 06/18. The same methodologies were used also to analyse the dry pasta samples. On the other hand, particle size distribution and colourimetric parameters of semolina were determined by dynamic light scattering (DLS), using a Malvern Mastersizer 2000 instrument (Malvern Instruments Ltd., Worcestershire, UK), and a colourimeter CR-400 (Konica Minolta Inc., Tokyo, Japan), respectively.

Together with the semolina, tap water was also used in this investigation for the production of pasta. For optimal pasta quality, the water must have specific physical and chemical characteristics, pH comprised between 6.6 and 6.9, a maximum mineral content of 400-500 mg/L, with a maximum content of calcium and magnesium carbonates of 180-200 mg/L, because of their influence on gluten network development (Manthey and Twombly, 2005). In the following tables (Table IV.6 and Table IV.7) the main characteristics of the semolina and water used in this Ph.D. investigation are listed.

Table IV.6 *Chemical and colour parameters of durum wheat semolina.*

(% dw)			Chamia	emical characterisation					Colourimetric			
			Chemic	ai ciiaiac	terisation	parameters						
Moisture	Protein	Ash	Gluten	Fibre	Starch	Lipid	Amylos e	L*	a*	b*		
14.3±	13.3±	0.6±0	11.3±	4.5±	66.4±	0.86±	19.4±	67.7	1.6±	20.8±		
0.9	0.5	.04	0.5	0.1	1.0	0.1	0.8	± 0.3	0.0	0.3		

Table IV.7 *Chemical and physical characteristics of tap water used in this Ph.D. investigation.*

рН	Residue at 180°C mg/L*	Hardness °F	Electrical Conductivity µS/cm	Calcium mg/L*	Magnesium mg/L*	Chloride mg/L*	Sodium mg/L*
7.7±	334	18.2±	472.0±	69	29	12	7
0.9		1.9	5.5				

All the values represent the average of at least three measurements. *Provided by GORI acqua.

The chemical and colour properties of the semolina sample are in agreement with the characteristics of high standard quality semolina as described elsewhere (Aravind et al., 2012; de Cindio and Baldino, 2015; Horvat et al., 2021; Sissons et al., 2012).

Likewise, the used semolina possessed a PSD profile with a representative second modal distribution with a mean diameter of 400 μ m, characteristic of coarse particles, in agreement with those reported for commercial semolina, where sizes from 150 to 450 μ m are preferentially required in large-scale manufacturing plants (Jalgaonkar and Jha, 2016).

IV.8 Solvents and chemicals

 α -amylase (A3176, \geq 5 U/mg) from porcine pancreas, pepsin (P7000, 674 U/mg) from porcine gastric mucosa, pancreatin (P3292, 4xUSP) from porcine pancreas, bile salts (B8756), and all the solvents, chemicals, and reagents involved in the analyses were purchased from Sigma Aldrich (Steinheim, Germany). All the standards used for HPLC–PDA analysis were provided by Acros Organics (Geel, Belgium). CellROX® Green Reagent was purchased from Invitrogen (Invitrogen S.r.l., Milan, Italy). Human THP-1 monocytic cell lines were obtained from the American Type Culture Collection, where they were authenticated, stored according to the supplier's instructions and used within 4 months after recovery of the frozen aliquots.

IV.9 Pasta Production – Sample processing

A fresh pasta production processing line was designed and implemented at lab-scale, focused on its standardisation for the subsequent scale-up of a defined and parameterised process to produce the functional pasta with optimal formulation.

To produce pasta, the following equipment was used:

- Heater (Argo LAB, M3-D, Modena, Italy)
- Pasta extruder (SIRMAN S.p.a., Pieve di Curtarolo (PD), Italy)
- Bronze die for maccheroncini shape (Figure IV.7)

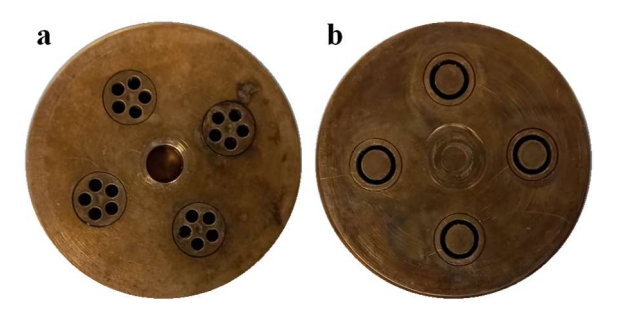


Figure IV.7 *Bronze die used in this Ph.D. investigation. Internal top view* (a), external top view (b).

 Tailor-made forced air convection chamber schematized in Figure IV 8

The main role of the movement, ventilation is to emulate the first predrying phase (trabatto, 1 min, air temperature $\approx 80~^{\circ}\text{C}$) able to dry the external surface of the pasta that lost 2-3% of moisture content, thus, allowing to separate the product, to avoid the sticking, and to preserve the original shape.

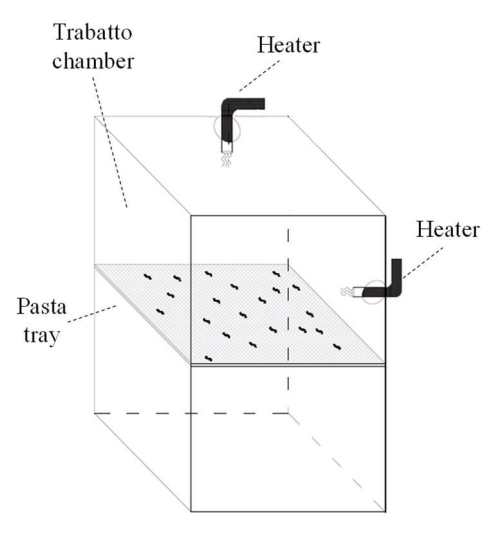


Figure IV.8 3D representation of the forced air convection chamber designed in ProdAl Scarl.

For the development of the pasta production process under standardised conditions, important factors were investigated to define the correct processing conditions (Figure IV.9).

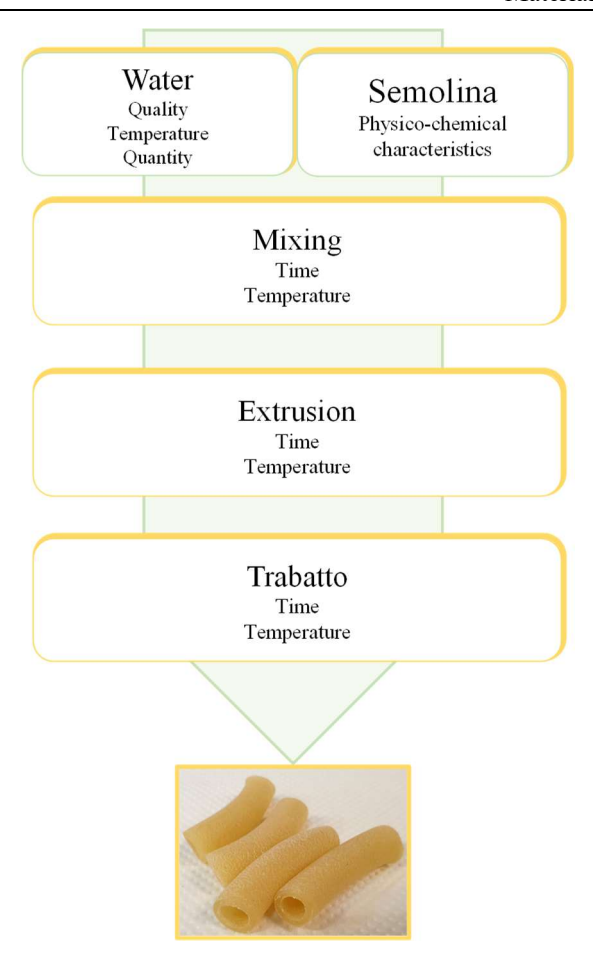


Figure IV.9 *Schematization of the pasta production process implemented at lab-scale and related investigated parameters.*

The first step of the pasta production process is the mixing step, in which the two main ingredients, semolina and water, are mixed. The main parameters that could be controlled and optimised were the mixing time (4 - 15 min), water content (28 - 32%), and water temperature (30 - 45 °C). The effect of their combination on the visual appearance and moisture content of the dough and final pasta was evaluated. The temperature of the dough and extruded pasta was monitored throughout the mixing and the extrusion phases using a probe thermometer (Delta Ohm S.r.l., HD 2128.2, Caselle di Selvazzano (PD), Italy), and no noticeable temperature increase or any overheating was recorded between the different experiments (Figure IV.10).

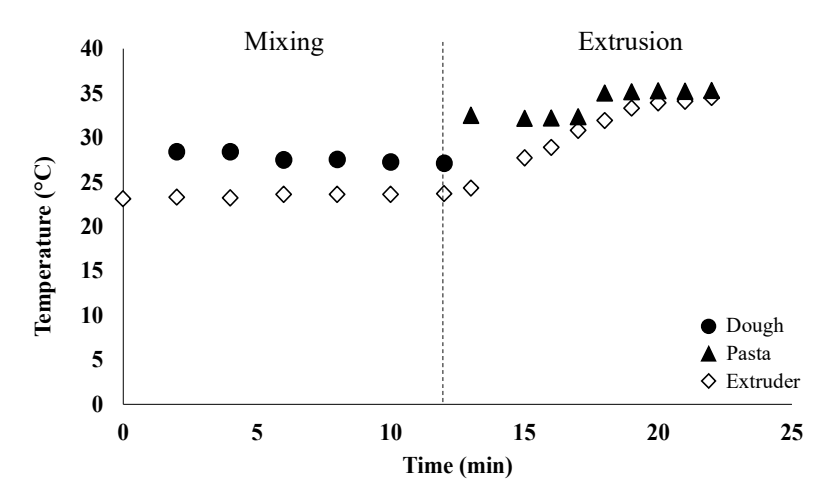


Figure IV.10 *Temperature profile of the dough, pasta and extruder after 15 min of mixing.*

The optimum mixing conditions were found to be 15 min of mixing time and 30% of water content at 45 °C. In fact, according to Dawe et al. (2001), water temperatures in the range of 40 °C improves the water absorption. Likewise, mixing times ranging from 10 to 15 min have been reported as optimal conditions for doughs formed with semolina at standardised chemical and physical properties (De Cindio and Baldino, 2015). In fact, the occurrence of white spots on pasta, indicating incomplete hydration of semolina (Manthey and Twombly, 2005), decreased with the increasing mixing time. The pasta obtained at the previously stated optimum conditions possessed a uniform texture and no superficial white spots were present.

After the standardisation of the mixing and extrusion conditions, to define the optimal concentration of extract to be added to the pasta, the effects of two different concentrations (C_1 , $C_2 = 2 C_1$), chosen according to the daily theoretic amount of the target bioactive compound to be taken for health benefits, on the moisture profile, colour, sensory profile, texture profile, microstructure, and bioactivity of pasta after mixing, extrusion, trabatto, and cooking phases (data not shown), were evaluated as described in § IV.10.

The obtained results led to select C_1 as the best concentration of extracts to be added to the pasta since a higher concentration showed a significant decrease in the compactness values of the final pasta than the control, and a strong influence on its colourimetric profile, which contributed to lower the acceptability in terms of colour, as emerged by the sensory analysis (Figure IV.11).

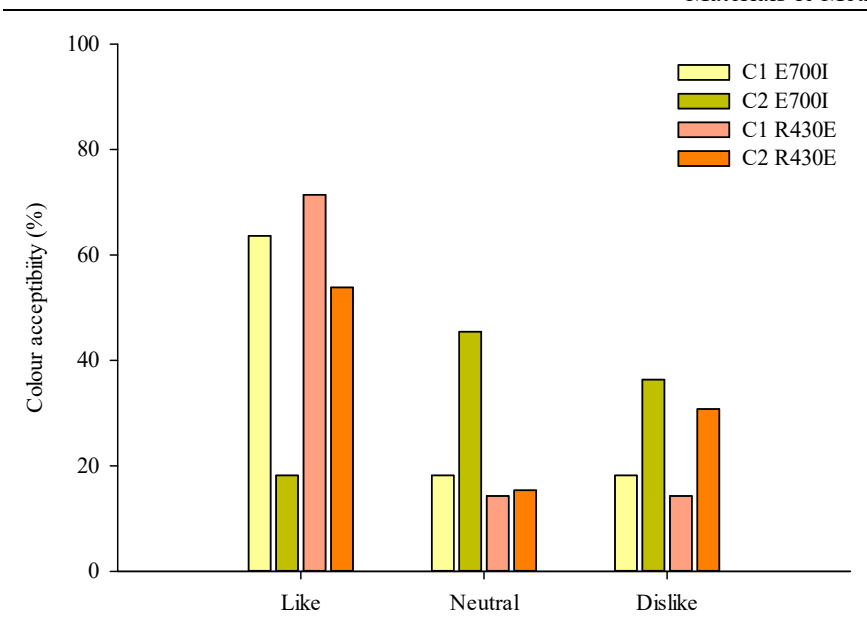


Figure IV.11 Acceptability by panelists in terms of colour of the E700I and R430E pasta samples.

Once the production process was standardised, the traditional pasta and six different types of pasta (R430E, E700I, D701GN, O112H, N309BN, B520GP), functionalized with the obtained natural ingredients (HPH-treated E706IT, A781M, B651S total suspensions, and pure extracts from PEF-treated A113H, N433W, and G300G, respectively) were produced on a pilot scale plant at FAVA S.p.a. (FAVA impianti per pastifici, Ferrara, Italy), (Figure IV.12) simulating industrial production processing conditions for durum wheat dry pasta (extrusion pressure: 100-120 bar, ultra-high temperature drying: 3 - 4 h at 80 - 120 °C).



Figure IV.12 *Schematization of the main pasta production processing phases conducted at FAVA S.p.a.*

IV.10 Analytical determinations

IV.10.1 Colourimetric analysis

Absolute measurements of colour parameters, namely lightness (L*), redness (a*) and yellowness (b*), of samples, were determined by the colourimeter CR-400 (Konica Minolta Inc., Tokyo, Japan). The colour difference (ΔE *) between the functional pasta and the control pasta was calculated according to Eq. (10), as reported by (Dattner and Bohn, 2015).

$$\Delta E^* = \sqrt{(\Delta L^*)^2 + (\Delta a^*)^2 + (\Delta b^*)^2}$$
 (10)

Ten measurements were conducted for each sample.

IV.10.2 Sensory analysis

Descriptive analysis was used to determine sensory profiles of pasta samples, following the procedure described by Sicignano (2015), with some modifications. A panel of fifteen judges was trained for the descriptive evaluation of pasta performed in the ProdAl Scarl laboratory at the University of Salerno. The characteristic parameters monitored were brightness, uniformity, colour, odour, vegetable odour (visual and olfactory evaluation); taste, hardness, vegetable flavour (tasting evaluation); colour, odour, and overall acceptability. These attributes were selected as important features of the pasta product with good discriminatory capability between samples. An open discussion with the panel leader as a moderator was conducted. Pasta samples were cooked in unsalted boiling water until reaching OCT and immediately drained for thirty seconds. Before the panel test, and to ensure the safety of pasta samples, the latter were subjected to microbiological analysis in terms of total microbial load (ISO 4833-1:2013), yeasts and moulds (ISO 21527-1:2008) with values lower than the detection limit of the method (< 1 log colony-forming units (CFU)/g of pasta). During each session the samples were identified with a three-digit numeric code. Water was used for rinsing between samples.

IV.10.3 Texture profile analysis

Through the texture analysis, it is possible to simulate the chewing of foods by measuring the load force in compression mode, being the cutting force an indicator of the pasta compactness and hardness. The texture profile analysis of the pasta samples was conducted according to the standardised method (AACC Method 66-52.01) by using an Instron Texture analyser (Instron 4442, Norwood, MA, USA), equipped with a plexiglass blade probe.

IV.10.4 Cooking quality

The determination of the optimal cooking time (OCT) and cooking loss (CL) of the pasta samples was carried out according to the official method AACC 66.50. Water absorption index (WAI) was measured as the weight increase of pasta before and after cooking and is expressed as percent weight gain concerning the weight of uncooked pasta (Bonomi et al., 2012).

IV.10.5 Thermal properties

The thermodynamic properties of semolina and pasta samples were determined in accordance with the method described by Marti et al. (2011), by scanning differential calorimetry (DSC 204 Phoenix, Netzsch, Wittelsbacherstraße, Germany). The start temperature (Tonset), peak temperature (Tpeak), end temperature (Tendset) and enthalpy (ΔH, J/g) associated to the starch gelatinization and the formation of amylose/lipid complexes were determined by the software Proteus Analysis Software (Version 4.2/3, Netzsch, Wittelsbacherstraße, Germany) provided with the equipment.

IV.10.6 Pasting analysis

Rheological determinations of the semolina and ground pasta samples were carried out in a controlled stress and strain rheometer (AR2000, TA instruments, New Castle, DE, USA), thermally regulated by a Peltier plate and a circulating water bath (DC10-Haake K10, Karlsruhe, Germany), in accordance to the official method AACC 76-21.01 (AACC, 1999), and following the methodology used by (Kaur et al., 2012) with some modifications. The instrument was fitted with a starch pasting cell geometry with a fixed gap of 5500 μm. For the analysis, 6 g of sample were poured into the pasting cell, and 24 g of distilled water was added and kept at a fixed measurement temperature (50 °C) for 2 min to allow stress relaxation and temperature equilibration. Dynamic and isothermal ramps were carried out to determine the rheological behavior of the samples. First, an isothermal ramp (50 °C) for 10 s with a shear rate of 16 1/s was applied to homogenize the mixture. Secondly, a dynamic heating ramp from 50 °C to 95 °C was applied at 5 °C/min with a shear of 10 1/s. The sample was maintained for 60 s at 95 °C and afterward cooled down at a rate of 5 °C/min up to 50 °C. Parameters recorded for each experimentation were peak time, peak viscosity, breakdown viscosity, and setback viscosity.

IV.10.7 Microstructure

The pasta surface and cross-section microstructure was observed using a field emission scanning electron microscope (FESEM, mod. LEO 1525, Carl Zeiss SMT AG, Oberkochen, Germany). Dry pieces (3 mm length) were attached to the specimen holders using carbon tape and sputter-coated with a gold layer (Agar Auto Sputter Coater mod. 108 A, Stansted, UK) at 40 mA for 120 s. Sample images were captured with secondary electron mode at 5 kV at a maximum magnification of 1.00K X (Renoldi et al., 2021).

IV.10.8 Chemical profile

To understand the stability of functional compounds in cooked pasta and the influence of the production processing conditions of pasta on the nutritional and functional properties of the final products, the bioactivity of the pasta samples was monitored after each production step and cooking phase. To extract TPC, the methodology reported by Crizel et al. (2015) was followed with some modifications. Briefly, uncooked and cooked pasta was freezedried, ground and sieved through 35 mesh (500 µm) sieve. The sample was homogenized with a methanol:water (80:20 v/v) solution acidified with 1% HCl (S/L ratio of 0.3 g/mL) in an Ultra-Turrax homogenizer (IKA, Ultra-Turrax T25 digital, Germany) for 2 min. The extract was then stirred for 2 hour at 25 °C, 160 rpm (Orbital incubator SI50 system, Bibby Sterilin LTD, UK) and centrifuged (ALC International S.r.l., model PK 130R, Milan, Italy) at 6500 × g and 4 °C, for 20 min.

For lycopene extraction, the method reported by Padalino et al. (2017) was followed. The determination of TPC, antioxidant activity, and lycopene present in control and functionalized pasta (uncooked and cooked) was performed by the spectrophotometric methods reported in § IV.5.1, § IV.5.3, and § IV.5.7, respectively. The results were expressed as milligrams of standard per gram of dry sample (mg/g).

IV.11 Simulated gastrointestinal digestion

The simulated gastrointestinal digestion was assessed on pasta samples, following the international consensus procedure described by Minekus et al. (2014), with slight modifications.

IV.11.1 Oral phase

A complete simulation of the mastication and swallowing processes was implemented. Briefly, 30 g of cooked pasta samples were mixed with an equal volume of simulated salivary fluid (SSF), consisting of 5 g/L of α -amylase, 0.117 g/L of sodium chloride, 0.149 g/L of potassium chloride, 2.1 g/L of monosodium carbonate, and 0.074 g/L of calcium carbonate. Prior to the oral phase digestion step, a size reduction step by means of a mincer (Kenwood Corporation, Tokio, Japan) emulating higher mastication forces was applied according to Hoebler et al. (2000). The samples were then subjected to a physical disruption process in a controlled homogenizer (Stomacher 400, Steward, England) at 200 rpm for 1 minute, simulating the mastication and swallowing process of the oral phase.

IV.11.2 Gastric phase

The entire sample from the oral digestion step was mixed (1:1 ratio) to the simulated gastric fluid (SGF), consisting of pepsin solution (3.2 g/L), 2 g/L of sodium chloride, and 7% (v/v) hydrochloric acid 37%. Then, the mixture was adjusted to pH 3 with 1 M hydrochloric acid and incubated at 37 °C for 120 min under continuous stirring at 130 rpm (Orbital incubator SI50 system, Bibby Sterilin LTD, UK).

IV.11.3 Intestinal phase

The entire sample from the gastric digestion step was mixed (1:1 ratio) to the simulated intestinal fluid (SIF) consisting of 5 g/L of pancreatin, 0.2 g/L of calcium carbonate, 0.2 g/L of calcium chloride, 1.75 g/L of sodium chloride, and 25 g/L of bile salts. The pH was adjusted to a final value of 7 by the addition of hydrochloric acid (0.1 M) and sodium hydroxide (0.05 M), and incubated at 37 °C for 120 min under continuous stirring at 130 rpm.

IV.11.4 Total phenolic content (TPC) release

Samples, which were withdrawn after the oral phase, 60 and 120 min of gastric phase, 20 and 120 min of intestinal phase, were centrifuged at 14000 rpm at 4 °C for 20 min using an Eppendorf centrifuge (Micro Centrifuge 5417R, Eppendorf Srl, Milan, Italy). TPC were determined as described in § IV.5.1. TPC release from the samples was determined according to the following equation (Eq. (11)):

$$Release_{TPC} = \frac{TPC_i}{TPC_T} * 100 \tag{11}$$

where TPC_i is the phenolic content detected in each sample during the digestive phases, and TPC_T is the total phenolic content measured in the sample taken after 180 min of the intestinal phase, assuming that, 60 min after the intestinal phase, the complete disintegration of the pasta matrix occurred.

IV.11.5 Starch digestibility

IV.11.5.1 Starch nutritional fractions

Starch can be classified by its digestibility in the human body, more specifically in the small intestine. For nutritional purposes, starch is classified into rapidly digestible starch (RDS), slowly digestible starch (SDS) and resistant starch (RS), depending on the rate and degree of its assimilation (Cummings, 1992).

The values of RDS, SDS and RS fractions in each sample were determined according to Eq. (11), (12), and (13):

$$RDS(\%) = \frac{H_{20}}{T_c} * 100, \tag{11}$$

$$SDS (\%) = \frac{H_{120} - H_{20}}{T_c} * 100, \tag{12}$$

$$RDS (\%) = \frac{H_{20}}{T_S} * 100, \tag{11}$$

$$SDS (\%) = \frac{H_{120} - H_{20}}{T_S} * 100, \tag{12}$$

$$RS (\%) = \frac{TS - H_{120}}{T_S} * 100, \tag{13}$$

where, H₂₀ and H₁₂₀ are the amounts of starch hydrolysed within 20 and 120 min of the intestinal digestion step, respectively (§ IV.11.5.3), and T_S is the initial weight of starch in the sample (§ IV.11.5.2).

IV.11.5.2 Total starch content

Total starch (TS) content in the samples was determined by a commercial kit (Megazyme K-TSHK, Wicklow Ireland) following the AOAC Method 996.11 and AACC Method 76-13.01 (determination of total starch content of samples containing resistant starch). Briefly, 0.2 mL of 80% v/v aqueous ethanol were added to an aliquot of 100 mg of sample and stirred on a vortex mixer to completely wet and disperse the sample. 2 mL of sodium hydroxide 1.7 M were added and stirred on a vortex mixer until complete dilution. 8 mL of sodium acetate buffer (600 mM) containing 5 mM of calcium chloride, 0.1 mL of thermostable α-amylase and 0.1 mL of amyloglucosidase were added to the mixture, which was then incubated in a water bath (PBI international N. 54270, Milan Italy) for 30 minutes at 50 °C. The solution was then removed from the water bath and cooled at room temperature.

2 mL of the sample were centrifuged at 13.000 rpm for 5 min. An aliquot of 0.1 mL was then mixed with 3 mL of GOPOD reagent. The resulting mixture was incubated for 20 minutes at 50 °C. The absorbance of the solution was measured at 510 nm against a blank consisting of 0.1 mL of sodium acetate buffer 100 mM and 3 mL of GOPOD reagent. The percentage of total starch in the sample was calculated according to Eq. (14), which was provided by the kit manufacturer.

$$T_S\% = \Delta A * F * \frac{EV}{0.1} * \frac{100}{W} * \frac{1}{1000} * \frac{162}{180}$$
 (14)

where:

 ΔA is the absorbance of sample solution read against reagent blank; F is a factor to convert absorbance values to µg glucose (100 µg glucose divided by the GOPOD absorbance value for 100 µg of glucose); EV is the sample extraction volume (equal to 10.4 mL in our case); 0.1 mL is the volume of sample analysed; 100/W is the conversion factor to 100 mg sample; W = sample weight in mg;

162/180 is the factor to convert from free glucose, as determined, to anhydroglucose, as occurs in starch.

IV.11.5.3 Hydrolysed starch

Due to a large amount of starch in the pasta samples, the digestibility was determined by the degree of hydrolysis of the starch in each digestive phase. Starch is hydrolysed by the enzymatic action of α -Amylase in salivary and intestinal fluids, transforming starch into maltodextrin.

Therefore, the following process quantifies the concentration of maltodextrin in the sample and evaluates the percentage of hydrolysed starch in the original sample. 0.2 mL of sample were diluted in 10 mL sodium acetate (100 mM) buffer solution and calcium chloride (5 mM) pH 5.0, then 0.1 mL amyloglucosidase were added. The test tube was shaken vigorously and then immersed in a hot water bath at 50 °C for 30 minutes. Blank solutions were prepared similarly, but replacing the sample and amyloglucosidase with the buffer solution. 2 mL of the sample were centrifuged at 13.000 rpm for 5 minutes. An aliquot of 0.1 mL of each sample was then mixed with 3 mL of GOPOD reagent. The resulting mixture was incubated for 20 minutes at 50 °C. The absorbance of the solution was measured at 510 nm against a blank consisting of 0.1 mL of sodium acetate buffer 100 mM and 3 mL of GOPOD reagent. The percentage of hydrolysed starch in the different digestion phases was calculated according to Eq. (14).

IV.12 Biological activity

IV.12.1 Sample preparation

To evaluate the potential health beneficial effects of the different produced functional pasta, the biological effects, in terms of cell viability, antiinflammatory properties, and glucose uptake, on human cell lines, such as hepatocarcinoma cells (Hep-G2), colorectal adenocarcinoma cells (CACO-2), liposarcoma cells (SW-872), and circulating monocytes of leukemia (THP-1) were investigated. The samples subjected to these analyses were obtained after cooking and in vitro digestion of the pasta samples (§ IV.11.1 - § IV.11.3), collected and freeze-dried (25 L VirTis Genesis freeze-drier (SP Scientific, USA) at P = 50 mbar for 24 h, by setting the plate temperature at 25°C). Subsequently, the dry samples were diluted in distilled water to obtain solutions at the different concentrations to investigate ($C_1 < C_2 < C_3 < C_4$), the range of which was assessed on the basis of the amount of extract (mg) present in the real average amount of dry pasta eaten per day per person, and the volume of fluid (mL) that flows from the terminal tract of the small intestine into the colon at the end of the digestive process. Specifically, C₃ corresponds to the addition of the functional ingredient to the pasta at the concentration C_1 .

IV.12.2 Cell Viability Assay

For the cell viability assay, 7000 Caco-2 and HepG2 cells were seeded into 96-well plates for 24 h. The cells were exposed for 12 h and 24 h to the different investigated sample concentrations, dissolved in distilled water. The 3-(4,5-dimethylthiazol- 2-yl)-2,5-diphenyltetrazolium (MTT) assay was used to evaluate the cell viability, as previously described elsewhere (Rovito et al., 2016). The absorbance was measured at a test wavelength of 570 nm in a Multiskan SkyHigh Photometer (Thermo Fisher Scientific, Milan, Italy). The data were reported as the percentage of viable cells compared to the control (100%).

IV.12.3 Real-Time RT-PCR Assays

From cells treated according to the experimental conditions reported in § IV.12.2, total RNA was extracted as previously reported by Giordano et al. (2016). Using SYBR Green Universal PCR Master Mix, 2 L of diluted (1:10) cDNA was determined in duplicate by real-time PCR, analysed in an iCycler iQ Detection System (Bio-Rad, Hercules, CA, USA), with 18S mRNA content being used to normalize each sample. Relative gene expression levels of Interleukin (IL)-6, and Monocyte Chemoattractant Protein (MCP)-1 were calculated as previously described by Augimeri et al. (2019).

IV.12.4 Enzyme-Linked Immunosorbent Assay (ELISA)

Interleukin (IL)-6, and Monocyte Chemoattractant Protein (MCP)-1 levels were measured in supernatants from M₀ macrophages (negative control) exposed for 1 h to different concentrations of sample, dissolved in distilled water and then treated with 10 ng/mL of lipopolysaccharides (LPS) for 24 h. M₀ macrophages treated with LPS were used as positive controls. IL-6, and MCP-1 concentrations were detected using the ELISA kit (Thermo Fisher Scientific, Waltham, MA, USA). The results were presented as pg/mL.

IV.12.5 Glucose uptake

Glucose uptake activity was analysed by measuring the uptake of 2-NBDG (2-(N-(7-Nitrobenz-2-oxa-1,3-diazol-4-yl)Amino)-2-Deoxyglucose) used as fluorescent tracer, according to the method used by Nwakiban et al. (2020). SW872 cells (human liposarcoma cells) were cultured in well black plates for 48 h. Cells were then incubated with the sample for 24 h. Finally, 500 μM H_2O_2 was then added for the last incubation hour. Subsequently, to determine 2-NBDG uptake, cells were incubated with 80 μM 2-NBDG and 0.1 mM

insulin (dissolved in glucose-free medium) for 1 h, and then were washed twice with ice-cold PBS to stop further uptake.

2-NBDG fluorescence intensities were measured using a microplate reader (EnSpire, PerkinElmer) at excitation and emission wavelengths of 465 and 540 nm, respectively. Results were expressed as Mean Fluorescent Intensity (MFI).

IV.13 Statistical analysis

All the analyses were carried out in triplicate and the results were reported as means \pm standard deviations. Differences among mean values were analysed by one-way variance (ANOVA), by using SPSS 20 (SPSS IBM., Chicago, USA) statistical package. Tukey test was performed for the physicochemical characterisation of the pasta samples, Student's t-test for the analysis of the biological effects in cell cultures. Statistical significance was set at p < 0.05.

Section I

Natural-based ingredients from agri-food by-products and herbs: production and characterisation

Chapter V – Pulsed Electric Fields - and High Pressure Homogenization - assisted extraction of intracellular compounds from the selected agri-food by-products and herbs

Chapter VI – Formulation and realization of the functional ingredients

Abstract

In this chapter, the efficiency of PEF-assisted extraction of bioactive compounds from G300G, A113H by-products, and N433W was investigated. Optimal PEF processing conditions (E = 3 - 4.6 kV/cm; WT = 5 - 20 kJ/kg) were determined based on the cell disintegration index (ZP) of the plant cell tissues for the subsequent PEF-assisted extraction experiments.

For solid-liquid extraction (SLE) process the effects of temperature, time, and solvent concentration on total phenolic content (TPC), flavonoid content (FC), total anthocyanin content (TAC), tannin content (TC), and antioxidant activity (FRAP) of the extracts from untreated and PEF-treated samples were assessed. Likewise, to fully recover the total matrix and investigate a more disruptive cell disintegration mechanism, able to unlock molecular complexes or high-molecular weight molecules, HPH treatment was applied for E706IT, A781M by-products, and B651S. The optimal treatment conditions (np = 10 - 15, P = 80 MPa, and T = 25 °C) were defined evaluating their extent on the recovery of intracellular compounds, particle size, and colourimetric profile in the case of E706IT. The phenolic composition of the obtained extracts were analyzed via HPLC-PDA analysis.

Results reveal that the application of PEF-assisted extraction at optimal processing conditions enhanced the extractability of FC (60%), TAC (23%), and TC (42%) from G300G, TPC (50%, on average) and FRAP values (45%, on average) from G300G, A113H, and N433W compared with the control extraction. HPLC-PDA analyses showed that the most abundant phenolic compounds were identified, among which catechin, epicatechin, chlorogenic acid, and phlorizin, and no degradation of the specific compounds occurred upon PEF application.

HPH induced a significant increment in the recovery of TPC (33%, on average), antioxidant activity (26%, on average), and lycopene (42%) from E706IT, A781M, and B651S. HPH treatment enhanced also the extractability of macromolecules, such as proteins and dietary fibres, and led to a significant reduction in the mean particle size of the HPH-treated suspensions (up to 8-fold) compared to the untreated ones, enhancing their homogeneity and smoothness.

V.1 Introduction

The raw materials selected in this investigation (G300G, A113H, E706IT, A781M) are among the most widely cultivated vegetable crops in the Mediterranean countries. Important amounts of these matrices are consumed in the form of processed products, therefore during the industrial processing large quantities of by-products are generated (Panzella et al., 2020; Zuin and Ramin, 2018). G300G, F500A, A113H, E706IT, A781M residues have been underexploited so far, being usually used for low value-added applications (Erinle et al., 2022), such as animal feed, or waste-based compost, while the majority is disposed of in landfills (Panzella et al., 2020). These matrices retain appreciable amounts of phenolic compounds with significant antioxidant activity, that can be recovered due to their nutritional properties and health-beneficial potential consisting in anti-inflammatory, antimicrobial, hypolipidemic, anticarcinogenic and prebiotic activities, among others (Anal, 2018; Cobb, 2014; Viuda-Martos et al., 2014; Carpentieri et al., 2021b).

In this line, the application of PEF treatment prior to SLE is gaining great interest as a mild, energy efficient, and scalable cell disruption technology (Carullo et al., 2020), leading to the permeabilization of cell membranes (Carpentieri et al., 2022a).

To date, only few studies focused on the optimization of the whole PEF-assisted extraction process of valuable compounds from these by-products, necessary to fully understand the possible benefits of PEF-assisted extraction process compared to SLE (Carpentieri et al., 2022a).

Therefore, the main aim of this chapter was to investigate the potential of PEF pre-treatment to enhance the extraction of intracellular valuable compounds from the selected matrices, through the optimization of the PEF-assisted extraction process. PEF processing conditions were optimized by RSM to

define the minimum treatment severity that maximize the cell disintegration index (Z_p) of the tissues, by assessing the effect of different combinations of electric field strength (E) and total specific energy input (W_T) on Z_p . RSM was also used to optimize the solid-liquid extraction (SLE) process during both conventional and PEF-assisted extraction process.

However, since several bioactives are localized inside the vesicles of the plastid arranged within the inner part of the lipid bilayer, appearing as complexes or solid microcrystals (Colle et al., 2010; Jurić et al., 2019), their recovery requires intensive thermal or mechanical treatments and organic solvents, with negative effects in terms of environmental sustainability. To this purpose, High-Pressure Homogenization (HPH) has been often used in food processing as a novel homogenization technology, that turned out to an effective method to micronise plant tissue in suspension, unlocking the high-molecular weight bioactive compounds entrapped in cells with high extraction yields (Jurić et al., 2019).

Therefore, the other goal of this chapter is to investigate the possibility to fully recover and valorise cheap sources of high-added value compounds, such as E706IT, A781M by-products, achieving the "zero waste" policy, through HPH technology and using water as solvent. Moreover, the present study aimed to evaluate the appropriate processing conditions for enhancing the recovery of intracellular compounds, such as lycopene, polyphenols, and polysaccharides, and to elucidate the effect of HPH structural changes on the physical properties of the processed suspensions.

This chapter also focused on investigating the extraction assisted by PEF and HPH of bioactive compounds from two matrices of herbaceous origin, namely N433W and B651S, respectively, allowing to forecast further applications of this kind of materials.

V.2 Materials and Methods

V.2.1 Raw materials and samples preparation

The preparation of raw materials and their sampling was described in § IV.1, and § IV.3.2.

V.2.2 Samples processing

PEF- and HPH- assisted extraction processes of target compounds from the selected matrices were reported in "Samples processing" section specifically for PEF § IV.3.2 (G300G, A113H, N433W) and for HPH § IV.4.2 (E706IT, A781M, B651S), respectively.

The experimental apparatus utilized for PEF and HPH treatments were described in § IV.3.1, and § IV.4.1, respectively. All the experiments were carried out at least in triplicate.

V.2.3 Analytical determinations

The obtained extracts from untreated, PEF-treated, and HPH-treated samples were analysed in terms of TPC, FC, TC, TAC, lycopene content, and antioxidant power as previously described in § IV.5. Untreated and HPH-treated suspensions were analysed also in terms of particle size distribution (PSD), optical microscopy, and colour measurements (§ IV.5.8 – § IV.5.10).

V.3 Results and discussion

V.3.1 Pulsed electric field-assisted extraction (G300G)

V.3.1.1 Optimization of PEF processing conditions

To obtain a quantitative measure of the degree of cell membrane permeabilization, the cell disintegration index (Z_p) has been evaluated for samples subjected to different PEF treatment conditions, as shown in Table V 1

Table V.1 Actual values of the two independent variables investigated and response of the dependent variable (Z_p) of the PEF-treated G300G tissue.

Run	Vari	ables	Response				
	E (kV/cm)	$W_T(kJ/kg)$	Z_p				
1	0.5	1	0.033 ± 0.003^a				
2	0.5	10.5	0.075 ± 0.002^{b}				
3	0.5	20	0.130 ± 0.015^{c}				
4	2.75	1	0.208 ± 0.034^d				
5	2.75	10.5	$0.513 \pm 0.020^{\rm f}$				
6	2.75	20	0.580 ± 0.010^g				
7	5.0	1	0.417 ± 0.009^{e}				
8	5.0	10.5	$0.521 \pm 0.010^{\rm f}$				
9	5.0	20	$0.700 \pm 0.007^{\rm h}$				

The results are expressed as mean \pm standard deviation (n=2 for factorial and axial points, n=5 for central point). Values with different lowercase letter within the same column are significantly different (p \leq 0.05).

It has been effectively demonstrated that Z_p is a reliable indicator of the cell membrane permeabilization degree induced by PEF treatment on several agrifood by-products tissues (Barba et al., 2015; Boussetta et al., 2009; Brianceau et al., 2015; Carpentieri et al., 2022a, 2021a; Frontuto et al., 2019; Pataro et al., 2020). Based on the experimental design, the effect of the input variables, such as electric field strength and energy input, on the Z_p value of PEF-treated G300G tissue were reported in Table V.1.

Results reveal that the extent of cell membrane permeabilization significantly $(p \le 0.05)$ increased with increasing the field strength and energy input, with the difference being not significant ($p \le 0.05$) only when the field strength was changed from 2.75 to 5 kV/cm at a fixed energy input (10.5 kJ/kg). Moreover, in the range of the investigated PEF treatment conditions, the effect of field strength appeared slightly more pronounced than that of the energy input. The highest Z_p (0.70) value was detected when the most intense PEF treatment was applied (5 kV/cm and 20 kJ/kg). The increment of Z_p values with increasing the intensity of PEF treatment is consistent with previously reported findings for different plant tissues (Carpentieri et al., 2022; Brianceau et al., 2015; Frontuto et al., 2019). As an example, in the study of Carpentieri et al. (2022a), who investigated the optimization of PEF-assisted extraction of phenolic compounds from white grape pomace, the electric field strength applied showed a remarkable influence on the Z_p value, while the effect of energy input appeared more evident especially at lower field strengths. In particular, the highest value of the cell disintegration index (0.80) was attained at an electric field strength of 5 kV/cm and an energy input of 10.5 kJ/kg. The apparent higher resistance to the electropermeabilization treatment exhibited by the G300G tissues in the present work might be ascribed to their higher content in insoluble dietary fibres (cellulose, hemicellulose, lignin), as compared to the matrix investigated by Carpentieri et al. (2022a), which, therefore, might hinder the electroporation of the cell envelope of G300G

A second-order polynomial model (Eq. (2)) was selected to better fit the obtained data from the experimental design (FC-CCD). The p values and significance, as well as the determination coefficient (R^2) and the Root Mean Square Error (RMSE) of each investigated variable and the polynomial model are reported in Table V.2.

Table V.2 Analysis of variance (ANOVA) of the second polynomial model for the cell disintegration index (Z_p) of PEF treated G300G tissue.

Coefficients	Z_p	
β_0	-0.14843	
$\beta_1(E)$	0.24029	***
$\beta_2 (W_T)$	0.01899	***
β_{12} (E x W _T)	-0.00217	ns
$\beta_{11}(E \times E)$	-0.02899	**
$\beta_{22}(W_T \times W_T)$	-0.00056	ns
p value of the model	0.0001	***
\mathbb{R}^2	0.9545	•
RMSE	0.3504	

ns not significant for p > 0.05

RMSE, Root Mean Square Error.

Results show that the linear terms of both factors (field strength and energy input) exerted a highly significant effect (p \leq 0.001) on the permeabilization degree of the plant tissue, while interactions between the single factors were not significant (p > 0.05). However, in agreement with the findings previously achieved in the by Carpentieri et al., (2022a), the electric field strength was the factor that exerted the most pronounced effect on the response variable Z_p , showing a statistically significant quadratic term with respect to the non-significant (p > 0.05) quadratic effect of the energy input. In addition, the significant negative value of the quadratic coefficient (β_{11}) suggests that the field strength can achieve an optimum value that maximizes the response variable.

The p-value of the model, also reported in the Table V.2, suggested that it was significant (p < 0.0001) for the selected response, thus corroborating the effectiveness of the model to describe the experimental data. In addition, the Root Mean Square Error (RMSE = 0.3504) and the determination coefficient $(R^2 = 0.9545)$ values indicated a good correlation between the experimental data and the predicted values. Figure V.1 depicts the 3D response surface graph that shows the interactions between field strength and energy input and their effect on the Z_p of PEF-treated G300G tissues. As previously discussed, the increase in the severity of the PEF treatment led to an increase in the cell membrane permeabilization of G300G tissues. In particular, in accordance with the coefficients and significance of each factor involved in the model, the graph demonstrates that Z_p increased almost linearly with increasing the energy input, whereas the field strength mainly affected the observed response in a quadratic way. These results confirmed the effectiveness of PEF to induce the cell membrane electroporation of G300G tissues in a mostly field strengthdependent way and allowed to select the optimal conditions with the minimum 100

^{*}Significant for $p \le 0.05$; ** significant for $p \le 0.01$; *** significant for $p \le 0.001$

electric field strength ($E_{opt} = 4.6 \text{ kV/cm}$) and total specific energy input ($W_{T,\text{opt}} = 20 \text{ kJ/kg}$) that led to the highest cell membrane permeabilization.

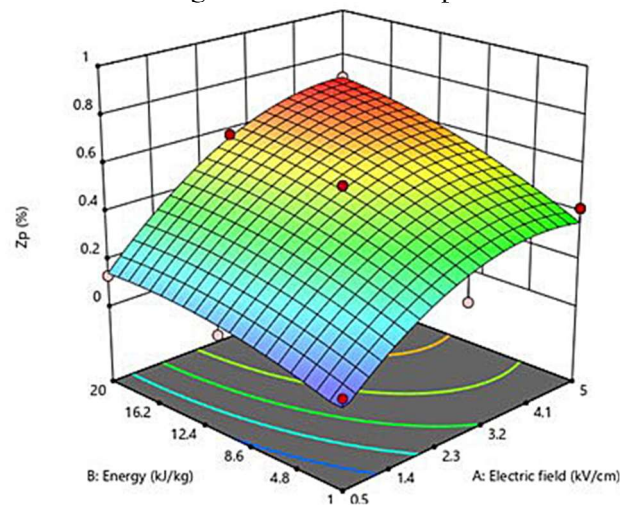


Figure V.1 Response surface for the permeabilization index (Z_p) of PEF treated G300G tissue as a function of electric field strength (kV/cm) and the energy input (kJ/kg).

V.3.1.2 Effect of PEF-assisted extraction on the recovery of bioactive compounds from G300G

V.3.1.2.1 Model fitting

In this study, the extent of three independent variables, such as extraction time, temperature, and ethanol concentration, on total phenolic content (TPC), flavonoid content (FC), antioxidant activity (FRAP), total anthocyanin content (TAC), tannin content (TC) of G300G extracts from both conventional SLE and PEF-assisted extraction was investigated (Tables V.3 and V.4) by means of the obtained experimental design (FC-CCD).

The results demonstrate that the three independent factors considerably affected all the investigated response variables. Specifically, regardless of the application of PEF pre-treatment, the maximum levels of response variables were attained at the highest extraction time (300 min), ethanol concentration (50%, v/v), and temperature (50 °C) investigated.

Results also show that the permeabilization induced by applying PEF pretreatment to G300G at the selected optimal conditions significantly intensified the extractability of TPC, FC, TAC, and TC, and led to obtain extracts with higher antioxidant activity with respect to those achieved by conventional SLE. To quantify the influence of the three investigated factors on the recovery of bioactive compounds and antioxidant activity of the extracts of either untreated or PEF-treated G300G, a two-factor interaction (2FI) model

(Eq. 3) was used to fit the experimental data obtained from the FC-CCD for all the investigated response variables.

The regression coefficients and significance of the predicted polynomial models, the determination coefficient (R²), and the Root Mean Square Error (RSME) for each variable are reported in Tables V.5 and V.6.

Results reveal that, for the extracts of either untreated or PEF-treated samples, all the investigated factors influenced, in a statistically significant linear manner, TPC, FC, and FRAP values, with a non-significant effect detected only for the linear terms of temperature and diffusion time for both TAC of untreated and TC of PEF-treated samples. Similarly, regardless of PEF pretreatment, all the interactions between single factors were significant for TPC and FRAP. In the case of FC, instead, all the interactions were significant for the control samples, while only the dependence of extraction temperature and ethanol concentration was detected in the case of PEF-treated samples. This implies that PEF-pre-treatment only amplifies the interaction of extraction temperature and ethanol concentration on the extractability of flavonoids, while decreasing the effect of temperature on diffusion time and that of diffusion time on ethanol concentration. Regarding TAC, all the interactions between single factors were not significant for the control extraction, whereas it was detected that only the extraction temperature exerted a not significant influence on the diffusion time for the PEF-treated samples. This implies that, in the investigated variables domain, PEF pre-treatment reduced the effect of extraction temperature on diffusion time, with respect to the untreated samples. Finally, only the temperature-ethanol concentration interaction for the untreated samples was found to be significant for TC. These results are partially in agreement with those found by Carpentieri et al. (2022a), who stated that all the investigated factors turned out in a statistically significant linear effect on most of the response variables (TPC, FC, and FRAP), except for the linear term of ethanol concentration in the case of FRAP values of PEF treated samples.

The analysis of variance (ANOVA) (Tables V.5 and V.6) confirmed the accurate correlation between the observed and predicted data with determination coefficients (R^2) ranging between 0.743 and 0.980. Results indicated that the selected model was significant ($p \le 0.04$) for all the responses, thus confirming its effective prediction ability.

Table V.3 Actual values of the three independent variables investigated and responses of the dependent variables (TPC, FC, and FRAP) in G300G extracts from either conventional SLE or PEF (4.6 kV/cm, 20 kJ/kg)-assisted extraction process.

Run	,	Variables	3		SLE		PEF-	-assisted extr	action
	E-W (%, v/v)	t (min)	T (°C)	TPC	FC	FRAP	TPC	FC	FRAP
1	0	30	20	$0.02 \pm$	2.44 ±	$0.69 \pm$	0.30 ±	3.94 ±	0.75 ±
				0.01^{a}	0.10^{a}	0.01^{a}	0.06^{b}	0.23 ^b	0.01^{b}
2	0	300	20	$0.12 \pm$	$4.37 \pm$	$0.68 \pm$	$0.19 \pm$	$13.26 \pm$	$0.70 \pm$
				0.11^{a}	0.54^{a}	0.03^{a}	0.15^{a}	$0.50^{\rm b}$	0.02^{a}
3	25	165	20	$1.11 \pm$	$7.03 \pm$	$0.44 \pm$	$1.17 \pm$	$7.92 \pm$	$0.47 \pm$
				0.22^{a}	0.54^{a}	0.04^{a}	0.07^{a}	0.44^{a}	0.01 ^a
4	50	30	20	$1.63 \pm$	$7.25 \pm$	$0.67 \pm$	$1.78 \pm$	$7.35 \pm$	$0.70 \pm$
				0.19^{a}	0.84^{a}	0.01^{a}	0.04^{b}	0.14^{a}	0.04^{a}
5	50	300	20	$2.42 \pm$	$13.03 \pm$	$0.99 \pm$	$2.65 \pm$	$14.11 \pm$	$1.21 \pm$
				0.20^{a}	0.72^{a}	0.10^{a}	0.26^{a}	0.21 ^b	0.02^{b}
6	0	165	35	$0.56 \pm$	$7.11 \pm$	$1.17 \pm$	$0.77 \pm$	$9.37 \pm$	$1.92 \pm$
				0.10^{a}	0.91 ^a	0.03^{a}	0.28^{a}	0.04^{b}	0.03^{b}
7	25	30	35	$0.70 \pm$	$5.27 \pm$	$0.20 \pm$	$0.94 \pm$	$7.25 \pm$	$0.34 \pm$
				0.14^{a}	0.42^{a}	0.04^{a}	0.07^{b}	0.44^{b}	0.01^{b}
8	25	165	35	$1.93 \pm$	$10.26\pm$	$1.05 \pm$	$2.77 \pm$	$17.13 \pm$	$1.08 \pm$
				0.10^{a}	0.04^{a}	0.02^{a}	0.56^{b}	0.08^{b}	0.04^{a}
9	25	300	35	$2.49 \pm$	$16.01 \pm$	$0.88 \pm$	$2.91 \pm$	$23.78 \pm$	$1.11 \pm$
				0.50^{a}	0.09^{a}	0.05^{a}	0.22^{a}	0.45 ^b	0.03^{a}
10	50	165	35	$5.20 \pm$	$19.98 \pm$	$2.28 \pm$	$5.39 \pm$	$26.22 \pm$	$2.72 \pm$
				0.11^{a}	0.21 ^a	0.22^{a}	0.07^{a}	0.94 ^b	0.10^{b}
11	0	30	50	$0.31 \pm$	$3.43 \pm$	$0.84 \pm$	$0.44 \pm$	$7.08 \pm$	$0.92 \pm$
				0.06^{a}	0.22^{a}	0.08^{a}	0.04^{b}	0.34^{b}	0.02^{a}
12	0	300	50	$1.25 \pm$	$13.40 \pm$	$1.22 \pm$	$1.39 \pm$	$15.05 \pm$	$1.23 \pm$
				0.07^{a}	0.06^{a}	0.07^{a}	0.21^{a}	0.63^{b}	0.10^{a}
13	25	165	50	$3.81 \pm$	$28.40\pm$	$2.09 \pm$	$4.37 \pm$	$29.40 \pm$	$2.10 \pm$
				0.10^{a}	0.84^{a}	0.10^{a}	0.21^{b}	0.34^{a}	0.05^{a}
14	50	30	50	$3.76 \pm$	$12.92 \pm$	$1.48 \pm$	$6.30 \pm$	$18.48 \pm$	$2.03 \pm$
				0.14^{a}	0.17^{a}	0.09^{a}	0.23^{b}	0.42^{b}	0.02^{b}
15	50	300	50	$8.30 \pm$	$36.68 \pm$	$4.58 \pm$	$9.51 \pm$	$58.53 \pm$	$5.99 \pm$
				0.11 ^a	0.48 ^a	0.15 ^a	0.02 ^b	0.39 ^b	0.12 ^b

TPC is expressed in mg GAE/g_{DM} G300G, FC is expressed in mg QE/g_{DM} G300G and FRAP in mg AAE/g_{DM} G300G. The results are expressed as mean \pm standard deviation (n = 2 for factorial and axial points, n = 5 for central point). E-W, ethanol percentage in ethanol-water mixture (%, ν/ν); t, extraction time (min) T, extraction temperature (°C).

Values of the same dependent variable with different lowercase letter within the same row are significantly different ($p \le 0.05$).

Table V.4 Actual values of the three independent variables investigated and responses of the dependent variables (TAC, TC) in G300G extracts from either conventional SLE or PEF (4.6 kV/cm, 20 kJ/kg)-assisted extraction process.

Run	,	ariables		Sl	LE	PEF-assiste	d extraction	
•	E-W (%, v/v)	t (min)	T (°C)	TAC	TC	TAC	TC	
1	0	30	20	0.02 ± 0.00^{a}	0.00 ± 0.00^{a}	0.03 ± 0.00^{b}	0.00 ± 0.00^{b}	
2	0	300	20	0.04 ± 0.01^a	0.21 ± 0.01^a	0.04 ± 0.05^b	0.22 ± 0.01^a	
3	25	165	20	0.15 ± 0.02^b	0.29 ± 0.02^a	0.12 ± 0.01^a	0.31 ± 0.01^a	
4	50	30	20	0.25 ± 0.02^a	0.66 ± 0.01^a	0.30 ± 0.01^b	0.70 ± 0.03^b	
5	50	300	20	0.41 ± 0.01^a	0.93 ± 0.01^{a}	0.44 ± 0.01^{b}	1.65 ± 0.10^{b}	
6	0	165	35	0.03 ± 0.00^a	0.15 ± 0.02^a	0.05 ± 0.00^b	0.26 ± 0.03^b	
7	25	30	35	0.10 ± 0.00^a	0.31 ± 0.10^a	0.12 ± 0.10^b	0.52 ± 0.12^a	
8	25	165	35	0.12 ± 0.01^a	0.66 ± 0.01^a	0.32 ± 0.02^b	1.62 ± 0.20^b	
9	25	300	35	0.24 ± 0.02^a	1.28 ± 0.10^a	0.34 ± 0.03^b	2.24 ± 0.20^b	
10	50	165	35	0.71 ± 0.05^a	$3.45 \pm 0.30a$	0.78 ± 0.03^b	3.19 ± 0.01^a	
11	0	30	50	0.04 ± 0.00^a	0.18 ± 0.01^a	0.05 ± 0.00^b	0.10 ± 0.01^b	
12	0	300	50	0.04 ± 0.01^a	0.40 ± 0.02^a	0.06 ± 0.01^{b}	1.21 ± 0.11^{b}	
13	25	165	50	0.56 ± 0.10^a	1.17 ± 0.10^{5a}	0.36 ± 0.10^a	1.68 ± 0.20^b	
14	50	30	50	0.23 ± 0.01^a	1.77 ± 0.10^a	0.46 ± 0.05^b	2.10 ± 0.30^a	
15	50	300	50	0.84 ± 0.05^a	3.84 ± 0.05^a	1.03 ± 0.06^{b}	5.45 ± 0.15^{b}	

TAC is expressed in mg C3G/g_{DM} G300G, TC is expressed in mg TC/g_{DM} G300G. The results are expressed as mean \pm standard deviation (n = 2 for factorial and axial points, n = 5 for central point). E-W, ethanol percentage in ethanol-water mixture (%, ν/ν); t, extraction time (min) T, extraction temperature (°C).

Values of the same dependent variable with different lowercase letter within the same row are significantly different ($p \le 0.05$).

Table V.5 Analysis of variance (ANOVA) of the two-factor interaction (2FI) models for the TPC, FC, and antioxidant activity (FRAP) in G300G extracts from either conventional SLE or PEF (4.6 kV/cm, 20 kJ/kg)-assisted extraction process.

Coefficients			SLE				PEF-assisted extraction TPC FC FRAP (mgGAE/gbM) (mgQE/gbM) (mgAAE/gbM))) 0.54185 10.9404 1.77311						
	TPC		FC		FRAP		TPC		FC		FRAP		
	(mgGAE/	(mgGAE/g _{DM}		(MD	(mgAAE/	g _{DM}	(mgGAE/	g _{DM}	(mgQE/g	g _{DM})	(mgAAE/g _{DM}		
))))		
β_0	0.71989		2.80043		1.30268		0.54185		10.9404		1.77311		
									1				
β ₁ (T)	-	**	-	**	-	*	-	**	-	***	-	**	
	0.02081	*	0.00085	*	0.01827	*	0.01224	*	0.18475		0.02757		
β ₂ (time)	-	**	-	**	-	*	-	**	-	***	-	*	
	0.00785		0.02866	*	0.00636		0.00524		0.03661		0.00805		
β ₃ (EtOH)	-	**	-	**	-	*	-	**	-	***	-	**	
	0.02682	*	0.09528	*	0.04034	*	0.04656	*	0.46701		0.06028		
β ₁₂ (T x t)	0.00028	*	0.00147	*	0.00020	*	0.00021	*	0.00197	ns	0.00024	*	
β ₁₃ (T x	0.00219	**	0.00659	*	0.00124	*	0.00335	**	0.01687	**	0.00180	**	
EtOH)								*					
β ₂₃ (t x	0.00016	*	0.00069	*	0.00011	*	0.00012	*	0.00109	ns	0.00016	*	
EtOH)													

p value of	< 0.000	**	0.0010	**	0.0062	*	< 0.000	**	0.0004	***	0.0090	**
the model	1	*		*			1	*				
\mathbb{R}^2	0.953		0.903		0.848		0.980		0.916		0.833	
RMSE	0.003		0.905		0.011		0.016		0.622		0.006	

ns not significant for p > 0.05

RMSE, Root Mean Square Error.

Table V.6 Analysis of variance (ANOVA) of the two-factor interaction (2FI) models for the TAC, TC in G300G extracts from either conventional SLE or PEF (4.6 kV/cm, 20 kJ/kg)-assisted extraction process.

Coefficients		SL	E	PEF-as	PEF-assisted extraction				
	TAC		TC		TAC		TC		
	(mgC3G/g	gdm)	(mgTC/g	$(mgTC/g_{DM})$		gdm)	$(mgTC/g_{DM})$		
$_{f eta_0}$	0.10299		-1.32124		0.12702		0.83264		
$\beta_1(T)$	-0.00221	ns	0.02295	***	-0.00342	**	-0.02976	ns	
β ₂ (time)	-0.00095	ns	0.00289	***	-0.00085	*	-0.00659	ns	
β ₃ (EtOH)	0.00005	***	0.00638	***	-0.00137	***	-0.01834	**	
$\beta_{12}(T \times t)$	0.00003	ns	-6.87·10	ns	0.00003	ns	0.00026	ns	
			6						
β_{13} (T x	0.00013	ns	0.0008	**	0.00024	*	0.00148	ns	
EtOH)									
β ₂₃ (t x	0.00003	ns	0.00005	ns	0.00003	*	0.00010	ns	
EtOH)									
p value of	0.0100	**	< 0.0001	***	0.0003	***	0.0410	*	
the model									
\mathbb{R}^2	0.815	•	0.970		0.929	•	0.743		
RMSE	0.028		0.705		0.120		0.469		

ns not significant for p > 0.05

RMSE, Root Mean Square Error.

V.3.1.2.2 Optimization of the extraction processing conditions

The single and interactive effects of extraction temperature (20 - 50 °C), diffusion time (30-300 min), and ethanol concentration (0-50%, v/v) on the level of TPC, FC, TAC, TC, and antioxidant activity of both extracts from untreated and PEF-treated G300G are depicted in the Response surface graphs reported in Figures V.2 – V.6. PEF treatment induced an increment in the concentration of TPC in the extracts as compared with the untreated samples. The same trend was observed for FC, TAC, TC, and the level of antioxidant activity.

^{*}Significant for $p \le 0.05$; **significant for $p \le 0.01$; ***significant for $p \le 0.001$

^{*}Significant for $p \le 0.05$; **significant for $p \le 0.01$; ***significant for $p \le 0.001$

Even though all the investigated variables had a statistically significant (p \leq 0.041) effect on the extraction yield of the target compounds, the ethanol concentration in water and the extraction temperature were the most influencing factors leading to the observed responses. This is also confirmed by the higher value of the linear coefficient of the ethanol concentration and temperature with respect to that of diffusion time (Tables V.5 and V.6). Moreover, regardless of the application of PEF treatment, the influence of ethanol concentration and especially that of diffusion time on the extraction yield of bioactive compounds appeared more pronounced only at extraction temperature higher than 35 °C.

The ethanol content was playing a non-negligible role in the extraction of phenolic compounds, representing one of the main factors affecting the efficiency of the extraction process (Canals et al., 2005). In addition, it is known that the exposure to ethanol of the phospholipid bilayer of plant cell membranes may alter the composition of the phospholipids, inducing a modification in the barrier properties and leading to the enhancement of the membrane permeability (Gurtovenko and Anwar, 2009). Similar results have been observed by Frontuto et al. (2019) who investigated the effect of ethanol concentration on the recovery of phenolic compounds from PEF-treated potato peels, and Aida, (2011), who reported that the extract from a medicinal plant obtained by using ethanol at 40%, v/v possessed higher amount of phenolic compounds than that obtained by using higher ethanol concentrations.

Likewise, Carpentieri et al. (2022a) found that the highest level of valuable compounds in the extract from white grape pomace was achieved at 50%, v/v of ethanol and that it decreased at higher ethanol concentrations.

Although the observed trend confirmed that the ethanol penetration-enhancing capability of solvent depends on ethanol concentration, however by exposing biological membranes to high ethanol concentrations the phospholipids dissolution is likely to occur causing the complete membrane disintegration and its subsequent death (Gurtovenko and Anwar, 2009).

Additionally, regardless of the application of PEF, results of Figures V.2 – V.6 reveal that, apart from the ethanol concentration, both extraction temperature and diffusion time significantly affected the TPC, FC, and FRAP values showing a significant linear effect on the extraction yield. It is evident that by applying an extraction temperature of 50 °C the diffusion time and ethanol concentration were more pronounced.

Results were greatly consistent with previous findings (Chanioti et al., 2021; Kwiatkowski et al., 2020; N. Rajha et al., 2013; Panzella et al., 2020), reporting that the antioxidant activity level, polyphenols, and flavonoids recovered from agri-food by-products reached the highest values at temperatures of 50 °C and 60 °C. Indeed, the temperature represents a key factor in a diffusion process, since it greatly affects the mass transfer, solubility, and diffusivity of intracellular compounds, directly and effectively

changing the properties of the biological membranes, including viscosity and permeability, through changes in the lipid composition and interactions between lipids and membrane proteins (Niu and Xiang, 2018). Nonetheless, when exposing the plant tissues to temperatures higher than 60 °C, the possible unlocking of certain phenolic compounds and the concurrent thermal degradation of others can occur.

Therefore, the values of the independent factors that maximize all the investigated variables such as TPC, FC, antioxidant activity, TAC, and TC were shown to be 50 °C, 50% ethanol-water mixture, and 300 min for extracts from untreated and PEF-treated G300G. Under these optimal conditions the TPC, FC, TAC, and TC values were 8.30 mgGAE/g_{DM}, 36.68 mgQE/g_{DM}, 0.84 mgC3G/g_{DM}, and 3.84 mgTC/g_{DM}, respectively, for the control sample, and 9.51 mgGAE/g_{DM}, 58.53 mgQE/g_{DM}, 1.03 mgC3G/g_{DM}, and 5.45 mgTC/g_{DM}, respectively, for the PEF-treated samples. A strong positive correlation was observed between the TPC, FC, TAC, FC and FRAP values, with a Pearson correlation coefficient in the range 0.88–0.89 for TPC, 0.86-0.92 for FC, 0.78-0.84 for TAC, and 0.82-0.89 TC, suggesting that phenolic compounds mostly contribute to the global antioxidant activity of the G300G extracts, as observed in previous literature works (Casazza et al., 2012; Carpentieri et al., 2022a). Therefore, the application PEF-assisted extraction process at the optimized conditions can be successfully used to intensify the extractability of phenolic compounds (15%), flavonoids (60%), anthocyanins (23%), and tannins (42%). These findings are correlated to the electroporation phenomenon that the cell membrane of plant tissue has undergone upon PEF treatment. The well-known ability of temperature and ethanol to further improve the solubility and diffusivity of the intracellular compounds through the plant tissue, and the synergistic effect of these factors with the PEF processing parameters may have contributed to ameliorating the extractability of the target compounds.

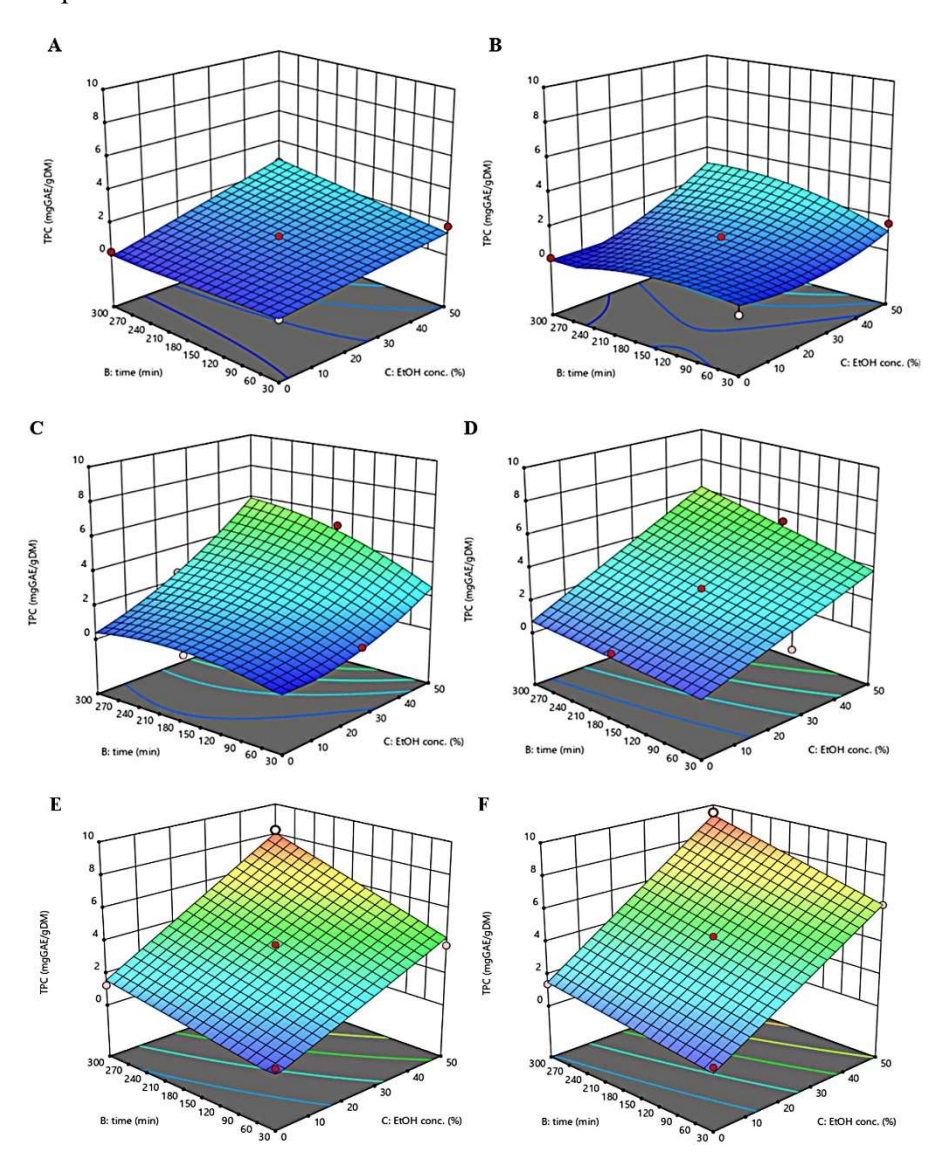


Figure V.2 Response surfaces for Total Phenolic Content (TPC) of extracts obtained from untreated (Control) (A,C,E) and PEF-treated (E = 4.6 kV/cm; $W_T = 20 \text{ kJ/kg}$) (B,D,F) G300G as a function of extraction time and ethanol concentration, with the extraction temperature set at 20°C (A,B), 35°C (C,D), 50°C (E,F).

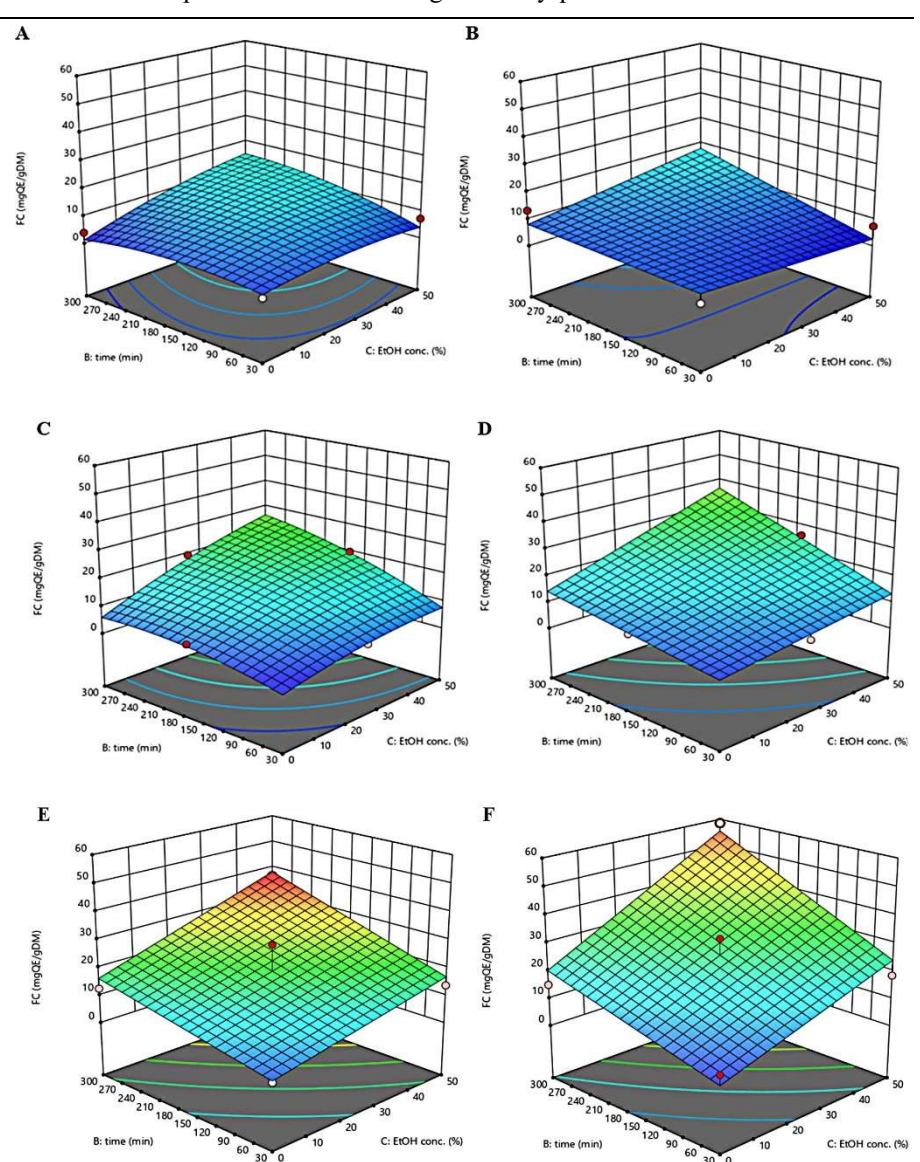


Figure V.3 Response surfaces for Flavonoid Content (FC) of extracts obtained from untreated (Control) (A,C,E) and PEF-treated (E = 4.6 kV/cm; $W_T = 20 \text{ kJ/kg}$) (B,D,F) G300G as a function of extraction time and ethanol concentration, with the extraction temperature set at 20°C (A,B), 35°C (C,D), 50°C (E,F).

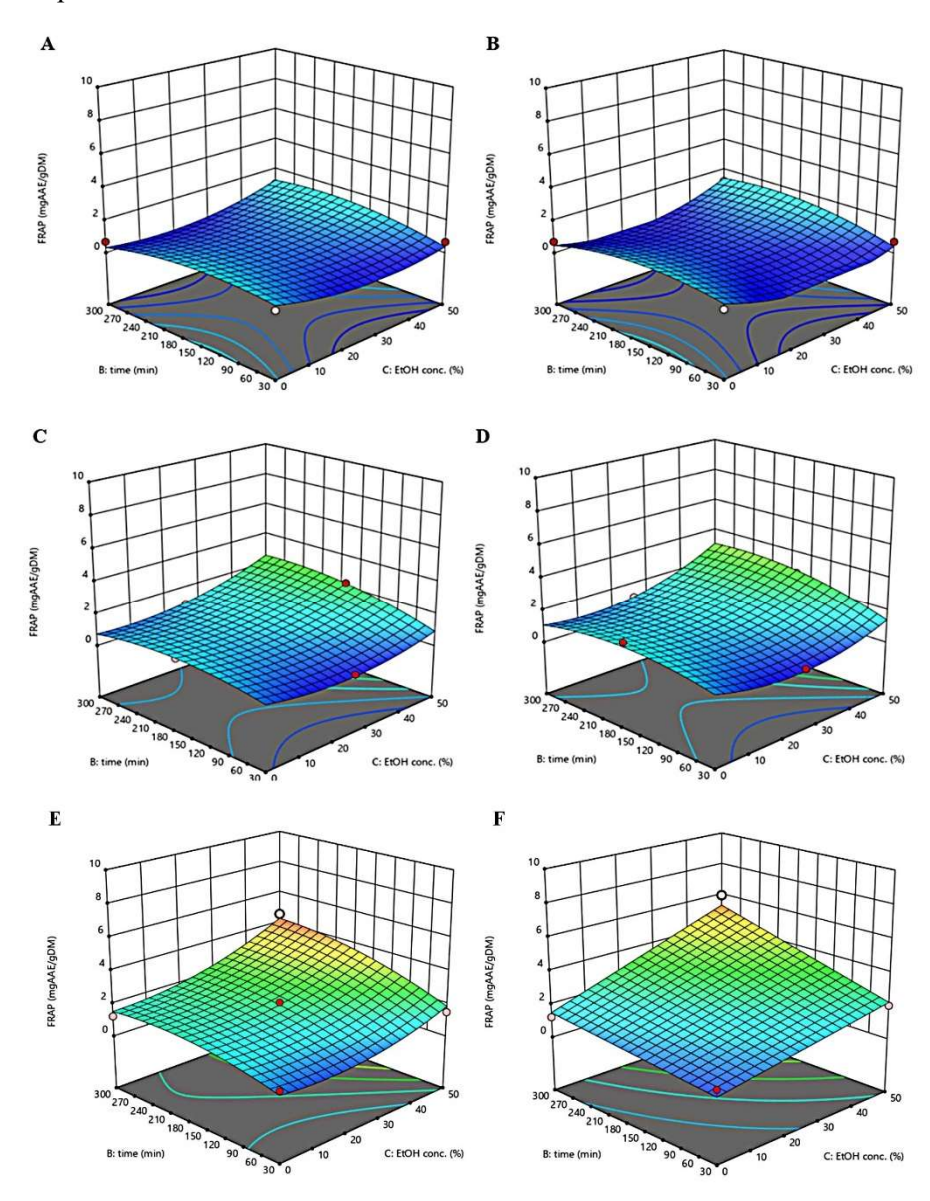


Figure V.4 Response surfaces for antioxidant activity (FRAP) of extracts obtained from untreated (Control) (A,C,E) and PEF-treated (E = 4.6 kV/cm; $W_T = 20 \text{ kJ/kg}$) (B,D,F) G300G as a function of extraction time and ethanol concentration, with the extraction temperature set at 20°C (A,B), 35°C (C,D), 50°C (E,F).

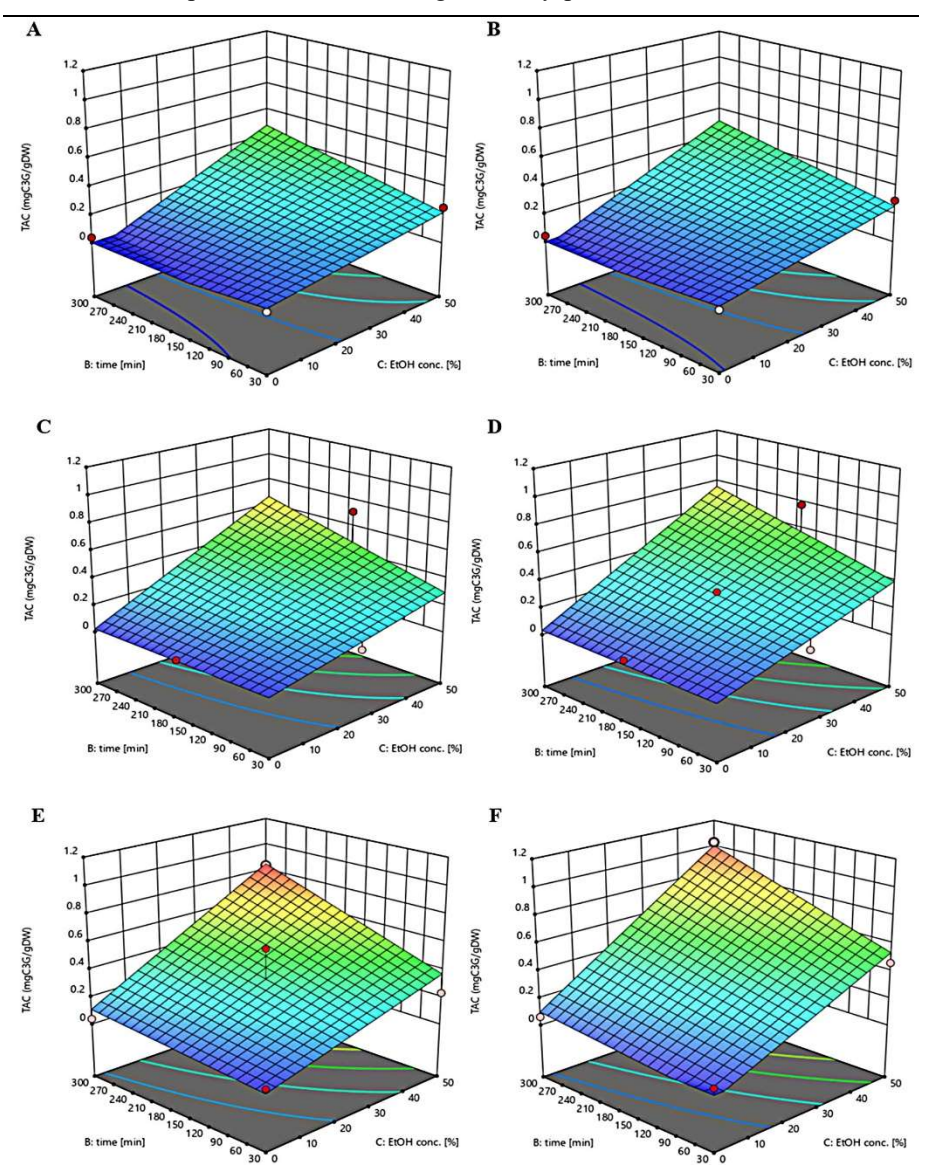


Figure V.5 Response surfaces for Total Anthocyanin Content (TAC) of extracts obtained from untreated (Control) (A,C,E) and PEF-treated (E = 4.6 kV/cm; $W_T = 20 \text{ kJ/kg}$) (B,D,F) G300G as a function of extraction time and ethanol concentration, with the extraction temperature set at 20°C (A,B), 35°C (C,D), 50°C (E,F).

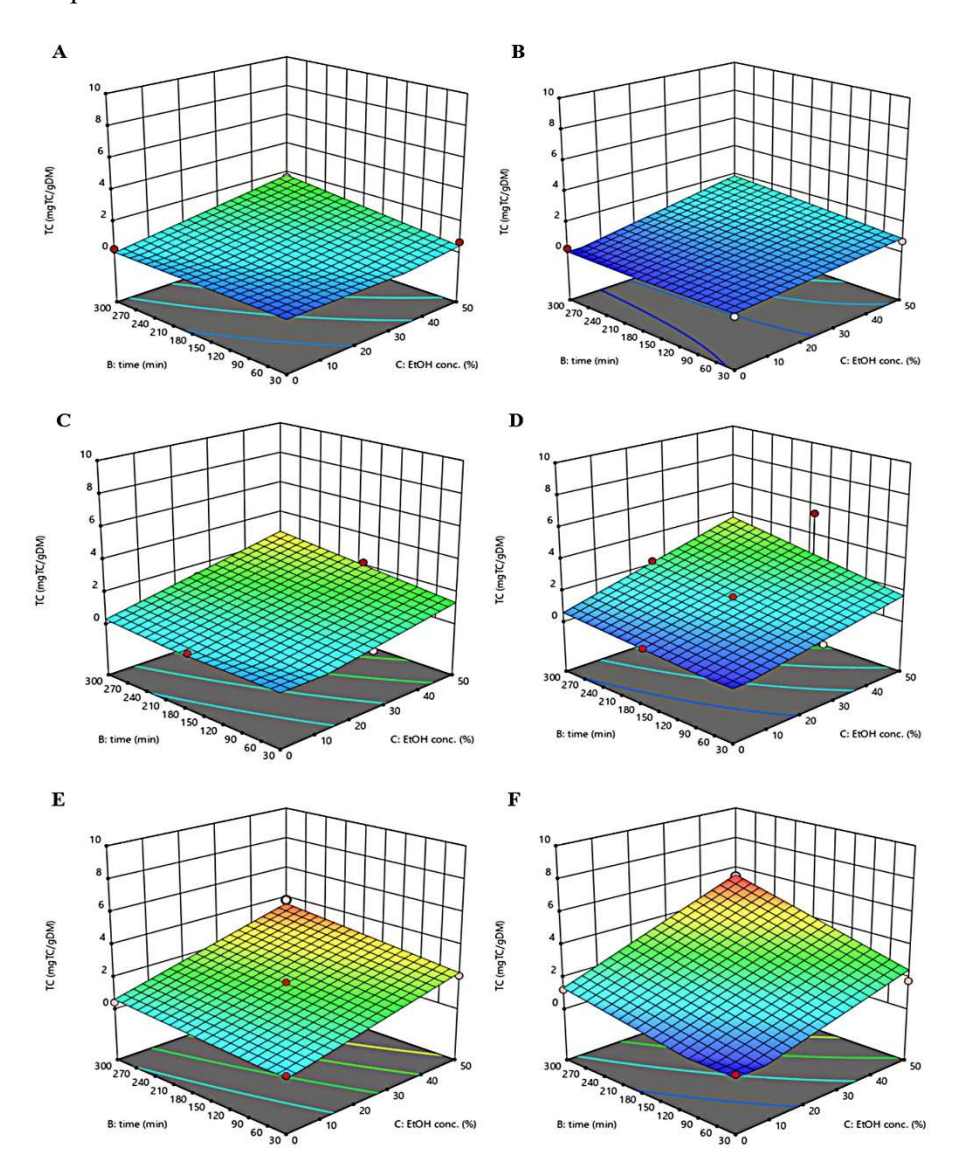


Figure V.6 Response surfaces for Tannin Content (TC) of extracts obtained from untreated (Control) (A,C,E) and PEF-treated (E = 4.6 kV/cm; W_T = 20 kJ/kg) (B,D,F) G300G as a function of extraction time and ethanol concentration, with the extraction temperature set at 20°C (A,B), 35°C (C,D), 50°C (E,F).

V.3.1.3 Quantification of the main phenolic compounds via HPLC-

PDA analysis

The identification and quantification of the main phenolic compounds in the extracts obtained from untreated and PEF-treated G300G at the selected PEFassisted extraction conditions (4.6 kV/cm - 20 kJ/kg; 50 °C - 50% ethanol concentration - 300 min), were carried out by HPLC-PDA analysis. The obtained chromatogram profiles and the concentrations of the specific identified phenolic compounds are reported in Figure V.7 and Table V.7, respectively. Results reveal that regardless of the application of PEF pretreatment, epicatechin (peak 4) was the most abundant phenolic compound detected in the extracts, followed by p-coumaric acid (peak 5), rutin (peak 7), naringin (peak 6), chlorogenic acid (peak 2), and to a lesser extent by caffeic acid (peak 3), gallic acid (peak 1), and phlorizin (peak 8). Moreover, it is interesting noting that, consistently with the findings reported by other scientists who investigated the recovery of phenolic compounds from several PEF pre-treated agri-food by-products (Bobinaitė et al., 2015; Brianceau et al., 2015; Carpentieri et al., 2022a; Frontuto et al., 2019; Pataro et al., 2017), the extracts from untreated and PEF pre-treated G300G showed comparable chromatographic profiles (Figure V.7). In comparison with the control samples, PEF pre-treatment determined an increase of the peak area of all phenolic compounds. In particular, the application of PEF pre-treatment caused a significant increment in the concentration of gallic acid (12%), chlorogenic acid (35%), epicatechin (62%), and p-coumaric acid (21%), whereas the increase of the other phenolic compounds was not statistically significant. As it can be seen in Figure V.8, one major peak corresponding to peonidin-3-O-glucoside (peak 1) with a concentration equal to 0.13 ± 0.004 mg/g_{DW} was detected in the control extract at an elution time of 27.91 min. The permeabilization of the cell membranes of G300G tissues upon PEF treatment significantly enhanced the extractability of anthocyanin compounds, leading to a final concentration of peonidin-3-O-glucoside in the extract of 0.16 ± 0.002 mg/g_{DW}, which was 23% higher than that detected in the control extract. This is in good agreement with previous findings (Brianceau et al., 2015), reporting that PEF pre-treatment led to an increase in the extractability of peonidin 3-O-glucoside of 5-20%.

Therefore, results demonstrated that the PEF technology was successful in selectively increasing the extraction yield of valuable compounds, especially epicatechin, p-coumaric acid, and peonidin 3-O-glucoside compared to the conventional extraction process.

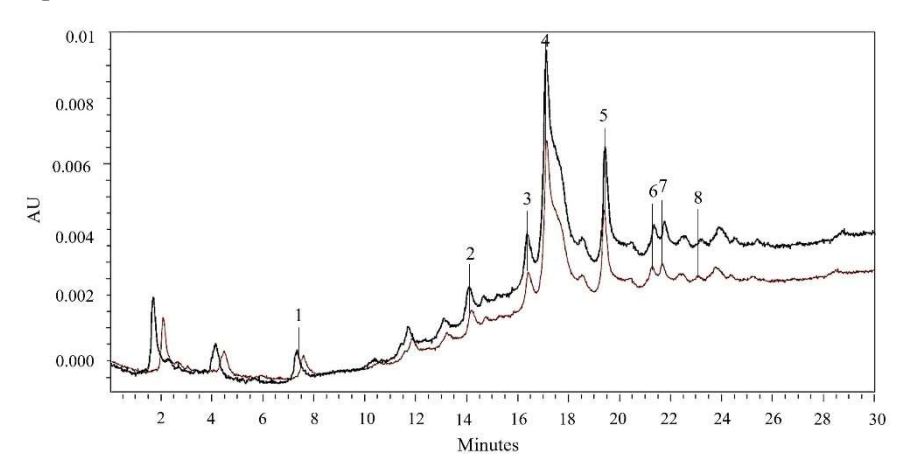


Figure V.7 HPLC-PDA chromatograms of 50% (v/v) ethanol-water extracts obtained after 300 min of extraction at 50 °C from untreated (brown line) and PEF-treated (black line) ($E_{opt} = 4.6 \text{ kV/cm}$; $W_{T,opt} = 20 \text{ kJ/kg}$) G300G. Peak identification: gallic acid (1); chlorogenic acid (2); caffeic acid (3); epicatechin (4), p-coumaric acid (5); naringin (6); rutin (7); phlorizin (8).

Table V.7 Concentrations (mg/g_{DW}) of gallic acid, chlorogenic acid, caffeic acid, epicatechin, p-coumaric acid, naringin, rutin and phlorizin (HPLC/PDA analysis) in the extracts from untreated and PEF-treated G300G.

Peak no.	Compound	Max absorption	Retention time		Concentration (mg/g _{DW})
		wavelength (nm)	(min)	Untreated	PEF-treated
1	Gallic acid	271	7.60	0.07 ± 0.01^a	0.08 ± 0.01^{b}
2	Chlorogenic acid	320	14.76	0.20± 0.01ª	0.27 ± 0.02^{b}
3	Caffeic acid	320	16.42	$0.10{\pm}~0.01^a$	0.12 ± 0.01^a
4	Epicatechin	280	17.15	2.99± 0.03a	4.83 ± 0.05^{b}
5	p-coumaric acid	320	19.40	0.38± 0.02ª	0.46 ± 0.03^{b}
6	Naringin	283	21.28	0.25± 0.01a	0.27 ± 0.02^{a}
7	Rutin	260	21.68	0.26± 0.02a	0.29 ± 0.03^{a}
8	Phlorizin	280	23.12	0.06 ± 0.01^{a}	0.06 ± 0.01^{a}

Values with different lowercase letters within the same row are significantly different ($p \le 0.05$).

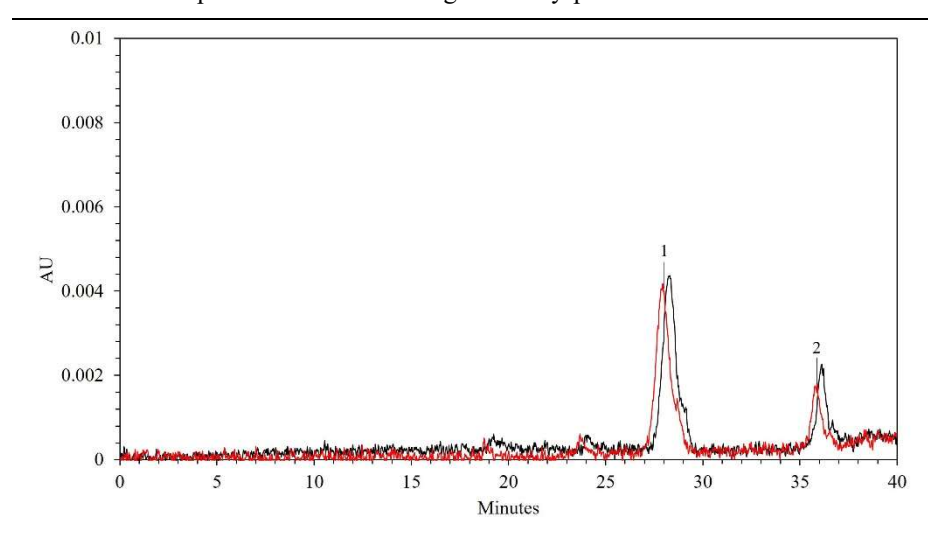


Figure V.8 HPLC-PDA chromatograms of 50% (v/v) ethanol-water extracts obtained after 300 min of extraction at 50 °C from untreated G300G (red line) and PEF-treated G300G (black line) ($E_{opt} = 4.6 \text{ kV/cm}$; $W_{T,opt} = 20 \text{ kJ/kg}$). Peak identification : (1) peonidin 3-O-glucoside.

V.3.2 Pulsed electric field-assisted extraction (A113H)

V.3.2.1 Total phenolic content, antioxidant activity and HPLC-PDA analysis of A113H extracts

The total phenolic content (TPC) and the antioxidant activity of the extract from untreated and PEF-treated A113H samples (processed at the optimal conditions defined according to previous results, namely 3 kV/cm - 5 kJ/kg; 25 °C - 120 min), were evaluated via Folin Ciocalteu, FRAP and DPPH assays. The values were 0.98 \pm 0.15 mg GAE/g_{DW}, 1.54 \pm 0.13 mg AAE/g_{DW}, and 67 \pm 2.03%, for untreated sample, and 1.91 \pm 0.15 mg GAE/g_{DW}, 2.48 \pm 0.17 mg AAE/g_{DW}, and 84 \pm 2.30% for the PEF-treated one.

Interestingly, it has been reported that A113H matrix is among the top 50 foods containing the most antioxidants per serving, including red berries, walnuts, cabbage, and broccoli, strengthening its competitiveness (Halvorsen et al., 2006). It is worth noting that the TPC values detected in the extract agreed with those found by other scientists, with slight differences depending on the variety, type of residue, and experimental protocol. The detected values for the TPC and antioxidant activity of the extracts from untreated and PEF-treated A113H allow us to conclude that the application of this extraction procedure, involving the combined use of PEF technology and water as a green extracting solvent, can be considered an effective and sustainable method for valorising A113H residues (+80% on average with respect to the

extracts from untreated samples). Moreover, the composition, in terms of the most abundant phenolic compounds, of the extract from untreated and PEF-treated A113H was assessed via HPLC-PDA analysis. The resulting chromatograms, depicted in Figure V.9, showed that the two extracts presented similar chromatographic profiles, and that PEF pre-treatment remarkably enhanced the amount of the major phenolic compounds in the extracts, corresponding to chlorogenic acid (peak 3), followed by naringin (peak 7), rutin (peak 8) catechin (peak 2), epicatechin (peak 4), sinapic acid (peak 6), phlorizin (peak 9), cynarine (peak 5), and gallic acid (peak 1). A variety of phenolic compounds, mainly phenolic acids, and flavonoids, which are the two major phenolic classes present in A113H, were detected. Indeed, 48.5% of the total phenolic compounds identified by HPLC-PDA analysis was represented by phenolic acids and derivatives (chlorogenic acid, sinapic acid, gallic acid, cynarine), while the remaining 51.5% were flavonoids (naringin, rutin, catechin, epicatechin, phlorizin).

The obtained results are consistent with previous findings reporting that, among phenolic compounds, caffeoylquinic acids were the most abundant hydroxycinnamic acids in this by-product, with chlorogenic acid being present to a greater extent. Specifically, as corroborated by the results reported in Table V.8, PEF-assisted extraction process led to a final concentration of chlorogenic acid in the extract of 0.84 ± 0.09 mg/g_{DW}, (+28% compared to the control sample) representing about the 93% of the phenolic acids identified in the extract. Additionally, in agreement with previous studies (Barbosa-Pereira et al., 2018; Bobinaitė et al., 2015; Carpentieri et al., 2021a; Giordano et al., 2016), it could be speculated that the identified phenolic compounds (1.87 \pm 0.15 mg/g_{DW}) were likely contributing to the detected antioxidant activity of the extract.

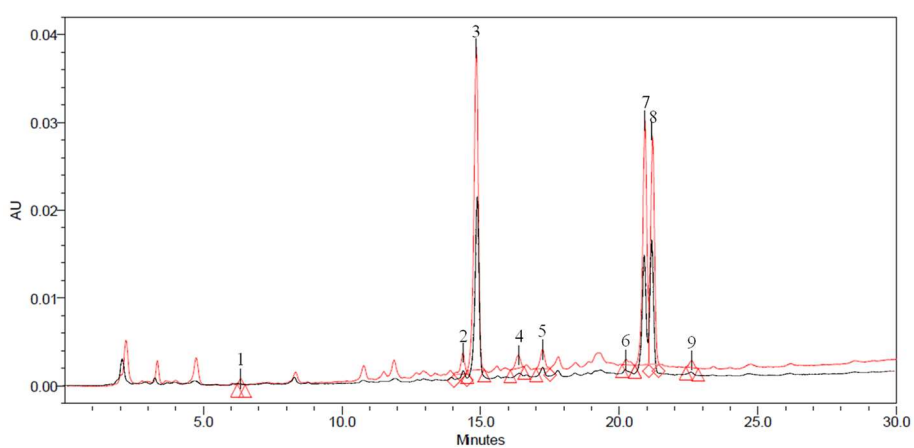


Figure V.9 HPLC-PDA chromatograms of the extract from untreated A113H (black line), and the extract from PEF-treated A113H (red line). Peak identification: gallic acid (1), catechin (2), chlorogenic acid (3),

epicatechin (4), cynarine (5), sinapic acid (6), naringin (7), rutin (8), phlorizin (9).

Table V.8 Concentrations (in mg/g_{DW}) of gallic acid, catechin, chlorogenic acid, epicatechin, cynarine, sinapic acid, naringin, rutin, and phlorizin (HPLC/PDA analysis) in the extracts from the untreated and PEF-treated A113H. Values with different lowercase letter within the same row are significantly different ($p \le 0.05$).

Peak	Compound	Max	Retention	Concentrat	tion (mg/g _{DW})
no.		absorption wavelength (nm)	time (min)	Untreated	PEF-treated
1	Gallic acid	271	6.35	/	0.01 ± 0.00
2	Catechin	280	14.36	0.05 ± 0.00^a	0.13 ± 0.01^{b}
3	Chlorogenic acid	320	14.83	0.66 ± 0.05^a	0.84 ± 0.09^{b}
4	Epicatechin	280	16.36	0.01 ± 0.00^a	0.05 ± 0.01^{b}
5	Cynarine	320	17.24	0.01 ± 0.00^a	0.02 ± 0.00^{b}
6	Sinapic acid	330	20.24	0.02 ± 0.00^a	0.04 ± 0.01^{b}
7	Naringin	283	20.93	0.29 ± 0.01^a	0.48 ± 0.05^{b}
8	Rutin	260	21.32	0.18 ± 0.01^a	0.27 ± 0.01^{b}
9	Phlorizin	280	22.61	0.01 ± 0.00^{a}	0.03 ± 0.00^{b}

Values with different lowercase letter within the same row are significantly different ($p \le 0.05$).

V.3.3 Pulsed electric field-assisted extraction (N433W)

The total phenolic content (TPC) and the antioxidant activity of the extract from untreated and PEF-treated N433W (at the optimal processing conditions defined according to previous results 3 kV/cm - 10 kJ/kg; 25 °C - 3 h), evaluated via Folin Ciocalteu, FRAP and DPPH assays, were 19.80 ± 2.08 mg GAE/gDW, 14.65 ± 0.31 mg AAE/gDW, and $78.10\pm2.00\%$ for the untreated sample, and 23.95 ± 0.37 mg GAE/gDW, 18.05 ± 0.02 mg AAE/gDW, and $93.23\pm1.55\%$ for the PEF-treated one. Interestingly, PEF pre-treatment induced an increment in TPC and antioxidant activity of about 22% in the extract with respect to those from untreated sample.

The phenolic profile of the extract from untreated and PEF-treated N433W was assessed via HPLC-PDA analysis. The chromatograms, reported in Figure V.10, showed that the two extracts presented similar chromatographic profiles, and that no degradation phenomena occurred upon PEF. PEF pretreatment also enhanced the extraction of several identified phenolic compounds present in the extracts, namely epicatechin (peak 3), representing the most abundant one, catechin (peak 2), rutin (peak 6), gallic acid (1), sinapic acid (5), p-coumaric acid (4), phlorizin (7), and luteolin (8). As reported in Table V.9, PEF-assisted extraction process led to a final concentration of rutin

in the extract of 6.81 ± 0.10 mg/g_{DW}, 3-fold higher than the amount of rutin present in the extract from untreated sample.

It is also noteworthy that no significant differences were observed between the values of TPC and antioxidant activity measured on pilot scale PEF-treated samples and laboratory scale PEF-treated samples, confirming the reproducibility of the results with scaling up the facilities.

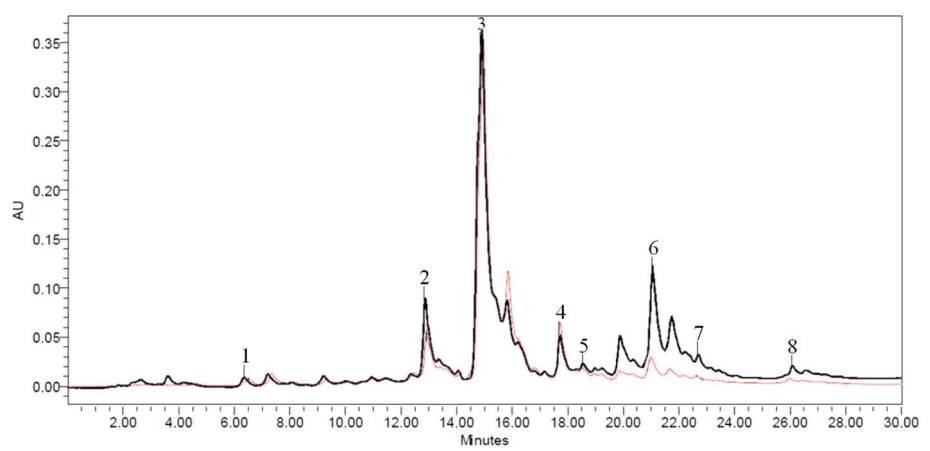


Figure V.10 HPLC-PDA chromatograms of the extract from untreated N433W (black line), and the extract from PEF-treated N433W (red line). Peak identification: gallic acid (1), catechin (2), chlorogenic acid (3), epicatechin (4), cynarine (5), sinapic acid (6), naringin (7), rutin (8), phlorizin (9).

Table V.9 Concentrations (in mg/g_{DW}) of gallic acid, catechin, chlorogenic acid, epicatechin, cynarine, sinapic acid, naringin, rutin, and phlorizin (HPLC/PDA analysis) in the extracts from the untreated and PEF-treated N433W. Values with different lowercase letter within the same row are significantly different ($p \le 0.05$).

		Max	Retenti	Concentrati	on (mg/g _{DW})
Peak no.	Compound	absorption wavelength (nm)	on time (min)	Untreated	PEF-treated
1	Gallic acid	271	6.50	0.10 ± 0.00^a	0.11 ± 0.00^{b}
2	Catechin	280	12.92	$1.22 \pm 0.01_a$	1.77 ± 0.03^{b}
3	Epicatechin	280	14.95	21.31 ± 0.28^a	23.09 ± 0.22^{b}
4	p-coumaric acid	310	17.72	0.04 ± 0.00^a	$0.05\pm0.00^{\mathrm{b}}$
5	Sinapic acid	330	18.53	0.05 ± 0.07^a	$0.05\pm0.01^{\mathrm{a}}$
6	Rutin	260	21.00	0.30 ± 0.07^a	0.89 ± 0.01^{b}
7	Phlorizin	280	22.62	0.03 ± 0.00^a	0.04 ± 0.00^{b}
8	Luteolin	350	26.43	0.02 ± 0.00^a	0.03 ± 0.00^{b}

Values with different lowercase letter within the same row are significantly different ($p \le 0.05$).

V.3.4 High-Pressure Homogenization-assisted extraction (E706IT)

V.3.4.1 Effect of HPH-treatment on the recovery of bioactive compounds from E706IT

In this study, RSM was used to relate the response variables to the input variables to define the optimal HPH processing conditions that maximize the extraction yields of TPC, antioxidant activity (FRAP), and lycopene content of untreated and HPH-treated E706IT suspensions. The selected independent variables were the HPH operating conditions, including the number of passes through the micronisation valve ($n_p = 0$ - 15), treatment temperature (T = 5 - 50 °C) and pressure (80 - 100 MPa).

The obtained results, reported in Table V.10, demonstrate that the independent factors considerably affected the TPC, FRAP values, and lycopene content of the suspensions.

More specifically, the maximum levels of response variables were attained at the lowest pressure applied (80 MPa), after 10 n_p , and at an intermediate temperature of 25 °C.

Results also show that HPH treatment applied at the selected optimal conditions significantly induced an increment in the extractability of TPC (31%), FRAP (25%), and lycopene content (42%) as compared with the control (HSH-treated suspension).

A linear model was used to fit the obtained data for all the investigated responses (data not shown).

Table V.10 Actual values of the three independent variables investigated and responses of the dependent variables (TPC, FRAP, and lycopene) in untreated and HPH-treated E706IT suspensions.

Run	Variables			HPH-treatment		
	P	n _P	T	TPC	Antioxidant activity	Lycopene content
Untreated	/	0	/	3.30 ± 0.40	3.63 ± 0.05	7.20 ± 0.10
1	80	2	5	2.67 ± 0.30	3.71 ± 0.00	9.97 ± 0.10
2	80	2	25	3.53 ± 0.01	4.47 ± 0.10	8.65 ± 0.10
3	80	2	50	3.44 ± 0.10	3.75 ± 0.02	8.15 ± 0.20
4	100	2	5	2.62 ± 0.22	3.04 ± 0.01	8.28 ± 0.10
5	100	2	25	2.71 ± 0.01	3.18 ± 0.01	7.48 ± 0.10
6	100	2	50	2.84 ± 0.05	3.49 ± 0.20	5.21 ± 0.15

7	80	5	5	3.26 ± 0.11	4.01 ± 0.10	8.55 ± 0.20
8	80	5	25	3.31 ± 0.01	4.76 ± 0.15	9.33 ± 0.02
9	80	5	50	4.07 ± 0.20	4.73 ± 0.50	10.19 ± 0.01
10	100	5	5	2.95 ± 0.10	3.08 ± 0.20	9.09 ± 0.35
11	100	5	25	2.97 ± 0.02	2.93 ± 0.30	9.57 ± 0.20
12	100	5	50	2.93 ± 0.07	3.65 ± 0.20	7.61 ± 0.01
13	80	10	5	3.69 ± 0.10	3.79 ± 0.20	9.90 ± 0.10
14	80	10	25	4.33 ± 0.08	4.52 ± 0.04	10.20 ± 0.10
15	80	10	50	3.77 ± 0.05	4.75 ± 0.30	8.66 ± 0.10
16	100	10	5	3.12 ± 0.05	3.35 ± 0.15	8.93 ± 0.20
17	100	10	25	3.21 ± 0.05	3.20 ± 0.10	9.57 ± 0.25
18	100	10	50	3.34 ± 0.05	3.95 ± 0.02	5.82 ± 0.30
19	80	15	5	3.85 ± 0.05	4.17 ± 0.20	10.03 ± 0.21
20	80	15	25	$3.54\ \pm0.05$	4.57 ± 0.10	9.55 ± 0.10
21	80	15	50	$4.05\ \pm0.05$	4.73 ± 0.30	8.32 ± 0.10
22	100	15	5	3.41 ± 0.05	3.06 ± 0.25	7.13 ± 0.15
23	100	15	25	3.46 ± 0.15	3.37 ± 0.30	9.47 ± 0.20
24	100	15	50	3.67 ± 0.10	4.03 ± 0.20	5.29 ± 0.10

TPC is expressed in mg GAE/ g_{DM} E706IT, FRAP in mg AAE/ g_{DM} E706IT, and lycopene in mg lycopene/ g_{DM} E706IT. The results are expressed as mean \pm standard deviation. P, pressure (MPa); n_p , number of passes through the valve, T, treatment temperature (\circ C).

The effects of the pressure, number of passes through the valve, and temperature on the level of TPC, FRAP values, and lycopene content are depicted in the Response surface graphs reported in Figure V.11.

Overall, in the investigated domain, HPH treatment induced a significant increment in TPC as compared with the untreated suspension when applying the lowest pressure investigated (80 MPa). Moreover, TPC level linearly increased as increasing the temperature and the number of passes through the valve (+34 % compared to the untreated suspension). The same trend was observed for the level of antioxidant activity (+28 % compared to the untreated suspension).

The regression coefficients and significance of the predicted polynomial models, show that even though all the investigated variables had a statistically significant effect (p \leq 0.05) on TPC, FRAP values, and lycopene content, the treatment temperature and pressure were the factors that mostly affected this latter response variable, whose concentrations slightly decreased as increasing the temperature up to 50 °C, and the pressure up to 100 MPa (-17% on average compared to the untreated suspension). The highest decrement in lycopene

content was detected when combining the highest pressure, temperature, and treatment time investigated (100 MPa, 50 °C, and 15 min, respectively).

Several studies concluded that the temperature exerts high effect on lycopene concentration during processing or drying that can be easily reduced by excessive heat treatment. High temperature can result in the discharge of hydroxyl enzymes which destroy lycopene, nevertheless, lycopene cannot get easily destroyed under mild heat exposure. However, this factor in combination with pressure, and treatment time can contribute to losing lycopene content (Jatau et al., 2019).

The reduction in particle size, due to the disruption of plant tissue occurring upon fluid-mechanical stresses induced by HPH treatment, has been shown to enhance carotenoid recovery and bioaccessibility (Jurić et al., 2019; Zhang et al., 2019). However, the increase in consistency, attributed to the formation of a fibre network by polymer–polymer interaction, has demonstrated to entrap the carotenoids and decrease their extraction (Colle et al., 2010; Jurić et al., 2021). Specifically, a decreasing trend of the lycopene recovery and bioaccessibility with increasing homogenisation pressure was noticed (Colle et al., 2010), resulting in the breakdown of the cell aggregate structures, as well as in a stronger fibre network.



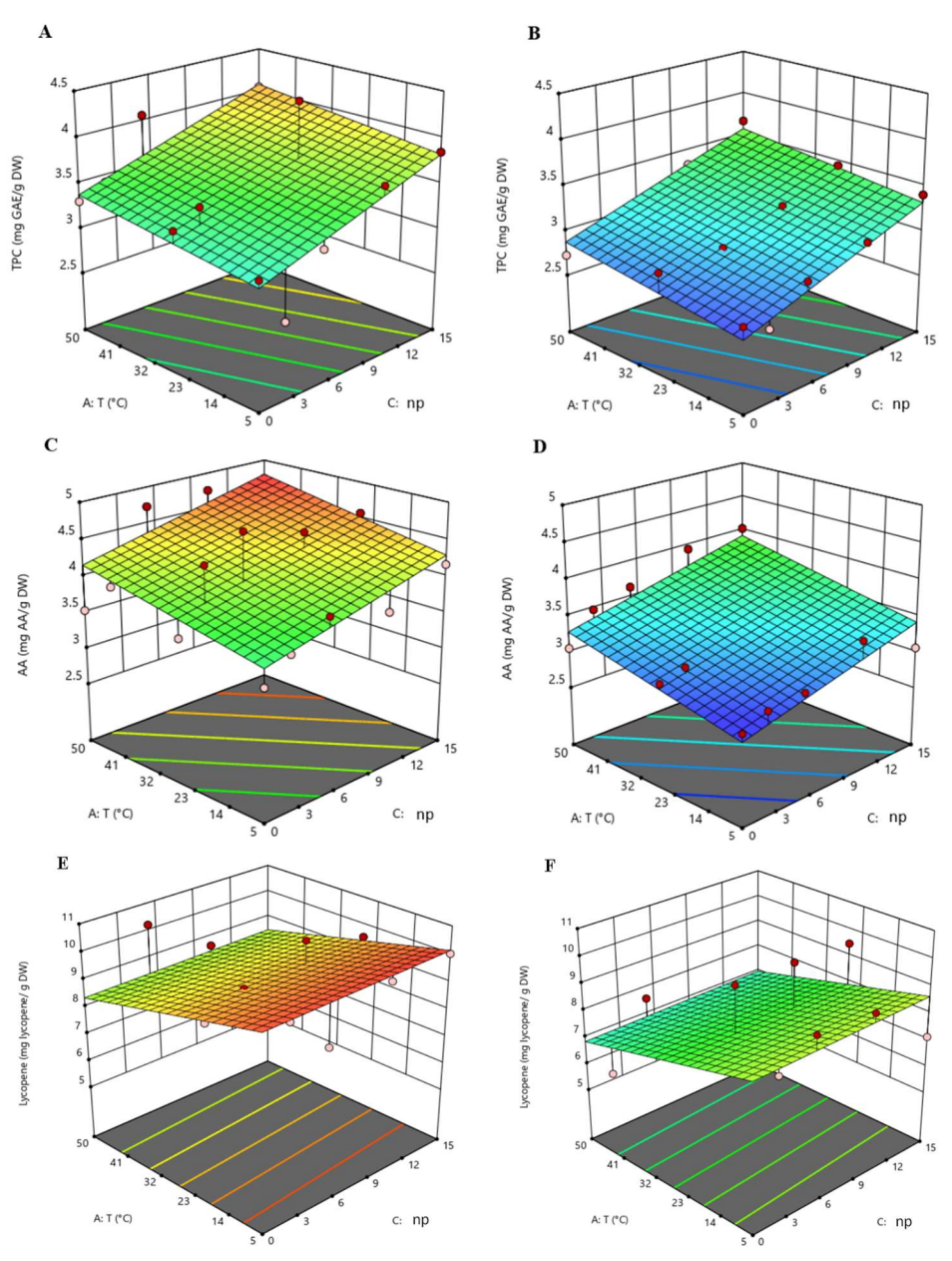


Figure V.11 Response surfaces for TPC, antioxidant activity and lycopene content in the untreated and HPH-treated suspensions at 80 MPa (A,C,E) and 100 MPa (B,D,F) as function of the process temperature and the number of passes through the homogenization valve.

Based on the previous considerations, the selected optimal conditions (the minimum conditions which maximize all the investigated response variables) together with the concentrations of the target compounds analysed in the HPH-treated and untreated suspension, as well as the resulting relative increment induced by HPH are summarized in Table V.11.

Table V.11 Optimal extraction conditions for each response variable analysed, for untreated and HPH-treated E706IT suspensions.

Response	Concer	ntration	Relative increment (%)	Temperature [°C]	Pressure [MPa]	Number of passes
	Control	HPH				
TPC [mgGAE/g _{DW}]	3.30 ± 0.40^{a}	4.33 ± 0.08 ^b	31.21	25	80	10
FRAP [mgAAE/g _{DW}]	3.63 ± 0.05 ^a	4.52 ± 0.04 ^b	24.52	25	80	10
DPPH [%]	35.30 ± 0.05^{a}	41.80 ± 0.05 ^a	20.77	25	80	10
Lycopene [mg lycopene/g _{DW}]	7.20 ± 0.20^{a}	10.20 ± 0.10^{b}	41.67	25	80	10
Total dietary fibre [g/100 g _{DW}]	$68.90 \pm \\0.50^a$	72.19 ± 0.10^{b}	4.78	25	80	10

Values with different lowercase letter within the same row are significantly different (p \leq 0.05).

Interestingly, the application of HPH at the processing conditions of 10 passes through the homogenization valve (corresponding to about 10 minutes of treatment), and using pure water as extraction solvent induced the recovery of 100% of the TPC with respect to that obtained by applying conventional extraction using a solution of acetone-water 80% (v/v) as solvent and an extraction time of 5 hours (§ IV.1.1).

V.3.4.2 Effect of HPH-treatment on the colourimetric profile of E706IT suspensions

Colour is one of the main sensory attributes that mostly affects the consumers' perception of food quality and their intention to buy a food product (Sant'Anna et al., 2013). Colour measurement of food products has been used as an indirect measure of other quality attributes, such as flavor and contents of pigments because it is simpler, faster, and correlates well with other physicochemical properties (Badin et al., 1947). Therefore, the effect of the HPH treatment temperature and number of passes on the colourimetric profile of the suspensions was investigated. In Table V.12 the colour parameters of E706IT suspensions as a function of HPH processing conditions (P = 80 MPa,

T = 5 °C – 50 °C, np = 0 – 15) are reported. Results demonstrated that all the suspensions obtained in this study showed positive values of a* (redness), in the range of 11.69 - 14.86, indicating that the red component was dominant in all cases. However, with increasing the treatment temperature to 50 °C, and after processing for 15 min, a* values of HPH-treated suspensions decreased (p<0.05) of about 40%, compared to the untreated suspension. Conversely, a* values increased when treating the suspension at 25 °C, with increasing the treatment time (+20%, with respect to the control). The parameter b* accounting for the tendency to yellow slightly increased with the processing time of 17%, 10%, and 23%, at 5 °C, 25 °C, and 50 °C, respectively, compared to the untreated suspension. These findings account for the influence of the processing conditions on the potential discolouration phenomenon of the suspensions rich in a natural pigment, namely lycopene. In this regard, Kaur et al. (2006) found a direct relationship between visual detection of colour and lycopene content.

To better understand whether the effects of the treatment conditions on colour parameters of the investigated suspensions could be detected by the human eye, ΔE parameter was evaluated. For the sake of comparison, ΔE was evaluated by comparing each HPH-treated suspension with the untreated one. Consistently with the previously discussed colour parameters, ΔE significantly increased as the severity of the processing conditions was increased of about 50% at 50 °C, and after 15 passes through the valve (Table V.12).

The chroma and the hue angle are the quantitative and qualitative attributes of colour, respectively. More specifically, the chroma provides information on the vividness of a colour, whereas the hue angle is the attribute according to which colours have been traditionally defined as reddish, orange, yellowish, corresponding to the three-dimensional colour diagram (i.e., 0° for red, 90° for yellow, 180° for green and 270° for blue) as seen by the human eye (Sant'Anna et al., 2013).

The treatment temperature did not induce significant changes in the chroma, conversely the hue angle, ranging between 56.21° and 70.13° (within the red – yellow region), slightly increased (+21%), shifting towards higher yellowness when increasing the treatment time and temperature. Conversely, hue values slightly decreased when treating the suspension at 25 °C and 80 MPa, shifting towards the red component, which is consistent with the enhanced release of lycopene upon the HPH treatment.

Table V.12 Colour parameters, colour differences (ΔE^*) among untreated and HPH-treated E706IT suspensions, hue angle, and chroma (C^*) of E706IT suspensions as a function of HPH processing conditions (P = 80 MPa, T = 5 °C - 50 °C, $n_p = 0 - 15$).

P (MPa))a)									80 MPa	Pa								
T (°C)	6			5 °C						25	25 °C					≥0°C	ွင		
Colour	ur :ters	*1	n*	*q	ΔE	Hue	C*	*1	**	p*	ΔE ab*	Hue	C*	r*	**	,*4	ΔE _a	Hue	Č.
	0	32.33 ± 0.02ª	14.86 ± 0.03^{a}	22.82 ± 0.03^{a}	,	56.93±	27.23±	32.45 ± 0.01ª	14.86 ± 0.04^{a}	$32.45 \pm 14.86 \pm 24.09 \pm 0.01^a 0.04^a 0.02^b$		58.33± 0.70 ^b	58.33± 28.30± 3	33.02 ± 0.02^{a}	$14.86 \pm 0.06^{\rm d}$	$14.86 \pm 23.68 \pm 0.06^{d} 0.04^{a}$	ı	57.89±	27.96 ± 0.06^{a}
	2	36.55 ± 0.05€	15.05 ± 0.10^{b}	23.64 ± 0.04 ^b	4.19± 0.01°	57.52± 0.60ª	57.52± 28.02± 3.060° 0.04°	35.96 ± 0.04 ^d	14.82 ± 0.05^{a}	$35.96 \pm 14.82 \pm 23.98 \pm 3.52 \pm 0.04^a 0.05^a 0.04^a 0.04^c$	3.52± 0.04°	58.28± 0.50 ^b	58.28± 28.19± 3	37.58 ± 0.06°	12.82 ± 0.03°	$12.82 \pm 24.73 \pm 0.03^{\circ}$ 0.06 ^b	5.11± 0.04ª	62.60± 0.80 ^b	$27.86\pm\\0.06^{a}$
HPH	Ś	33.64 ± 0.05 ^b	15.77 ± 0.22^{d}	24.79 ± 0.04°	$\begin{array}{c} 2.46 \pm \\ 0.05^{a} \end{array}$	57.53± 0.50ª	57.53± 29.38± 3	34.08 ± 0.00 ^b	15.89 ± 0.02 ^b	34.08 ± 15.89 ± 24.12 ± 1.93 ± 0.00 ^b 0.02 ^b 0.05 ^a	1.93 ± 0.05^{a}	56.62± 0.50a	56.62± 28.88± 3	36.22 ± 0.01°	11.1 ± 0.03 ^b	25.93 ± 0.01°	5.43± 0.02 ^b	66.82± 0.60°	66.82± 28.21± 0.60° 0.02 ^b
	10	33.77 ± 0.01°	15.26 ± 0.05°	24.78 ± 0.04°	$\begin{array}{c} 2.53 \pm \\ 0.06^{b} \end{array}$	58.37± 0.50 ^b	29.10± 3.04°	34.8 ± 0.01°		$16.77 \pm 25.3 \pm 0.02^{\circ}$	$\begin{array}{c} 3.26 \pm \\ 0.01^{b} \end{array}$	56.46± 0.40ª	56.46± 30.35± 30.40° 0.40°	35.27 ± 0.01 ^b	10.57 ± 0.03^{a}	$10.57 \pm 26.89 \pm 0.03^{a}$	5.81± 0.01°	68.54± 0.55 ^d	28.89± 0.04°
	15	34.07 ± 0.01 ^d	14.90 ± 0.04^{a}	26.63 ± 0.04 ^d	4.30± 0.06 ^d	60.77± 0.50b°	60.77± 30.51± 3	34.79 ± 0.01°	17.69 ± 0.03 ^d	34.79 ± 17.69 ± 26.44 ± 4.36± 0.01° 0.03 ^d 0.05 ^d 0.04 ^d	4.36± 0.04 ^d	56.21±	56.21± 31.81± 36.32± 0.70a 0.04° 0.01 ^d		10.54 ± 0.03^{a}	$10.54 \pm 29.16 \pm 0.03^a 0.04^c$	7.72± 0.02 ^d	70.13± 0.70°	70.13± 31.01± 0.70° 0.04 ^d

Values with different lowercase letter within the same column are significantly different ($p \le 0.05$).

V.3.4.3 Effect of HPH-treatment on the particle size of E706IT suspensions

The D_{4,3} (mean particle size) of untreated and HPH-treated E706IT suspensions treated at a pressure of 80 MPa, as a function of the number of passes (2 - 15) and temperature $(5 \, ^{\circ}\text{C} - 50 \, ^{\circ}\text{C})$ are reported in Figure V.12. Results show that HPH treatment induced a significant decrease ($p \le 0.05$) in the mean particle size of the suspension, with a drastic reduction of D_{4,3} from 474 μm to 172 μm after only 2 passes through the valve, and achieving an 8fold reduction (51 µm) after 10 passes, due to the fragmentation of the cells. Consistently with the significant decrease in D_{4,3} with respect to control samples, the particle size distribution curve of the HPH treated suspensions, reported in Figure V.13, showed a marked shift towards smaller sizes with respect to untreated cells suggesting a high cell disruption efficiency. A decreasing trend of the mean particle size as well as a significant increase in the sample homogeneity and monodispersion were detected as the treatment time increases. These observations are supported by the microscopic images reported in Figure V.14, that visibly highlight the decreasing size of the particles.

Remarkably, the results of Figures V.12-V.14 clearly show that HSM treatment was not able to destroy individual plant cells, whereas HPH treatment, after 10 passes, was able to completely disrupt the plant cells, with most of the intracellular content being released in the suspension (Jurić et al., 2019). These results could contribute to strengthen the possibility to add to the pasta a homogeneous and smooth suspension, potentially reducing the negative impact on the sensory characteristics of the product.

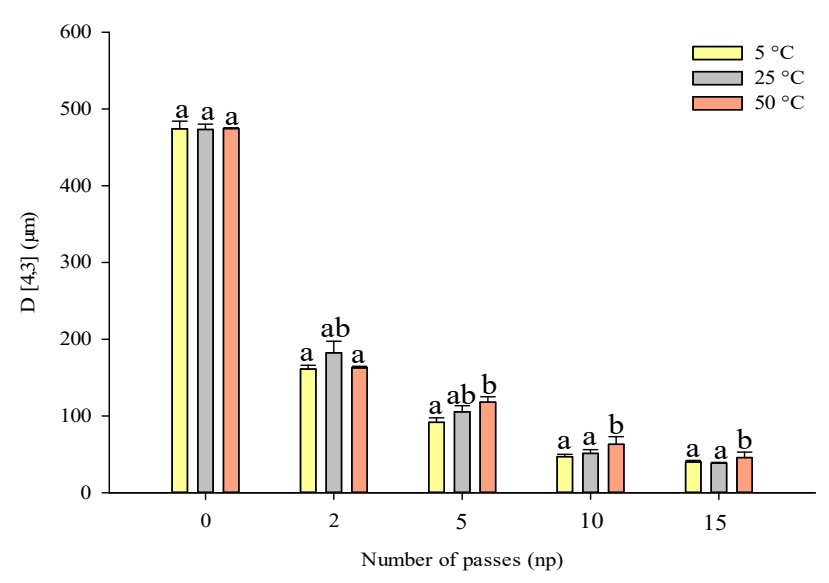


Figure V.12 Mean particle size of untreated $(n_p = 0)$, and HPH-treated $(P = 80 \text{ MPa}, T = 5 \text{ °C} - 50 \text{ °C}, n_p = 2 - 15)$ E706IT suspensions. Different letters above the bars indicate significant differences $(p \le 0.05)$ among the mean values of the samples treated with the same number of passes (n_p) .

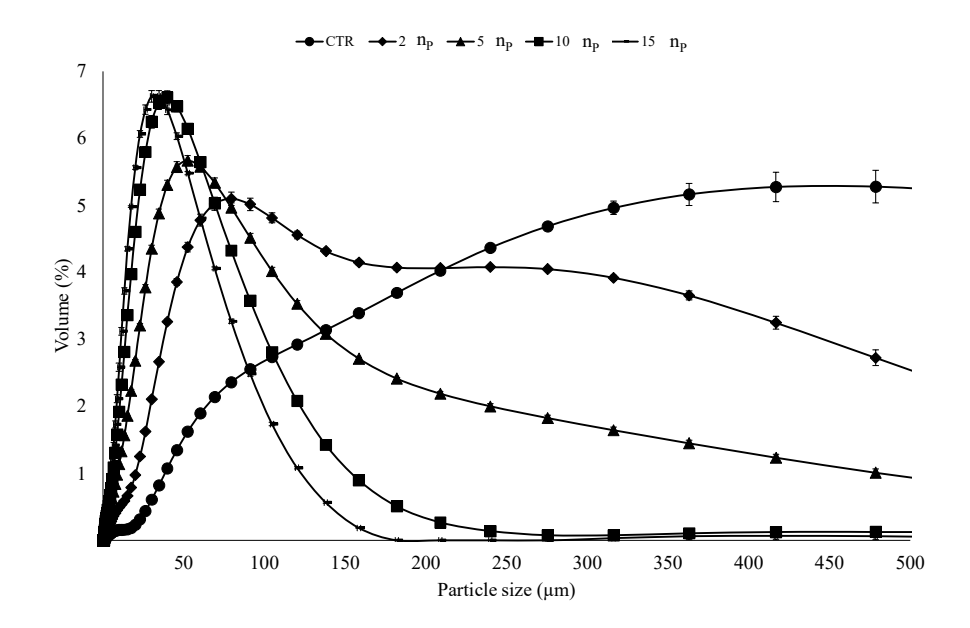


Figure V.13 Particle size distribution (PDI) of untreated $(n_p = 0)$, and HPH-treated (P = 80 MPa, T = 25 °C, $n_p = 2 - 15$) E706IT suspensions. Different letters above the bars indicate significant differences among the mean values of the samples ($p \le 0.05$).



Figure V.14 *Micrographs at 10x of untreated* $(n_p = 0, control)$ *and HPH-treated* $(P = 80 MPa, T = 5 °C - 50 °C, n_p = 2 - 15)$ *E706IT suspensions.*

V.3.5 High-Pressure Homogenization-assisted extraction (A781M)

V.3.5.1 Effect of HPH-treatment on the recovery of bioactive compounds and particle size of A781M suspensions

The selected optimal conditions for HPH treatment of A781M residues are given in Table V.13, with the concentrations of the target compounds analysed in the untreated and HPH-treated suspensions and the relative increase of each target compound of HPH-treated suspensions compared with the control.

Table V.13 Optimal extraction conditions for each response variable analysed, for untreated and HPH-treated A781M suspensions.

Response	Concen	tration	Relative increment (%)	T [°C]	P [MPa]	Number of passes
	Control	HPH				
TPC	7.16 ±	9.35 ±	30.58	25	80	10
$[mgGAE/g_{DW}]$	0.50^{a}	0.40^{b}				
FRAP	4.93 ±	6.48 ±	23.92	25	80	10
$[mgAAE/g_{DW}]$	0.60^{a}	0.23^{b}				
DPPH [%]	52.30 ±	70.3 ±	34.53	25	80	10
	1.81 ^a	3.00^{b}				
Total dietary fibre	$73.52 \pm$	79.9 ±	8.68	25	80	10
$[g/100 g_{DW}]$	0.80^{a}	1.00^{b}				

Values with different lowercase letter within the same row are significantly different (p \leq 0.05).

Results demonstrate that HPH treatment induced a significant increase in TPC, antioxidant activity (FRAP values), and DPPH inactivation capacity in the suspensions of about 31%, 24%, and 35%, respectively. Additionally, consistently with previous studies (Carullo et al., 2018; Jurić et al., 2019), 128

HPH treatment at the optimal processing conditions also led to enhanced macromolecules extractability, including total dietary fibre, and proteins (data not shown) of about 9%, and 20%, respectively.

The effectiveness of HPH technology in improving the extraction of bioactive compounds, including polyphenols, was corroborated also observing the obtained phenolic profiles, shown in the chromatograms reported in Figure V.15.

Figure V.15 showed that the two suspensions presented similar chromatographic profiles, and no degradation phenomena occurred upon HPH treatment that potentially stabilised the bioactives by the eventual with complexation the concurrently extracted macromolecules (polysaccharides and proteins). HPH treatment also enhanced the recovery of several identified phenolic compounds, namely catechin (peak 1), chlorogenic acid (2), epicatechin (3), rutin (peak 4), and phlorizin (5). Specifically, as reported in Table V.14, HPH process led to a significant increase in the content of phlorizin, the most abundant identified phenolic compounds in the analysed suspensions, equal to the 29% compared with that detected in the untreated suspension.

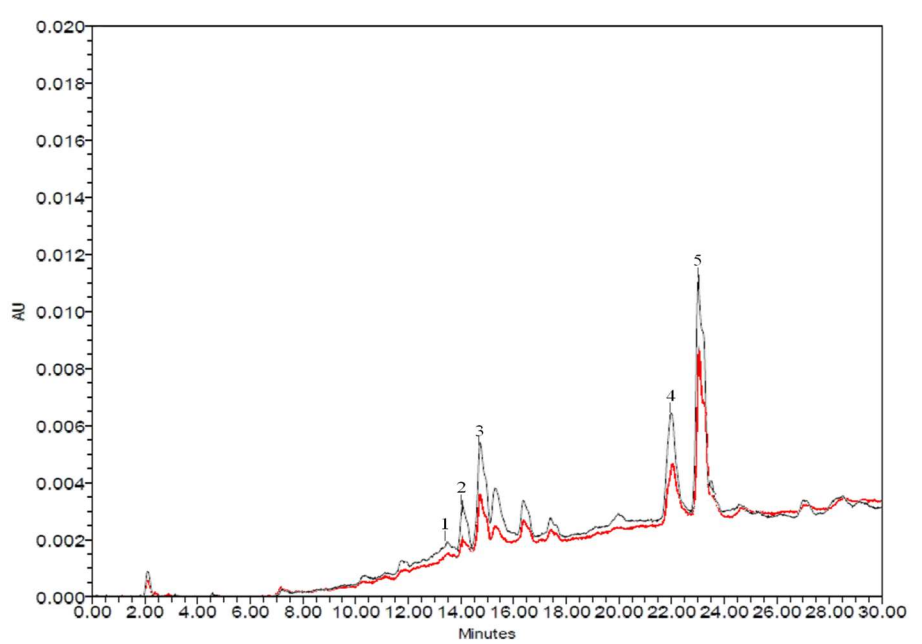


Figure V.15 HPLC-PDA chromatograms of the untreated A781M suspension (red line), and HPH-treated A781M suspension (black line). Peak identification: catechin (1), epicatechin (2), chlorogenic acid (3), rutin (4), phlorizin (5).

Table V.14 Concentrations (in mg/g_{DW}) of catechin, epicatechin, chlorogenic acid, rutin, and phlorizin (HPLC/PDA analysis) in the untreated and HPH-treated A781M suspensions.

D		Max	Retention	Concentration	on (mg/g _{DW})
Peak no.	Compound	absorption wavelength (nm)	time (min)	Untreated	HPH-treated
1	Catechin	280	13.51	0.03 ± 0.00^a	0.05 ± 0.00^b
2	Chlorogenic acid	320	14.74	0.20 ± 0.03^a	0.33 ± 0.05^b
3	Epicatechin	280	14.06	0.12 ± 0.01^a	0.28 ± 0.02^b
4	Rutin	260	22.05	0.39 ± 0.03^a	0.52 ± 0.02^b
5	Phlorizin	280	23.01	0.49 ± 0.05^a	0.63 ± 0.10^{b}

Values with different lowercase letter within the same row are significantly different ($p \le 0.05$).

Interestingly, the application of HPH with 10 passes through the homogenization valve (corresponding to about 10 minutes of treatment) and using pure water as extraction solvent induces the recovery of 84% of the TPC higher than that obtained with conventional extraction using an ethanol-water solution 50% (v/v) and an extraction time of 5 hours (§ IV.1,1).

The enhanced release of intracellular compounds from A781M samples upon HPH treatment, was confirmed by the significant reduction in the mean particle size of the suspensions (Figure V.16) as function of the HPH treatment time (from 493 μm , for the untreated suspension, to 56 μm , for the HPH-treated suspension at 10 $n_p,~80$ MPa, and 25 °C). These results were comparable to the main findings obtained for the E706IT suspensions, due to the similar structural characteristics and proximate composition, especially in terms of dietary fibre content (74% on average).

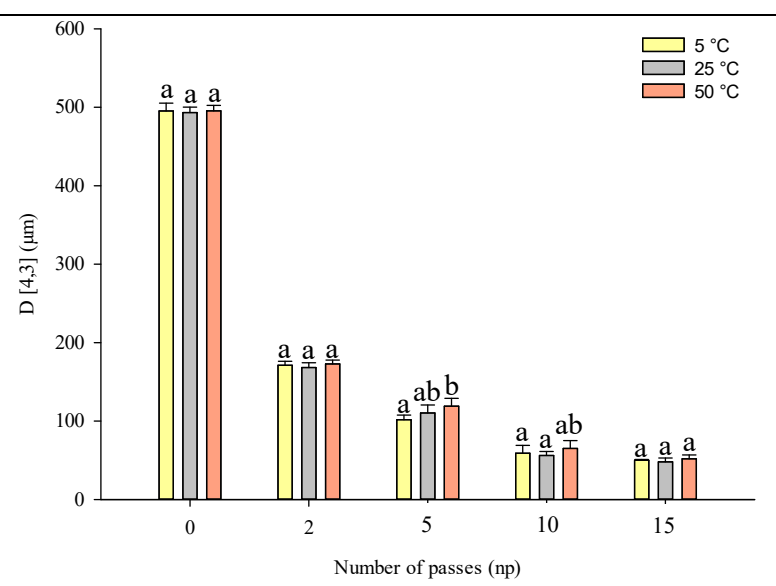


Figure V.16 Mean particle size of untreated $(n_p = 0)$, and HPH-treated $(P = 80 \text{ MPa}, T = 5 \text{ °C} - 50 \text{ °C}, n_p = 2 - 15)$ A781M suspensions. Different letters above the bars indicate significant differences $(p \le 0.05)$ among the mean values of the samples treated with the same number of passes (n_p) .

V.3.6 High-Pressure Homogenization-assisted extraction (B651S)

V.3.6.1 Effect of HPH-treatment on the recovery of bioactive compounds and particle size of B651S suspensions

The selected optimal conditions for HPH treatment of B651S sample together with the concentrations of the extracted compounds in the untreated and HPH-treated suspensions and their relative increase compared with the control are reported in Table V.15. Results demonstrate that HPH treatment significantly enhanced the TPC, antioxidant activity (FRAP values), and DPPH inactivation capacity in the suspensions of 36%, 29%, and 35%, respectively. However, due to the low moisture content of the raw material, and the higher compactness, and hardness, associated to the presence of predominant insoluble dietary fibres (cellulose, lignin, and hemicellulose, respectively), with respect to the other HPH-treated matrices, a higher number of passes through the micrometric valve and, thus, a longer treatment time was needed to maximize the extraction yield of the target investigated compounds.

Table V.15 Optimal extraction conditions for each response variable analysed, for untreated and HPH-treated B651S suspensions.

Response	Concer	ntration	Relative increment (%)	T [°C]	P [MPa]	Number of passes
	Control	НРН				
TPC [mgGAE/g _{DW}]	$\begin{array}{c} 24.51 \pm \\ 0.80^a \end{array}$	$\begin{array}{c} 33.46 \pm \\ 0.90^b \end{array}$	36.52	25	80	15
FRAP [mgAAE/g _{DW}]	17.83 ± 0.80^{a}	$\begin{array}{c} 23.05 \pm \\ 0.80^b \end{array}$	29.28	25	80	15
DPPH [%]	63.21 ± 1.34 ^a	85.05 ± 2.50 ^b	34.55	25	80	15
Total dietary fibre [g/100 g _{DW}]	64.50 ± 0.70^{a}	70.40 ± 0.60^{b}	9.15	25	80	10

Values with different lowercase letter within the same row are significantly different ($p \le 0.05$).

In Figure V.17 the phenolic profiles, obtained by HPLC-PDA analysis, of untreated and HPH-treated suspensions are depicted.

The investigated suspensions showed similar chromatogram profiles, indicating that no degradation phenomena occurred upon HPH treatment. Moreover, the treatment led to a significant increase in the main identified phenolic compounds, such as gallic acid (1), catechin (peak 2), chlorogenic acid (3), epicatechin (4), p-coumaric acid (5), naringin (6), rutin (peak 7), quercetin (8), and phlorizin (9). Specifically, as reported in Table V.16, HPH treatment led to a significant increase in the content of catechin (+20%, compared with the control), representing the predominant identified phenolic compound, as well as the most abundant flavonoid (48% of the identified flavonoids) among epicatechin, naringin, rutin, quercetin, and phlorizin.

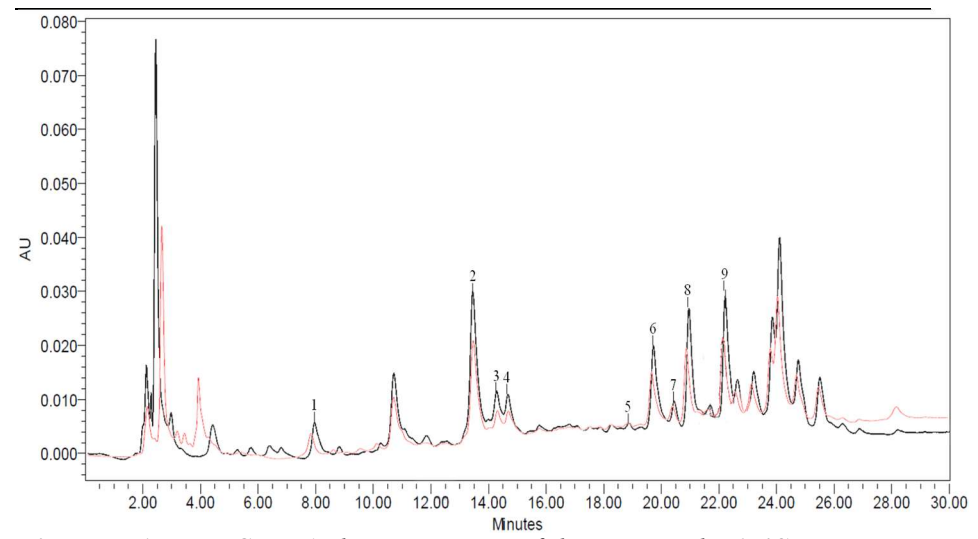


Figure V.17 HPLC-PDA chromatograms of the untreated B651S suspension (red line), and HPH-treated B651S suspension (black line). Peak identification: gallic acid (1), catechin (2), chlorogenic acid (3), epicatechin (4), p-coumaric acid (5), naringin (6), rutin (7), quercetin (8), phlorizin (9).

Table V.16 Concentrations (in mg/g_{DW}) of catechin, chlorogenic acid, epicatechin, p-coumaric acid, naringin, rutin, quercetin, and phlorizin (HPLC/PDA analysis) in the untreated and HPH-treated B651S suspensions.

Peak		May absorption	Retention	Concentrati	on (mg/g _{DW})
no.	Compound	Max absorption wavelength (nm)	time (min)	Untreated	HPH- treated
1	Gallic acid	271	7.75	0.13 ± 0.01^a	0.20 ± 0.04^{b}
2	Catechin	280	13.56	0.67 ± 0.05^a	0.80 ± 0.04^{b}
3	Chlorogenic acid	320	14.43	0.06 ± 0.00^a	0.10 ± 0.01^{b}
4	Epicatechin	280	14.86	0.10 ± 0.02^a	0.18 ± 0.04^{b}
5	P-coumaric acid	310	18.91	0.02 ± 0.00^a	0.03 ± 0.00^{b}
6	Naringin	283	19.87	0.14 ± 0.05^a	0.25 ± 0.04^b
7	Rutin	260	20.52	0.11 ± 0.03^{a}	0.14 ± 0.02^a
8	Quercetin	260	21.04	0.32 ± 0.05^a	0.40 ± 0.01^b
9	Phlorizin	280	22.41	0.25 ± 0.01^{a}	0.30 ± 0.02^{b}

Values with different lowercase letter within the same row are significantly different ($p \le 0.05$).

The efficacy of HPH treatment in improving the extractability of intracellular compounds from B651S samples was associated with its ability in inducing the disruption of plant cell tissues. This observation is supported by the $D_{4,3}$

mean particle size values (Figure V.18), that clearly highlight the decreasing trend of the suspension's particle size as function of the HPH treatment time. The application of HPH treatment at 80 MPa, 25 °C, and 10 n_{p} reduced the particle size from 509 μm to 90 μm (4.7-fold reduction), and to 75 μm after 15 passes through the valve (5.8-fold reduction). As previously stated, this matrix was subjected to a slower decrease in the mean particle size when compared to the other investigated matrices, since a 2-fold reduction was observed after only 2 passes through the valve for A781M and E706IT samples, respectively.

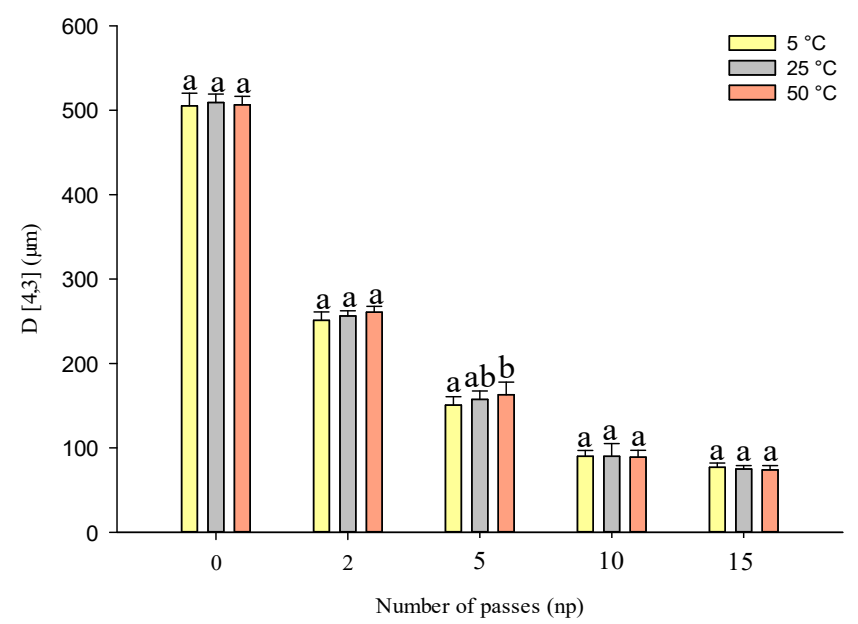


Figure V.18 Mean particle size of untreated $(n_p = 0)$, and HPH-treated $(P = 80 \text{ MPa}, T = 5 ^{\circ}\text{C} - 50 ^{\circ}\text{C}, n_p = 2 - 15) B651S suspensions. Different letters above the bars indicate significant differences <math>(p \le 0.05)$ among the mean values of the samples treated with the same number of passes (n_p) .

V.4 Conclusions

Results obtained in this chapter have shown the possibility to exploit PEF-assisted extraction and HPH treatment for valorising agri-food by-products (G300G, A113H, E706IT, A781M), and herbs (N433W, B651S), through the recovery of intracellular bioactive compounds.

More in details, the optimization step of the processing conditions involved in the whole PEF-assisted extraction process allowed to determine the optimal processing conditions, summarized in Table V.17, able to maximize the

permeabilization of the plant cell tissues, and the extraction yields of valuable compounds, such as TPC (+15%), FC (+60%), TAC (+23%), TC (+42), and the antioxidant activity (+31) of extracts from G300G.

Similar findings were obtained for A113H and N433W, where the exposure to a PEF treatment at the optimized processing conditions, and the subsequent diffusion step, led to significant (p < 0.05) increase of TPC and antioxidant activity of the extracts, as compared to the control samples. The HPLC analyses also confirmed that PEF pre-treatment selectively improved the extraction yield of the identified phenolic compounds, indicating that no degradation phenomena of the target bioactive compounds upon the PEF application occurred.

Likewise, HPH treatment enabled the recovery of the total plant matrix by significantly reducing the particle size of the treated suspensions, namely E706IT, A781M, B651S (up to 8-fold), showing a smooth, and homogeneous appearance. These results were also confirmed by a significant unlocking of bioactive compounds and macromolecules, such as proteins and fibres, induced by HPH treatment when applied at the optimal processing conditions (Table V.18). Moreover, the use of water as operating solvent represents a useful solution to reduce the risks associated with the large amount of organic solvents that are usually implied to increase the extraction yields.

The integration of novel technologies, such as PEF-assisted extraction, positively affect the selectivity of the SLE process, intensifying the extractability of target phenolic compounds from plant matrices. Moreover, HPH wet milling can fully exploit low-cost by-products and to unlock valuable macromolecules. The introduction of this kind of technologies in the food industry to complement existing unit operations and achieve the total use of the resources will be steered by the driving forces dictated by the needs of increasing the sustainability of food processes, which in the medium/long term might create environmental, economic, and social benefits.

The results illustrated in this chapter demonstrated that high value-added extracts and total suspensions can be obtained. However, downstream processes, necessary for the purification and increase of shelf life, must be individuated, and assessed together with the determination of the stability of these compounds during the processing of foods. To the latter purpose thermal stability kinetic studies are planned and the main outcomes should be discussed to confirm the potential utilization of the extracts and total suspensions as functional ingredients to be incorporated into food products, particularly into pasta, which can be considered as a study case.

 Table V.17 Optimal HPH processing conditions for E706IT, A781M, and B651S

samples.

sumpies.				
	T [°C]	P [MPa]	Number of passes	Solvent
E706IT	25	80	10	Water
A781M	25	80	10	Water
B651S	25	80	15	Water

Table V.18 Optimal PEF-assisted extraction processing conditions for G300G, A113H, and N433W samples.

ATTITI, and N433W samples.										
	E [kV/cm]	W _T [kJ/kg]	t [min]	T [°C]	Solvent					
G300G	4.6	20	300	50 °C	EtOH-					
					H2O [%,					
					v/v]					
A113H	3	5	120	20 °C	Water					
N433W	3	10	180	20 °C	Water					

Chapter VI Formulation and realization of the functional ingredients

Abstract

In this chapter, the freeze-dried HPH-treated suspensions, and extracts from PEF-treated samples, obtained in Chapter V, were characterised in terms of chemical stability (TPC and antioxidant activity) under the conditions of interest simulating the phases of transformation (extrusion, and drying) and preparation (cooking) of pasta.

Water absorption capacity (WAC) and water solubility index (WSI) of the samples were also evaluated, particularly relevant in the case of extrudates, which are playing a crucial role in the determination of extrusion conditions. Results demonstrated that the extracts showed good thermal stability when exposed at 25 °C, 40 °C, 70 °C, and 100 °C up to 8 hours. However, some degrading effects were observed after 3 - 4 h at 70 °C, and 2 h at 100 °C, which are more severe conditions with respect to those that pasta undergoes during the production process and preparation. The highest degradation was detected in the case of lycopene (2-fold reduction), and for the antioxidant activity of A113H extract (40% reduction), compared with the initial samples (t = 0), after 8 h at 100 °C.

The results obtained highlighted that the use of PEF and HPH technologies to obtain extracts and total suspensions from agri-food biomasses are also efficient in guaranteeing the stabilisation of these products, possessing good WAC ($2.40-5.18~\mathrm{g/g}$) and WSI (45.02%-84.83%), and do not induce significant degradation and loss of functionality of the target bioactive compounds.

VI.1 Introduction

The effectiveness of functional food products in preventing health-related diseases depends on the preservation of bioactivity and bioaccessibility of the active ingredients incorporated in the food matrix. This represents a formidable challenge, given that only a small proportion of molecules remain available following oral administration, due to instability under conditions encountered in food processing, or in the gastrointestinal (GI) tract (Bell, 2001).

In fact, while in the field of liquid foods functionalization (fruit juices, milk derivatives and beverages) several examples of applications have already been reported, there are still few studies related to the functionalization of solid foods due to the marked problems of chemical and physical stability caused by the severe conditions of transformation processes, conservation, and preparation for consumption (Carpentieri et al., 2022b).

Polyphenols degradation after processing (by 46%) and after cooking of pasta (by 53%) due to heat sensitivity and solubility of polyphenols in the cooking water was observed in previous studies (Bustos et al., 2015; Oliviero and Fogliano, 2016).

To further explain the phenolic and antioxidant losses incurred during processing and cooking, the chemical stability of the bioactive ingredients prior to their incorporation into pasta need to be properly investigated (Biney and Beta, 2014).

Therefore, in this chapter, in view of producing the newly formulated pasta, the functional ingredients will be characterised in terms of chemical stability, being affected by the type of extract (supernatant (obtained upon PEF) or total suspension (produced by HPH)), by its different components and physicochemical characteristics, in the conditions that simulate the stages of transformation (extrusion and drying) and preparation (cooking) of pasta.

In addition, WAC and WSI, two indices linked to the behavior of non-conventional ingredients during the formulation and kneading of pasta, were determined for all the obtained extracts. PEF-assisted extraction, and especially HPH treatment, if compared with traditional comminution methods, enable obtaining particles with larger surface area that result in improved water absorption, flavor release, soft mouthfeel, and high solubility of nutritive components, easily absorbed by the human body (van Buggenhout et al., 2015; Yu et al., 2016).

VI.2 Materials and Methods

VI.2.1 Raw materials and samples processing

The obtained dry extracts were analysed in terms of proximate composition (§ IV.1), and thermal stability kinetics were determined, as described in § IV.5.13.

WAC, and WSI were evaluated for all the investigated extracts (§ IV.5.14).

VI.2.2 Analytical determinations

The extracts were analysed in terms of total polyphenols (§ IV.5.1), antioxidant activity (§ IV.5.3), and lycopene content (§ IV.5.7).

VI.3 Results and discussion

VI.3.1 Chemical stability of the extracts under conditions simulating the transformation and preparation of dry pasta

An optimal thermal process of food always requires a trade-off between the beneficial and the destructive influences of heat on the food itself (Badin et al., 1947). Therefore, thermal stability kinetics in terms of the main classes of bioactive compounds of the obtained potential functional ingredients, exposed at different temperatures (25, 40, 70, 100 °C) up to 8 hours, were determined. The isothermal degradation curves reported in Figures VI.1 and VI.2 highlight the effect of different temperatures over time on lycopene content, and antioxidant activity values in HPH-treated (P = 80 MPa, $n_p = 10$, T = 25 °C) E706IT suspensions.

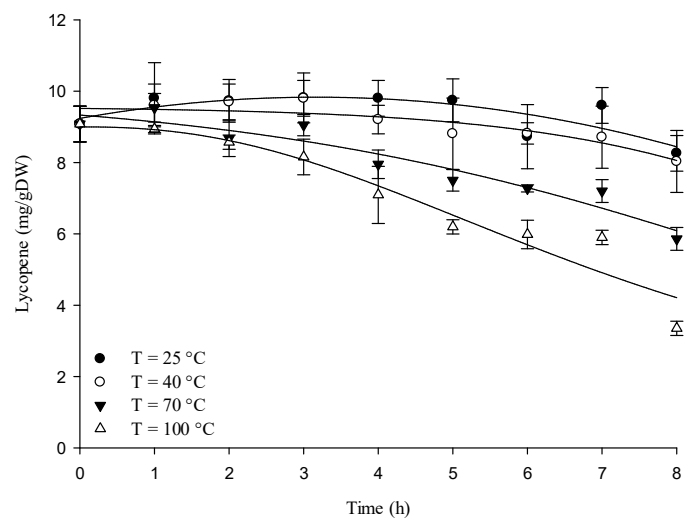


Figure VI.1 Isothermal degradation of lycopene in E706IT suspension, obtained upon HPH treatment, exposed at different temperatures (25, 40, 70, $100\,^{\circ}$ C). The lines represent model fits to the experimental data. The bars represent the mean \pm standard deviation.

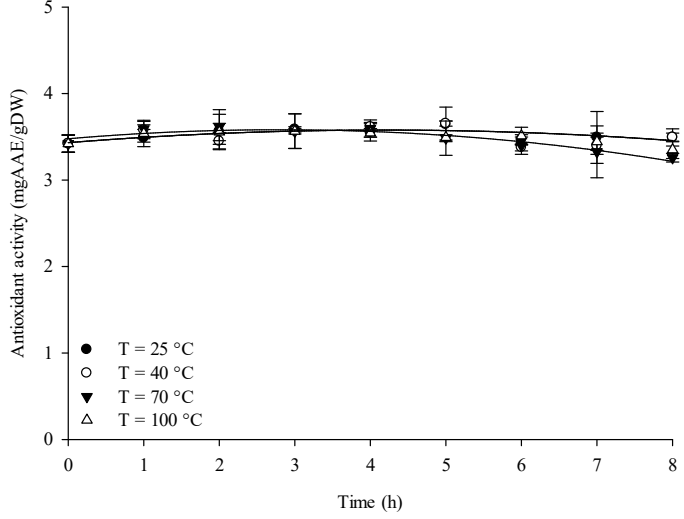


Figure VI.2 Isothermal degradation of antioxidant activity in E706IT suspension, obtained upon HPH treatment, exposed at different temperatures (25, 40, 70, 100 °C). The lines represent model fits to the experimental data. The bars represent the mean \pm standard deviation.

From the thermal stability kinetics of lycopene, it can be noted that, although a slight decrement of lycopene content is visible, no statistically significant differences between the extracts subjected to 25 °C and 40 °C compared with the initial lycopene content of the sample were detected. It is possible that in

a complex system, including multiple components, the hydrophobic nature of lycopene may result in the formation of molecular complexes, which might help increase its chemical stability (Liang et al., 2019), but might also hinder lycopene extractability. However, a degradation of lycopene can be clearly noted when extracts were exposed to temperatures of 70 °C and 100 °C, reaching a 1.5-fold, and 2.7- fold reduction, respectively after 8 hours of exposure, with respect to the initial suspension (t = 0).

In the case of thermal stability kinetics of antioxidant activity of E706IT suspension, it can be observed that, although there are no statistically significant differences, a reduction of the antioxidant activity is, however, visible with temperature increase. A similar trend was also observed in the case of TPC and antioxidant activity in A781M suspension (Figures VI.3 - VI.4). Interestingly, an initial increment of TPC and antioxidant activity was detected up to 70 °C, and after 3 - 4 hours of exposure.

These observations could be corroborated by the fact that the degradation of some bioactive compounds and, therefore, the reduction of their antioxidant activity could be balanced by the increase of the antioxidant activity of other bioactive compounds, of which the temperature favors the diffusion and the release from the cellular walls (Ciccoritti et al., 2017; Fares et al., 2010). This behavior is especially true in the case of total HPH-treated extract, where the cell debris is present in the final suspensions. In addition, the possible formation of some products of non-enzymatic browning reactions can contribute to the total antioxidant activity (Yilmaz et al., 2005). Indeed, Molaveisi et al. (2019) showed a strong correlation between the formation of pigments (brown pigment formation (BPF)) on antioxidant activity, and on TPC as increasing the time and temperature. This phenomenon is particularly evident in the case of A781M suspensions (Figure VI.5).

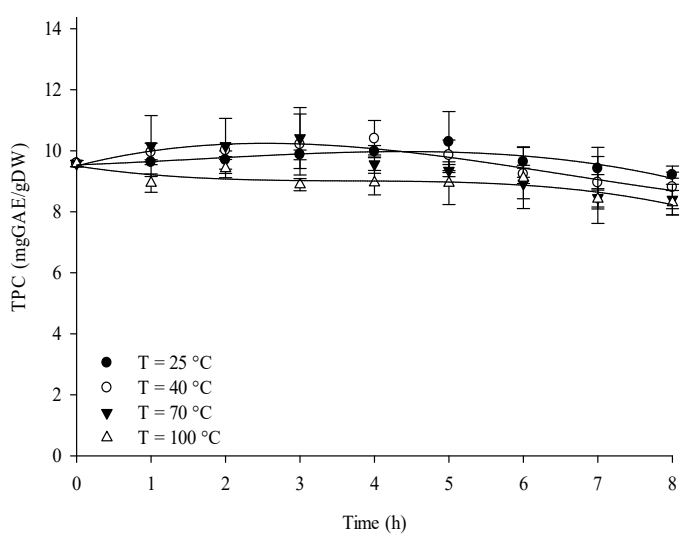


Figure VI.3 Isothermal degradation of TPC in A781M suspension, obtained upon HPH treatment, exposed at different temperatures (25, 40, 70, 100 °C). The lines represent model fits to the experimental data. The bars represent the mean \pm standard deviation.

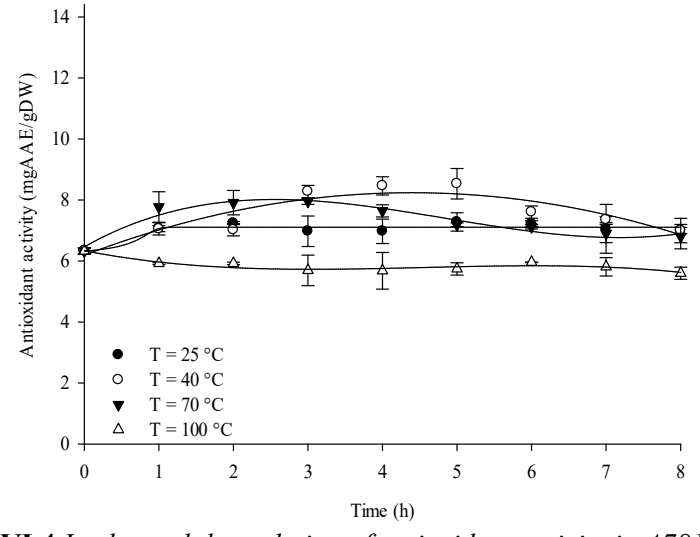


Figure VI.4 Isothermal degradation of antioxidant activity in A781M suspension, obtained upon HPH treatment, exposed at different temperatures (25, 40, 70, 100 °C). The lines represent model fits to the experimental data. The bars represent the mean \pm standard deviation.

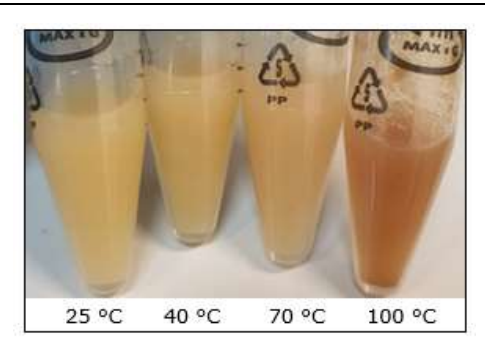


Figure VI.5 *Picture of A781M suspensions, obtained upon HPH treatment, exposed at different temperatures (25, 40, 70, 100 °C) after 8 hours of exposure.*

In addition, stabilization by complexation with the concurrently extracted macromolecules (polysaccharides and proteins) to form colloidal particles, could occur, without any measurable degradation of the bioactive compounds. As an example, the application of HPH on orange pulp resulted in a more homogeneous appearance, smoother suspension and increased the relative presence of water-extractable pectin, enhancing the physicochemical stability of the suspensions (Van-Buggenhout et al., 2015).

Based on these considerations, also HPH-treated B651S suspensions demonstrated to be stable in terms of TPC (Figure VI.6) and antioxidant activity (Figure VI.7) when exposed at temperatures simulating the pasta production process and the cooking phase. More in detail, a significant decrement of the antioxidant activity, with respect to the initial sample (t = 0), was observed (- 20%) after 8 hours of exposure at 70 °C and 100 °C.

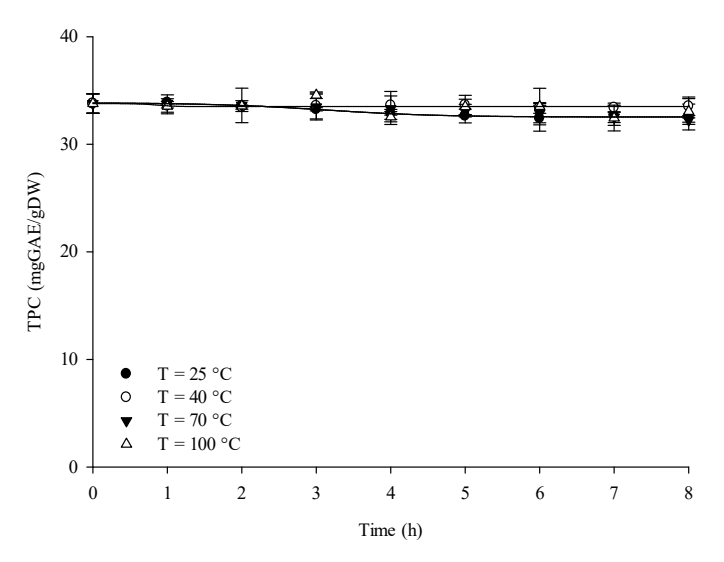


Figure VI.6 Isothermal degradation of TPC in B651S suspension, obtained upon HPH treatment, exposed at different temperatures (25, 40, 70, 100 °C). The lines represent model fits to the experimental data. The bars represent the mean \pm standard deviation.

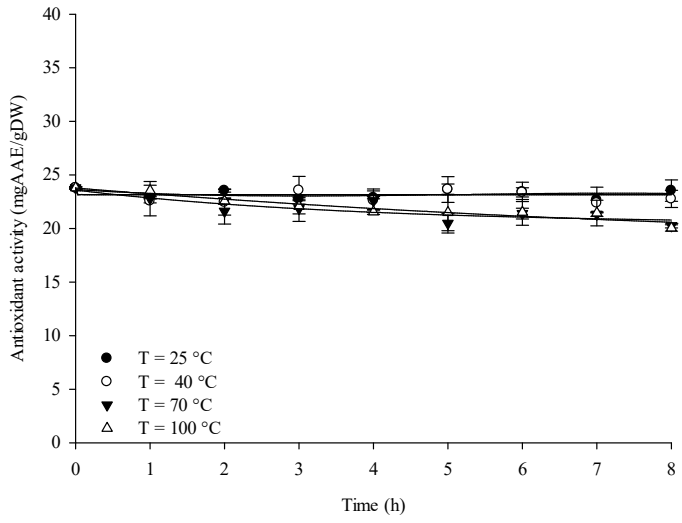


Figure VI.7 Isothermal degradation of antioxidant activity in B651S suspension, obtained upon HPH treatment, exposed at different temperatures (25, 40, 70, 100 °C). The lines represent model fits to the experimental data. The bars represent the mean \pm standard deviation.

In the case of thermal stability kinetics of TPC and antioxidant activity of extracts from PEF-treated G300G (Figures VI.8 – VI.9), A113H (Figures VI.10 – VI.11) and N433W (Figures VI.12 – VI.13), similar trends were 144

measured. Specifically, all the analysed extracts show a good chemical stability at 25 °C and 40 °C, even at the longest investigated exposure time. These observations could be supported by the proximate composition of the dry extracts, characterised by the predominant presence of sugars (85.8% – 57.9% on a dry basis) that can bind to phenolic compounds, increasing their stability.

Among the common plant polyphenols are phenolic acids, and flavonoids which are capable of strongly binding to polymers, especially proteins (Amoako and Awika, 2016). Likewise, sugars engage in the stability of polyphenols in the form of conjugated sugar or glycoside via a glycosidic bond to one or more hydroxyl groups that may inhibit the autoxidation of polyphenols and contribute to high antioxidant activities (Zayapor et al., 2021). This trend is particularly evident in the case of G300G and N433W extracts, that demonstrated to possess the highest amount of phenolic compounds, and flavonoids (§ IV.3.1 – § IV.3.3) with respect to all the investigated extracts.

Nevertheless, significant decrements in TPC and antioxidant activity were detected when exposing the extracts at 70 °C after 4 hours, and at 100 °C after 2 hours. Specifically, the highest reduction in TPC (- 33%) and antioxidant activity (- 41%) was observed for A113H extract (Figures VI.10 – VI.11) with respect to the initial sample (t = 0).

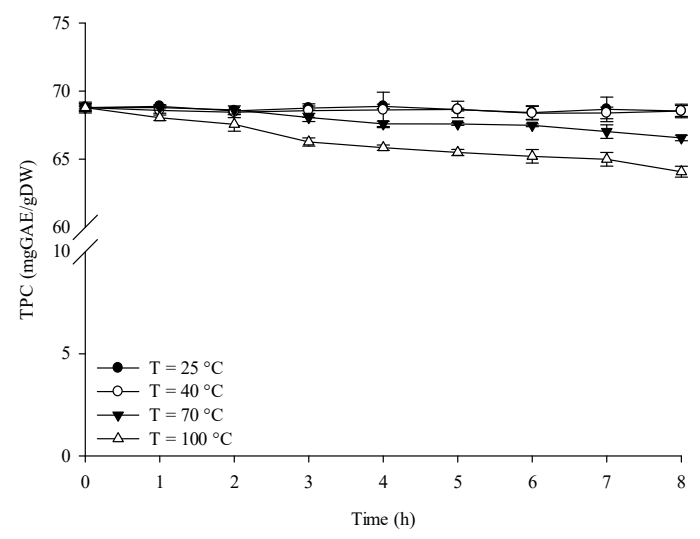


Figure VI.8 Isothermal degradation of TPC in G300G extract, obtained upon PEF-assisted extraction, exposed at different temperatures (25, 40, 70, $100\,^{\circ}$ C). The lines represent model fits to the experimental data. The bars represent the mean \pm standard deviation.

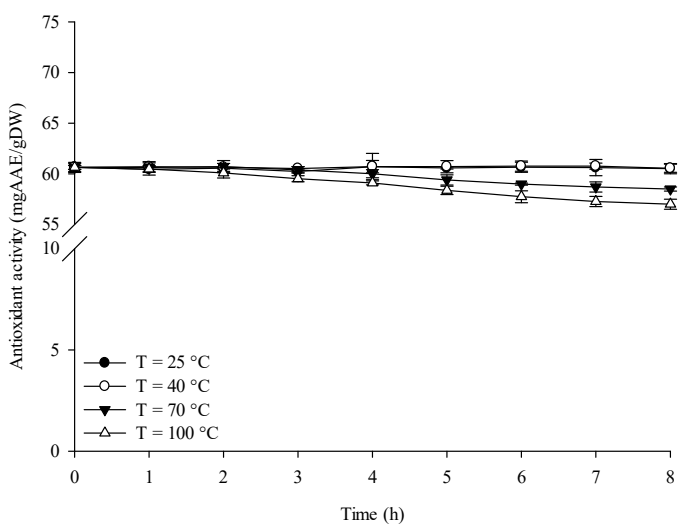


Figure VI.9 Isothermal degradation of antioxidant activity in G300G extract, obtained upon PEF-assisted extraction, exposed at different temperatures (25, 40, 70, 100 °C). The lines represent model fits to the experimental data. The bars represent the mean \pm standard deviation.

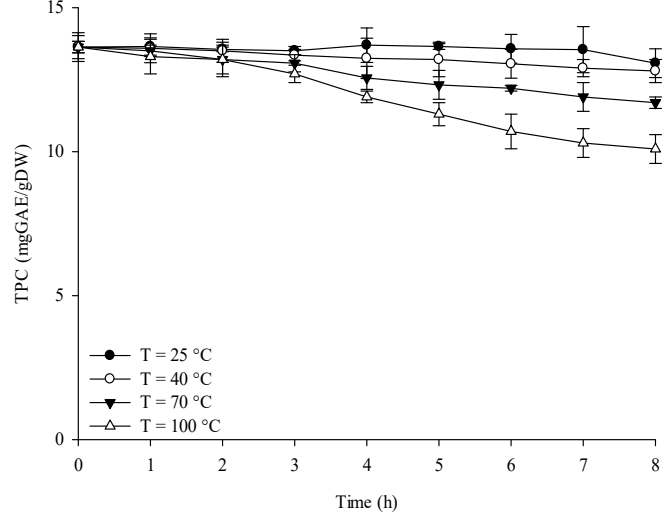


Figure VI.10 Isothermal degradation of TPC in A113H extract, obtained upon PEF-assisted extraction, exposed at different temperatures (25, 40, 70, $100\,^{\circ}$ C). The lines represent model fits to the experimental data. The bars represent the mean \pm standard deviation.

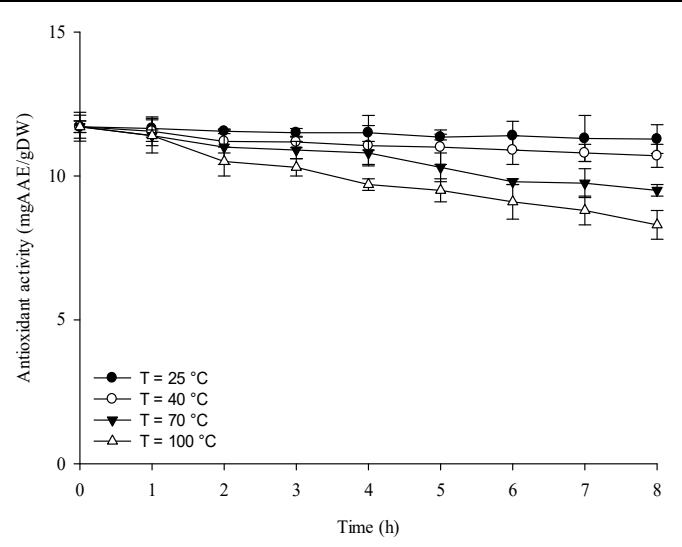


Figure VI.11 Isothermal degradation of antioxidant activity in A113H extract, obtained upon PEF-assisted extraction, exposed at different temperatures (25, 40, 70, 100 °C). The lines represent model fits to the experimental data. The bars represent the mean \pm standard deviation.

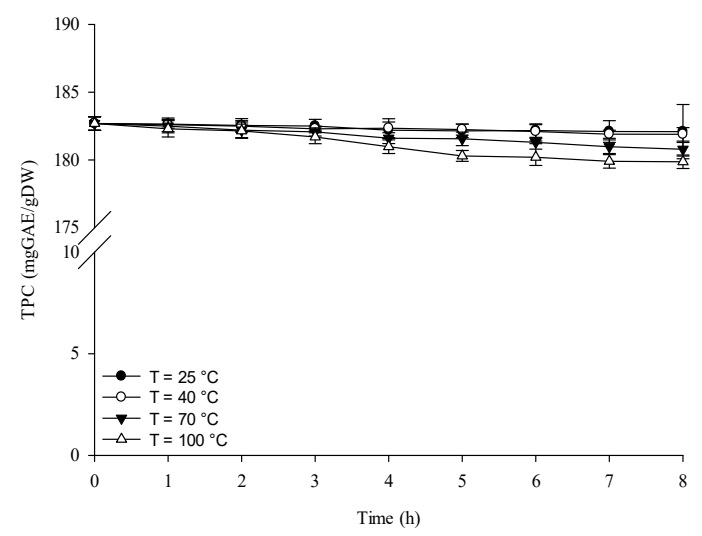


Figure VI.12 Isothermal degradation of TPC in N433W extract, obtained upon PEF-assisted extraction, exposed at different temperatures (25, 40, 70, $100\,^{\circ}$ C). The lines represent model fits to the experimental data. The bars represent the mean \pm standard deviation.

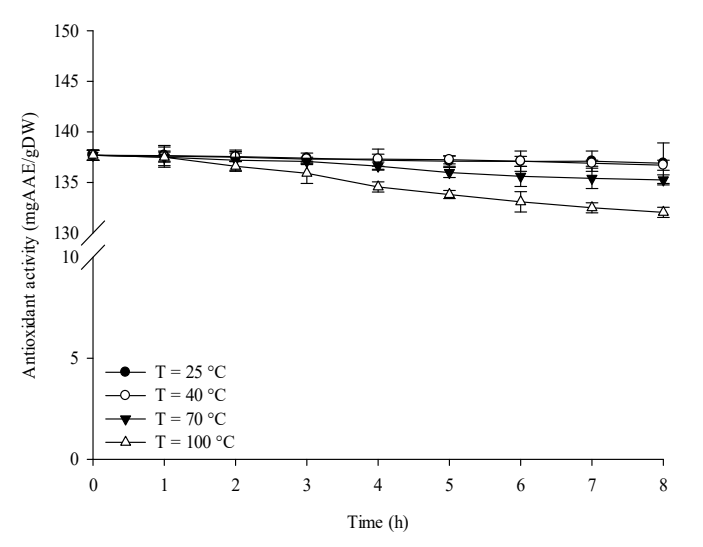


Figure VI.13 Isothermal degradation of antioxidant activity in N433W extract, obtained upon PEF-assisted extraction, exposed at different temperatures (25, 40, 70, 100 °C). The lines represent model fits to the experimental data. The bars represent the mean \pm standard deviation.

Results demonstrated that all the investigated extracts were stable under the conditions simulating the pasta production process (extrusion, and drying), and cooking phase.

VI.3.2 Water absorption capacity (WAC) and solubility index (WSI)

The hydration properties, described by the ability to retain water, and the water solubility index of the investigated extracts are reported in Table VI.1.

Table VI.1 Water absorption capacity (WAC) and water solubility index (WSI) and of E706IT, A781M, B651S HPH-treated suspensions, and G300G, A113H, N433W extracts from PEF-treated samples.

	E706IT	A781M	B651S	G300G	A113H	N433W
WAC (g/g)	2.40 ± 0.21 ^a	3.63 ± 0.10°	2.98 ± 0.13 ^b	4.25 ± 0.06 ^d	4.93 ± 0.08 ^e	5.18 ± 010 ^f
WSI (%)	45.02 ± 0.54 ^a	61.05 ± 0.26°	55.23 ± 0.36 ^b	74.09 ± 1.13 ^d	$\begin{array}{c} 84.83 \pm \\ 0.80^{\rm f} \end{array}$	79.28 ± 1.09 ^e

WAC represents the ability of a product to associate with water, while the WSI determines the amount of free polysaccharide or polysaccharide released from the sample on addition of excess water (Joshi et al., 2022).

The increase in the WAC has always been associated with the increase in solubility of the powdery sample (Gull et al., 2015).

Differences in water absorption may be related to differences in proximate composition. Specifically, high water absorption powders may have more hydrophilic components, such as polysaccharides, while the lower WAC in some samples may be due to the lower availability of polar amino acids (Gull et al., 2015).

The difference in protein concentrations, their degree of interaction with water, their conformational characteristics (Butt & Batool, 2010), as well as fibre content are known to affect water binding ability (Aydogdu et al., 2018). For example, cellulose and lignin (main components of insoluble dietary fibres) tend to have low water binding capacity, on the contrary hemicellulose and pectin (main components of soluble dietary fibres) possess high water binding capacity.

Soluble fibres were shown to be correlated with water binding capacity (r = 0.92, $p \le 0.05$) (Aydogdu et al., 2018).

The results obtained showed differences particularly related to the different chemical composition of the extracts analysed. In particular, among the HPH-treated suspensions, A181M due to its higher water-soluble fibre content among other fibres, mainly pectin, showed a higher WAC and WSI compared to the other suspensions. Conversely, E706IT, due to higher lipid (1.5% on a dry basis), and dietary fibre content (75.9% on a dry basis), showed the lowest WAC and WSI with respect to the other investigated samples.

G300G, A113H, and N433W, being purer extracts compared with the suspensions from total residues (E706IT, A181M, B651S), and obtained by separating the supernatant from the solid pellet, are mainly characterised by hydrophilic components, such as polysaccharides (85.8% – 57.9% on a dry basis) and have shown to possess a higher solubility index and water absorption capacity.

Interestingly, the obtained results were consistent with the main findings achieved by other authors, highlighting that powder samples of fruit, vegetables, cereals, and plants such as apple, wheat, sugar beet, pea, carrot, Moringa oleifera leaves (Aydogdu et al., 2018; Thierry et al., 2013), agri-food by-products (López-Valdez et al., 2020), and plant-based extracts (Susantikarn and Donlao, 2016) represented a WHC ranging between 2.5 and 10 g/g dry weight, and a solubility index between 41.6% (López-Valdez et al., 2020) and 98.53% (Susantikarn and Donlao, 2016).

VI.4 Conclusions

Results demonstrated that all the investigated potential functional ingredients are stable under the processing conditions, temperature and time, simulating the pasta production processing phases, and cooking phase.

Specifically, they underwent a significant reduction in TPC and antioxidant activity, only after exposure at 70 °C and 100 °C for 3 - 4 hours. These conditions, are, however, far from the milder conditions to which pasta is subjected both during drying, in which it reaches lower bulk temperatures, and during cooking, that lasts no more than 10-15 minutes.

The results obtained highlighted the potential of PEF and HPH technologies enable the stabilization of extracts and induce minimal degradation and loss of functionality of bioactive compounds. Furthermore, the application of HPH, by recovering the total by-product, may have enhanced the stabilisation of bioactive compounds in the suspensions by their complexation with the concurrently extracted macromolecules to form colloidal particles. Nevertheless, these observations should be corroborated by further investigations.

Additionally, the investigated samples demonstrated to possess good water absorption capacity and solubility index, ranging between 2.40-5.18~g/g, and 45.02% - 84.83%, respectively, well-correlated with the differences found in their proximate composition.

Section II

Production of functional pasta at pilot scale and its comprehensive characterisation and technoscientific validation

Chapter VII – Functional pasta production and its physicochemical, microstructural, and sensorial characterisation

Chapter VIII – Health validation of the new functional pasta: in vitro digestibility and biological activity

Chapter VII Functional pasta production and its physicochemical, microstructural, and sensorial characterisation

Abstract

In this chapter the pilot scale production of functional pasta by using optimized methodologies and processing parameters, previously identified at laboratory scale, as well as its comprehensive characterisation were carried out. Six different types of dry pasta (R430E, E700I, O112H, N309BN, D701GN, B520GP) functionalized with the obtained natural extracts (Chapter V), together with the traditional pasta (control), were produced, and characterised in terms of sensory profile, colourimetric parameters, texture, cooking properties and microstructural properties. In addition, the determination of the chemical profile of all the investigated pasta samples was also carried out with the aim of monitoring their bioactivity during the different stages of pasta production process and cooking phase.

Results demonstrate that three representative groups of functional pasta could be identified based on the overall difference in colourimetric parameters (ΔE) compared with the control (E700I and O112H, $\Delta E < 3$; R430E and N309BN, $10 < \Delta E < 15$; D701GN and B520GP, $\Delta E > 15$). It is interesting to note that the sensory analysis results showed that about 80% of panelists expressed the highest colour acceptability for R430E sample.

Interestingly, the different types of functional pasta showed similar texture and residual moisture properties compared to traditional pasta. All the functional pasta samples possessed a water absorption capacity and losses during cooking comparable to those of the traditional pasta (generally < 4.5 g/100 g). These results were also confirmed by the microstructural analysis

which showed that, in general, no significant differences between the sample structures can be observed. However, the surface of E700I, R430E and D701GN, functionalized with HPH-treated total suspensions, was characterised by a reduced roughness and a denser network, with starch granules strongly embedded in the glutinous matrix.

Finally, the addition of the natural extracts into pasta significantly contributed to enhancing its bioactivity with respect to the control, and the bioactive compounds were found to be stable during the pasta production and preparation phases, including extrusion, trabatto, drying, and cooking.

VII.1 Introduction

Choosing a fortification route through the addition of a bioactives has resulted in several technical challenges for food manufacturers, and demonstration of successful and effective incorporation of bioactives into selected food matrices is important for the commercialization of new functional foods. Although maintaining bioactivity of the 'active' ingredient after processing is important, the quality of the product is even more critical, particularly its appearance (Laureati et al., 2016).

To date, most of the studies available in the literature focused on the addition of powdery plant-based products obtained through dry milling techniques, rather than extracts from the by-products that will less affect the structural properties of pasta itself and will increase the bioavailability of the bioactives. Several researchers (Foschia et al., 2013; Sant'Anna et al., 2014; Padalino et al., 2013) stated that the main challenge of adding non-conventional ingredients in cereal products is the adverse effects on the product quality, mainly due to changes on texture, aftertaste, and colour properties.

In this sense, the use of PEF and HPH technologies as pre-processing steps (for extraction or micronisation) represents a strategy to mitigate the impact of the addition of non-conventional ingredients from agri-food by-products on the sensory attributes of pasta, by reducing the amount of the required additives and quality-enhancers, as well as to improve its specific health-beneficial properties.

The application of these technologies allowed also to understand and differentiate the effects of the addition of newly formulated ingredients on the techno-functional and structural properties of the final pasta by attributing them to the different physicochemical characteristics and bioactive components of pure extracts, obtained from the more selective PEF pretreatment, and total suspensions, produced upon the HPH treatment.

Moreover, the addition of high-antioxidant ingredients into pasta products is still very new since pasta is a complex matrix and the mechanisms of interaction of plant residues with pasta matrix remain unknown. More research is needed specially to understand the stability of functional

compounds in cooked pasta and the influence of the processing conditions of pasta on the nutritional and functional properties of the final products.

VII.2 Materials and Methods

VII.2.1 Raw materials and samples processing

Pasta samples were produced on pilot scale, as reported in § VI.9, according to a preliminary phase of pasta production on laboratory scale, conducted to optimise all the process parameters involved in the formulation, kneading, extrusion and drying phases, based on the proximate composition of the raw materials (water, durum wheat semolina, plant extracts).

VII.2.2 Analytical determinations

The pasta samples were comprehensively characterised in terms of colour parameters (§ IV.10.1), sensory attributes (§ IV.10.2), texture profile (§ IV.10.3), cooking properties (§ IV.10.4), thermal properties (§ IV.10.5), pasting properties (§ IV.10.6), microstructure (§ IV.10.7), chemical profile (§ IV.10.8).

VII.3 Results and discussion

VII.3.1 Physicochemical characterisation of the pasta products

VII.3.1.1 Colour determination

Colour is one of the most important attributes considered as indicator of the quality of a food product, that influences the purchase decision of consumers. The colour space L*a*b*, also called CIELAB, is one of the most reliable and widely used instrumental methods for colour determination, and the measured colourimetric parameters of the produced dry functional and traditional pasta (Figure VII.1) are reported in Figure VII.2.

Specifically, O112H, N309BN, and B520GP pasta samples have been functionalized with the addition of A113H, N433W, and G300G extracts, respectively, from PEF-treated matrices; while A181M, E706IT, and B651S HPH-treated total suspensions have been used to functionalize E700I, R430E, and D701GN pasta samples, respectively.

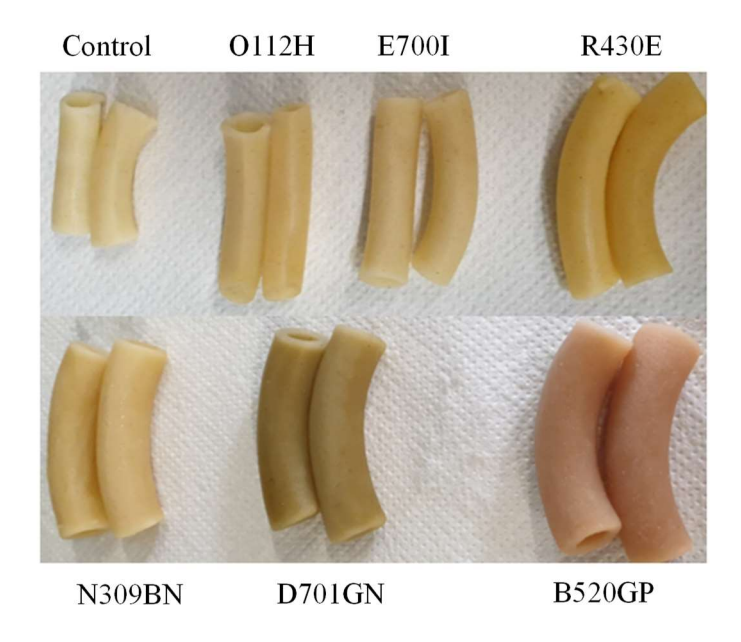


Figure VII.1 *Pictures of the traditional pasta (control) and the pasta functionalized with the obtained natural extracts.*

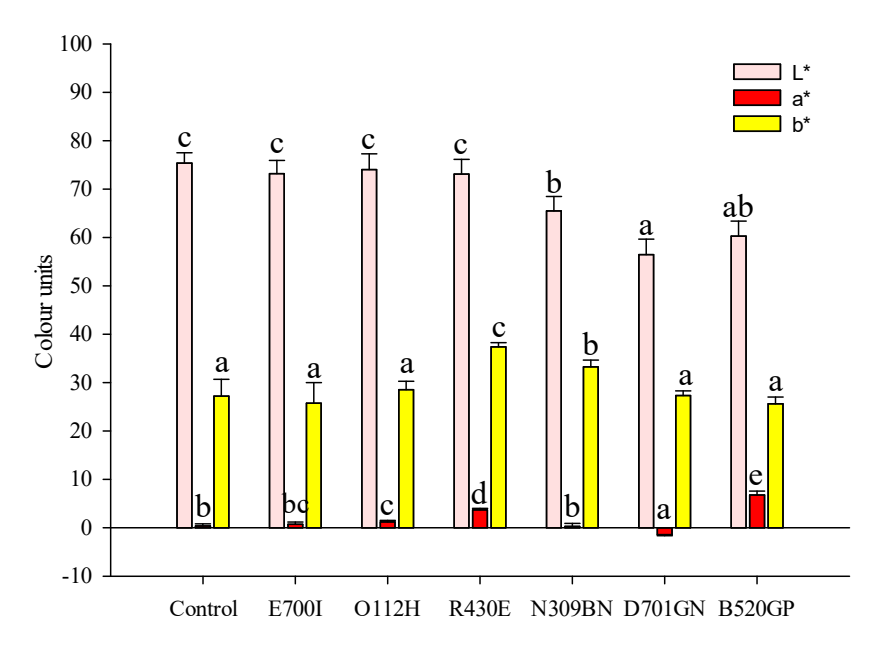


Figure VII.2 Colourimetric profile of the different types of functional and traditional pasta (control). 156

Different letters above the bars indicate significant differences ($p \le 0.05$) among the mean values of each colourimetric parameter of the investigated samples.

Results reported in Figure VII.2 show that the addition of the different extracts from agri-food by-products to the pasta matrix influenced the colourimetric profile of the pasta itself. Specifically, all the pasta samples obtained in this study showed positive values of L*, in the range 60 - 75, indicating that the lightness component was dominant in all cases. However, N309BN, D701GN, and B520GP pasta samples were statistically significantly darker than those made from durum wheat semolina, consistently with previous findings demonstrating that the addition of non-conventional ingredients, such as rice flour, defatted soy flour, and cereal brans induced a substantial decrement in the whiteness of pasta (Kaur et al., 2012; Sereewat et al., 2015).

Nevertheless, changes in colourimetric parameters were noticeable in the case of some types of functional pasta, including R430E and B520GP, which showed a significant increase in the parameter a* (redness) (4-fold, and 8-fold increase, respectively, compared with the control), mainly due to the presence of natural pigments such as carotenoids and anthocyanins. Likewise, D701GN pasta, functionalized with the herbaceous HPH-treated suspension (B651S) possessed a negative value of the parameter a*, highlighting its tendency to green attributed to the leaf pigments, mainly chlorophyll (Figure VII.2).

For the sake of comparison, the overall difference (ΔE) of the colourimetric parameters between each functionalized pasta and those of the traditional pasta was evaluated, and the obtained results are depicted in Figure VII.3.

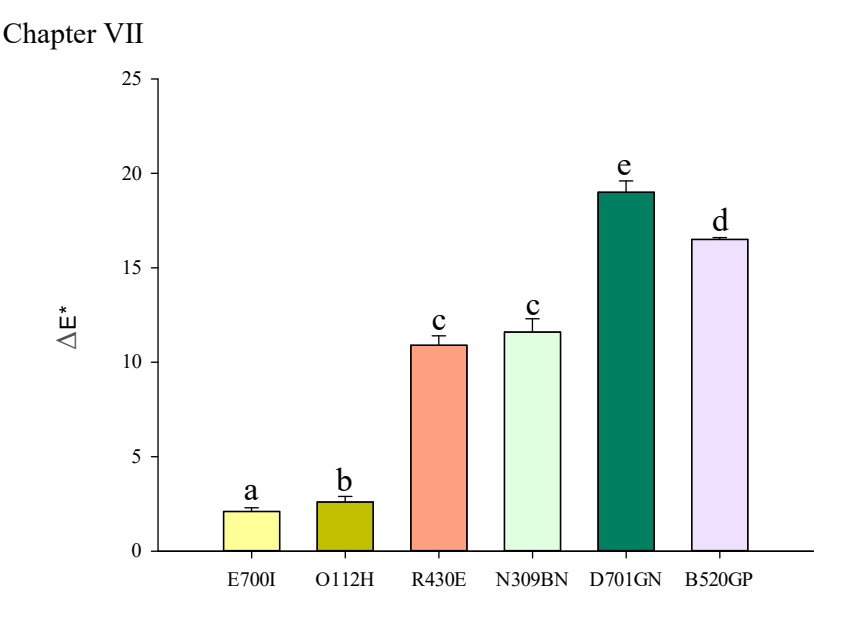


Figure VII.3 Overall difference (ΔE^*) between the main colourimetric parameters of functional pasta samples and those of traditional pasta (control). Different letters above the bars indicate significant differences ($p \le 0.05$) among the mean values of the samples.

From the obtained results, it was possible to identify three representative groups of pasta samples based on ΔE values compared with the control sample. E700I and O112H are characterised by $\Delta E < 3$, R430E and N309BN by $10 < \Delta E < 15$, D701GN and B520GP by $\Delta E > 15$. The latter samples represent the two types of pasta that mostly differ from the control in terms of colour profile, while E700I and O112H samples exhibited colour profile like that of traditional pasta, since no colour differences can be detected by human eye ($\Delta E < 3$).

VII.3.1.2 Sensory analysis

The sensory attributes of the pasta samples were determined by a panel test of 20 previously trained judges, who evaluated, by means of a descriptive analysis, the different pasta samples according to the intensity of the main characteristic descriptors of the pasta product. The descriptive test was divided into two types of evaluations: visual and olfactory evaluations and tasting evaluation. In particular, the parameters analysed were the brightness, uniformity, colour, odour, vegetable odour, compactness, taste, vegetable taste, overall acceptability. The obtained scores are reported in Figure VII.4.

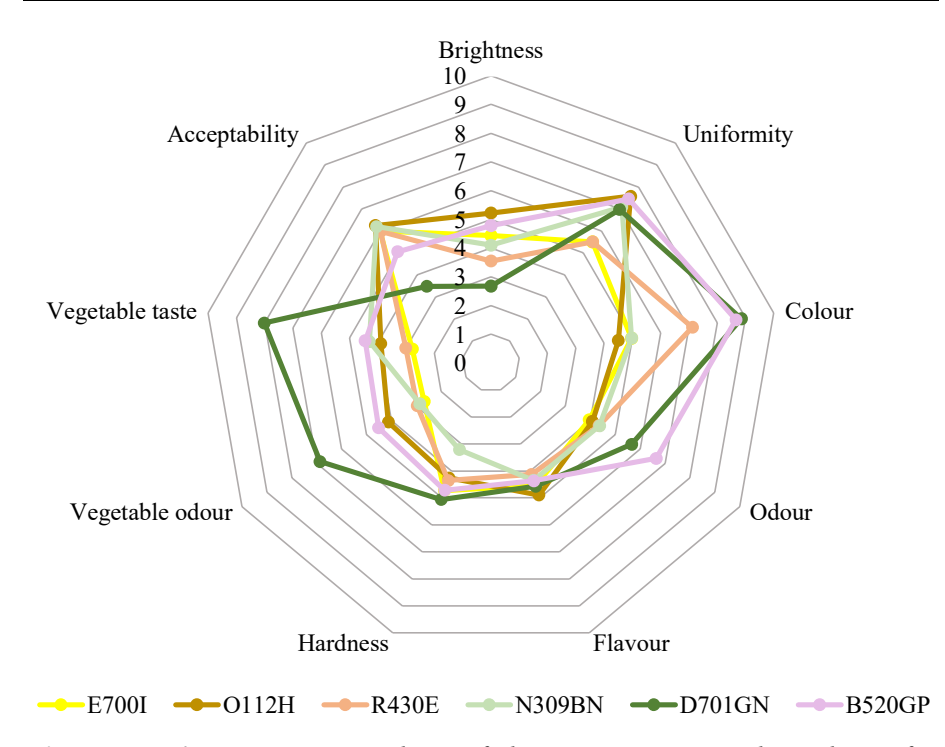


Figure VII.4 Descriptive analysis of the main investigated attributes for functional pasta samples.

Interestingly, the qualitative results related to the colour of the investigated samples, depicted in Figure VII.4, are in good agreement with the quantitative results obtained from the analysis of the colourimetric parameters (§ VII.3.1.1).

Specifically, R430E, B520GP and D701GN pasta received higher scores than the other types of functional pasta in terms of colour, indicating the greater difference in colour perceived by the judges compared with the control sample. Moreover, based on the scores in terms of brightness, D701GN sample is the sample that received the lowest value, consistently with the detected L* parameter (§ VII.3.1.1). Overall, D701GN pasta had high scores in terms of vegetable odour and taste, and it was found to be the least acceptable by the involved panelists, given the particularly pronounced chromatic profile and vegetable smell.

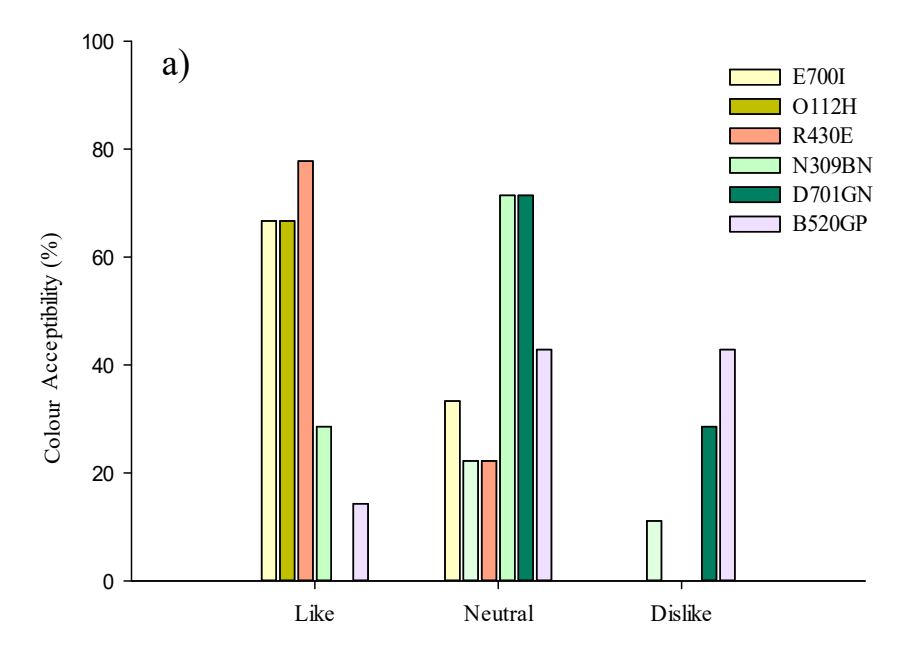
Another important pasta quality indicator is uniformity. E700I and R430E were considered the samples with the uniformity most like that of the control, highlighting the effectiveness of the wet micronisation of the plant residue by HPH treatment to obtain homogeneous and smooth total suspensions with negligible phase separation, increased consistency and stability (Van

Buggenhout et al., 2015; Yu et al., 2016) with reduced adverse effect on the sensory attributes when incorporated in pasta.

However, all the investigated samples received good scores in terms of uniformity, indicating that the separated hydration of semolina and natural additives before the kneading step contributed to effectively distribute the functional ingredients in the dough, improving the organoleptic properties of the final pasta (la Gatta et al., 2017). In addition, the use of cell disruption or permeabilization technologies, leading to a significant increase in the bioactivity of the obtained extracts, allowed adding a lower amount of non-conventional ingredients (1%, on a dry basis) compared to those usually incorporated into the pasta product, as emerged from the literature (Table II.2), which is expected to reduce the negative impact on the processability of the pasta dough and on the sensorial characteristics of pasta.

Likewise, according to the panelists, the hardness all the different types of functional pasta did not significantly differ from the control.

Additionally, to give a clearer idea of the acceptability of the investigated pasta samples, the values of acceptability (like, neutral, dislike) by the panelists in terms of colour and odour, (the two characteristic parameters that mostly influence the consumers' purchase decision) were determined and reported in Figure VII.5.



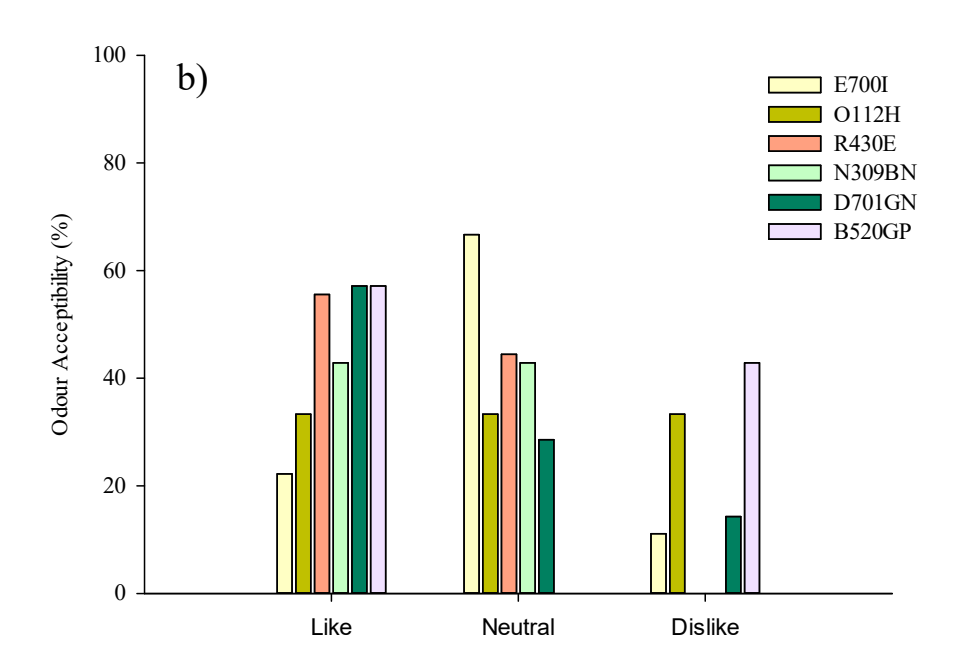


Figure VII.5 Acceptability by panelists in terms of colour (a) and odour (b) of the functional pasta samples.

From the graphs depicted in Figure VII.5 it is possible to notice that R430E, O112H and E700I were the most appreciated samples, in terms of colour, by approximately the 75% of panellists. It is interesting to notice that, despite R430E significantly differed from the control pasta in terms of detected colourimetric parameters (§ VII.3.1.1), it was found to be the most appreciated sample by the panellists. Conversely, the less appreciated samples in terms of colour were D701GN and B520GP (about 30% of panellists disliked their colour). These findings are in good agreement with the previously reported overall colourimetric difference of D701GN compared with the traditional pasta ($\Delta E > 15$). However, although D701GN received the highest score in terms of vegetable odour (Figure VII.4), most of the panellists (57%) liked its olfactory profile.

Results demonstrated that the addition of natural non-conventional ingredients to pasta did not negatively affect its homogeneity, colour, taste, and odour, that are the parameters that most influenced the evaluation of the overall quality of dry pasta.

VII.3.1.3 Texture profile analysis (TPA)

Through the texture analysis it is possible to define the critical factors, such as processing conditions and sensorial parameters, which affect the compactness and hardness of a food product and, consequently, its acceptability by consumers.

In this study, the compression force needed to cut the functional and traditional pasta samples with the incisors was determined by a single compression test. The results obtained showed that, despite the slightly higher hardness value detected for the control compared to the other samples, the addition of natural extracts did not negatively affect the compactness of the functional pasta after cooking (Figure VII.6). All types of functional pasta produced do not show cutting force values with statistically significant differences (p<0.05) compared to those of the control pasta.

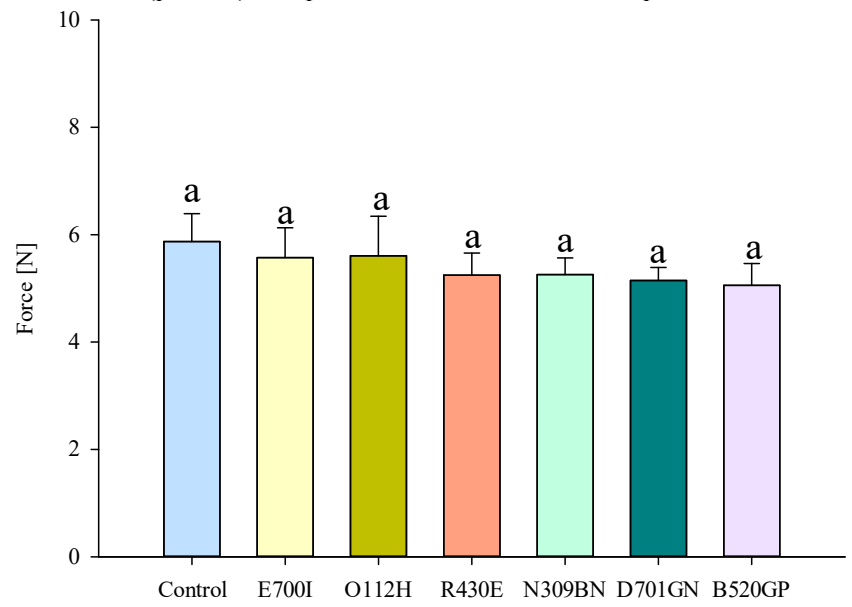


Figure VII.6 *Texture profile of functional and traditional pasta samples (control). Different letters above the bars indicate significant differences* $(p \le 0.05)$ *among the mean values of the samples.*

In conclusion, the obtained results, in agreement with previous findings (Biernacka et al., 2019; Cimini et al., 2022; Monteiro et al., 2019), and coherently with the sensory profile evaluations of pasta (§ VII.3.1.2), have shown that neither the production process of functional pasta nor the texture characteristics of the product after cooking differ from those traditionally considered as acceptable by the pasta consumers.

VII.3.1.4 Cooking properties

The amount of water absorbed per gram of dry pasta during the cooking phase of the different pasta samples has been determined and reported in Figure VII.7. The main evidence found was that no significant differences were observed among the different samples, and that water absorption index was stable for all the samples analysed, even after 10 minutes from the end of the cooking phase.

Results also demonstrate that the weight of cooked pasta ranged from 0.9 to 2.3 times the initial weight of dry pasta samples, in agreement with the expected ideal cooked weight for durum wheat pasta that should not be more than three times the dry weight (Piwińska et al., 2016).

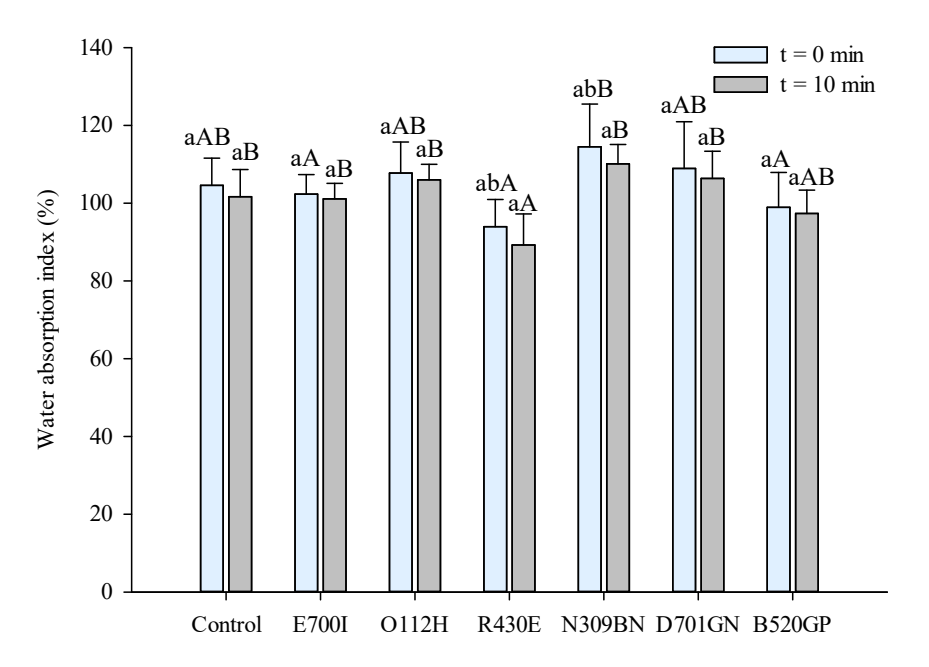


Figure VII.7 Water absorption index (WAI) of functional and traditional pasta samples (control), at cooling time of 0 min and 10 min after cooking. Different lowercase letters above the bars indicate significant differences ($p \le 0.05$) among the mean values of the same samples at different cooling times (0 min, 10 min).

Different uppercase letters above the bars indicate significant differences $(p \le 0.05)$ among the mean values of the different samples at the same cooling time.

In addition, despite the slight differences among the WAI of the investigated samples, the obtained results were affected by the differences in the proximate composition of the natural additives.

Specifically, N309BN pasta showed a slightly higher WAI compared to that of the other samples, due to the association of water absorption capacity and water solubility with hydrophilic constituents, such as polysaccharides. The extract used to obtain N309BN pasta, namely N433W, showed the highest WAC and WSI (as previously discussed in § VI.3.2), due to the highest content of water-soluble polysaccharides (57.9% on a dry basis). On the contrary, R430E pasta, functionalized with the E706IT suspension showed the lowest water absorption capacity, coherently with the lowest WAC and WSI detected for the extract (§ VI.3.2), and with the highest amount of lipids in its composition, compared to the other investigated extracts (1.5% on a dry basis).

It is worth noting that the higher is the water uptake, the higher are the amylose leaching, cooking losses, and loss of starch crystalline structure (Syah et al., 2022). Therefore, in agreement with the values of WAI, N309BN and B520GP pasta showed the highest losses during cooking, while R430E pasta showed the lowest ones (Table VII.1).

However, all types of functional pasta, as reported in Table VII.1, showed losses during cooking comparable to those of durum wheat pasta.

High-quality durum wheat pasta should be characterised by cooking loss values that should not exceed 7 - $8 \, g/100 \, g$ (Piwińska et al., 2016). Therefore, it can be concluded that all the tested pasta formulations can be considered acceptable in terms of cooking losses.

Additionally, within the cooking properties, the optimal cooking times (OCT) of the pasta samples were determined and reported in Table VII.1. The obtained results show slightly lower values for functional pasta compared with the control, indicating that the addition of natural extracts in the matrix, could induce a better distribution of water within it, reducing also the time needed to obtain the gelatinization of components.

TableVII.1 Optimal cooking time (OCT), and cooking losses (CL) of functional and traditional pasta samples (control).

	Control	О112Н	R430E	E700I	N309BN	D701GN	B520GP
OCT (min)	10	9.30	9.30	9.00	9.30	8.30	9.30
CL (per 100 g di pasta)	$\begin{array}{c} 3.6 \pm \\ 0.2^{ab} \end{array}$	4.4 ± 0.1°	3.6 ± 0.1 ^a	4.0 ± 0.2b ^c	5.2 ± 0.1 ^d	4.4 ± 0.2°	5.6 ± 0.1 ^d

Values with different lowercase letter within the same row are significantly different ($p \le 0.05$).

VII.3.1.5 Thermal properties

Thermal analysis is a valuable tool for investigating the effect of thermal processing on the main components of raw materials and the phase transition of starch. It is well known that the drying and cooking processes of pasta cause structural changes on starch and gluten network of the dough. In fact, during heating starch gelatinization process, such as the transition of insoluble starch granules to a solution composed of individual molecules, takes place (Romano et al., 2015).

Durum wheat starches show two endotherms during heating. The first, with transition peak temperature (T_{peak}) generally ranging between 51 °C and 79 °C (Romato et al., 2015), corresponds to the gelatinization of starches, while the second, with a T_{peak} between 90 °C - 120 °C (Detchewa et al., 2016), represents the melting/dissociation of amylose-lipids complexes.

In Table VII.2 are reported the DSC parameters, such as transition onset temperature (T_{on}), transition peak temperature (T_{peak}), transition end temperature (T_{end}), and transition enthalpy (ΔH) associated to the starch gelatinization and the dissociation of amylose/lipids complexes for all the investigated samples. Values of T_{peak} obtained in this study fall within the ranges associated with wheat starches. Specifically, T_{peak1} ranges between 67.35 °C and 69.19 °C, while T_{peak2} is between 89.50 °C and 103.76 °C.

Table VII.2 Thermal properties of the analysed samples: ΔH , transition enthalpy, T_{on} , onset temperature; T_{peak} , peak temperature; T_{end} , end temperature.

Sample	Ton ₁ (°C)	Tpeak ₁ (°C)	Tend ₁ (°C)	ΔH ₁ (J/g)	Ton ₂ (°C)	Tpeak ₂ (°C)	Tend ₂ (°C)	ΔH ₂ (J/g)
Control	63.29 ± 0.32^{b}	68.19 ± 0.42^{a}	74.07 ± 0.22^{abc}	$\begin{array}{l} 0.76 \pm \\ 0.02^{abc} \end{array}$	96.26 ± 0.30 ^e	$103.76 \\ \pm 1.50^d$	106.31 ± 0.52°	$\begin{array}{c} 0.09 \pm \\ 0.00^{b} \end{array}$
О112Н	61.83 ± 0.21 ^a	67.80 ± 1.02^{a}	$74.84 \pm \\ 0.20^{ab}$	$\begin{array}{l} 0.72 \pm \\ 0.01^{ab} \end{array}$	85.77 ± 0.10^{ab}	89.50 ± 0.92^{a}	98.15 ± 0.90^{a}	$\begin{array}{c} 0.08 \pm \\ 0.00^a \end{array}$
R430E	62.08 ± 0.11 ^a	67.35 ± 0.50^{a}	75.13 ± 0.30^{bc}	0.79 ± 0.05^{bc}	87.70 ± 0.21°	95.68 ± 2.00 ^{bc}	$101.52 \pm \\ 1.10^{b}$	0.16±0 .00 ^d
E700I	61.65 ± 0.20^{a}	$67.36 \pm \\ 0.20^a$	73.71 ± 0.40°	0.80 ± 0.03°	85.51 ± 0.60^{ab}	95.15 ± 0.80 ^{bc}	$102.13 \pm \\ 1.20^{ab}$	0.12 ± 0.00°
N309BN	61.67 ± 0.42 ^a	67.70 ± 0.92^{a}	74.51 ± 0.30 ^{abc}	$\begin{array}{l} 0.72 \pm \\ 0.03^{ab} \end{array}$	$84.87 \pm \\ 0.20^a$	90.60 ± 1.80^{a}	100.18 ± 0.95^{b}	0.08 ± 0.00^{a}
D701GN	61.98 ± 0.41 ^a	67.85 ± 0.70^{a}	75.90 ± 0.40^{d}	0.77 ± 0.03 ^{bc}	86.90 ± 0.60 ^{bc}	93.55 ± 2.00^{ab}	101.71 ± 1.16 ^b	0.12 ± 0.00°

B520GP	$62.08 \pm$	$68.09 \pm$	$75.81 \pm$	$0.69 \pm$	$90.80 \pm$	$97.68 \pm$	$102.16 \pm$	$0.09 \pm$
	0.10^{a}	0.19^{a}	0.12^{d}	0.02^{a}	1.50^{d}	$0.50^{\rm c}$	0.80^{b}	0.00^{b}

Values with different lowercase letter within the same column are significantly different ($p \le 0.05$).

It is interesting to notice that the control pasta showed a statistically significant higher transition onset temperature (T_{onl}) compared with the other samples. This observation appeared consistent with the OCT of control pasta, that was slightly higher (30 s) than those of the other samples (§ VII.3.1.4), since the cooking time is related to the transition temperatures of starch gelatinization (Kaur et al., 2016).

Likewise, strong positive correlations between wheat starch transition enthalpy of pasta and dietary fibres, fat, and protein content, were observed by several authors (Lu et al., 2018; Romano et al., 2015), who speculated that fibres (especially insoluble dietary fibres) and fat exert a protective role during processing, reducing the degree of starch granule gelatinisation during pasta production process and cooking phase. R430E, E700I, D701GN pasta, functionalized with the E706IT, A781M, and B651S total suspensions obtained via HPH, showed the highest values of the transition enthalpy (ΔH_1), coherently with the highest fibre (73.8% – 75.9% on a dry basis), protein (10.6% – 15.1% on a dry basis), and lipid content (1.1% – 1.5% on a dry basis) of the natural extracts.

The higher enthalpy values indicated a higher order of crystallinity in these samples, while the decrease in transition temperature and gelatinization enthalpy (ΔH) could be attributed to the destruction of amylopectin chains and reduction in the overall crystallinity of the starch (Romano et al., 2015).

Results also demonstrated that R430E sample had the highest transition enthalpy ($\Delta H_2 = 0.16 \text{ J/g}$) associated with the dissociation of amylose/lipids complexes, appearing consistent with the lipid content of E706IT suspension, and with the lowest investigated water absorption index of R430E (§ VII.3.1.4), as the increase of amylose-lipids complexes contributes to lowering water absorption of pasta (Zhang et al., 2013).

VII.3.1.6 Pasting analysis

The pasting properties of a sample represent the modifications that occur inside it due to the application of heat in the presence of water. Pasting viscosities are indicators of the degree of interaction between the different components of a food system and the effect of any modification on its functionality when it is processed (Meares et al., 2004). The peak time, peak viscosity, breakdown viscosity, and setback viscosity of the analysed pasta samples are reported in Table VII.3.

Interestingly, the control pasta showed a higher pasting time (300 s), that is the time at which the structural changes start, than that of the functional pasta 166

samples (273 s - 288 s). These findings are coherent with the measured peak onset temperature for starch gelatinisation (\S VII.3.1.5), and with the OCT (\S VII.3.1.4) of the pasta samples. Likewise, the peak viscosity time was greatly correlated with the OCT of the pasta samples, with a Pearson correlation coefficient of 0.928.

The peak viscosity indicates the maximum viscosity that occurs at the equilibrium point between swelling and polymer leaching, indicating the capacity and ability of water absorption of starch granules (Punia et al., 2021). In the present study, the decrease observed in viscosity values for R430E compared with the control pasta might be partially attributed to the increased fat and fibre levels that compete with starch for water binding, increasing hydrogen bonding and stability within granules and depriving starch of binding water (Gull et al., 2018; Sayar et al., 2005).

Table VII.3 *Pasting properties of the analysed samples.*

Sample	Pasting time (s)	Peak time (s)	Peak viscosity (Pa*s)	Breakdown viscosity (Pa*s)	Setback viscosity (Pa*s)
Control	300±0.9e	470±0.30 ^d	55.6±2.9 ^{ab}	30.8±0.1°	52.9±1.4a
R430E	276±1.30 ^b	460±0.41°	49.2±2.7 ^a	22.6±2.3 ^a	51.5±2.2 ^a
E700I	280±1.00°	450±0.50 ^b	54.4±1.3 ^{ab}	27.0±0.9bc	52.5±0.3ª
О112Н	275±0.70 ^b	460±0.12°	56.5±0.9 ^{ab}	31.0±1.6°	50.2±2.7 ^a
B520GP	275±0.90 ^b	450±0.10 ^b	57.9±3.3 ^b	42.8±1.7 ^d	45.3±6.7 ^a
D701GN	273±0.80 ^a	440±0.31ª	50.8±4.9 ^{ab}	26.2±0.8 ^{ab}	53.2±0.5 ^a
N309BN	288±1.50 ^d	460±0.20°	52.2±1.2 ^{ab}	27.9±1.1 ^{bc}	50.9±1.5 ^a

Values with different lowercase letter within the same column are significantly different ($p \le 0.05$).

The breakdown viscosity, defined as the difference between peak and holding viscosity, is related to the starch granules disintegration or stability during the

holding time with the viscosity test. It gives information on the hydration, starch swelling power and shear resistance of starch during heating (Shafie et al., 2016). The highest breakdown viscosity could be linked with its higher peak viscosity value (Rani et al., 2019). Statistically significant reduction in the breakdown viscosity of R430E and D701BN pasta samples compared to that of the control might be associated with the restricted swelling behaviour of starch granules in consequence of total extracts incorporation. Reduced breakdown viscosity is suggestive of a higher resistance of the sample toward shear thinning during the cooking process, and together with reduced peak viscosity is essential for a good pasta texture attribute (Rani et al., 2019).

The setback viscosity, calculated by subtracting holding viscosity from final viscosity, is related to retrogradation tendency, and reordering of starch after gelatinization and cooling (Patil et al., 2020). Low setback values indicate low rate of starch retrogradation and syneresis (Rani et al., 2019). As indicated in Table VII.3 setback viscosities of the pasta samples did not differ significantly from each other (p < 0.05), suggesting good compatibility among the different investigated functional pasta samples.

VII.3.1.7 Microstructural analysis

Scanning electron microscopy (SEM) was used to investigate the surface (Figure VII.8) and cross section (Figure VII.9) structure of all the investigated dry pasta samples.

The results of cooking properties, texture profiles, thermal and pasting properties of the pasta samples were coherent with the microstructural analysis of both the functional and traditional pasta.

The obtained surface micrographs, reported in Figure VII.8, showed minor differences among the structure of the several samples upon the addition of non-conventional ingredients.

Specifically, the surface area of E700I, R430E and D701GN samples, functionalized with HPH-treated total suspensions (A781M, E706IT, and B651S, respectively), was characterised by a reduced roughness, a network with denser areas, and starch granules strongly embedded in the glutinous matrix.

This may be due to the increased interactions between starch-gluten-extract and the presence of lipids and macromolecules, such as fibres and proteins, that tend to exert a protective effect on starch granules, in agreement with previous studies showing that pasta enriched with insoluble dietary fibres and proteins exhibited a more compact surface than the control, with starch granules coated by a smooth film (Aravind et al., 2012; Lu et al., 2018).

However, O112H, N309BN, and B520GP samples displayed a rough, less compact, and more porous surfaces.

These considerations were confirmed by taking the cross-section micrographs (Figure VII.9), where less distinct starch granules could be observed in the

case of R430E, E700I, and D701GN samples. Similarly, SEM from a study incorporating pollard showed that pasta with 40% replacement were minimally disrupted compared with the control pasta (Aravind et al., 2012).

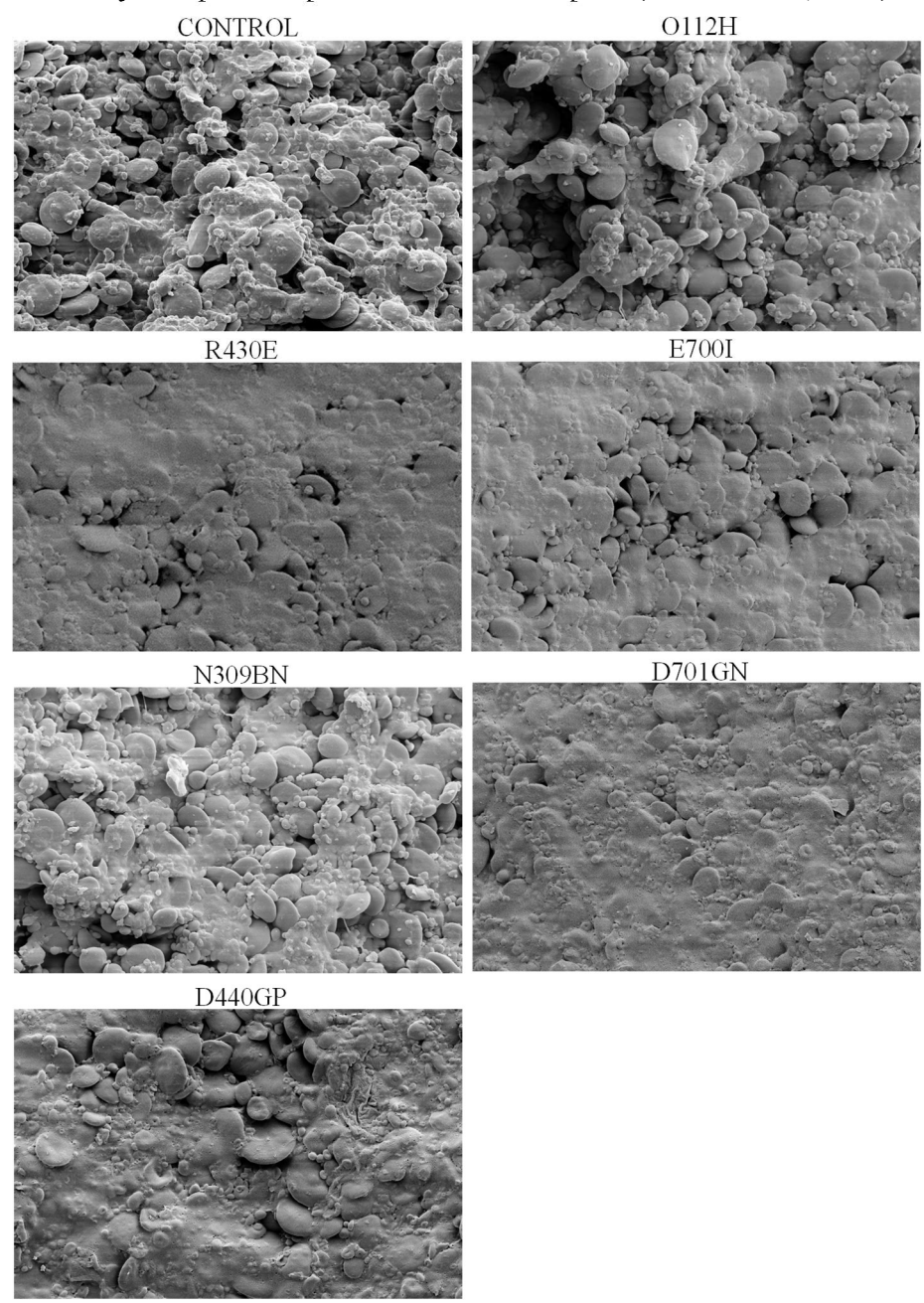


Figure VII.8 Scanning electron micrographs of raw pasta surface.

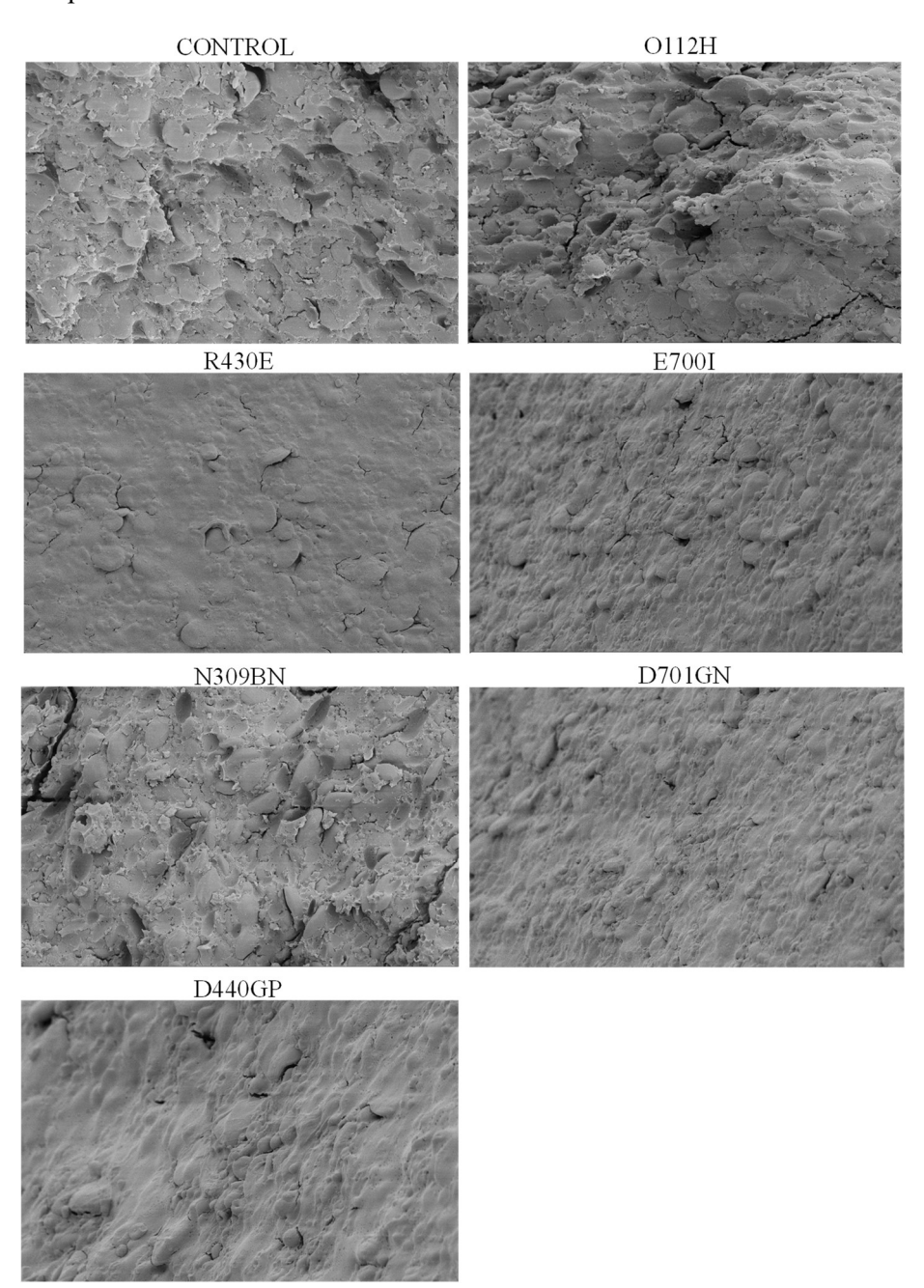


Figure VII.9 Scanning electron micrographs of raw pasta section.

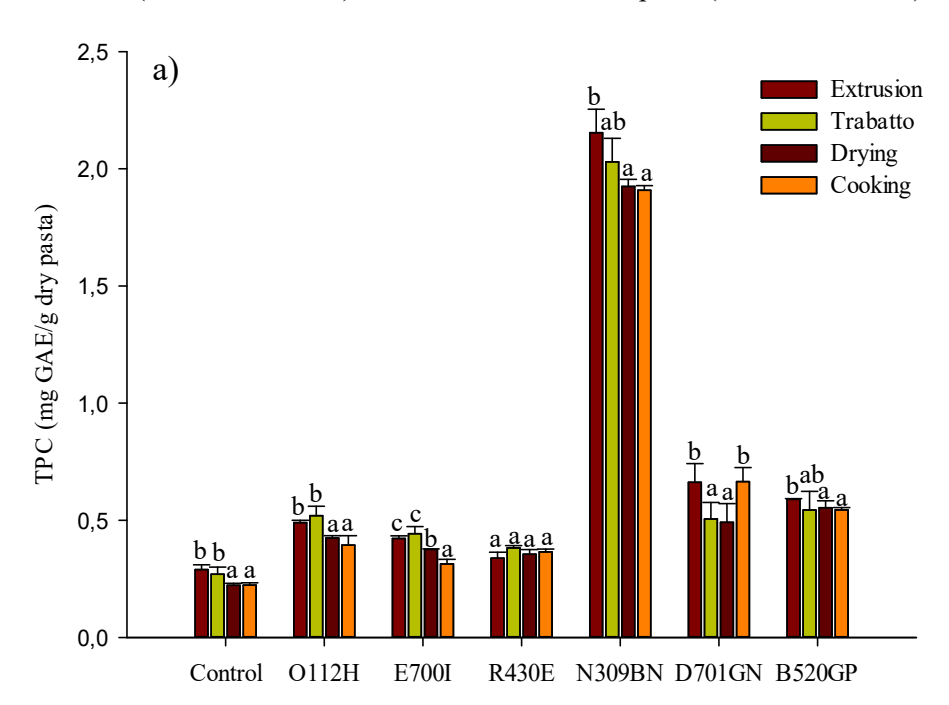
VII.3.1.8 Chemical profile

Total phenolic content (TPC) and antioxidant activity (FRAP values) of pasta samples before and after each production processing phase (extrusion, trabatto, drying), and cooking phase are reported in Figure VII.10.

It is known that traditional durum wheat semolina pasta has important levels of functionality due to its composition, with a total phenolic content of 0.29 mgGAE/g pasta, in agreement with that found elsewhere for durum wheat dry pasta (Gull et al., 2016).

However, as shown in Figure VII.10, the addition of natural extracts from the selected agri-food by-products significantly increased the bioactivity of the traditional pasta in terms of phenolic compounds and antioxidant activity, regardless of the type of extract added.

Specifically, in agreement with the bioactivity of the investigated natural extracts (§ V.3), those that mostly contributed to the increase in the level of TPC and antioxidant activity of control pasta are the extracts used to produce N309BN (6.4-fold increase), B520GP and D701GN pasta (1.2-fold increase).



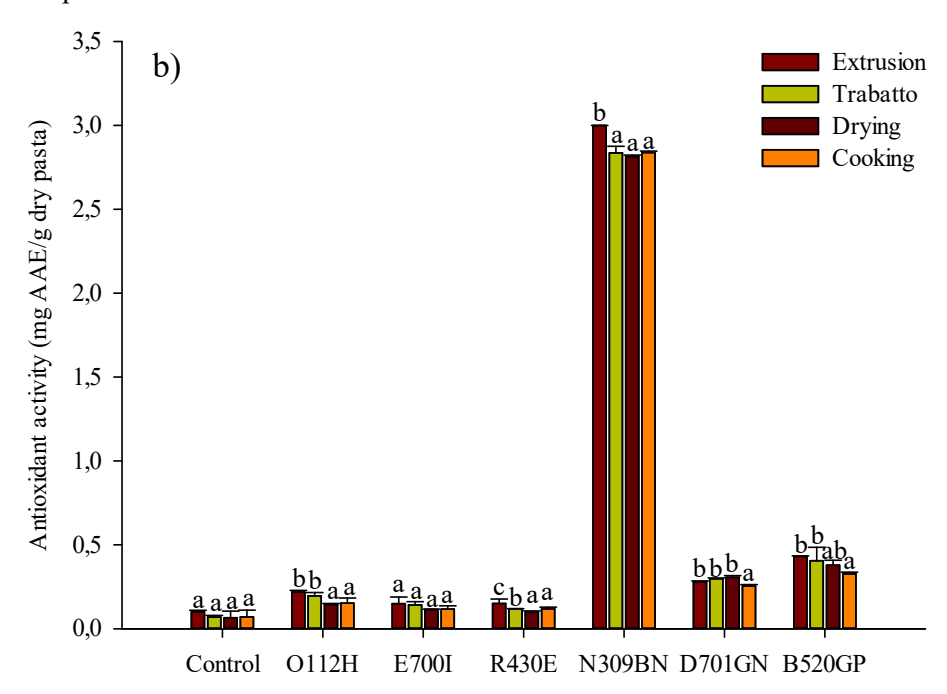


Figure VII.10 Chemical profile in terms of total polyphenols (a) and antioxidant activity (b) of functional and traditional pasta samples (control), downstream of the main phases of dry pasta production and cooking. Different letters above the bars indicate significant differences ($p \le 0.05$) among the mean values of the same samples at different processing phases.

The obtained results showed that the concentration of bioactive compounds added to the different types of pasta had not undergone a drastic degradation after each production and cooking phases. Specifically, TPC level and antioxidant activity of the cooked pasta samples decreased of about 13% and 20% on average, respectively, compared with fresh pasta samples (after extrusion).

Interestingly, the decrements in TPC and antioxidant activity in cooked pasta detected in this study are much lower than those found by other authors when investigating the thermal degradation of polyphenols and antioxidant activity of pasta during the production process and cooking. Verardo et al. (2011), studied the effects of pasta-making process (mixing, extrusion, drying) and boiling step on total free phenolic compounds that decreased of about 74.5% from whole buckwheat flour to cooked spaghetti.

Likewise, Gull et al. (2018) concluded that the TPC and antioxidant activity of cooked pasta samples decreased significantly of 51% and 55%, respectively, due to thermal degradation during cooking and leaching of phenolic compounds into cooking water.

As an example, in Figure VII.11 the chromatogram obtained by HPLC of the O112H sample before and after the cooking phase (dry and cooked pasta) is reported. The two samples showed similar phenolic profiles confirming that the cooking phase did not lead to any significant degradation phenomena, with the concentration of some phenolic compounds slightly increasing upon cooking.

In some cases, phenolics in cereal products were reported to increase with cooking, since the process can soften the hard structure and break cellular components, allowing an easier extraction from the matrix (Carcea et al., 2017). Fares et al. (2010) reported an increase of bound phenolic acids (from 22 to 46%) in cooked pasta with respect to raw durum wheat pasta enriched with debranning fractions of wheat. Changes of phenolic compounds upon cooking could result from oxidative degradation, release of free acids from conjugate forms, and formation of complex structures of phenolic substances from related compounds (Carcea et al., 2017).

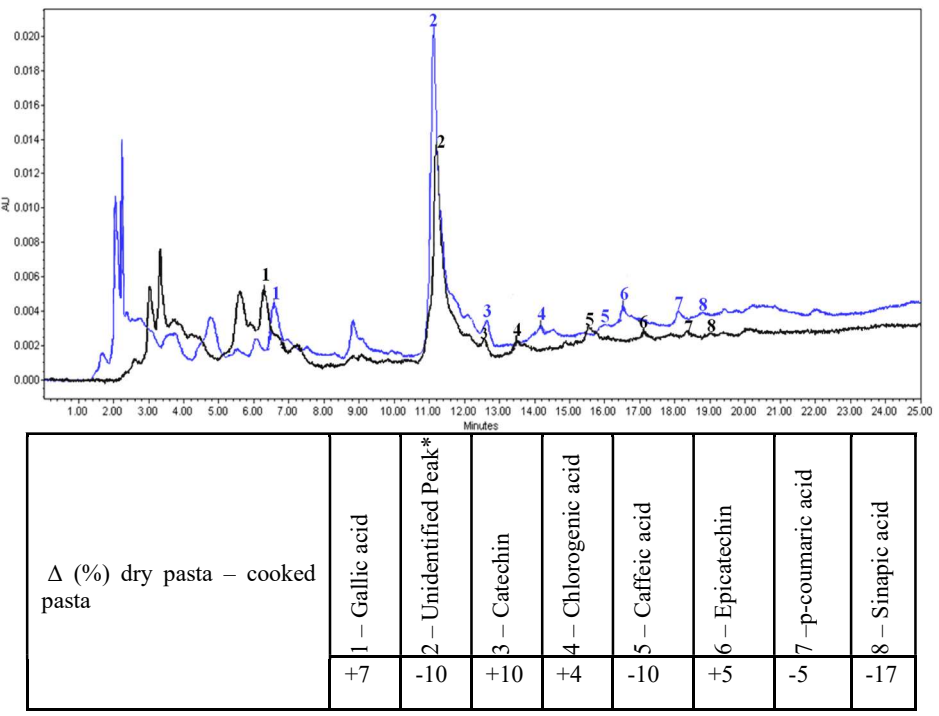


Figure VII.11 Chromatogram (HPLC) of extracts from B520GP dry pasta (blue curve) and cooked pasta (black curve) samples and change in the concentration of the identified phenolic compounds between B520GP pasta before and after cooking.

*Peak 2: unidentified compound at 11.30 min, that could correspond to hydroxybenzoic acid, being one of the most abundant free phenolic

acids in durum wheat semolina (Bueno-Herrera and Pérez-Magariño, 2020).

VII.4 Conclusions

The results obtained in this chapter highlighted the potentiality of the natural extracts obtained from the selected agri-food residues to be used as bioactive non-conventional ingredients for pasta functionalization, without sacrificing the sensory aspect of the final pasta, and a significant increase of its bioactivity has been detected.

The sensory analysis of the dry functional pasta samples showed that the addition of these extracts at the selected concentration did not led to any drastic change in the organoleptic characteristics of the final product, which were well-correlated with the previously detected colourimetric parameters and hardness values. Moreover, the results of the structural analysis and cooking properties were in good agreement with the thermal and pasting properties of the pasta samples and were coherently related to the proximate composition, mainly in terms of fat, fibre, and protein content, of the natural extracts.

Interestingly, the production process and the cooking phase of the pasta did not induce significant degradative effects and loss of bioactivity in the samples.

These results can be attributed to the use of emerging cell disruption technologies, such as HPH and PEF, which contributed to reducing the negative effects of the incorporation of natural extracts in the pasta on its appearance and sensory attributes, improving the extractability of bioactive compounds from plant matrices, and, therefore, reducing the amount of extracts to be added to the pasta. This helped to retain a good sensory acceptance of the final products, without affecting the appearance, texture and cooking quality, and at the same time improving the bioactivity of the newly formulated pasta.

Nevertheless, further investigations are needed to assess the chemical stability of these compounds through *in vitro* digestive studies, as well as their potential health-beneficial effects.

Chapter VIII Health validation of the new functional pasta: in vitro digestibility and biological activity

Abstract

In this chapter, *in vitro* total phenolic compounds (TPC) release and starch digestibility during oral, gastric, and intestinal digestion phases were performed, considered among the most important steps to investigate when validating a newly formulated functional food product. In addition, the potential biological effects of the functional pasta samples, after *in vitro* digestion, on human cell lines, including hepatocarcinoma, colorectal adenocarcinoma, and liposarcoma cell lines, were also evaluated.

Results showed that all the pasta samples had a similar TPC release profile during digestion reaching the maximum release in the intestinal phase (76% - 98%). Likewise, average values of digested starch of about 10% in the oral phase, 23% in the gastric phase, and 70% in the intestinal phase were detected in the pasta samples. Nevertheless, rapidly and slowly digestible starch fractions of the pasta samples functionalized with the total suspensions fully recovered by the plant matrices (R430E, E700I, D701GN) exhibited notable reductions, while resistant starch fractions showed a corresponding increase compared with the control. These findings could support the potential of functionalized pasta for the prevention of the metabolic syndrome due to a slowed glucose release in the blood. Moreover, B520GP pasta digestate was able to significantly reduce the secretion of the pro-inflammatory mediators Interleukin-6 and Monocyte Chemoattractant Protein-1 in LPS-stimulated macrophages, even at the lowest investigated concentration. Conversely,

R430E digestate exerted a positive effect on glucose uptake in liposarcoma cell lines. These results highlighted the anti-inflammatory properties and the ability to modulate the glucose uptake of the investigated pasta samples, differentiating their specific biological effects in relation to the type of extract incorporated into the pasta and the main components constituting the functional ingredients.

VIII.1 Introduction

In vitro release studies are among the most important steps to consider when developing and validating a newly formulated functional food product. A successful food system not only has to protect the bioactive compound ensuring its bioavailability, but also needs to guarantee the intended release behaviour (temporal and target oriented) (Celli et al., 2015).

In this sense, phenolic extracts, together with individual phenolic compounds, are the most studied bioactives for food product design, nevertheless, studies dealing with final food applications, *in vitro* digestion, and biological effects are much scarcer (Dias et al., 2015).

The human digestive system is a complex, multi-phase (i.e., oral, stomach, small intestine, and large intestine compartments) biologic process in which food products undergo a series of steps that transform them into smaller and more basic components, in order to be absorbed (mostly in the small intestine) and reach the bloodstream. Therefore, studying the different physicochemical conditions of the digestive system and their impact on the most abundant components of the food product is of utmost importance.

In the case of functional pasta, investigating the starch digestibility during the human digestive phases could represent a strategy to understand the potential effects of the addition of non-conventional ingredients to the pasta on glucose release, which reflects blood glucose level, glycaemic index, diabetes, and metabolic syndrome. Results reported in the recent literature indicate that the starch digestibility in pasta with non-wheat flours is a complex process strongly affected by the addition of protein and dietary fibre (Garcia-Valle et al., 2021).

In addition, to the best of our knowledge, no studies have been carried out so far on the evaluation of the biological effects of the functionalized food product, after its *in vitro* digestion, using human cell lines.

Therefore, the aim of the present chapter was to explore the potential health-beneficial effects of the functional pasta samples, by evaluating the phenolic compounds bioaccessibility, the starch digestibility, and the biological effects of pasta digestates in human lipopolysaccharide-stimulated THP-1 macrophages, hepatocarcinoma, colorectal adenocarcinoma, and liposarcoma cell lines with specific emphasis on their anti-inflammatory activities and glucose uptake. This chapter has also the objective of understanding if the different types of digestate exerted specific health-beneficial effects

attributable to the nature of the non-conventional ingredients used to functionalize pasta and characterised by different chemical components.

VIII.2 Materials and Methods

VIII.2.1 Raw materials and samples preparation

Pasta samples were subjected to *in vitro* digestion studies, as reported in § IV.11.1 – IV.11.3, and subjected to further analyses (§ VII.2.2).

The pasta digestates were then characterised in terms of biological activity, and the samples prepared according to § IV.12.1.

VIII.2.2 Analytical determinations

The pasta samples were analysed in the different *in vitro* digestive phases in terms of TPC (§ IV.11.4), starch content and its nutritional fractions, rapidly digestible starch (RDS), slowly digestible starch (SDS) and resistant starch (RS), (§ IV.11.5). Pasta digestates were analysed in terms of cytotoxicity (§ IV.12.2), anti-inflammatory activity (§ IV.12.3 - IV.12.4), and glucose uptake (§ IV.12.5).

VIII.3 Results and discussion

VIII.3.1 In vitro digestion studies

During the *in vitro digestion* study of pasta, the concentration of bioactive compounds released from the functional and traditional pasta (control) samples after each digestion phase was monitored.

The TPC bioactive compounds were measured to understand how they behave during digestion, and in which part of the gastrointestinal tract they are mostly released or degraded.

The obtained results, reported in Figure VIII.1, showed total polyphenols from all the different investigated pasta samples are constantly released during digestion, and the maximum release occurred in the intestinal phase (76% - 98%). Due to the hydrolysis of starch taking place in the intestine, the bioactives are unlocked and their release in the digestive fluid is enhanced. Previous studies (Pigni et al., 2020; Podio et al., 2019) stated that the oral step allows the release of 37% and 50% of the TPC found in cooked control and supplemented pasta, respectively. Gastric and intestinal phases cause a much higher increase in TPC indicating that the action of enzymes (pepsin, pancreatin) and pH at these stages effectively favour the release of polyphenols from the food matrix. Nevertheless, it should also be highlighted

that the Folin Ciocalteu assay is not specific for polyphenols, since other reducing agents can react with the reagent (Pigni et al., 2020). Armellini et al. (2019) also found that the bioaccessibility (%) of each pasta, estimated as total crocin content at the end of gastrointestinal digestion with respect of total crocin in pasta before digestion, reached values up to $97 \pm 3\%$.

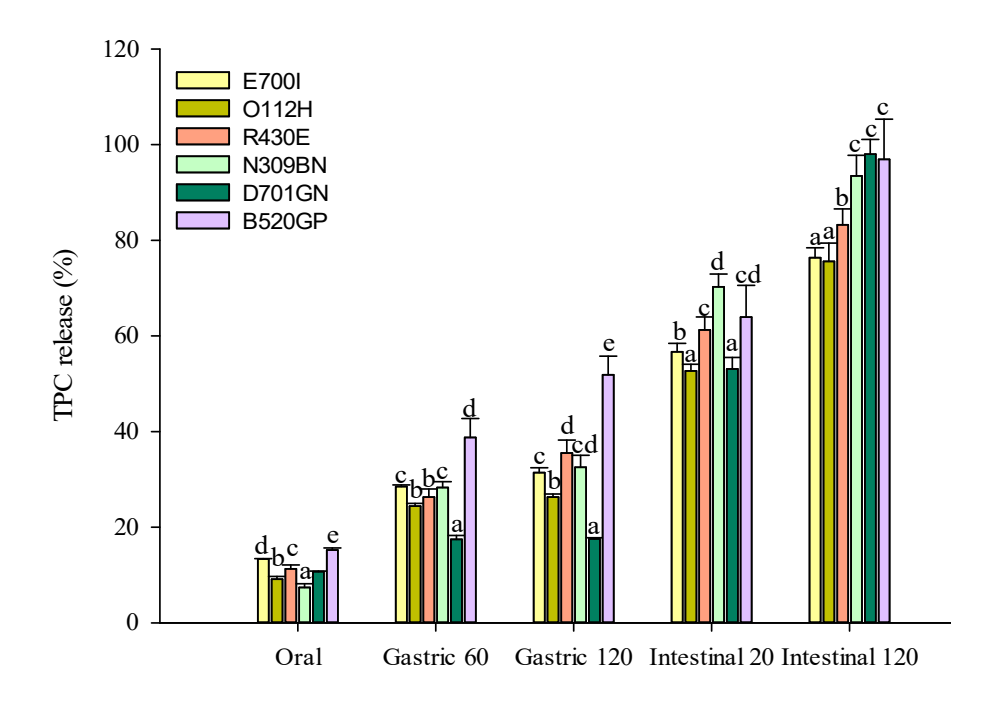


Figure VIII.1 Release of total phenolic compounds (TPC) during the digestive phases of functional and traditional pasta (control) samples. Different letters above the bars indicate significant differences ($p \le 0.05$) among the mean values of the different samples at the same digestive phase.

Regarding the starch digestibility, in general, all the samples presented a similar digestion profile (Figure VIII.2), reaching average values of digested starch of about 10% in the oral phase by the action of alpha-amylase, 23% in the gastric phase, and 70% in the intestinal phase. Similarly, Lucas-Gonzàlez et al., (2021) found that the starch hydrolysis of spaghetti with persimmon flours coproducts started in the oral phase, where around 10% of starch was released from the spaghetti matrix (p < 0.05). Then, in the gastric phase, around 13–19% of starch was transformed into glucose, reaching the highest ratios of starch hydrolysis (around 50–60%) during the intestinal phase. Results of the starch nutritional fractions of the investigated pasta samples, reported in Figure VIII.3, showed that, interestingly, the natural extracts added

to some types of pasta, including E700I, R430E, and D701GN, significantly contributed to increase the resistant starch fraction (RS, less easily digestible) in the intestinal phase of about 2.5 times compared to the control pasta, and led to a corresponding reduction in rapidly digestible starch (RDS).

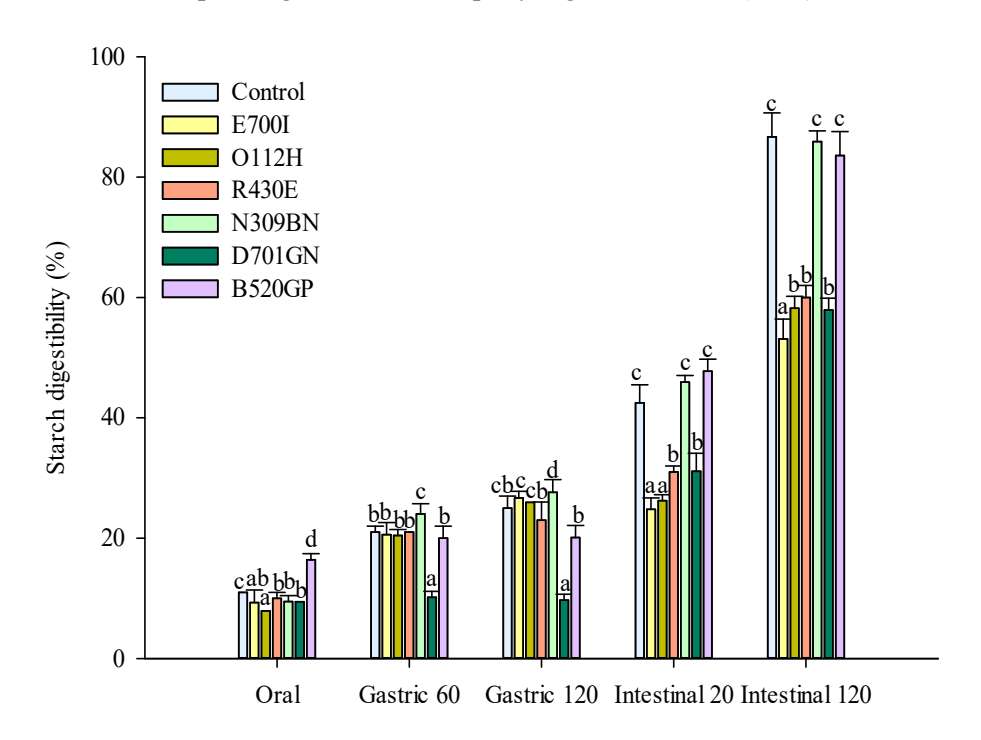


Figure VIII.2 Digestibility of starch in functional and traditional pasta (control) samples during each digestive phase. Different letters above the bars indicate significant differences ($p \le 0.05$) among the mean values of the different samples at the same digestive phase.

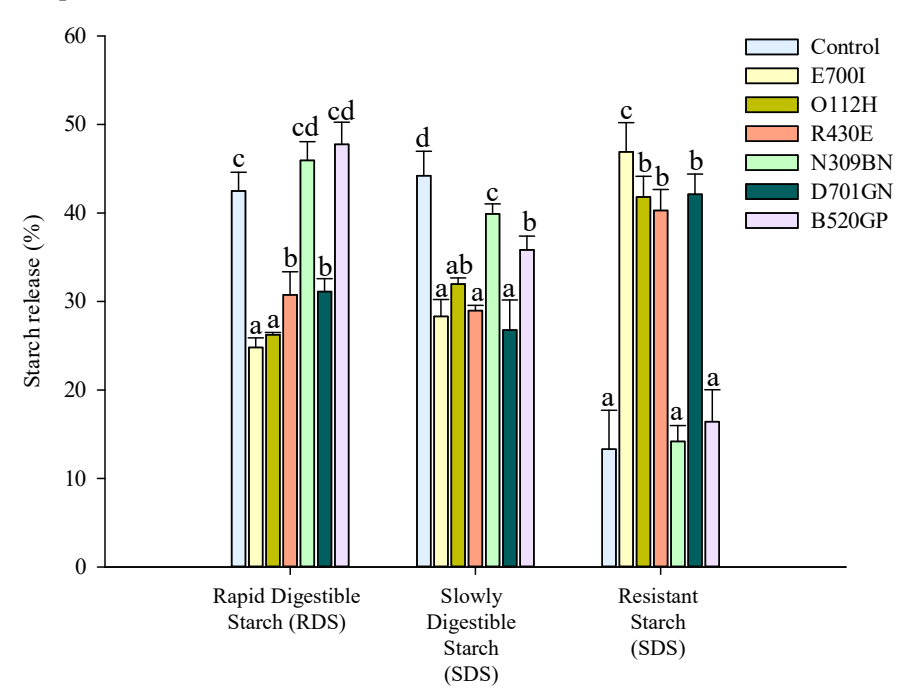


Figure VIII.3 *Nutritional fractions of starch in functional and traditional pasta (control) samples. RDS: rapid digestible starch, SDS: slowly digestible starch, RS: resistant starch.*

Different letters above the bars indicate significant differences ($p \le 0.05$) among the mean values of the different samples at the same digestive rate.

This phenomenon could be related to the presence of polysaccharides (fibres, 73.8% - 75.9% on a dry basis), protein (10.6% - 15.1% on a dry basis), and fat (1.1% - 1.5% on a dry basis) in the total extracts obtained from the full exploitation of the plant matrices by HPH and incorporated in E700I, R430E, and D701GN pasta samples (A781M, E706IT, B651S suspensions, respectively), which may have exerted a protective effect on the starch granules, making them less accessible to the action of the hydrolytic enzymes. These findings were consistent with the main results found by Garcia-Valle et al. (2021), who concluded that the rapidly and slowly digestible starch fractions exhibited notable reductions of up 45%, which was attributed to the formation of complexes and to protective physical barriers of proteins on the starch granules when adding chickpea flour to pasta.

A similar trend was observed for durum wheat pasta supplemented with sorghum flour (Khan et al., 2014), and with mushroom powder (Lu et al., 2018) that inhibited enzyme accessibility to starch granules within the pasta matrix, limiting the release of reducing sugars during starch digestion. This effect was attributed to protein-starch complex formation mediated by intermolecular disulphide crosslinking, and to dietary fibres that also

negatively affect starch digestibility by acting as a physical barrier against the hydrolytic action of amylolytic enzymes (Garcia-Valle et al., 2021).

These findings could be related to a more controlled starch digestion and a slowdown in the glucose release into the blood, which could potentially have a positive effect on the glycaemic index and on the prevention of the metabolic syndrome. Indeed, a study conducted by Kim and White (2012) demonstrated that the fats and phenolic compounds get adsorbed on the starch surface restricting its access to enzymatic breakdown resulting in lowered glycaemic index.

VIII.3.2 Biological activity of the pasta samples

VIII.3.2.1 Cytotoxicity

To exclude any cytotoxic effects on cells upon treatment with pasta digestates, its biological effects were assessed in LPS (lipopolysaccharide)-stimulated THP-1 macrophages (human circulating monocytes of leukemia) (data not shown), HepG2 cells (human hepatocarcinoma), and Caco-2 cells (human colorectal adenocarcinoma) by MTT assay. These analyses were conducted for all the different types of dry functional pasta samples, including the control (traditional pasta), however in Figures VIII.4 and VIII.5, the cell viability of the most promising two functional pasta samples (R430E, and B520GP) in terms of biological effects on human cell lines were reported.

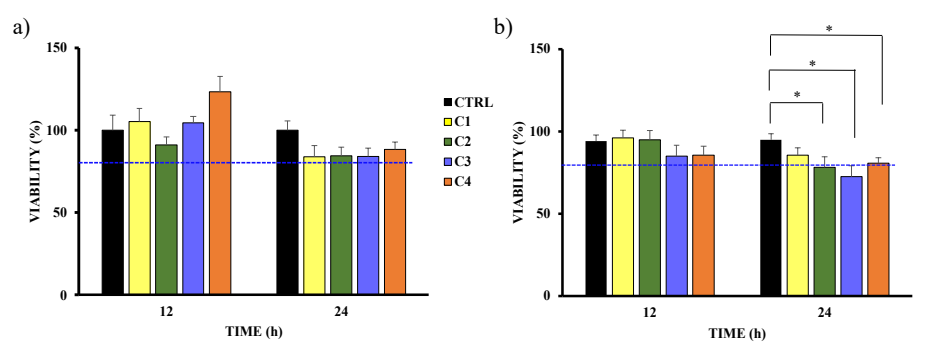


Figure VIII.4 MTT (3-(4,5-Dimethylthiazol-2-yl)-2,5-Diphenyltetrazolium Bromide) growth in Caco-2 (a), and HepG2 (b) cells untreated (CTRL) or treated for 12 - 24 h with R430E pasta digestate ($C_1 < C_2 < C_3 < C_4$). Cell viability is expressed as % of control (CTRL). The value represents the means \pm SEMs of three different experiments, each performed with triplicate samples. * p < 0.05, *** p < 0.005, **** p < 0.001, **** p < 0.0001.

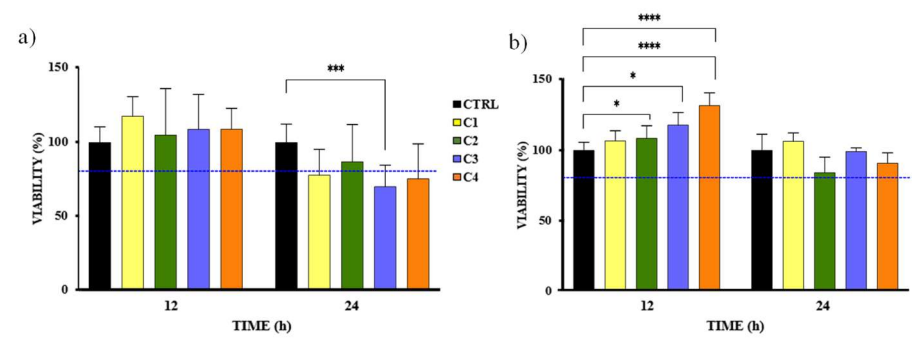


Figure VIII.5 MTT (3-(4,5-Dimethylthiazol-2-yl)-2,5-Diphenyltetrazolium Bromide) growth in Caco-2 (a), and HepG2 (b) cells untreated (CTRL) or treated for 12 - 24 h with B520GP pasta digestate ($C_1 < C_2 < C_3 < C_4$). Cell viability is expressed as % of control (CTRL). The value represents the means \pm SEMs of three different experiments, each performed with triplicate samples. * p < 0.05, *** p < 0.005, **** p < 0.001, **** p < 0.0001.

Results reveal that the exposure of cells for 12 and 24 h to pasta digestates (R430E, and B520GP), at the investigated concentrations, did not significantly hamper cell viability, considering 80% confluence as the threshold level (Ker et al., 2011). However, a slight cytotoxicity was observed when Caco-2 cells were exposed for the longest time tested (24 h) at a concentration C_3 of B520GP digestate. Therefore, R430E and B520GP pasta digestates did not induce any toxic effect on Caco-2 and HepG2 cells after treatment for 12 h at increasing concentrations ($C_1 < C_2 < C_3 < C_4$). Similar results (data not shown) were obtained for LPS-stimulated THP-1 macrophages exposed to the pasta digestates at the same concentrations.

VIII.3.2.2 Anti-inflammatory effects in LPS stimulated human macrophages

To investigate the potential anti-inflammatory effects of the pasta digestates, the gene and protein expression levels of pro-inflammatory cytokines (Interleukin (IL)-6, and Monocyte Chemoattractant Protein (MCP)-1/C-C motif chemokine ligand 2 (CCL-2)) were measured by qRT-PCR and ELISA, respectively, in human M_1 macrophages treated with increasing R430E (Figure VIII.6) and B520GP (Figure VIII.7) concentrations ($C_1 < C_2 < C_3 < C_4$).

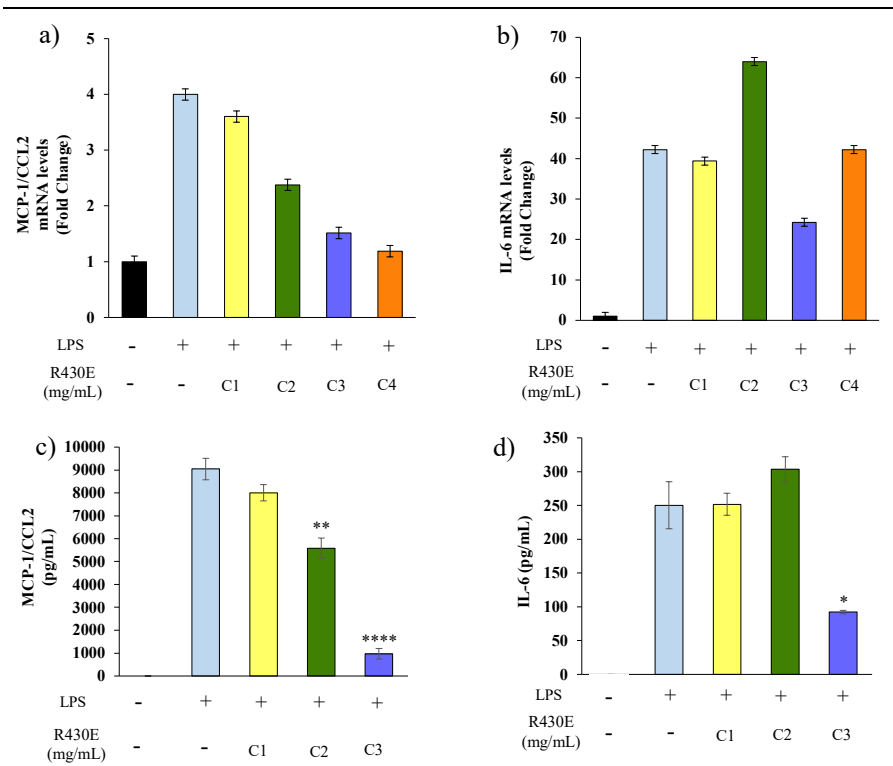


Figure VIII.6 Anti-inflammatory effects of R430E digestate in M1 macrophages. Real Time RT-PCR assay for (a) Monocyte Chemoattractant Protein (MCP)-1/C-C motif chemokine ligand 2 (CCL-2) and (b) interleukin-6 (IL-6), mRNA expression in human THP-1 derived macrophages untreated (-) or treated for 1 h with digestate ($C_1 < C_2 < C_3 < C_4$) and then stimulated with 10 ng/mL of lipopolysaccharides (LPS) for 24 h. Enzyme-linked immunosorbent assay (ELISA) for (c) CCL-2 and (d) IL-6 and in human THP-1 derived macrophages. The values represent the means \pm SEMs of three different experiments, performed in duplicate. * p < 0.05, *** p < 0.005, *** p < 0.001, **** p < 0.0001.

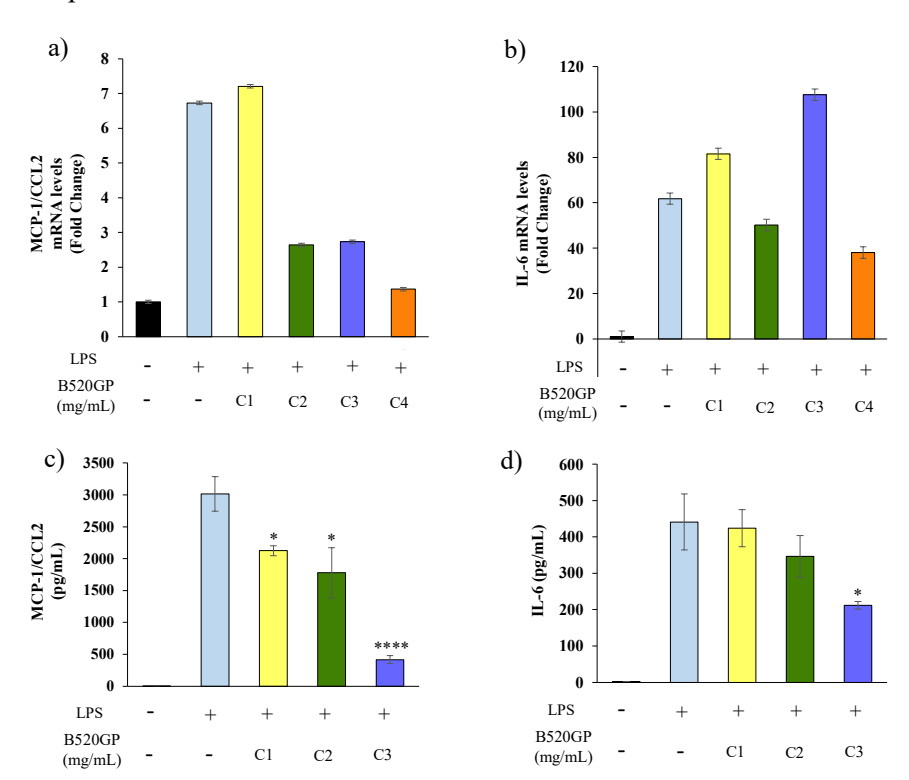


Figure VIII.7 Anti-inflammatory effects of B520GP digestate in M1 macrophages. Real Time RT-PCR assay for (a) Monocyte Chemoattractant Protein (MCP)-1/C-C motif chemokine ligand 2 (CCL-2) and (b) interleukin-6 (IL-6), mRNA expression in human THP-1 derived macrophages untreated (-) or treated for 1 h with digestate ($C_1 < C_2 < C_3 < C_4$) and then stimulated with 10 ng/mL of lipopolysaccharides (LPS) for 24 h. Enzyme-linked immunosorbent assay (ELISA) for (c) CCL-2 and (d) IL-6 and in human THP-1 derived macrophages. The values represent the means \pm SEMs of three different experiments, performed in duplicate. * p < 0.05, *** p < 0.005, *** p < 0.001, **** p < 0.0001.

As expected, the treatment with LPS induced the expression of IL-6 and MCP-1/CCL2 in M_1 macrophages, whereas the samples were able to dampen the inflammation in a concentration-dependent manner (Figures VIII.6 and VIII.7 (c) – (d)). Specifically, in the case of R430E a significant reduction (68%) of IL-6 secretion in THP-1 cells at C_3 concentration level, and a reduction of MCP-1 secretion at C_2 and C_3 concentrations, (40% and 90%, respectively) were observed (Figure VIII.6 (c) – (d)).

Likewise, B520GP led to the reduction (55%) of IL-6 secretion in THP-1 cells at C₃ concentration level (Figure VIII.6 (d)).

It is interesting to notice that B520GP sample induced a strong reduction of MCP-1 secretion in THP-1 cells even at the lowest concentration investigated (33%, 43%, and 80%, at C₁, C₂, and C₃ levels) (Figure VIII.6 (c)).

Consistently with the high antioxidant activity level detected in the extract used to functionalize B520GP pasta (G300G), the antioxidant compounds can promote the expression of key proinflammatory cytokines, IL-6 and CCL2, which sustain inflammation. Moreover, these findings could also be attributed to the higher purity of G300G extract, especially in terms of epicatechin (4.83 mg/g_{DW}, Table V.7, § V.3.1.3) obtained from PEF-assisted extraction, when compared to the less pure E706IT total suspension obtained via HPH used to functionalize R403E pasta sample. It is well known that low-grade chronic inflammation is a risk factor for the development of several chronic pathological conditions, including cardiovascular disease and cancer. Therefore, reducing systemic inflammatory processes through natural anti-inflammatory agents which impair cytokine production may prevent or delay the onset of chronic illness.

Using an in vitro model of cellular inflammation represented by LPS-stimulated human THP-1 macrophages, it was found that, especially B520GP, reduced the gene expression and protein secretion of IL-6 and MCP-1/CCL2, suggesting strong anti-inflammatory properties.

VIII.3.2.3 Glucose uptake

The effects of R430E and B520GP digestates on glucose uptake were tested by using SW872 cell model as a potential adipocyte model. The obtained results are reported in Figure VIII.8 (for R430E sample) and Figure VIII.9 (for B520GP sample).

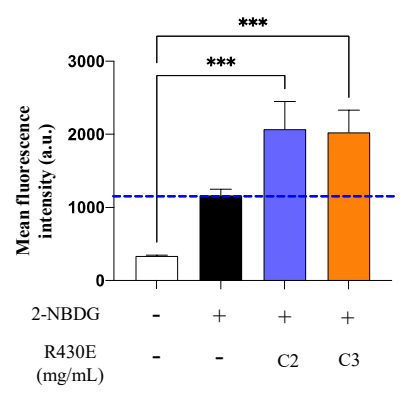


Figure VIII.8 *Effect of the exposure of SW872 cells for 24 h at R430E digestate* ($C_2 < C_3$) *on glucose uptake (MFI).*

Chapter VIII

The values represent the means \pm SEMs of three different experiments, performed in triplicate. * p < 0.05, *** p < 0.005, *** p < 0.001, **** p < 0.001.

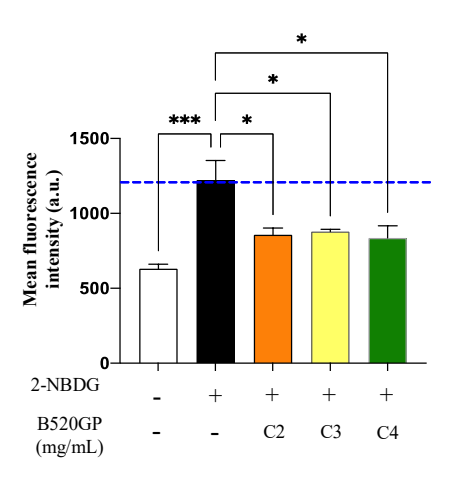


Figure VIII.9 Effect of the exposure of SW872 cells for 24 h at B520GP digestate ($C_2 < C_3 < C_4$) on glucose uptake (MFI). The values represent the means \pm SEMs of three different experiments, performed in triplicate. * p < 0.05, ** p < 0.005, *** p < 0.001, **** p < 0.001.

Results showed that B520GP led to a modest reduction of glucose uptake in SW872 cells (30%, p < 0.05) at C_2 , C_3 , and C_4 concentration levels (Figure VIII.9). Interestingly, the cells responded better to insulin when exposed to R430E digestate (C_2 , C_3). In particular, results (Figure VIII.8) demonstrated that glucose uptake of the cells almost doubled compared with the control (p < 0.001) when treated with R430E sample.

Increased glucose uptake is an indicator of increased sensitivity of adipose to insulin, behaving similarly to hypoglycemic drugs like metformin, which stimulates fat tissues to use glucose, delaying its absorption in the gut. These observations are coherent with the main findings related to the *in vitro* starch digestibility of R430E pasta sample functionalized with the total HPH-treated E706IT suspension that was found to reduce the resistant starch fraction (Figure VIII.3, § VIII.3.1). This type of extract, obtained from the total valorisation of the biomass, is less pure in terms of phenolic compounds than the purest G300G extract, but characterised by higher extraction yields regarding macromolecular components to which a better effect on glucose uptake is attributable.

VIII.4 Conclusions

The results reported in this chapter have highlighted the potential biological activity of the newly formulated functional pasta samples. Specifically, results showed that during *in vitro* digestion of the pasta samples a constant release of total polyphenols was observed, with the maximum release occurring in the intestinal phase (87% on average).

All pasta samples presented a similar total starch digestion profile. It is interesting, however, to highlight that the composition of the different natural extracts, especially in terms of protein and dietary fibre content, had an important role in the reduced starch digestibility of cooked pasta (increased resistant starch fraction), which is an important result given the adverse effects (e.g., metabolic syndrome) of a high intake of digestible carbohydrates on human health.

Promising results were also obtained from *in vitro* experiments on the antiinflammatory properties and glucose-uptake of functional pasta digestate in human cell lines.

The obtained findings support the potential of B520GP functional pasta to bring significant anti-inflammatory effects on human health, according to the high levels of antioxidant activity observed in the extract used for its formulation (G300G). Results also reveal that R430E pasta positively affected glucose uptake in human cell lines, supporting the possible prevention of the metabolic syndrome coherently with the starch digestibility profile.

Therefore, these findings reinforce the fact that different types of natural ingredients can exert specific health benefits based on the nature of the extract and its main constituents that possess specific biological properties.

Nevertheless, these findings need to be supported by *in vivo* clinical trials to validate the potential health benefits of these new functional pasta products compared with the traditional durum wheat pasta.

Chapter IX General conclusion and future perspectives

Results shown in Chapter V-VIII have highlighted that the application of innovative technologies for the recovery of natural bioactive compounds from agri-food by-products could be an opportunity and a strength for the development of novel functional pasta, preserving the traditional pasta-like sensory profile and improving its health-promoting effect.

The determination of optimal product formulation, pilot scale production, and comprehensive characterisation, including *in vitro* digestibility and biological activity of the newly formulated pasta functionalized with different natural extracts from agri-food by-products, by PEF and HPH technologies, represented a clear advancement of the knowledge on the field.

Specifically, the application of these technologies contributed to enhancing the extractability of bioactives from agri-food by-products, allowing to obtain extracts with specific characteristics that improved the bioactivity of functional pasta, which remained stable even after the production process and cooking phase.

The resulting lower amount of natural ingredients to be added to the pasta, compared to the usually used ranges, as emerged from the literature, allowed to obtain functional pasta with properties, such as consistency, residual moisture, water absorption capacity, cooking losses, and microstructure comparable to those of traditional pasta. Moreover, differently from the findings of most of the previous studies reported in the literature, it was found that the impact of the incorporation of bioactive compounds on the sensory attributes of the final pasta is minimized and the addition of hydrocolloids can be avoided.

Interestingly, the application of the two technologies proposed has led to the production of high value-added ingredients, in the form of supernatant from PEF-assisted extraction and in the form of total suspension from the complete micronisation of the plant matrix by HPH, with different physicochemical characteristics and specific health benefits.

Chapter IX

The pasta sample functionalized with the HPH-treated total suspension induced a significant reduction in rapidly digestible starch compared to the control pasta, supporting the potential prevention of glycaemic peaks. This could be associated with the presence of macromolecules in the total extracts, such as fibres and proteins, which may have exerted a protective effect on the starch granules, making them less accessible to hydrolytic enzymes.

Results also reveal that R430E pasta positively affected glucose uptake in human cell lines, supporting the possible prevention of the metabolic syndrome, coherently with the starch digestibility profile. In addition, the obtained findings supported the potential of B520GP functional pasta to positively affect human health bringing significant anti-inflammatory effects, due to the high antioxidant activity values detected in the pure extract used for its formulation (G300G).

Therefore, as the main positive outcome of this Ph.D. thesis, it has been demonstrated that bioactive compounds recovered utilizing unconventional technologies can be successfully utilized in food product formulation and design. Moreover, their application for the valorisation of agri-food biomasses and side streams could stimulate the technological development of PEF and HPH technologies which, despite being intensively investigated in recent years for different food-related applications, still struggle to find economically viable industrial applications.

The exploitation of their respective strengths (higher extraction yield and lower operative costs than conventional processes), while compensating their weaknesses (high investment costs) in the recovery of bioactive compounds from agri-food by-products might facilitate their industrial implementation.

The compensation of the high required investment costs might happen only if lower operating costs or larger revenues than conventional processes are achieved, which, in turn, means higher extraction yield, and reduced use of organic solvents. Interestingly, a preliminary evaluation of the variable production costs of the selected extracts reveal that the operative costs associated with the conventional solid-liquid extraction are about 40% on average higher than those required by PEF- and HPH- assisted extraction processes.

Another significant economic impact is expected from the development of the novel functional pasta with potential health benefits, exploiting natural, low-cost sources, retaining the traditional pasta-like sensory attributes, and, at the same time, meeting consumers' demand for greener products and cleaner labels.

In this sense, one of the most promising novel functional pasta (B520GP) exhibited a good market potential on a national scale, as emerged from a market research conducted within the "Pasta for fun" project, consisting in qualitative and quantitative interviews with potential consumers. The obtained results highlighted that the concept of the new functional pasta received high

ratings, even higher than the benchmark, especially in terms of liking, relevance, credibility, involvement, and purchase intention.

The approach and the results obtained in this Ph.D. thesis can represent a useful baseline for opening up new scenarios of this novel food product that will join on the market the traditional pasta offer, innovating while respecting the tradition.

Nevertheless, environmental and economic impact assessment of the proposed production line, as well as health validation of the product through *in vivo* studies should be carried out to further support the industrial transferability of the novel functional pasta.

In this sense, within the "Pasta for fun project", of which this Ph.D. activities were part, *in vivo* clinical trials, involving 20 patients who will daily consume traditional dry pasta and 20 patients who will daily consume the new functional dry pasta, as well as Life Cycle Assessment (LCA) studies are currently ongoing.

References

Ahmad Shiekh, K., Odunayo Olatunde, O., Zhang, B., Huda, N., Benjakul, S., 2021. Pulsed electric field assisted process for extraction of bioactive compounds from custard apple (Annona squamosa) leaves. Food Chem 359. https://doi.org/10.1016/j.foodchem.2021.129976

Aida, W., 2011. Effect of ethanol concentration, extraction time and extraction temperature on the recovery of phenolic compounds and antioxidant capacity of Centella asiatica extracts-ethylbenzothiazoline-6-sulphonic acid) (ABTS) radical-scavenging capacity, 2,2'-Diphenyl-1-picrylhydrazyl (DPPH) radical-scavenging capacity, International Food Research Journal.

Altamore, L., Bacarella, S., Columba, P., Chironi, S., Ingrassia, M., 2017. The Italian consumers' preferences for pasta: Does environment matter? Chem Eng Trans 58, 859–864. https://doi.org/10.3303/CET1758144

Alzuwaid, N.T., Fellows, C.M., Laddomada, B., Sissons, M., 2020. Impact of wheat bran particle size on the technological and phytochemical properties of durum wheat pasta. J Cereal Sci 95. https://doi.org/10.1016/j.jcs.2020.103033

Amagliani, L., O'Regan, J., Kelly, A.L., O'Mahony, J.A., 2017. The composition, extraction, functionality and applications of rice proteins: A review. Trends Food Sci Technol 64, 1–12. https://doi.org/10.1016/j.tifs.2017.01.008

Amoako, D., Awika, J.M., 2016. Polyphenol interaction with food carbohydrates and consequences on availability of dietary glucose. Curr Opin Food Sci 8, 14–18. https://doi.org/10.1016/J.COFS.2016.01.010

Anal, A.K., 2018. Food processing by-products and their utilization, in: Anal, A.K. (Ed.), Wiley Blackwell, New Jersey. ISBN:9781118432884

Aranibar, C., Pigni, N.B., Martinez, M., Aguirre, A., Ribotta, P., Wunderlin, D., Borneo, R., 2018. Utilization of a partially-deoiled chia flour to improve the nutritional and antioxidant properties of wheat pasta. LWT - Food Science and Technology 89, 381–387. https://doi.org/10.1016/j.lwt.2017.11.003

- Aravind, N., Sissons, M., Egan, N., Fellows, C., 2012. Effect of insoluble dietary fibre addition on technological, sensory, and structural properties of durum wheat spaghetti. Food Chem 130, 299–309. https://doi.org/10.1016/j.foodchem.2011.07.042
- Armellini, R., Peinado, I., Asensio-Grau, A., Pittia, P., Scampicchio, M., Heredia, A., Andres, A., 2019. In vitro starch digestibility and fate of crocins in pasta enriched with saffron extract. Food chemistry 283, 155-163. https://doi.org/10.1016/j.foodchem.2019.01.041
- Attanzio, A., Diana, P., Barraja, P., Carbone, A., Spanò, V., Parrino, B., Cascioferro, S.M., Allegra, M., Cirrincione, G., Tesoriere, L., Montalbano, A., 2019. Quality, functional and sensory evaluation of pasta fortified with extracts from Opuntia ficusindica cladodes. J Sci Food Agric 99, 4242–4247. https://doi.org/10.1002/jsfa.9655
- Augimeri, G., Plastina, P., Gionfriddo, G., Rovito, D., Giordano, C., Fazio, A., Barone, I., Catalano, S., Andò, S., Bonofiglio, D., Meijerink, J., Witkamp, R., 2019. N-eicosapentaenoyl dopamine, a conjugate of dopamine and eicosapentaenoic acid (EPA), exerts anti-inflammatory properties in mouse and human macrophages. Nutrients 11. https://doi.org/10.3390/nu11092247
- Aydogdu, A., Sumnu, G., Sahin, S., 2018. Effects of addition of different fibers on rheological characteristics of cake batter and quality of cakes. J Food Sci Technol 55, 667–677. https://doi.org/10.1007/s13197-017-2976-y
- Badin, E.E., Quevedo-Leon, & R., Ibarz, & A., Ribotta, P.D., Lespinard, & A.R., 1947. Kinetic Modeling of Thermal Degradation of Color, Lycopene, and Ascorbic Acid in Crushed Tomato. https://doi.org/10.1007/s11947-021-02579-1/Published
- Badwaik, L.S., Prasad, K., Seth, D., 2014. Optimization of ingredient levels for the development of peanut based fiber rich pasta. J Food Sci Technol. https://doi.org/10.1007/s13197-012-0779-8
- Baiano, A., di Chio, A.G., Scapola, D., 2019. Analysis of cracking and breakage in dried pasta: A case study. Quality Assurance and Safety of Crops and Foods 11, 713–717. https://doi.org/10.3920/QAS2019.1580
- Balli, D., Cecchi, L., Innocenti, M., Bellumori, M., Mulinacci, N., 2021. Food by-products valorisation: Grape pomace and olive pomace (pâté) as sources of phenolic compounds and fiber for enrichment of tagliatelle pasta. Food Chem 355, 129642. https://doi.org/10.1016/j.foodchem.2021.129642
- Banach, J.K., Majewska, K., Żuk-Gołaszewska, K., 2021. Effect of cultivation system on quality changes in durum wheat grain and flour produced in North-Eastern Europe. PLoS One 16, 1–25. https://doi.org/10.1371/journal.pone.0236617
- Barba, F.J., Brianceau, S., Turk, M., Boussetta, N., Vorobiev, E., 2015. Effect of Alternative Physical Treatments (Ultrasounds, Pulsed Electric Fields, and High-Voltage Electrical Discharges) on Selective Recovery of Bio-compounds from

Fermented Grape Pomace. Food Bioproc Tech 8, 1139–1148. https://doi.org/10.1007/s11947-015-1482-3

Barba, F.J., Grimi, N., Vorobiev, E., 2014. New Approaches for the Use of Non-conventional Cell Disruption Technologies to Extract Potential Food Additives and Nutraceuticals from Microalgae. Food Engineering Reviews. https://doi.org/10.1007/s12393-014-9095-6

Barba, F.J., Zhu, Z., Koubaa, M., Sant'Ana, A.S., Orlien, V., 2016. Green alternative methods for the extraction of antioxidant bioactive compounds from winery wastes and by-products: A review. Trends Food Sci Technol 49, 96–109. https://doi.org/10.1016/j.tifs.2016.01.006

Barbosa-Pereira, L., Guglielmetti, A., Zeppa, G., 2018. Pulsed Electric Field Assisted Extraction of Bioactive Compounds from Cocoa Bean Shell and Coffee Silverskin. Food Bioproc Tech 11, 818–835. https://doi.org/10.1007/s11947-017-2045-6

Bell, L.N., 2001. Stability Testing of Nutraceuticals and Functional Foods. In: Wildman, R.E.C. (Ed.), Handbook of Nutraceuticals and Functional Foods, CRC Press, New York, 501-516. ISBN: 9780429195570

Ben-Othman, S., Jõudu, I., Bhat, R., 2020. Bioactives from agri-food wastes: Present insights and future challenges, Molecules. https://doi.org/10.3390/molecules25030510

Benzie, I.F.F., Strain, J.J., 1996. The Ferric Reducing Ability of Plasma (FRAP) as a Measure of "Antioxidant Power": The FRAP Assay. Anal Biochem 239, 70–76. https://doi.org/10.1006/ABIO.1996.0292

Biernacka, B., Dziki, D., Gawlik-Dziki, U., Różyło, R., 2021. Common wheat pasta enriched with cereal coffee: Quality and physical and functional properties. Lwt 139. https://doi.org/10.1016/j.lwt.2020.110516

Biernacka, B., Dziki, D., Miś, A., Rudy, S., Krzykowski, A., Polak, R., Różyło, R., 2019. Changes in pasta properties during cooking and short-time storage. Int Agrophys 33, 323–330. https://doi.org/10.31545/intagr/110806

Biney, K., Beta, T., 2014. Phenolic profile and carbohydrate digestibility of durum spaghetti enriched with buckwheat flour and bran. LWT - Food Science and Technology 57, 569–579. https://doi.org/10.1016/j.lwt.2014.02.033

Bobinaitė, R., Pataro, G., Lamanauskas, N., Šatkauskas, S., Viškelis, P., Ferrari, G., 2015. Application of pulsed electric field in the production of juice and extraction of bioactive compounds from blueberry fruits and their by-products. J Food Sci Technol 52, 5898–5905. https://doi.org/10.1007/s13197-014-1668-0

Bodie, A.R., Micciche, A.C., Atungulu, G.G., Rothrock, M.J., Ricke, S.C., 2019. Current Trends of Rice Milling Byproducts for Agricultural Applications and

Alternative Food Production Systems. Front Sustain Food Syst 3, 1–13. https://doi.org/10.3389/fsufs.2019.00047

Boggia, R., Zunin, P., Turrini, F., 2020. Functional foods and food supplements. Applied Sciences (Switzerland). https://doi.org/10.3390/app10238538

Bolarinwa, I.F., Oyesiji, O.O., 2021. Gluten free rice-soy pasta: proximate composition, textural properties and sensory attributes. Heliyon 7, e06052. https://doi.org/10.1016/j.heliyon.2021.e06052

Bonomi, F., D'Egidio, M.G., Iametti, S., Marengo, M., Marti, A., Pagani, M.A., Ragg, E.M., 2012. Structure-quality relationship in commercial pasta: A molecular glimpse. Food Chem 135, 348–355. https://doi.org/10.1016/j.foodchem.2012.05.026

Bouasla, A., Wójtowicz, A., Zidoune, M.N., 2017. Gluten-free precooked rice pasta enriched with legumes flours: Physical properties, texture, sensory attributes and microstructure. LWT - Food Science and Technology 75, 569–577. https://doi.org/10.1016/j.lwt.2016.10.005

Boukid, F., 2021. Cereal-Based Foodstuffs: The Backbone of Mediterranean Cuisine, Cereal-Based Foodstuffs: The Backbone of Mediterranean Cuisine. https://doi.org/10.1007/978-3-030-69228-5

Boussetta, N., Lebovka, N., Vorobiev, E., Adenier, H., Bedel-Cloutour, C., Lanoisellé, J.L., 2009. Electrically assisted extraction of soluble matter from chardonnay grape skins for polyphenol recovery. J Agric Food Chem 57, 1491–1497. https://doi.org/10.1021/jf802579x

Boussetta, N., Vorobiev, E., 2014. Extraction of valuable biocompounds assisted by high voltage electrical discharges: A review. Comptes Rendus Chimie 17, 197–203. https://doi.org/10.1016/j.crci.2013.11.011

Boussetta, N., Vorobiev, E., Reess, T., de Ferron, A., Pecastaing, L., Ruscassié, R., Lanoisellé, J.L., 2012. Scale-up of high voltage electrical discharges for polyphenols extraction from grape pomace: Effect of the dynamic shock waves. Innovative Food Science and Emerging Technologies 16, 129–136. https://doi.org/10.1016/j.ifset.2012.05.004

Brianceau, S., Turk, M., Vitrac, X., Vorobiev, E., 2015. Combined densification and pulsed electric field treatment for selective polyphenols recovery from fermented grape pomace. Innovative Food Science and Emerging Technologies 29, 2–8. https://doi.org/10.1016/j.ifset.2014.07.010

Bueno-Herrera, M., Pérez-Magariño, S., 2020. Validation of an extraction method for the quantification of soluble free and insoluble bound phenolic compounds in wheat by HPLC-DAD. J Cereal Sci 93, 102984. https://doi.org/10.1016/J.JCS.2020.102984

Bustos, M.C., Perez, G.T., Leon, A.E., 2015. Structure and quality of pasta enriched with functional ingredients. RSC Adv 5, 30780–30792. https://doi.org/10.1039/c4ra11857j

Bustos, M.C., Vignola, M.B., Paesani, C., León, A.E., 2020. Berry fruits-enriched pasta: effect of processing and in vitro digestion on phenolics and its antioxidant activity, bioaccessibility and potential bioavailability. Int J Food Sci Technol. https://doi.org/10.1111/ijfs.14453

Byun, J., Han, J., 2020. Sustainable development of biorefineries: Integrated assessment method for co-production pathways. Energy Environ Sci 13, 2233–2242. https://doi.org/10.1039/d0ee00812e

Canals, R., Llaudy, M.C., Valls, J., Canals, J.M., Zamora, F., 2005. Influence of ethanol concentration on the extraction of color and phenolic compounds from the skin and seeds of tempranillo grapes at different stages of ripening. J Agric Food Chem 53, 4019–4025. https://doi.org/10.1021/jf047872v

Cappa, C., Alamprese, C., 2017. Brewer's spent grain valorization in fiber-enriched fresh egg pasta production: Modelling and optimization study. LWT - Food Science and Technology 82, 464–470. https://doi.org/10.1016/j.lwt.2017.04.068

Carcea, M., Narducci, V., Turfani, V., Giannini, V., 2017. Polyphenols in raw and cooked cereals/pseudocereals/legume pasta and couscous. Foods 6. https://doi.org/10.3390/foods6090080

Carpentieri, S., Ferrari, G., Pataro, G., 2022a. Optimization of Pulsed Electric Fields-Assisted Extraction of Phenolic Compounds From White Grape Pomace Using Response Surface Methodology. Front Sustain Food Syst 6. https://doi.org/10.3389/fsufs.2022.854968

Carpentieri, S., Larrea-Wachtendorff, D., Donsì, F., Ferrari, G., 2022b. Functionalization of pasta through the incorporation of bioactive compounds from agri-food by-products: Fundamentals, opportunities, and drawbacks. Trends Food Sci Technol. https://doi.org/10.1016/j.tifs.2022.02.011

Carpentieri, S., Mazza, L., Nutrizio, M., Jambrak, A.R., Ferrari, G., Pataro, G., 2021a. Pulsed electric fields- and ultrasound-assisted green extraction of valuable compounds from Origanum vulgare L. and Thymus serpyllum L. Int J Food Sci Technol 1–9. https://doi.org/10.1111/ijfs.15159

Carpentieri, S., Soltanipour, F., Ferrari, G., Pataro, G., Dons, F., 2021b. Emerging Green Techniques for the Extraction of Antioxidants from Agri-Food By-Products as Promising Ingredients for the Food Industry.

Carullo, D., Abera, B.D., Casazza, A.A., Donsì, F., Perego, P., Ferrari, G., Pataro, G., 2018. Effect of pulsed electric fields and high pressure homogenization on the

- aqueous extraction of intracellular compounds from the microalgae Chlorella vulgaris. Algal Res 31, 60–69. https://doi.org/10.1016/j.algal.2018.01.017
- Carullo, D., Pataro, G., Donsì, F., Ferrari, G., 2020. Pulsed Electric Fields-Assisted Extraction of Valuable Compounds From Arthrospira Platensis: Effect of Pulse Polarity and Mild Heating. Front Bioeng Biotechnol 8. https://doi.org/10.3389/fbioe.2020.551272
- Cecchi, L., Schuster, N., Flynn, D., Bechtel, R., Bellumori, M., Innocenti, M., Mulinacci, N., Guinard, J.X., 2019. Sensory Profiling and Consumer Acceptance of Pasta, Bread, and Granola Bar Fortified with Dried Olive Pomace (Pâté): A Byproduct from Virgin Olive Oil Production. J Food Sci 84, 2995–3008. https://doi.org/10.1111/1750-3841.14800
- Cedola, A., Cardinali, A., D'Antuono, I., Conte, A., del Nobile, M.A., 2020. Cereal foods fortified with by-products from the olive oil industry. Food Biosci 33, 100490. https://doi.org/10.1016/j.fbio.2019.100490
- Celli, G.B., Ghanem, A., Brooks, M.S.L., 2015. Bioactive Encapsulated Powders for Functional Foods—a Review of Methods and Current Limitations. Food Bioproc Tech 8, 1825–1837. https://doi.org/10.1007/s11947-015-1559-z
- Chanioti, S., Katsouli, M., Tzia, C., 2021. Novel processes for the extraction of phenolic compounds from olive pomace and their protection by encapsulation. Molecules 26. https://doi.org/10.3390/molecules26061781
- Chemat, F., Vian, M.A., Cravotto, G., 2012. Green extraction of natural products: Concept and principles. Int J Mol Sci. https://doi.org/10.3390/ijms13078615
- Chiang, J.H., Ong, D.S.M., Ng, F.S.K., Hua, X.Y., Tay, W.L.W., Henry, C.J., 2021. Application of chia (Salvia hispanica) mucilage as an ingredient replacer in foods. Trends Food Sci Technol 115, 105–116. https://doi.org/10.1016/j.tifs.2021.06.039
- Chuyen, H. v., Nguyen, M.H., Roach, P.D., Golding, J.B., Parks, S.E., 2018. Microwave-assisted extraction and ultrasound-assisted extraction for recovering carotenoids from Gac peel and their effects on antioxidant capacity of the extracts. Food Sci Nutr 6, 189–196. https://doi.org/10.1002/fsn3.546
- Ciccoritti, R., Nocente, F., Sgrulletta, D., Gazza, L., 2019. Cooking quality, biochemical and technological characteristics of bran-enriched pasta obtained by a novel pasta-making process. Lwt 101, 10–16. https://doi.org/10.1016/j.lwt.2018.11.034
- Ciccoritti, R., Taddei, F., Nicoletti, I., Gazza, L., Corradini, D., D'Egidio, M.G., Martini, D., 2017. Use of bran fractions and debranned kernels for the development of pasta with high nutritional and healthy potential. Food Chem 225, 77–86. https://doi.org/10.1016/j.foodchem.2017.01.005

- Cimini, A., Poliziani, A., Antonelli, G., Sestili, F., Lafiandra, D., Moresi, M., 2022. Characterization of Fresh Pasta Made of Common and High-Amylose Wheat Flour Mixtures. Foods 11. https://doi.org/10.3390/foods11162510
- Çoban, D.İ., Babiker, E.F.E., al Juhaimi, F., Uslu, N., Özcan, M.M., Ghafoor, K., Mohamed Ahmed, I.A., Almusallam, I.A., 2021. Fatty acid composition, mineral contents, and glycemic index values of chips produced with different cooking methods and lupine (Lupinus albus L.) flour formulations. J Food Process Preserv 45, 0–2. https://doi.org/10.1111/jfpp.15161
- Yu, J., Ahmedna, M., Bansode, R.R., 2014. Agricultural by-products as important agricultural by-products as important food sources of polyphenols, in: Dean T. Cobb (Ed.), Polyphenols. Nova Science Publishers, Inc., Chapter 1, pp. 1–32. ISBN: 978-1-63117-857-3
- Coelho, M.C., Pereira, R.N., Rodrigues, A.S., Teixeira, J.A., Pintado, M.E., 2020. The use of emergent technologies to extract added value compounds from grape by-products. Trends Food Sci Technol 106, 182–197. https://doi.org/10.1016/j.tifs.2020.09.028
- Colle, I., Lemmens, L., van Buggenhout, S., van Loey, A., Hendrickx, M., 2010. Effect of Thermal Processing on the Degradation, Isomerization, and Bioaccessibility of Lycopene in Tomato Pulp. J Food Sci 75. https://doi.org/10.1111/j.1750-3841.2010.01862.x
- Comunian, T.A., Silva, M.P., Souza, C.J.F., 2021. The use of food by-products as a novel for functional foods: Their use as ingredients and for the encapsulation process. Trends Food Sci Technol 108, 269–280. https://doi.org/10.1016/j.tifs.2021.01.003
- Comuzzo, P., Calligaris, S., 2019. Potential Applications of High Pressure Homogenization in Winemaking: A Review. Beverages 5, 56. https://doi.org/10.3390/beverages5030056
- Conte A, P.L., Likyova D, L.A., Pellicanò TM, S. v, 2015. Durum Wheat Whole-meal Spaghetti with Tomato Peels: How By-product Particles Size Can Affect Final Quality of Pasta. J Food Process Technol 6. https://doi.org/10.4172/2157-7110.1000500
- Crizel, T. de M., Rios, A. de O., Thys, R.C.S., Flôres, S.H., 2015. Effects of orange by-product fiber incorporation on the functional and technological properties of pasta. Food Science and Technology 35, 546–551. https://doi.org/10.1590/1678-457X.6719
- Cummings, J.H., 1992. Classification and Measurement of Nutritionally Important Starch Fractions, Article in European Journal of Clinical Nutrition.
- Czaja, T., Kuzawińska, E., Sobota, A., Szostak, R., 2018. Determining moisture content in pasta by vibrational spectroscopy. Talanta 178, 294–298. https://doi.org/10.1016/j.talanta.2017.09.050

Dalvi-Isfahan, M., Hamdami, N., Le-Bail, A., Xanthakis, E., 2016. The principles of high voltage electric field and its application in food processing: A review, Food Research International. Elsevier B.V. https://doi.org/10.1016/j.foodres.2016.09.002

Dattner, M., Bohn, D., 2015. Characterization of Print Quality in Terms of Colorimetric Aspects, in: Printing on Polymers: Fundamentals and Applications. Elsevier Inc., pp. 329–345. https://doi.org/10.1016/B978-0-323-37468-2.00020-8

Day, L., Seymour, R.B., Pitts, K.F., Konczak, I., Lundin, L., 2009. Incorporation of functional ingredients into foods. Trends Food Sci Technol 20, 388–395. https://doi.org/10.1016/j.tifs.2008.05.002

De Arcangelis, E., Cuomo, F., Trivisonno, M.C., Marconi, E., Messia, M.C., 2020. Gelatinization and pasta making conditions for buckwheat gluten-free pasta. J Cereal Sci 95, 103073. https://doi.org/10.1016/j.jcs.2020.103073

De Cindio, B., Baldino, N., 2015. Pasta: Manufacture and Composition, 1st ed, Encyclopedia of Food and Health. Elsevier Ltd. https://doi.org/10.1016/B978-0-12-384947-2.00522-5

De la Peña, E., Manthey, F.A., 2017. Effect of Formulation and Dough Hydration Level on Extrusion, Physical and Cooked Qualities of Nontraditional Spaghetti. J Food Process Eng 40, 1–12. https://doi.org/10.1111/jfpe.12301

De Paula, R., Abdel-Aal, E.S.M., Messia, M.C., Rabalski, I., Marconi, E., 2017. Effect of processing on the beta-glucan physicochemical properties in barley and semolina pasta. J Cereal Sci. https://doi.org/10.1016/j.jcs.2017.03.030

Detchewa, P., Thongngam, M., Jane, J.L., Naivikul, O., 2016. Preparation of glutenfree rice spaghetti with soy protein isolate using twin-screw extrusion. J Food Sci Technol 53, 3485–3494. https://doi.org/10.1007/s13197-016-2323-8

Dey, D., Richter, J.K., Ek, P., Gu, B.J., Ganjyal, G.M., 2021. Utilization of Food Processing By-products in Extrusion Processing: A Review. Front Sustain Food Syst 4, 1–18. https://doi.org/10.3389/fsufs.2020.603751

Dias, M.I., Ferreira, I.C.F.R., Barreiro, M.F., 2015. Microencapsulation of bioactives for food applications. Food Funct 6, 1035–1052. https://doi.org/10.1039/c4fo01175a

Dima, C., Assadpour, E., Dima, S., Jafari, S.M., 2020. Bioavailability and bioaccessibility of food bioactive compounds; overview and assessment by in vitro methods. Compr Rev Food Sci Food Saf 19, 2862–2884. https://doi.org/10.1111/1541-4337.12623

Dobrinčić, A., Repajic, M., Elez Garofulić, I., Tuđen, L., Dragović-Uzelac, V., Levaj, B., 2020. Comparison of Di ff erent Extraction Methods for the. Processes 8, 1008.

- Donsì, F., Ferrari, G., Fruilo, M., Pataro, G., 2010. Pulsed electric field-assisted vinification of aglianico and piedirosso grapes. J Agric Food Chem 58, 11606–11615. https://doi.org/10.1021/jf102065v
- Donsì, F., Velikov, K.P., 2020. Mechanical cell disruption of mustard bran suspensions for improved dispersion properties and protein release. Food Funct. https://doi.org/10.1039/d0fo00852d
- Duba, K.S., Casazza, A.A., Mohamed, H. ben, Perego, P., Fiori, L., 2015. Extraction of polyphenols from grape skins and defatted grape seeds using subcritical water: Experiments and modeling. Food and Bioproducts Processing 94, 29–38. https://doi.org/10.1016/j.fbp.2015.01.001
- Erinle, T.J., Oladokun, S., MacIsaac, J., Rathgeber, B., Adewole, D., 2022. Dietary grape pomace effects on growth performance, intestinal health, blood parameters, and breast muscle myopathies of broiler chickens. Poult Sci 101. https://doi.org/10.1016/j.psj.2021.101519
- Espinosa-Solis, V., Zamudio-Flores, P.B., Tirado-Gallegos, J.M., Ramírez-Mancinas, S., Olivas-Orozco, G.I., Espino-Díaz, M., Hernández-González, M., García-Cano, V.G., Sánchez-Ortíz, O., Buenrostro-Figueroa, J.J., Baeza-Jiménez, R., 2019. Evaluation of cooking quality, nutritional and texture characteristics of pasta added with oat bran and apple flour. Foods 8. https://doi.org/10.3390/foods8080299
- European Commission, 2013. Horizon 2020 work programme 2014-2015: 8. Health, demographic change and wellbeing 2015, 95.
- Fares, C., Platani, C., Baiano, A., Menga, V., 2010. Effect of processing and cooking on phenolic acid profile and antioxidant capacity of durum wheat pasta enriched with debranning fractions of wheat. Food Chem 119, 1023–1029. https://doi.org/10.1016/j.foodchem.2009.08.006
- Faustino, M., Veiga, M., Sousa, P., Costa, E.M., Silva, S., Pintado, M., 2019. Agrofood byproducts as a new source of natural food additives. Molecules 24, 1–23. https://doi.org/10.3390/molecules24061056
- Fish, W.W., Perkins-Veazie, P., Collins, J.K., 2002. A quantitative assay for lycopene that utilizes reduced volumes of organic solvents. Journal of Food Composition and Analysis 15, 309–317. https://doi.org/10.1006/jfca.2002.1069
- Foschia, M., Peressini, D., Sensidoni, A., Brennan, M.A., Brennan, C.S., 2015. Synergistic effect of different dietary fibres in pasta on in vitro starch digestion? Food Chem 172, 245–250. https://doi.org/10.1016/j.foodchem.2014.09.062
- Fradinho, P., Oliveira, A., Domínguez, H., Torres, M.D., Sousa, I., Raymundo, A., 2020. Improving the nutritional performance of gluten-free pasta with potato peel autohydrolysis extract. Innovative Food Science and Emerging Technologies 63, 102374. https://doi.org/10.1016/j.ifset.2020.102374

Frontuto, D., Carullo, D., Harrison, S.M., Brunton, N.P., Ferrari, G., Lyng, J.G., Pataro, G., 2019. Optimization of Pulsed Electric Fields-Assisted Extraction of Polyphenols from Potato Peels Using Response Surface Methodology. Food Bioproc Tech 12, 1708–1720. https://doi.org/10.1007/s11947-019-02320-z

Gadioli Tarone, A., Keven Silva, E., Dias de Freitas Queiroz Barros, H., Baú Betim Cazarin, C., Roberto Marostica Junior, M., 2021. High-intensity ultrasound-assisted recovery of anthocyanins from jabuticaba by-products using green solvents: Effects of ultrasound intensity and solvent composition on the extraction of phenolic compounds. Food Research International 140, 110048. https://doi.org/10.1016/J.FOODRES.2020.110048

Galanakis, C.M., 2021. Functionality of food components and emerging technologies. Foods 10, 1–26. https://doi.org/10.3390/foods10010128

Gali, L., Bedjou, F., Ferrari, G., Donsì, F., 2022. Formulation and characterization of zein/gum arabic nanoparticles for the encapsulation of a rutin-rich extract from Ruta chalepensis L. Food Chem 367. https://doi.org/10.1016/j.foodchem.2021.129982

Gali, L., Bedjou, F., Velikov, K.P., Ferrari, G., Donsì, F., 2020. High-pressure homogenization-assisted extraction of bioactive compounds from Ruta chalepensis. Journal of Food Measurement and Characterization 14, 2800–2809. https://doi.org/10.1007/s11694-020-00525-x

Gallego, R., Bueno, M., Herrero, M., 2019. Sub- and supercritical fluid extraction of bioactive compounds from plants, food-by-products, seaweeds and microalgae – An update. TrAC - Trends in Analytical Chemistry 116, 198–213. https://doi.org/10.1016/j.trac.2019.04.030

Garcia-Valle, D.E., Bello-Pérez, L.A., Agama-Acevedo, E., Alvarez-Ramirez, J., 2021. Effects of mixing, sheeting, and cooking on the starch, protein, and water structures of durum wheat semolina and chickpea flour pasta. Food Chem 360. https://doi.org/10.1016/j.foodchem.2021.129993

Gasparre, N., Betoret, E., Rosell, C.M., 2019. Quality Indicators and Heat Damage of Dried and Cooked Gluten Free Spaghetti. Plant Foods for Human Nutrition 74, 481–488. https://doi.org/10.1007/s11130-019-00765-3

Giannetti, V., Boccacci Mariani, M., Colicchia, S., 2021a. Furosine as marker of quality in dried durum wheat pasta: Impact of heat treatment on food quality and security — A review. Food Control 125, 108036. https://doi.org/10.1016/j.foodcont.2021.108036

Giannetti, V., Boccacci Mariani, M., Marini, F., Biancolillo, A., 2021b. Effects of thermal treatments on durum wheat pasta flavour during production process: A modelling approach to provide added-value to pasta dried at low temperatures. Talanta 225, 121955. https://doi.org/10.1016/j.talanta.2020.121955

Giordano, C., Barone, I., Vircillo, V., Panza, S., Malivindi, R., Gelsomino, L., Pellegrino, M., Rago, V., Mauro, L., Lanzino, M., Panno, M.L., Bonofiglio, D., Catalano, S., Andò, S., 2016. Activated FXR Inhibits Leptin Signaling and Counteracts Tumor-promoting Activities of Cancer-Associated Fibroblasts in Breast Malignancy. Sci Rep 6. https://doi.org/10.1038/srep21782

Grassi, S., Gulli, M., Visioli, G., Marti, A., 2021. Gluten aggregation properties as a tool for durum wheat quality assessment: A chemometric approach. Lwt 142, 111048. https://doi.org/10.1016/j.lwt.2021.111048

Gull, A., Prasad, K., Kumar, P., 2018. Nutritional, antioxidant, microstructural and pasting properties of functional pasta. Journal of the Saudi Society of Agricultural Sciences 17, 147–153. https://doi.org/10.1016/j.jssas.2016.03.002

Gull, A., Prasad, K., Kumar, P., 2015. Effect of millet flours and carrot pomace on cooking qualities, color and texture of developed pasta. LWT - Food Science and Technology 63, 470–474. https://doi.org/10.1016/j.lwt.2015.03.008

Gurtovenko, A.A., Anwar, J., 2009. Interaction of ethanol with biological membranes: The formation of non-bilayer structures within the membrane interior and their significance. Journal of Physical Chemistry B 113, 1983–1992. https://doi.org/10.1021/jp808041z

Halvorsen, B.L.; Carlsen, M.H.; Phillips, K.M.; Bohn, S.K.; Holte, K.; Jacobs, D.R., Jr.; Blomhoff, R. Content of redox-active compounds (ie, antioxidants) in foods consumed in the United States. Am. J. Clin. Nutr. 2006, 84, 95–135.

Hare, R., 2017. Durum Wheat: Grain-Quality Characteristics and Management of Quality Requirements, Second Edi. ed, Cereal Grains: Assessing and Managing Quality: Second Edition. Elsevier Ltd. https://doi.org/10.1016/B978-0-08-100719-8.00006-1

Hoebler, C., Devaux, M.-F., Karinthi, A., Belleville, C., Barry, J.-L., 2000. Particle size of solid food after human mastication and in vitro simulation of oral breakdown.

Horvat, D., Šimić, G., Dvojković, K., Ivić, M., Plavšin, I., Novoselović, D., 2021. Gluten protein compositional changes in response to nitrogen application rate. Agronomy 11. https://doi.org/10.3390/agronomy11020325

Iafelice, G., Caboni, M.F., Cubadda, R., Criscio, T. di, Trivisonno, M.C., Marconi, E., 2008. Development of functional spaghetti enriched with long chain omega-3 fatty acids. Cereal Chem 85, 146–151. https://doi.org/10.1094/CCHEM-85-2-0146

Iuga, M., Mironeasa, S., 2021. Simultaneous optimization of wheat heat moisture treatment and grape peels addition for pasta making. Lwt 150, 112011. https://doi.org/10.1016/j.lwt.2021.112011

Jalgaonkar, K., Jha, S., Mahawar, M., 2018a. Influence of die size and drying temperature on quality of pearl millet based pasta. Food Science and Technology 35, 626–632.

Jalgaonkar, K., Jha, S.K., 2016. Influence of particle size and blend composition on quality of wheat semolina-pearl millet pasta. J Cereal Sci 71, 239–245. https://doi.org/10.1016/j.jcs.2016.09.007

Jalgaonkar, K., Jha, S.K., Mahawar, M.K., 2018b. Influence of incorporating defatted soy flour, carrot powder, mango peel powder, and moringa leaves powder on quality characteristics of wheat semolina-pearl millet pasta. J Food Process Preserv 42, 1–11. https://doi.org/10.1111/jfpp.13575

Jatau, S.H., Birnin-Yauri, U.A., Sokoto, A.M., Zubairu, A.Y., 2017. Effect of heat processing on lycopene content of fresh tomatoe (Solanum Lycoperiscuml), International Journal of Engineering & Environmental Technology, 13, 1-7. DOI: 10.13140/RG.2.2.34885.81126

Jaworska, D., Królak, M., Przybylski, W., Jezewska-Zychowicz, M., 2020. Acceptance of Fresh Pasta with β-Glucan Addition: Expected Versus Perceived Liking. Foods 9, 1–17. https://doi.org/10.3390/foods9070869

John Camm, A., 2012. European Perspective. Cardiac Mapping: Fourth Edition. https://doi.org/10.1002/9781118481585

Joshi, A.A., Kshirsagar, R.B., Sadawarte, S.K., Patil, B.M., Sawate, A.R., 2022. Comparative evaluation of baking and functional qualities of black wheat flour. ~ 229 ~ The Pharma Innovation Journal 11, 229–234.

Jurić, S., Ferrari, G., Velikov, K.P., Donsì, F., 2019. High-pressure homogenization treatment to recover bioactive compounds from tomato peels. J Food Eng 262, 170–180. https://doi.org/10.1016/j.jfoodeng.2019.06.011

Jurić, S., Jurić, M., Ferrari, G., Režek Jambrak, A., Donsì, F., 2021. Lycopene-rich cream obtained via high-pressure homogenisation of tomato processing residues in a water—oil mixture. Int J Food Sci Technol 56, 4907–4914. https://doi.org/10.1111/ijfs.15243

Kaur, A., Shevkani, K., Katyal, M., Singh, N., Ahlawat, A.K., Singh, A.M., 2016. Physicochemical and rheological properties of starch and flour from different durum wheat varieties and their relationships with noodle quality. J Food Sci Technol 53, 2127–2138. https://doi.org/10.1007/s13197-016-2202-3

Kaur, D., Sogi, D.S., Wani, A.A., 2006. Degradation kinetics of lycopene and visual color in tomato peel isolated from pomace. Int J Food Prop 9, 781–789. https://doi.org/10.1080/10942910600596357

- Kaur, G., Sharma, S., Nagi, H.P.S., Dar, B.N., 2012. Functional properties of pasta enriched with variable cereal brans. J Food Sci Technol 49, 467–474. https://doi.org/10.1007/s13197-011-0294-3
- Ker, D.F.E., Weiss, L.E., Junkers, S.N., Chen, M., Yin, Z., Sandbothe, M.F., Huh, S. il, Eom, S., Bise, R., Osuna-Highley, E., Kanade, T., Campbell, P.G., 2011. An engineered approach to stem cell culture: Automating the decision process for real-time adaptive subculture of stem cells. PLoS One 6. https://doi.org/10.1371/journal.pone.0027672
- Khan, I., Yousif, A.M., Johnson, S.K., Gamlath, S., 2014. Effect of sorghum flour addition on in vitro starch digestibility, cooking quality, and consumer acceptability of durum wheat pasta. J Food Sci 79. https://doi.org/10.1111/1750-3841.12542
- Kim, H.J., White, P.J., 2012. In vitro digestion rate and estimated glycemic index of oat flours from typical and high β -glucan oat lines. Journal of Agricultural and Food Chemistry 60, 5237-5242, 10.1021/jf300429u
- Kostas, E.T., Wilkinson, S.J., White, D.A., Cook, D.J., 2016. Optimization of a total acid hydrolysis based protocol for the quantification of carbohydrate in macroalgae, J. Algal Biomass Utln.
- Kwiatkowski, M., Kravchuk, O., Skouroumounis, G.K., Taylor, D.K., 2020. Response surface parallel optimization of extraction of total phenolics from separate white and red grape skin mixtures with microwave-assisted and conventional thermal methods. J Clean Prod 251, 119563. https://doi.org/10.1016/j.jclepro.2019.119563
- la Gatta, B., Rutigliano, M., Padalino, L., Conte, A., del Nobile, M.A., di Luccia, A., 2017. The role of hydration on the cooking quality of bran-enriched pasta. LWT Food Science and Technology 84, 489–496. https://doi.org/10.1016/j.lwt.2017.06.013
- Lalegani, S., Ahmadi Gavlighi, H., Azizi, M.H., Amini Sarteshnizi, R., 2018. Inhibitory activity of phenolic-rich pistachio green hull extract-enriched pasta on key type 2 diabetes relevant enzymes and glycemic index. Food Research International 105, 94–101. https://doi.org/10.1016/j.foodres.2017.11.003
- Laureati, M., Conte, A., Padalino, L., del Nobile, M.A., Pagliarini, E., 2016. Effect of Fiber Information on Consumer's Expectation and Liking of Wheat Bran Enriched Pasta. J Sens Stud 31, 348–359. https://doi.org/10.1111/joss.12218
- Lee, J., Durst, R.W., Wrolstad, R.E., Barnes, K.W., Eisele, ; T, Giusti, ; M M, Haché, ; J, Hofsommer, ; H, Koswig, ; S, Krueger, D.A., Kupina, ; S, Martin, ; S K, Martinsen, ; B K, Miller, T.C., Paquette, ; F, Ryabkova, ; A, Skrede, ; G, Trenn, ; U, Wightman, J.D., 2001. Determination of Total Monomeric Anthocyanin Pigment Content of Fruit Juices, Beverages, Natural Colorants, and Wines by the pH Differential Method: Collaborative Study.

- Lee, J., Rennaker, C., Wrolstad, R.E., 2008. Correlation of two anthocyanin quantification methods: HPLC and spectrophotometric methods. Food Chem 110, 782–786. https://doi.org/10.1016/j.foodchem.2008.03.010
- Levent, H., Koyuncu, M., Bilgiçli, N., Adıgüzel, E., Dedeoğlu, M., 2020. Improvement of chemical properties of noodle and pasta using dephytinized cereal brans. LWT Food Science and Technology 128, 109470. https://doi.org/10.1016/j.lwt.2020.109470
- Liang, X., Ma, C., Yan, X., Liu, X., Liu, F., 2019. Advances in research on bioactivity, metabolism, stability and delivery systems of lycopene. Trends Food Sci Technol. https://doi.org/10.1016/j.tifs.2019.08.019
- Lin, T., Liu, Y., Lai, C., Yang, T., Xie, J., Zhang, Y., 2018. The effect of ultrasound assisted extraction on structural composition, antioxidant activity and immunoregulation of polysaccharides from Ziziphus jujuba Mill var. spinosa seeds. Ind Crops Prod 125, 150–159. https://doi.org/10.1016/j.indcrop.2018.08.078
- López-Valdez, F., Maldonado-Torres, R., Morales-Camacho, J.I., Huerta-González, L., Luna-Suárez, S., 2020. Assessment of techno-functional and nutraceutical potential of tomato (Solanum lycopersicum) seed meal. Molecules 25. https://doi.org/10.3390/molecules25184235
- Lu, X., Brennan, M.A., Serventi, L., Liu, J., Guan, W., Brennan, C.S., 2018. Addition of mushroom powder to pasta enhances the antioxidant content and modulates the predictive glycaemic response of pasta. Food Chem 264, 199–209. https://doi.org/10.1016/j.foodchem.2018.04.130
- Lucas-González, R., Pérez-Álvarez, J.A., Moscaritolo, S., Fernández-López, J., Sacchetti, G., Viuda-Martos, M., 2021. Evaluation of polyphenol bioaccessibility and kinetic of starch digestion of spaghetti with persimmon (Dyospyros kaki) flours coproducts during in vitro gastrointestinal digestion. Food Chemistry 338, 128142. https://doi.org/10.1016/j.foodchem.2020.128142
- Manoj Kumar, C.T., Sabikhi, L., Singh, A.K., Raju, P.N., Kumar, R., Sharma, R., 2019. Effect of incorporation of sodium caseinate, whey protein concentrate and transglutaminase on the properties of depigmented pearl millet based gluten free pasta. LWT Food Science and Technology 103, 19–26. https://doi.org/10.1016/j.lwt.2018.12.071
- Manthey, F.A., Twombly, W., 2005. Extruding and drying of pasta. Handbook of Food Science, Technology, and Engineering 4 Volume Set 2829–2843. https://doi.org/10.1201/b15995-178
- Marinelli, V., Padalino, L., Conte, A., del Nobile, M.A., Briviba, K., 2018. Red grape marc flour as food ingredient in durum wheat spaghetti: Nutritional evaluation and bioaccessibility of bioactive compounds. Food Sci Technol Res 24, 1093–1100. https://doi.org/10.3136/fstr.24.1093

- Marinelli, V., Padalino, L., Conte, D., del Nobile, M.Alesandro., Conte, A., 2015. New Approach to Enrich Pasta with Polyphenols from Grape Marc. J Chem 2015. https://doi.org/10.1155/2015/734578
- Marti, A., D'Egidio, M.G., Pagani, M.A., 2016. Pasta: Quality Testing Methods. Reference Module in Food Science 1–5. https://doi.org/10.1016/b978-0-08-100596-5.00132-3
- Marti, A., Pagani, M.A., Seetharaman, K., 2011. Understanding starch organisation in gluten-free pasta from rice flour. Carbohydr Polym 84, 1069–1074. https://doi.org/10.1016/j.carbpol.2010.12.070
- Martin, C., Morel, M.H., Reau, A., Cuq, B., 2019. Kinetics of gluten protein-insolubilisation during pasta processing: Decoupling between time- and temperature-dependent effects. J Cereal Sci 88, 103–109. https://doi.org/10.1016/j.jcs.2019.05.014
- Martini, D., Ciccoritti, R., Nicoletti, I., Nocente, F., Corradini, D., D'Egidio, M.G., Taddei, F., 2018. From seed to cooked pasta: influence of traditional and non-conventional transformation processes on total antioxidant capacity and phenolic acid content. Int J Food Sci Nutr 69, 24–32. https://doi.org/10.1080/09637486.2017.1336751
- Masato, O., Kentaro, M., Tatsuro, M., Akio, F., Yukako, H., Yasuki, M., 2021. Effects of drying temperature on the properties of starch in pasta. Lwt 145, 111171. https://doi.org/10.1016/j.lwt.2021.111171
- Maskey, B., Subedi, S., Shrestha, N.K., 2020. Effect of Incorporation of Jackfruit (Artocarpus heterophyllus) Seed Flour on the Quality of Cookies. Dristikon: A Multidisciplinary Journal 10, 60–72. https://doi.org/10.3126/dristikon.v10i1.34541
- Meares, C.A., Bogracheva, T.Y., Hill, S.E., Hedley, C.L., 2004. Development and testing of methods to screen chickpea flour for starch characteristics. Starch/Staerke 56, 215–224. https://doi.org/10.1002/star.200300276
- Meerts, M., Cardinaels, R., Oosterlinck, F., Courtin, C.M., Moldenaers, P., 2017. The Impact of Water Content and Mixing Time on the Linear and Non-Linear Rheology of Wheat Flour Dough. Food Biophys 12, 151–163. https://doi.org/10.1007/s11483-017-9472-9
- Melini, V., Melini, F., Acquistucci, R., 2020. Phenolic compounds and bioaccessibility thereof in functional pasta. Antioxidants 9, 1–30. https://doi.org/10.3390/antiox9040343
- Merendino, N., Molinari, R., Costantini, L., Mazzucato, A., Pucci, A., Bonafaccia, F., Esti, M., Ceccantoni, B., Papeschi, C., Bonafaccia, G., 2014. A new "functional" pasta containing tartary buckwheat sprouts as an ingredient improves the oxidative status and normalizes some blood pressure parameters in spontaneously hypertensive rats. Food Funct 5, 1017–1026. https://doi.org/10.1039/c3fo60683j

Mesa, J., Barrera, C., Betoret, E., Betoret, N., 2020. High Homogenization Pressures to Improve Food. Molecules 25, 1–19.

Messia, M.C., Cuomo, F., Falasca, L., Trivisonno, M.C., Arcangelis, E. de, Marconi, E., 2021. Nutritional and technological quality of high protein pasta. Foods 10. https://doi.org/10.3390/foods10030589

Meullemiestre, A., Breil, C., Abert-Vian, M., Chemat, F., 2016. Microwave, ultrasound, thermal treatments, and bead milling as intensification techniques for extraction of lipids from oleaginous Yarrowia lipolytica yeast for a biojetfuel application. Bioresour Technol 211, 190–199. https://doi.org/10.1016/j.biortech.2016.03.040

Minekus, M., Alminger, M., Alvito, P., Ballance, S., Bohn, T., Bourlieu, C., Carrière, F., Boutrou, R., Corredig, M., Dupont, D., Dufour, C., Egger, L., Golding, M., Karakaya, S., Kirkhus, B., le Feunteun, S., Lesmes, U., MacIerzanka, A., MacKie, A., Marze, S., McClements, D.J., Ménard, O., Recio, I., Santos, C.N., Singh, R.P., Vegarud, G.E., Wickham, M.S.J., Weitschies, W., Brodkorb, A., 2014. A standardised static in vitro digestion method suitable for food-an international consensus. Food Funct 5, 1113–1124. https://doi.org/10.1039/c3fo60702j

Molaveisi, M., Beigbabaei, Adel, Akbari, E., Noghabi, S., Mohamadi, M., Beigbabaei, A, Kinetics, M.M., 2019. Kinetics of temperature effect on antioxidant activity, phenolic compounds and color of Iranian jujube honey. Heliyon 5, e01129. https://doi.org/10.1016/j.heliyon.2019

Monteiro, M.L.G., Mársico, E.T., Deliza, R., Castro, V.S., Mutz, Y.S., Soares Junior, M.S., Caliari, M., dos Santos, E.A., Conte-Junior, C.A., 2019. Physicochemical and sensory characteristics of pasta enriched with fish (Oreochromis niloticus)waste flour. LWT 111, 751–758. https://doi.org/10.1016/j.lwt.2019.05.075

Mustafa, W., Pataro, G., Ferrari, G., Donsì, F., 2018. Novel approaches to oil structuring via the addition of high-pressure homogenized agri-food residues and water forming capillary bridges. J Food Eng 236, 9–18. https://doi.org/10.1016/j.jfoodeng.2018.05.003

N. Rajha, H., Darra, N. el, Vorobiev, E., Louka, N., Maroun, R.G., 2013. An Environment Friendly, Low-Cost Extraction Process of Phenolic Compounds from Grape Byproducts. Optimization by Multi-Response Surface Methodology. Food Nutr Sci 04, 650–659. https://doi.org/10.4236/fns.2013.46084

Naidu, D.S., Hlangothi, S.P., John, M.J., 2018. Bio-based products from xylan: A review. Carbohydr Polym 179, 28–41. https://doi.org/10.1016/j.carbpol.2017.09.064

Nilusha, R.A.T., Jayasinghe, J.M.J.K., Perera, O.D.A.N., Perera, P.I.P., 2019. Development of pasta products with nonconventional ingredients and their effect on selected quality characteristics: A brief overview. Int J Food Sci 2019. https://doi.org/10.1155/2019/6750726

Niu, D., Ren, E.F., Li, J., Zeng, X.A., Li, S.L., 2021. Effects of pulsed electric field-assisted treatment on the extraction, antioxidant activity and structure of naringin. Sep Purif Technol 265, 118480. https://doi.org/10.1016/j.seppur.2021.118480

Niu, D., Zeng, X.A., Ren, E.F., Xu, F.Y., Li, J., Wang, M.S., Wang, R., 2020. Review of the application of pulsed electric fields (PEF) technology for food processing in China. Food Research International 137, 109715. https://doi.org/10.1016/j.foodres.2020.109715

Niu, Y., Xiang, Y., 2018. An Overview of Biomembrane Functions in Plant Responses to High-Temperature Stress. Front. Plant Sci 9, 915. https://doi.org/10.3389/fpls.2018.00915

Nwakiban, A.P.A., Cicolari, S., Piazza, S., Gelmini, F., Sangiovanni, E., Martinelli, G., Bossi, L., Carpentier-Maguire, E., Tchamgoue, A.D., Agbor, G., Kuiaté, J.R., Beretta, G., Dell'Agli, M., Magni, P., 2020. Oxidative stress modulation by cameroonian spice extracts in HepG2 cells: Involvement of Nrf2 and improvement of glucose uptake. Metabolites 10. https://doi.org/10.3390/metabo10050182

Obiang-Obounou, B.W., Ryu, G.H., 2013. The effect of feed moisture and temperature on tannin content, antioxidant and antimicrobial activities of extruded chestnuts. Food Chem. https://doi.org/10.1016/j.foodchem.2013.06.129

Ogawa, T., Adachi, S., 2017. Detection of cracks in dried spaghetti using transmission images. Biosci Biotechnol Biochem 81, 750–754. https://doi.org/10.1080/09168451.2016.1274641

Oliviero, T., Fogliano, V., 2016. Food design strategies to increase vegetable intake: The case of vegetable enriched pasta. Trends Food Sci Technol 51, 58–64. https://doi.org/10.1016/j.tifs.2016.03.008

Oniszczuk, A., Kasprzak, K., Wójtowicz, A., Oniszczuk, T., Olech, M., 2019. The impact of processing parameters on the content of phenolic compounds in new glutenfree precooked buckwheat pasta. Molecules 24, 1–9. https://doi.org/10.3390/molecules24071262

Özcan, M.M., Juhaimi, F. al, Gülcü, M., Uslu, N., Geçgel, Ü., Ghafoor, K., Dursun, N., 2017. Effect of harvest time on physico-chemical properties and bioactive compounds of pulp and seeds of grape varieties. J Food Sci Technol 54, 2230–2240. https://doi.org/10.1007/s13197-017-2658-9

Padalino, L., Conte, A., Lecce, L., Likyova, D., Sicari, V., Pellicanò, T.M., Poiana, M., del Nobile, M.A., 2017. Functional pasta with tomato by-product as a source of antioxidant compounds and dietary fibre. Czech Journal of Food Sciences 35, 48–56. https://doi.org/10.17221/171/2016-CJFS

- Padalino, L., D'Antuono, I., Durante, M., Conte, A., Cardinali, A., Linsalata, V., Mita, G., Logrieco, A.F., del Nobile, M.A., 2018. Use of olive oil industrial by-product for pasta enrichment. Antioxidants 7, 1–15. https://doi.org/10.3390/antiox7040059
- Padayachee, A., Day, L., Howell, K., Gidley, M.J., 2017. Complexity and health functionality of plant cell wall fibers from fruits and vegetables. Crit Rev Food Sci Nutr 57, 59–81. https://doi.org/10.1080/10408398.2013.850652
- Panzella, L., Moccia, F., Nasti, R., Marzorati, S., Verotta, L., Napolitano, A., 2020. Bioactive Phenolic Compounds From Agri-Food Wastes: An Update on Green and Sustainable Extraction Methodologies. Front Nutr. https://doi.org/10.3389/fnut.2020.00060
- Parizad, P.A., Marengo, M., Bonomi, F., Scarafoni, A., Cecchini, C., Pagani, M.A., Marti, A., Iametti, S., 2020. Bio-functional and structural properties of pasta enriched with a debranning fraction from purple wheat. Foods 9, 1–13. https://doi.org/10.3390/foods9020163
- Parniakov, O., Barba, F.J., Grimi, N., Lebovka, N., Vorobiev, E., 2016. Extraction assisted by pulsed electric energy as a potential tool for green and sustainable recovery of nutritionally valuable compounds from mango peels. Food Chem 192, 842–848. https://doi.org/10.1016/j.foodchem.2015.07.096
- Pasqualone, A., Gambacorta, G., Summo, C., Caponio, F., di Miceli, G., Flagella, Z., Marrese, P.P., Piro, G., Perrotta, C., de Bellis, L., Lenucci, M.S., 2016. Functional, textural and sensory properties of dry pasta supplemented with lyophilized tomato matrix or with durum wheat bran extracts produced by supercritical carbon dioxide or ultrasound. Food Chem 213, 545–553. https://doi.org/10.1016/j.foodchem.2016.07.006
- Pasqualone, A., Punzi, R., Trani, A., Summo, C., Paradiso, V.M., Caponio, F., Gambacorta, G., 2017. Enrichment of fresh pasta with antioxidant extracts obtained from artichoke canning by-products by ultrasound-assisted technology and quality characterisation of the end product. Int J Food Sci Technol 52, 2078–2087. https://doi.org/10.1111/ijfs.13486
- Pataro, G., Bobinaitė, R., Bobinas, Č., Šatkauskas, S., Raudonis, R., Visockis, M., Ferrari, G., Viškelis, P., 2017. Improving the Extraction of Juice and Anthocyanins from Blueberry Fruits and Their By-products by Application of Pulsed Electric Fields. Food Bioproc Tech 10, 1595–1605. https://doi.org/10.1007/s11947-017-1928-x
- Pataro, G., Carullo, D., Falcone, M., Ferrari, G., 2020. Recovery of lycopene from industrially derived tomato processing by-products by pulsed electric fields-assisted extraction. Innovative Food Science and Emerging Technologies 63, 102369. https://doi.org/10.1016/j.ifset.2020.102369
- Patil, S., Sonawane, S.K., Mali, M., Mhaske, S.T., Arya, S.S., 2020. Pasting, viscoelastic and rheological characterization of gluten free (cereals, legume and

underutilized) flours with reference to wheat flour. J Food Sci Technol 57, 2960–2966. https://doi.org/10.1007/s13197-020-04328-2

Perito, M.A., di Fonzo, A., Sansone, M., Russo, C., 2019. Consumer acceptance of food obtained from olive by-products: A survey of Italian consumers. British Food Journal 122, 212–226. https://doi.org/10.1108/BFJ-03-2019-0197

Pigni, N.B., Aranibar, C., Lucini Mas, A., Aguirre, A., Borneo, R., Wunderlin, D., Baroni, M.V., 2020. Chemical profile and bioaccessibility of polyphenols from wheat pasta supplemented with partially-deoiled chia flour. Lwt 124, 109134. https://doi.org/10.1016/j.lwt.2020.109134

Pillai, D.S., Prabhasankar, P., Jena, B.S., Anandharamakrishnan, C., 2012. Microencapsulation of garcinia cowa fruit extract and effect of its use on pasta process and quality. Int J Food Prop 15, 590–604. https://doi.org/10.1080/10942912.2010.494756

Piwińska, M., Wyrwisz, J., Kurek, M.A., Wierzbicka, A., 2016. Effect of drying methods on the physical properties of durum wheat pasta. CYTA - Journal of Food 14, 523–528. https://doi.org/10.1080/19476337.2016.1149226

Plazzotta, S., Ibarz, R., Manzocco, L., Martín-Belloso, O., 2021. Modelling the recovery of biocompounds from peach waste assisted by pulsed electric fields or thermal treatment. J Food Eng 290, 110196. https://doi.org/10.1016/j.jfoodeng.2020.110196

Plazzotta, S., Manzocco, L., 2018. Effect of ultrasounds and high pressure homogenization on the extraction of antioxidant polyphenols from lettuce waste. Innovative Food Science and Emerging Technologies. https://doi.org/10.1016/j.ifset.2018.10.004

Podio, N.S., Baroni, M. v., Pérez, G.T., Wunderlin, D.A., 2019. Assessment of bioactive compounds and their in vitro bioaccessibility in whole-wheat flour pasta. Food Chem 293, 408–417. https://doi.org/10.1016/j.foodchem.2019.04.117

Postma, P.R., Pataro, G., Capitoli, M., Barbosa, M.J., Wijffels, R.H., Eppink, M.H.M., Olivieri, G., Ferrari, G., 2016. Selective extraction of intracellular components from the microalga Chlorella vulgaris by combined pulsed electric field-temperature treatment. Bioresour Technol 203, 80–88. https://doi.org/10.1016/j.biortech.2015.12.012

Preedy, V., 2014. Processing and Impact on Active Components in Food, Processing and Impact on Active Components in Food. https://doi.org/10.1016/C2012-0-02526-4

Puértolas, E., Barba, F.J., 2016. Electrotechnologies applied to valorization of by-products from food industry: Main findings, energy and economic cost of their

industrialization. Food and Bioproducts Processing 100, 172–184. https://doi.org/10.1016/j.fbp.2016.06.020

Punia, S., Kumar, M., Siroha, A.K., Kennedy, J.F., Dhull, S.B., Whiteside, W.S., 2021. Pearl millet grain as an emerging source of starch: A review on its structure, physicochemical properties, functionalization, and industrial applications. Carbohydr Polym. https://doi.org/10.1016/j.carbpol.2021.117776

Puraikalan, Y., 2018. Current research in nutrition and food science characterization of proximate, phytochemical and antioxidant analysis of banana (Musa sapientum) peels / skins and objective evaluation of ready to eat / cook product made with banana peels. Current Research in Nutrition and Food Science 06, 382–391. https://doi.org/http://dx.doi.org/10.12944/CRNFSJ.6.2.13

Ramos-Diaz, J.M., Kince, T., Sabovics, M., Gürbüz, G., Rauma, A., Lampi, A.M., Piironen, V., Straumite, E., Klava, D., Jouppila, K., 2020. Relationship of compositional, mechanical, and textural properties of gluten-free pasta using different quinoa (Chenopodium quinoa) varieties. Foods 9. https://doi.org/10.3390/foods9121849

Rani, S., Singh, R., Kamble, D.B., Upadhyay, A., Kaur, B.P., 2019. Structural and quality evaluation of soy enriched functional noodles. Food Biosci 32, 100465. https://doi.org/10.1016/J.FBIO.2019.100465

Rapisarda, P., Tomaino, A., lo Cascio, R., Bonina, F., de Pasquale, A., Saija, A., 1999. Antioxidant effectiveness as influenced by phenolic content of fresh orange juices. J Agric Food Chem 47, 4718–4723. https://doi.org/10.1021/jf9901111

Raso, J., Frey, W., Ferrari, G., Pataro, G., Knorr, D., Teissie, J., Miklavčič, D., 2016. Recommendations guidelines on the key information to be reported in studies of application of PEF technology in food and biotechnological processes. Innovative Food Science & Emerging Technologies. https://doi.org/10.1016/j.ifset.2016.08.003

Reddy Surasani, V.K., Singh, A., Gupta, A., Sharma, S., 2019. Functionality and cooking characteristics of pasta supplemented with protein isolate from pangas processing waste. LWT - Food Science and Technology 111, 443–448. https://doi.org/10.1016/j.lwt.2019.05.014

Renoldi, N., Brennan, C.S., Lagazio, C., Peressini, D., 2021. Evaluation of technological properties, microstructure and predictive glycaemic response of durum wheat pasta enriched with psyllium seed husk. LWT 151. https://doi.org/10.1016/j.lwt.2021.112203

Rezende, E.S.V., Lima, G.C., Naves, M.M.V., 2021. Dietary fibers as beneficial microbiota modulators: A proposal classification by prebiotic categories. Nutrition 89. https://doi.org/10.1016/j.nut.2021.111217

Rocchetti, G., Lucini, L., Chiodelli, G., Giuberti, G., Montesano, D., Masoero, F., Trevisan, M., 2017. Impact of boiling on free and bound phenolic profile and antioxidant activity of commercial gluten-free pasta. Food Research International 100, 69–77. https://doi.org/10.1016/j.foodres.2017.08.031

Romano, A., di Luccia, A., Romano, R., Sarghini, F., Masi, P., 2015. Microscopic and thermal characteristics of experimental models of starch, gliadins, glutenins and gluten from semolina. Chem Eng Trans 43, 163–168. https://doi.org/10.3303/CET1543028

Romano, A., Gallo, V., Ferranti, P., Masi, P., 2021. Lentil flour: nutritional and technological properties, in vitro digestibility and perspectives for use in the food industry. Curr Opin Food Sci 40, 157–167. https://doi.org/10.1016/j.cofs.2021.04.003

Romero, M.E., Toro, M.T., Noriega, F., Lopez, M.D., 2019. Wellness ingredients and functional foods, in: The Role of Alternative and Innovative Food Ingredients and Products in Consumer Wellness. https://doi.org/10.1016/b978-0-12-816453-2.00001-2

Roselló-Soto, E., Koubaa, M., Moubarik, A., Lopes, R.P., Saraiva, J.A., Boussetta, N., Grimi, N., Barba, F.J., 2015. Emerging opportunities for the effective valorization of wastes and by-products generated during olive oil production process: Nonconventional methods for the recovery of high-added value compounds. Trends Food Sci Technol 45, 296–310. https://doi.org/10.1016/j.tifs.2015.07.003

Rovito, D., Gionfriddo, G., Barone, I., Giordano, C., Grande, F., de Amicis, F., Lanzino, M., Catalano, S., Andò, S., Bonofiglio, D., 2016. Ligand-activated PPARγ downregulates CXCR4 gene expression through a novel identified PPAR response element and inhibits breast cancer progression.

Sahin, A.W., Hardiman, K., Atzler, J.J., Vogelsang-O'Dwyer, M., Valdeperez, D., Münch, S., Cattaneo, G., O'Riordan, P., Arendt, E.K., 2021. Rejuvenated Brewer's Spent Grain: The impact of two BSG-derived ingredients on techno-functional and nutritional characteristics of fibre-enriched pasta. Innovative Food Science & Emerging Technologies 68, 102633. https://doi.org/10.1016/j.ifset.2021.102633

Saini, A., Panesar, P.S., 2020. Beneficiation of food processing by-products through extraction of bioactive compounds using neoteric solvents. Lwt 134, 110263. https://doi.org/10.1016/j.lwt.2020.110263

Sant'Anna, V., Christiano, F.D.P., Marczak, L.D.F., Tessaro, I.C., Thys, R.C.S., 2014. The effect of the incorporation of grape marc powder in fettuccini pasta properties. LWT - Food Science and Technology 58, 497–501. https://doi.org/10.1016/j.lwt.2014.04.008

Sant'Anna, V., Gurak, P.D., Ferreira Marczak, L.D., Tessaro, I.C., 2013. Tracking bioactive compounds with colour changes in foods - A review. Dyes and Pigments. https://doi.org/10.1016/j.dyepig.2013.04.011

- Sarkis, J.R., Boussetta, N., Blouet, C., Tessaro, I.C., Marczak, L.D.F., Vorobiev, E., 2015. Effect of pulsed electric fields and high voltage electrical discharges on polyphenol and protein extraction from sesame cake. Innovative Food Science and Emerging Technologies 29, 170–177. https://doi.org/10.1016/j.ifset.2015.02.011
- Sarris, D., Papanikolaou, S., 2016. Biotechnological production of ethanol: Biochemistry, processes and technologies. Eng Life Sci 16, 307–329. https://doi.org/10.1002/elsc.201400199
- Sayar, S., Koksel, H., Turhan, M., 2005. The effects of protein-rich fraction and defatting on pasting behavior of chickpea starch. Starch/Staerke 57, 599–604. https://doi.org/10.1002/star.200500397
- Sereewat, P., Suthipinittham, C., Sumathaluk, S., Puttanlek, C., Uttapap, D., Rungsardthong, V., 2015. Cooking properties and sensory acceptability of spaghetti made from rice flour and defatted soy flour. LWT 60, 1061–1067. https://doi.org/10.1016/j.lwt.2014.10.001
- Setford, P.C., Jeffery, D.W., Grbin, P.R., Muhlack, R.A., 2019. Mathematical modelling of anthocyanin mass transfer to predict extraction in simulated red wine fermentation scenarios. Food Research International 121, 705–713. https://doi.org/10.1016/j.foodres.2018.12.044
- Shafie, B., Cheng, S.C., Lee, H.H., Yiu, P.H., 2016. Characterization and classification of whole-grain rice based on rapid visco analyzer (RVA) pasting profile, International Food Research Journal.
- Sharma, S.K., Bansal, S., Mangal, M., Dixit, A.K., Gupta, R.K., Mangal, A.K., 2016. Utilization of food processing by-products as dietary, functional, and novel fiber: A review. Crit Rev Food Sci Nutr 56, 1647–1661. https://doi.org/10.1080/10408398.2013.794327
- Sicignano, Dott.A., 2015. Effects of raw material, technological process and cooking procedure on quality of pasta from durum wheat semolina. PhD. Thesis, University Degli Studi Di Napoli Federico, Italy, 71 p. 71.
- Siemer, C., Toepfl, S., Heinz, V., 2012. Mass Transport Improvement by PEF Applications in the Area of Extraction and Distillation. Distillation Advances from Modeling to Applications. https://doi.org/10.5772/37746
- Simonato, B., Trevisan, S., Tolve, R., Favati, F., Pasini, G., 2019. Pasta fortification with olive pomace: Effects on the technological characteristics and nutritional properties. Lwt 114. https://doi.org/10.1016/j.lwt.2019.108368
- Singh, B., Singh, J.P., Kaur, A., Singh, N., 2017. Phenolic composition and antioxidant potential of grain legume seeds: A review. Food Research International 101, 1–16. https://doi.org/10.1016/j.foodres.2017.09.026

Sissons, M., Abecassis, J., Marchylo, B., Cubadda, R., 2012. Methods Used to Assess and Predict Quality of Durum Wheat, Semolina, and Pasta, Second Edi. ed, Durum Wheat Chemistry and Technology: Second Edition. AACC International, Inc. https://doi.org/10.1016/B978-1-891127-65-6.50017-9

Sissons, M., Cutillo, S., Marcotuli, I., Gadaleta, A., 2021. Impact of durum wheat protein content on spaghetti in vitro starch digestion and technological properties. J Cereal Sci 98, 103156. https://doi.org/10.1016/j.jcs.2020.103156

Spinelli, S., Padalino, L., Costa, C., del Nobile, M.A., Conte, A., 2019. Food by-products to fortified pasta: A new approach for optimization. J Clean Prod 215, 985–991. https://doi.org/10.1016/j.jclepro.2019.01.117

Steglich, T., Bernin, D., Moldin, A., Topgaard, D., Langton, M., 2015. Bran particle size influence on pasta microstructure, water distribution, and sensory properties. Cereal Chem. https://doi.org/10.1094/CCHEM-03-15-0038-R

Susantikarn, P., and Donlao, N., 2016. Optimization of green tea extracts spray drying as affected by temperature and maltodextrin content, International Food Research Journal, 23, 1327-1331.

Syah, I.T., Irundu, D., Bahmid, N.A., Indrastuti, Karim, I., 2022. Changes in functional properties during fermentation of Amorphophallus paeoniifolius (Dennst.) Nicolson yam using Lactobacillus plantarum, in: IOP Conference Series: Earth and Environmental Science. IOP Publishing Ltd. https://doi.org/10.1088/1755-1315/978/1/012015

Tempel, A.S., 1982. Tannin-measuring techniques - A review. J Chem Ecol 8, 1289–1298. https://doi.org/10.1007/BF00987762

Thierry, N.N., Léopold, T.N., Didier, M., Moses, F.M.C., 2013. Effect of Pure Culture Fermentation on Biochemical Composition of <i>Moringa oleifera</i> Lam Leaves Powders. Food Nutr Sci 04, 851–859. https://doi.org/10.4236/fns.2013.48111

Torres, O.L., Lema, M., Galeano, Y. v., 2021. Effect of Using Quinoa Flour (Chenopodium quinoa Willd.) on the Physicochemical Characteristics of an Extruded Pasta. Int J Food Sci 2021. https://doi.org/10.1155/2021/8813354

Tournour, H.H., Segundo, M.A., Magalhães, L.M., Barreiros, L., Queiroz, J., Cunha, L.M., 2015. Valorization of grape pomace: Extraction of bioactive phenolics with antioxidant properties. Ind Crops Prod 74, 397–406. https://doi.org/10.1016/j.indcrop.2015.05.055

Tzima, K., Brunton, N.P., Lyng, J.G., Frontuto, D., Rai, D.K., 2021. The effect of Pulsed Electric Field as a pre-treatment step in Ultrasound Assisted Extraction of phenolic compounds from fresh rosemary and thyme by-products. Innovative Food

Science and Emerging Technologies 69, 102644. https://doi.org/10.1016/j.ifset.2021.102644

Ungureanu-Iuga, M., Dimian, M., Mironeasa, S., 2020. Development and quality evaluation of gluten-free pasta with grape peels and whey powders. Lwt 130. https://doi.org/10.1016/j.lwt.2020.109714

van Buggenhout, S., Wallecan, J., Christiaens, S., Debon, S.J.J., Desmet, C., van Loey, A., Hendrickx, M., Mazoyer, J., 2015. Influence of high-pressure homogenization on functional properties of orange pulp. Innovative Food Science & Emerging Technologies 30, 51–60. https://doi.org/10.1016/J.IFSET.2015.05.004

Verardo, V., Arráez-Román, D., Segura-Carretero, A., Marconi, E., Fernández-Gutiérrez, A., Caboni, M.F., 2011. Determination of free and bound phenolic compounds in buckwheat spaghetti by RP-HPLC-ESI-TOF-MS: Effect of thermal processing from farm to fork. J Agric Food Chem 59, 7700–7707. https://doi.org/10.1021/jf201069k

Vieira, M. v., Pastrana, L.M., Fuciños, P., 2020. Microalgae Encapsulation Systems for Food, Pharmaceutical and Cosmetics Applications. Mar Drugs 18. https://doi.org/10.3390/md18120644

Vinatoru, M., Mason, T.J., Calinescu, I., 2017. Ultrasonically assisted extraction (UAE) and microwave assisted extraction (MAE) of functional compounds from plant materials. TrAC - Trends in Analytical Chemistry 97, 159–178. https://doi.org/10.1016/j.trac.2017.09.002

Viuda-Martos, M., Sanchez-Zapata, E., Sayas-Barberá, E., Sendra, E., Pérez-Álvarez, J.A., Fernández-López, J., 2014. Tomato and Tomato Byproducts. Human Health Benefits of Lycopene and Its Application to Meat Products: A Review. Crit Rev Food Sci Nutr 54, 1032–1049. https://doi.org/10.1080/10408398.2011.623799

Wahanik, A.L., Chang, Y.K., Clerici, M.T.P.S., 2018. How to make pastas healthier? Food Reviews International 34, 52–69. https://doi.org/10.1080/87559129.2016.1210634

Yadav, D.N., Balasubramanian, S., Kaur, J., Anand, T., Singh, A.K., 2014. Non-wheat pasta based on pearl millet flour containing barley and whey protein concentrate. J Food Sci Technol 51, 2592–2599. https://doi.org/10.1007/s13197-012-0772-2

Yousf, N., Nazir, F., Salim, R., Ahsan, H., Sirwal, A., 2017. Water solubility index and water absorption index of extruded product from rice and carrot blend. Journal of Pharmacognosy and Phytochemistry 6, 2165-2168.

Yu, Z.Y., Jiang, S.W., Cao, X.M., Jiang, S.T., Pan, L.J., 2016. Effect of high pressure homogenization (HPH) on the physical properties of taro (Colocasia esculenta (L). Schott) pulp. J Food Eng 177, 1–8. https://doi.org/10.1016/J.JFOODENG.2015.10.042

Zayapor, M.N., Aminah, A., Wan Aida, W.M., 2021. Influence of sugar concentration and sugar type on the polyphenol content and antioxidant activity in spiced syrup preparation. Italian Journal of Food Science 33, 96–105. DOI: 10.15586/ijfs.v33i1.1874P

Zhang, L., Nishizu, T., Hayakawa, S., Nakashima, R., Goto, K., 2013. Effects of Different Drying Conditions on Water Absorption and Gelatinization Properties of Pasta. Food Bioproc Tech 6, 2000–2009. https://doi.org/10.1007/s11947-012-0976-5

Zhang, Q.W., Lin, L.G., Ye, W.C., 2018. Techniques for extraction and isolation of natural products: A comprehensive review. Chinese Medicine (United Kingdom) 13, 1–26. https://doi.org/10.1186/s13020-018-0177-x

Zhang, W., Yu, Y., Xie, F., Gu, X., Wu, J., Wang, Z., 2019. High pressure homogenization versus ultrasound treatment of tomato juice: Effects on stability and in vitro bioaccessibility of carotenoids. LWT 116. https://doi.org/10.1016/j.lwt.2019.108597

Zhu, X., Cheng, Y., Chen, P., Peng, P., Liu, S., Li, D., Ruan, R., 2016. Effect of alkaline and high-pressure homogenization on the extraction of phenolic acids from potato peels. Innovative Food Science and Emerging Technologies 37, 91–97. https://doi.org/10.1016/j.ifset.2016.08.006

Zuin, V.G., Ramin, L.Z., 2018. Green and Sustainable Separation of Natural Products from Agro-Industrial Waste: Challenges, Potentialities, and Perspectives on Emerging Approaches. Top Curr Chem. https://doi.org/10.1007/s41061-017-0182-z